ANALYTICAL APPLICATIONS
OF
ION SELECTIVE DEVICES.

by

Janice Dick

Thesis submitted to the University of Newcastle-upon-Tyne
for the Degree of Doctor of Philosophy.

November 1991

NEWCASTLE UNIVERSITY LIBRARY
091 51186 4
Thesis L3897

Aknowledgements.

I am grateful to Professor A.K. Covington for his supervision and helpful advice and discussions throughout this research. I should like to take this oportunity to thank the workshop and technical staff of the Chemistry Department for their support.

Thanks must also also go to Bellhouse Medical Products Ltd., for an ISFET flow cell, and to I.C.I plc. for fertilizer samples. I wish to express my gratitude to the Centre for Urban and Rural Studies (CURDS), of the University of Newcastle-upon-Tyne, for allowing me to use their digitiser.

To my fellow students and workers of the AKC group, I extend warmest thanks for making life in the lab more enjoyable, especially to Miss P.M. Kelly who has had to contend with my continual bullying.

Finally, I must thank my parents and Doug, for their unfailing support and encouragement throughout the writing of this thesis.

Abstract.

Ion selective electrodes, ISEs, and ion sensitive field effect transistors, ISFETs, are small, relatively simple to operate and easily automated sensors and, therefore, have a wide range of uses e.g. for field measurements in portable detectors,for on-line measurements in industrial flow systems and in clinical work.

Several flow systems were studied for use with ion selective devices. New design ISE flow cells, designed at Newcastle, were found to minimise dead space and carry-over of sample solutions, allowing more rapid sample throughput. An ISFET flow cell studied, however, was found to have serious design faults. The constant volume dilution method of calibration and selectivity determination was shown to be a simple easy-to-use method but must be implemented with caution. The selectivity of sensors to the primary ion was determined, where applicable, and the optical sensitivity of ISFETs was examined.

Potassium concentrations in fertilizers were determined, using ISEs, in both flow systems described above; more accurate results were obtained using the newer flow-cells. Failure of ISEs after prolonged use in fertilizer solutions is believed to be have been caused by Donnan Breakdown due to HPO_4^{2-} ions.

A computer controlled titration system was developed which can be used for volumetric or coulometric titrations. Coulometry, an absolute method, is particularly suitable for titration of sub micro-litre samples and for chemically labile species as sample manipulation is minimised and avoids addition of solution reagent, obviating CO_2 contamination of hydroxide. The advantages of coulometry were exploited in work to confirm the second dissociation constant for hydrogen sulphide. Aerial oxidation and sample carbon dioxide uptake are common problems associated with sulphide solutions. Using degassed water for sample

preparation, keeping all solutions under nitrogen and using a sulphide anti-oxidant buffer it was possible to reduce sulphide oxidation.

Coulometry was used to generate hydrogen ions and potentiometric measurements of the pH and sulphide ion concentrations, made simultaneously, were used to calculate the pK_2^d of hydrogen sulphide for a range of 50 µl sodium sulphide solutions.

A non-linear least squares programme, SUPERQUAD, was used to obtain a better value for pK_2^d. Though a coulometric option exists in SUPERQUAD, it is not often implemented. ISE titration results have not been used much with SUPERQUAD; this work examined the potential of expanding the application of SUPERQUAD.

Values of pK_2^d of 12.08 ± 1.0 and 11.83 ± 0.4 were obtained by visual inspection and SUPERQUAD refinement, respectively. These values agree well with the text-book value, of 11.96, and demonstrate the accuracy of coulometry.

The auto-titration system developed has advantages in many areas, particularly in clinical chemistry where determinations of available species in sub micro-litre samples, delivered in a flow system are required.

Chapter 1. Introduction

1.1 Introduction 1

1.2 Ion Exchange Processes 2

1.3 Membrane Components 6

1.4 Transfer Processes occurring in Glass Electrodes 8

1.5 Classification of Electroactive Membranes 10

1.6 Ion Selective Devices 11

1.7 Classification of Ion Selective Electrodes 11

1.7.1 Primary Electrodes 11

1.7.2 Sensitized Electrodes 11

1.8 Objectives of this Work 11

Chapter 2. Description of Ion Selective Devices.

2.1 Introduction 18

2.2 Cell Design 18

2.3 Ion Selective Electrodes 18

2.3.1 Electrode Construction 18

2.3.2 Reference Electrodes 20

a) Calomel Electrode 20

b) Silver / Silver Chloride Electrode 21

c) Preparation of Thermal Electrolytic 21

Silver / Silver Chloride Electrodes

2.4 Ion Sensitive Field Effect Transistors (ISFETs) 22

2.4.1 Introduction 22

2.4.2 Insulated Gate Field Effect Transistors (IGFETs) 22

2.4.3 Charge Distribution of the IGFET 23

a) Threshold Voltage and Inversion Layer 23

b) Enhancement and Depletion Mode 24

c) Saturated and Unsaturated Mode 24

2.4.4 Construction of ISFETs 25
a) Eμ-146 Device 25
b) Eμ-358A (OPTRAN) Device 26
2.4.5 Flow Through Sensors 26
2.4.6 Epoxy Encapsulation 26
2.4.7 Membrane Deposition 26
2.5 Electrode Response 27
2.6 Selectivity and Interference 28
2.7 Methods of Determining k_{ij} 29
2.7.1 Separate Solution Method 29
2.7.2 Mixed Solution Method 29
a) Constant Interferent Concentration 29
b) Constant Primary Ion Concentration 30
2.8 Response Limits 30
2.9 Response Time 31
2.10 Liquid Junction Potentials 31

Chapter 3. Instrumentation and Calibration Methods.

3.1 Introduction 35
3.2 Buffer Amplifiers 35
3.3 ISFET Operation 36
3.3.1 Methods of Measuring the Drain Current, I_D 36
i) Constant Applied Gate Voltage, V_G 36
ii) Constant Drain Current, I_D 37
3.4 Display of Signal 37
3.5 Thermal Effects 37
3.5.1 Thermal Characteristics of FETs 38
3.6 Effect of Stirring 38
3.7 Pretreatment of Electrodes 39

3.8 Dip Tests 39
3.8.1 Beaker to Beaker Method 39
3.8.2 Standard Addition Technique 39
3.9 Flow Methods 40
3.9.1 Response Time 40
3.9.2 Dip Methods *versus* Flow Methods 41
3.9.3 Conventional Continuous Flow Methods 41
3.10 Unsegmented Flow Techniques 42
3.10.1 Flow Injection Analysis (FIA) 42
3.11 Flow Cells 42
3.11.1 Introduction 42
3.11.2 Experimental 43
3.11.3 Results 43
3.11.4 Conclusion 44
3.12 Constant Volume Dilution Method 44
3.12.1 Introduction 44
3.12.2 Experimental 45
3.12.3 Results and Discussion 47
3.12.4 Conclusion 49
Chapter 4. Development of a Sensor-Actuator Titration System.
4.1 Introduction 53
4.2 Historical 53
4.3 Background 54
4.4 Design and Development of Apparatus 57
4.4.1 General Cell Features 57
4.4.2 Cell Design 57
4.4.3 Separators 57
4.4.4 Depolarizers 58
4.4.5 The Working Electrode 58

4.4.6 The Auxiliary Electrode 59
4.4.7 Supporting Electrolyte 60
4.4.8 Stirring 60
4.4.9 Detectors 61
a) The Indicator Electrode 61
b) The Reference Electrode 61
4.4.10 Atmospheric Gases 62
i) Removal of Dissolved Oxygen 62
ii) Removal of Dissolved Carbon Dioxide 62
4.4.11 Constant Current Systems 63
4.4.12 Pulse Generation 63
4.4.13 Computer Control 64
4.5 Experimental 65
4.5.1 Reagents 65
4.5.2 Apparatus 66
4.6 Method 66
4.7 Designing the Sensor-Actuator System 69
4.8 Results and Discussion 71
4.8.1 Experimental Details 71
4.8.2 A.C. Impedance Studies 74
4.8.3 Using SUPERQUAD 78
4.8.4 Titration Results 79
4.9 Conclusions 81
Chapter 5. Determination of pK_2 for Hydrogen Sulphide.
5.1 Introduction 88
5.2 Hydrolysis of Hydrogen Sulphide 89
5.3 Review of Previous Spectroscopic Work 91
5.4 Experimental 98

5.4.1 Reagents 98

5.4.2 Experimental Set-up 99

5.5 Calibration of Electrodes 100

5.5.1 Experimental 100

5.5.2 Calibration Results 100

5.6 Coulometric Titrations 103

5.6.1 Experimental 103

5.6.2 Titration Results 104

5.7 Calculation of pK_1^d 105

5.8 Calculation of pK_2^d 105

5.9 Using SUPERQUAD to Determine pK_1^d, pK_2^d for Hydrogen Sulphide 108

5.9.1 Manipulation of the Titration Curves 108

5.9.2 Setting up SUPERQUAD 108

5.10 Results of SUPERQUAD Analysis 112

5.11 Determining the β Formation Constants 112

5.12 Experimental *versus* Calculated Data 116

5.13 Further Work 119

5.14 Comparison of Results of Spectroscopic and Potentiometric Studies 120

5.15 Conclusions 121

Chapter 6. Clinical Analysis.

6.1 Introduction 130

6.2 Ex-vivo *versus* In-vivo Methods 130

6.3 Clinical Methods 130

6.3.1 Flame Photometry 130

6.3.2 Potentiometric Methods 131

6.4 Ion Sensitive Field Effect Transistors (ISFETs) 131

6.5 Blood Constituents 132

6.6 Protein Interference 134
6.7 Sterilization Techniques 136
6.7.1 Autoclaving 136
6.7.2 Chemical Methods 136
6.7.3 Cold Gas Method 136
6.7.4 Irradiation 136
6.8 Ion Selective Membranes 137
6.9 Calibration of Sensors 138
6.10 The ChemFET Device 139
6.10.1 Preliminary Tests 139
6.10.2 Optical Sensitivity 140
6.10.3 Thermal Sensitivity 140
6.10.4 Electrostatic Damage 140
6.11 Assembly of the Bellhouse Flow Cell 140
6.12 Results and Discussion 141
6.12.1 Membrane Studies 141
6.12.2 Optical Sensitiivity 143
6.12.3 Thermal Sensitivity 143
6.13 The Bellhouse Flow Cell 143
6.14 Conclusions 145
Chapter 7. Analysis of Fertilizers
7.1 Introduction 151
7.2 The Fertilizer Samples 151
7.3 Ion Selective Electrodes 151
7.3.1 Home made Electrodes 151
7.3.2 Commercial Electrodes 153
7.3.3 ISFETs 153
7.4 Calibration Methods and Standards 153

7.5 Experimental 154
7.5.1 Analyses 154
7.5.2 pH Effects. Pretreatment of Samples 155
7.5.3 Ionic Strength Adjustor 155
7.5.4 Selectivity Studies 155
7.5.5 Effect of Phosphate 155
7.6 Electrode Poisoning 155
7.7 Drift Studies 156
7.8 Results and Discussion 156
7.9 pH Effects 160
7.10 Selectivity Studies 162
7.10.1 Ammonium Solutions 162
7.10.2 Phosphate Solutions 164
7.11 Electrode Poisoning 166
7.12 The Donnan Exclusion Principle 169
7.13 Drift Studies 170
7.14 Conclusions 170

Chapter 8. Conclusions.

8.1 Introduction 174
8.2 Calibration and Measuring Systems 174
8.3 Potentiometric Titrations 176
8.4 Determination of the pK_2^d Value of Hydrogen Sulphide 177
8.4.1 Potentiometric *versus* Spectroscopic Methods 177
8.4.2 Sulphide Anti-Oxidant Buffers 178
8.5 Modifying SUPERQUAD 179
8.6 Novel Designs of Flow Cells 180
8.6.1 Ion Selective Field Effect Transistors 180
8.6.2 Ion Selective Electrodes 180

8.7 Experimental Considerations 181
8.8 Fertilizer Analyses 181
8.8.1 Matrix Effects 181
8.8.2 Electrode Poisoning 182
8.9 Summary 183

Appendices.

A (i) Distillation of Tetrahydrofuran (THF) 185
(ii) Preparation of Silver Oxide 185
B ChemFET Encapsulation using Polyimide / Photoresist 186
C Composition of Buffers 189
D BASIC Sensor-Actuator Proogramme for Volumetric 190
and Coulometric Titrations
E (i) HELP File to assist in using SUPERQUAD 193
(ii) Starting to use SUPERQUAD 195
Documentation to assist in setting up SUPERQUAD
F (i) Composition of Sulphide Anti-Oxidant Buffers 203
(ii) Dissociation Constants of Reagents Present in SAOB 204

CHAPTER ONE

INTRODUCTION

1.1 Introduction.

The ability of solids to conduct was first reported by Lord Kelvin as long ago as 1875 [1] during experiments with hot glasses. However, it was not for another thirty years that Cremer [2] showed that a potential difference arose when a thin glass membrane was placed between two aqueous solutions. This potential difference was found to be pH sensitive and was shown [3] to give the same potential difference as for the hydrogen electrode.

It was discovered [4-7] that a glass membrane could respond to ions other than the hydrogen ion e.g. Na^+, K^+, Li^+ [8]. During the 1930's, Tendeloo [8], and Kolthoff and Saunders [9] showed that natural alumino-silicates in clays could be used as ion sensitive materials, though these were not ion specific. Tendeloo[11] investigated the use of a paraffin support for calcium selective membranes, but this attempt was unsuccessful. Using the same support material, however, Pungor and Hollos-Rokosinyi [12] produced the first anion specific ion selective electrode. This was an iodide precipitate based membrane which could selectively identify iodide ions over chloride ions. During the late 1960's, there was a surge in the development of ion sensing membranes, the highlights of this period may be found elsewhere [13], however, a few of the major 'milestones' of this era are included.

In 1966, Frant and Ross [14], working at Orion Inc., published a paper describing what is still considered the most selective ion selective membrane, the single crystal lanthanum fluoride, fluoride electrode, and in 1969, Ross [15] identified the advantages of liquid membranes over solid state membranes. In 1964, neutral antibiotics, e.g. valinomycin, nonactin, were used as effective cation selective ionophores [16]. In line with this, Pederson [17] synthesised *ca.* 50 tailor-made neutral ligands known as crown ethers, similar in function to the macrocyclic antibiotics.

Advances in synthetic ionophore production, particularly by Simon's

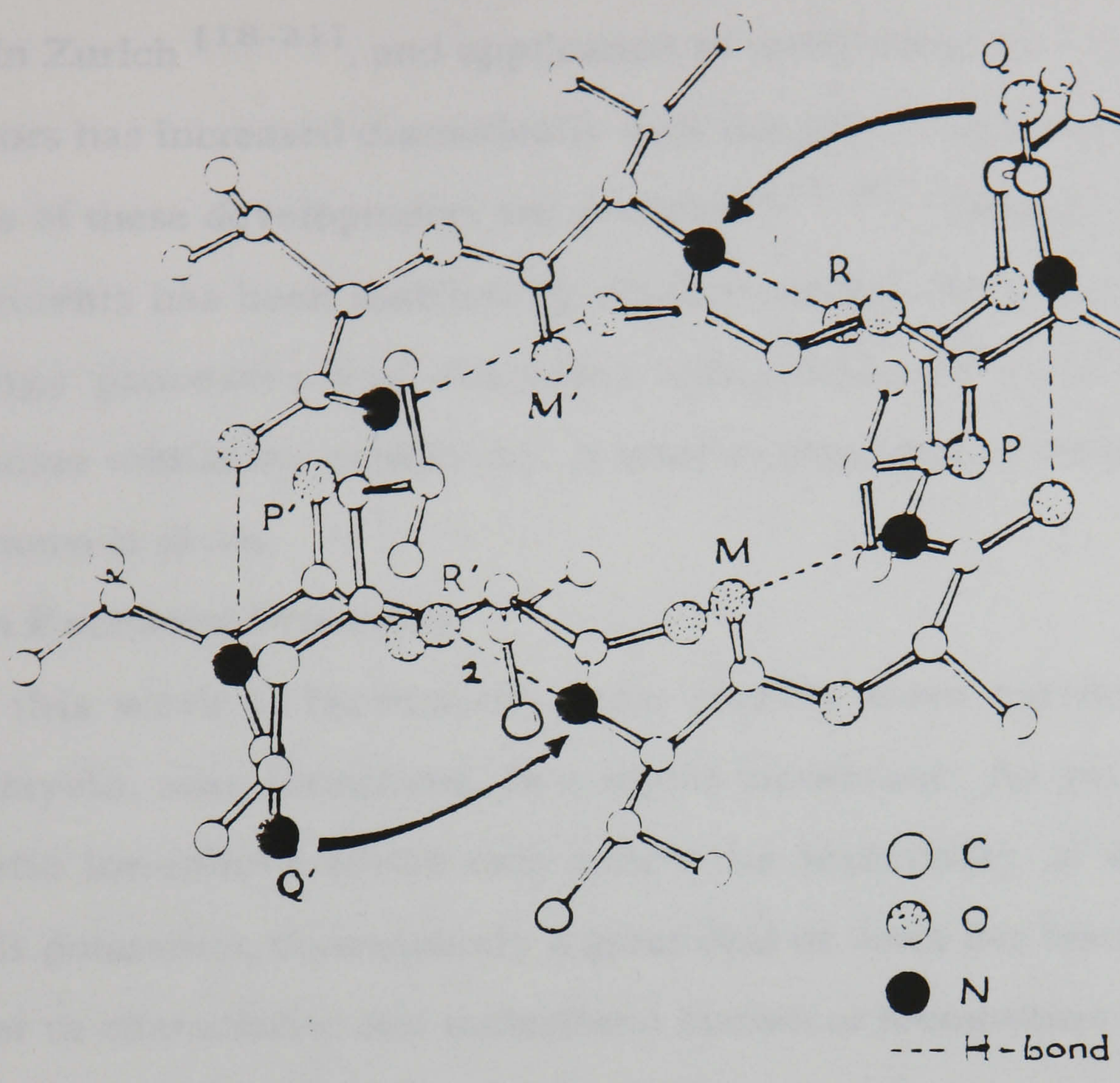

Figure 1:1 Conformation of Free Valinomycin.

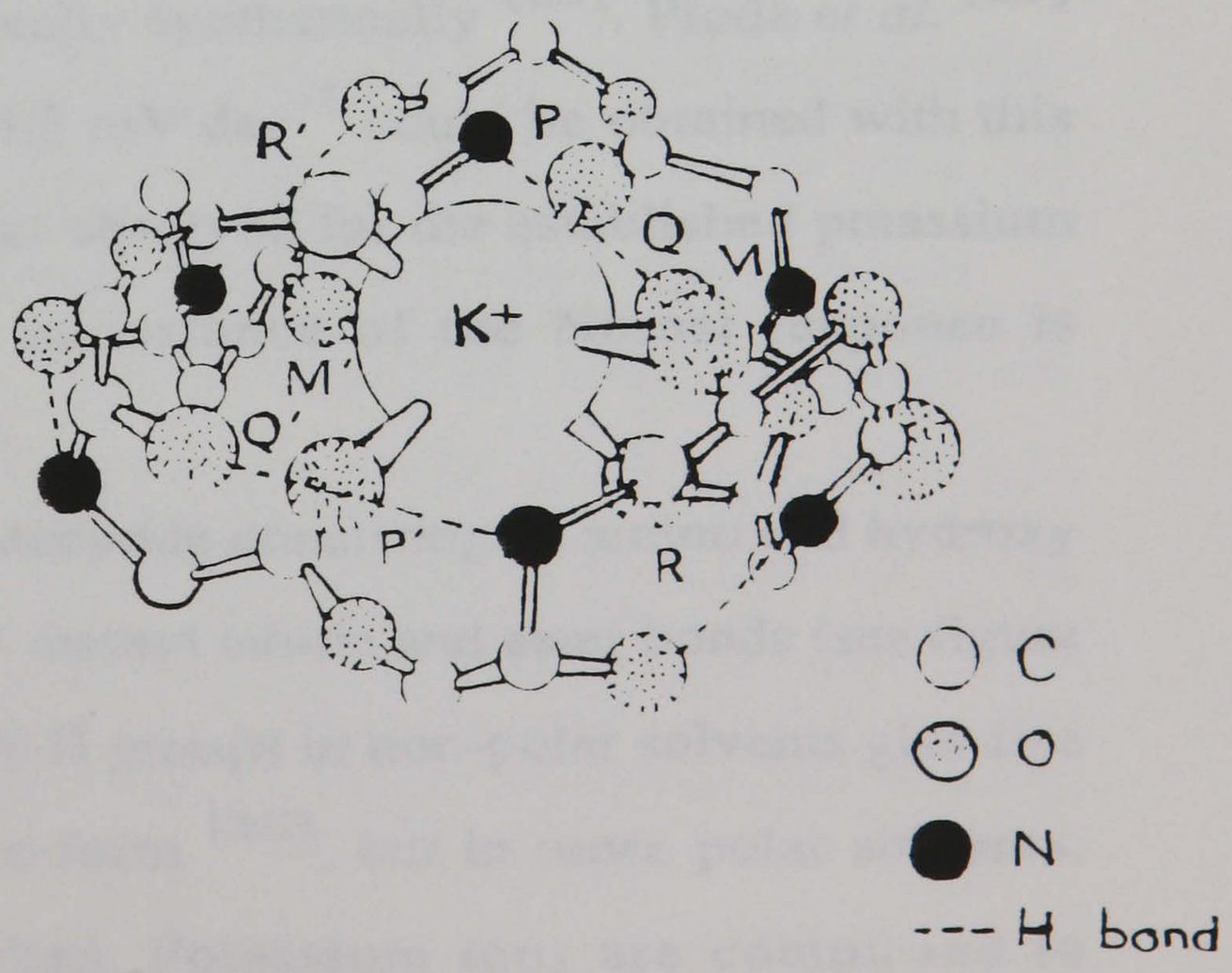

Figure 1:2 Conformation of Potassium Complexed Valinomycin.

Advances in synthetic ionophore production, particularly by Simon's group in Zurich [18-21], and application of membranes to a broader range of sensors has increased dramatically over the past twenty years; numerous reviews of these developments are available [22-25]. Modelling ionophore requirements has been assisted by studies carried out to understand ion exchange processes and chemical recognition of specific ions by ionophores within the membrane. A brief explanation of these membrane phenomena is given.

1.2 Ion Exchange Processes.

In this work at Newcastle, most studies were carried out using valinomycin, asan ionophore, in a liquid membrane. As yet, there is no synthetic ionophore which can match the selectivity of valinomycin towards potassium, consequently a great deal of work has been undertaken in order to characterise and understand chemical recognition processes of the valinomycin membrane.

Moore and Pressman [16] found that in living organisms, antibiotics induced mitochondrial cation permeation. Valinomycin was one of these antibiotics, isolated by Brockmann *et al.*[26, 27] from *Streptomyces fulvissimus* and now prepared totally synthetically [28]. Pioda *et al.* [29] showed that a Nernst slope of 58.3 mV dec^{-1} could be obtained with this macrocycle, much better than that observed for the established potassium selective glass electrode (the importance of the Nernst response is explained in detail in Chapter 2).

Valinomycin is a cyclic depsipeptide consisting of amino and hydroxy acid residues linked by amide, N-methyl amide and ester bonds (see figure 1:1). Hydrogen bonding by the N-H groups in non-polar solvents give rise to a bracelet structure in its free form [30], but in more polar solvents, these hydrogen bonds are broken. Potassium ions are complexed to valinomycin in a 1:1 ratio in an octahedral configuration (figure 1:2). Other cyclo depsipeptides exist which can bind to alkali metal ions, e.g.

valinomycin's high selectivity, probably since the central ion is better enclosed in valinomycin than in e.g. enniatin. Features influencing cation selectivity are considered in the following sections.

In liquid membranes, with plasticized poly (vinyl) chloride as 'inert' support, complex formation (MV^+) with valinomycin (V) is believed to go via a two stage process [31];

$$V + M^+_{(solvent)} \underset{k_{21}}{\overset{k_{12}}{\rightleftharpoons}} VM^+_{(solvent)} \underset{k_{32}}{\overset{k_{23}}{\Leftrightarrow}} MV^+ \qquad (1.1)$$

The first equilibrium process occurs rapidly, it is the second equilibrium process which determines the reaction characteristics, which in turn relies on the radius of the reacting cation. With respect to equilibrium processes, the free energies of the final *versus* initial states of the complex must be favourable, that is, whether the incoming ligand group is more, or less, tightly bound than the replaced solvent molecule. Selectivity towards a particular ion relies on the cavity size of the macrocyclic; determined by steric interference and electronic energies at the lower limit and by conformational flexibility of binding sites in the molecule as the upper size limit. Thus, for a smaller metal ion, stronger electrostatic forces are exerted at the surface, but the rate of substitution is lower since solvent molecules are more tightly bound. In the free molecule, a wide cavity is observed which shrinks on complexation as the cavity adapts to the size of the unsolvated metal ion. In PVC membranes, as for other ionic conductors, the conductivity, σ, of any dissolved salt depends on the extent of salt dissolution in the membrane and the mobility of ions formed within the membrane. This is shown in equation (1.2)

$$\sum \sigma = \quad z_i e c_i u_i \qquad (1.2)$$

where $z_i e$ = charge of ion, i

c_i = volume concentration of ion, i

u_i = mobility of ion, i

Two theories were proposed to explain the mechanism of ion transport across the membrane;

i) the macrocycle membrane component forms an ion specific channel directly through the membrane

ii) the macrocycle substance is the ion carrier, and the complex formed is transported in the direction in which its electrochemical potential is decreasing [32].

The first of these theories was rejected due to the large number of macrocyclic molecules required to produce an ion specific channel; in general only 1 weight percent of ionophore is present in the membrane. In equation (1.1), the first equilibrium process occurred rapidly, and in thick liquid membranes it was shown [33] that ions exhibited rapid exchange, or 'carrier relay' with different macrocyclic molecules. A schematic of this process is shown in figure 1:3 [33].

Figure 1:3

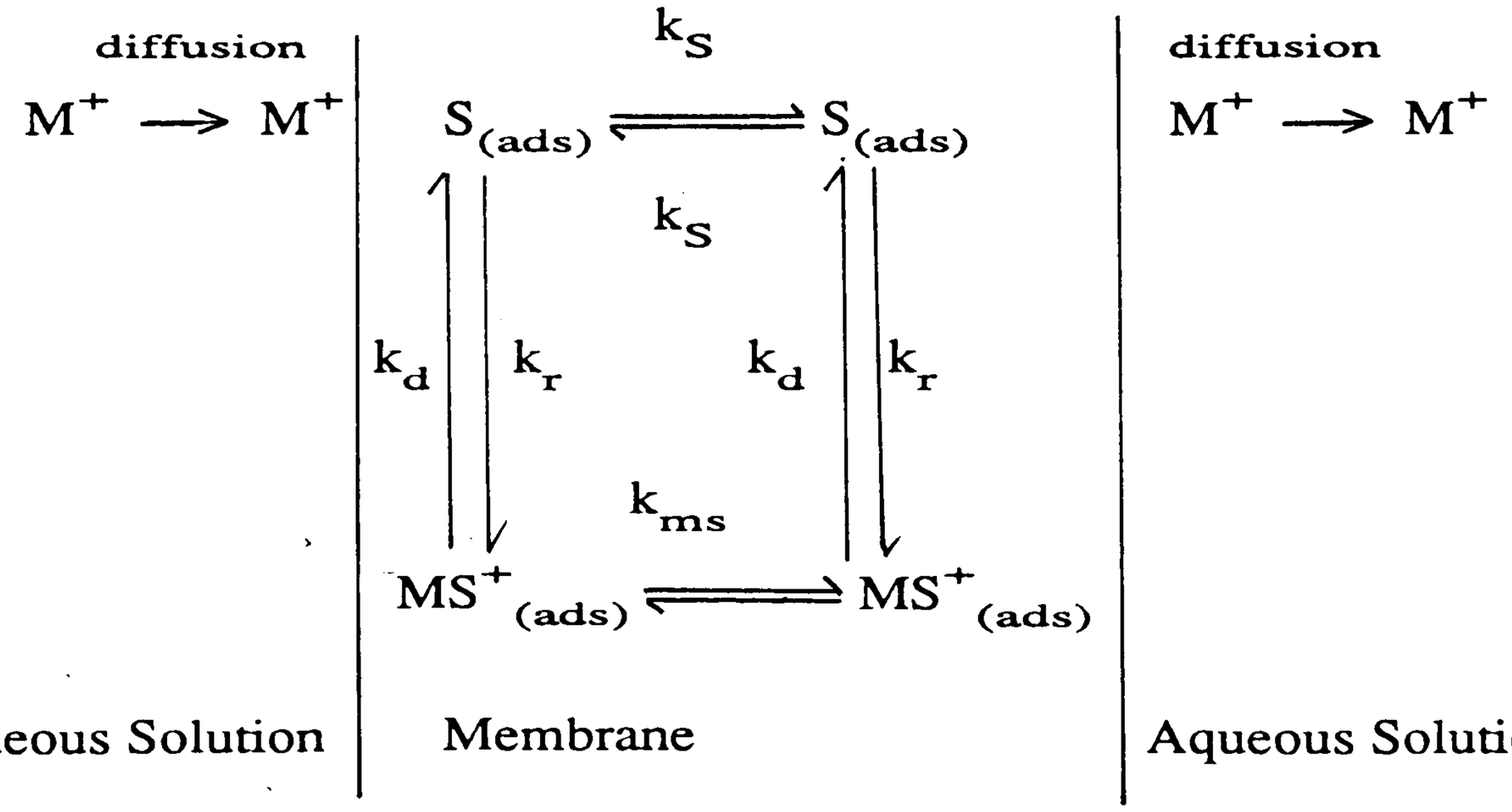

where

M^+ = metal cation

S = carrier

k_r, k_d = rate constants of complex formation and dissociation, respectively

k_{ms}, k_s = constants characterizing transport of the complex and carrier

As figure 1:3 shows, the carrier mechanism relies on complexation of valinomycin with the cation, then migration through the interior of the lipid membrane to the opposite membrane / solution interface where the ion is released into solution. This carrier mechanism theory is held by Armstrong *et al.*[34-36], who suggested that the presence of almost immobile anions in the membrane contribute to the membrane transport phenomenon. Buck *et al.*[37] stated that so long as anionic sites are present, it is irrelevant that these sites are fixed or mobile.

Horvai *et al.*[38] also carried out experiments to observe the effects of anion salt additions on ion selective membranes. Addition of lipophilic anions, such as tetraphenyl borate to the membrane composition reduced interference by anions and decreased the specific resistance of the membrane. The lowest membrane resistance was observed when a 1:1 ratio of quaternary ammonium tetraphenyl borate: valinomycin was used, above a 1:1 ratio, no potassium ion selectivity was observed.

A recent review by Armstrong and Horvai [39] summarises the experimental work carried out in PVC valinomycin membranes, and gives guidelines as to suitable membrane compositions. If a 1:1 tetraphenylborate : valinomycin is exceeded, excess salt is spontaneously lost to the aqueous solution, thus explaining the loss of potassium selectivity. However, sufficient anionic salt must be taken to swamp variability due to impurities. These impurities are mainly sulphonate residues, the remains of PVC polymerisation, which are present in the membrane. The concentration of impurities in the membrane is 0.05 - 5 mM, typically, which can be determined chemically [40]. Originally in PVC valinomycin membranes, no anion salt was added, therefore pre-conditioning was required to allow ion exchange processes between the

sample solution and membrane to occur. Radio-tracer studies [41, 42] showed that the exchange selectivity constant, k, is in good agreement with the potential selectivity coefficient, K_{pot}, and this is also the case in the presence of anion salt with less than 1:1 salt : valinomycin ratio.

Thus, in liquid membranes, ion exchange processes occur as a result of a carrier mechanism. The ion of interest is exchanged at the membrane - solution interface to form a cation-ionophore complex. This is carried through the membrane via a rapid exchange process, before arriving at the second membrane-solution interface where it is lost from the membrane. Selectivity of the macrocyclic to a particular ion depends on the electronic and steric interaction of the ionophore and the ion; the free energy of the ligand-ion must be favourable compared with that of the solvent molecule-ion, and the cavity of the macrocyclic must be suitable for the size of the cation of interest.

1.3 Membrane Components.

Armstrong and Horvai's review [39] drew attention to variation in membrane behaviour when different manufacturers' PVC was used. This must be because of the different method e.g. photolytic, thermolytic or mediators used to induce polymerisation, which leads to different fixed (anion) sites in the membrane.

Arami [43] carried out studies to determine the optimum percentage of plasticizer necessary in ISE membranes. He found that without a plasticizer, membranes, not unexpectedly, were too brittle. Using greater than 70 % plasticizer, membranes were jelly-like and difficult to manipulate and with only 30 % plasticizer, sub-Nernstian membrane responses (47 mV dec^{-1}) were observed and the membranes did not respond to the primary ion in mixed ion solutions. The best Nernst slope and selectivity was observed for those membranes prepared with 60 - 70 % plasticizer. A study of PVC electrodes by Fiedler and Ruzicka [44] showed that electrodes will function only above the glass-transition

temperature, T_g, thus, the polymer must exist in a liquid-like state at room temperature; hence the necessity of use a suitable plasticizer such as dioctyl sebacate (DOS).

A new support material for liquid membrane ion selective electrodes has been proposed by Wotring *et al.* [45], poly (vinyl diene) chloride (PVDC) which is similar in structure to PVC but has a lower T_g, removing the need for a plasticizer. As leaching of plasticizer is a common source of electrode failure [46, 47], and since PVDC does not require a mediator (plasticizer) [48-50] or have a high resistance, as silicone rubber[51], this, or similar materials, should be considered as important developments in the production of long-life membranes. The only drawback of PVDC is its photosensitivity; these electrodes should be stored in air, protected from light.

In analyses of body fluids, serum, plasma and urine which have a high lipophilicity, will favourably extract non-lipophilic membrane components, leading to depletion of membrane constituents on the sample side of the membrane [52]. Lipophilicity of the membrane appears to be the factor most affecting membrane lifetimes; on replacing DOS with a highly lipophilic plasticizer, such as ETH-2041, greatly improved membrane lifetime and stability was observed [53, 54]. Oesch *et al.* [55] recommended that the lipophilicity term, lg P, of the plasticizer be at least 12.8 for ISEs used in clinical applications (lg P for DOS is 10.2). P is the partition coefficient of the component between 1-octanol and water [56] determined in the standard manner using thin layer chromotography with reversed-phase silica plates[57]. ETH-2041 is a tetra carboxylated benzophenone, tetra-n-undecyl 3,3',4,4'-benzophenone tetracarboxylate (figure 1:4), which has long alkyl chains giving rise to lipophilic character.

In addition, ionophores should also be lipophilic for devices to be used for analyses in body fluids. Grehrig *et al.*[58] announced the

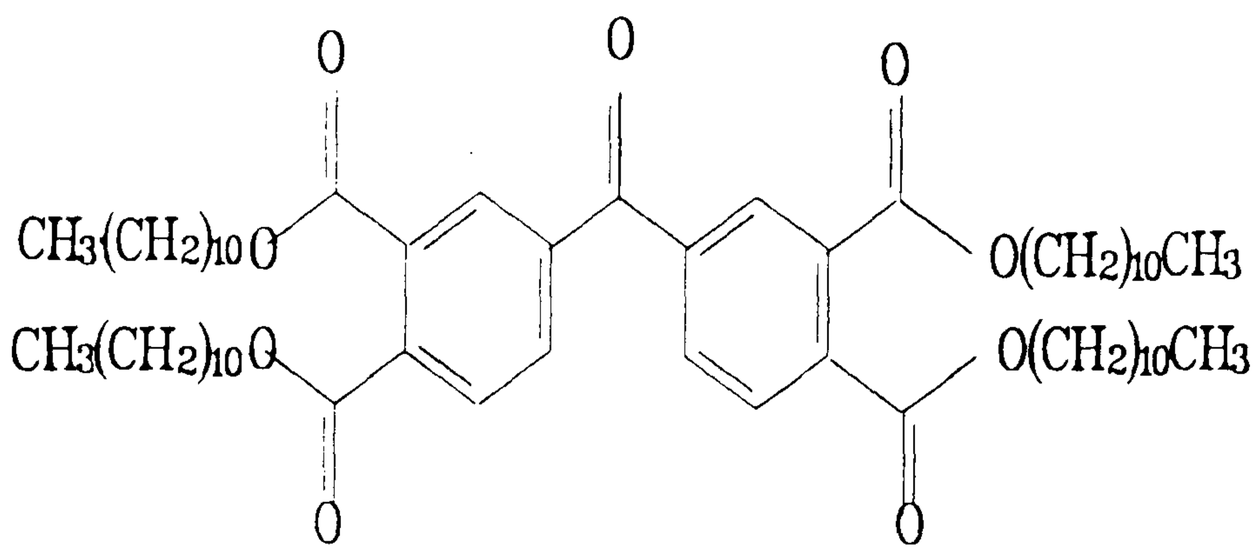

Figure 1:4 Structure of ETH 2041

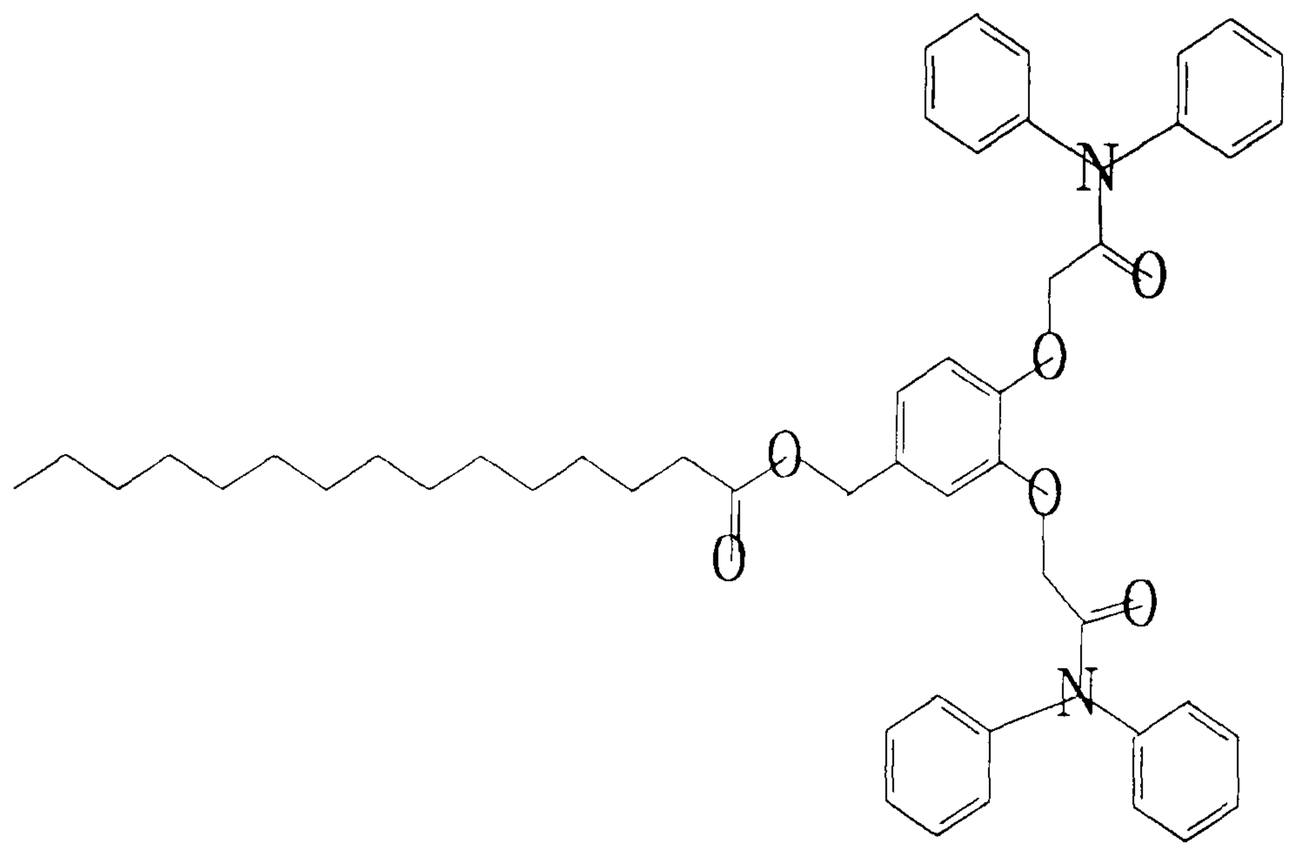

Figure 1:5 Structure of ETH 4120

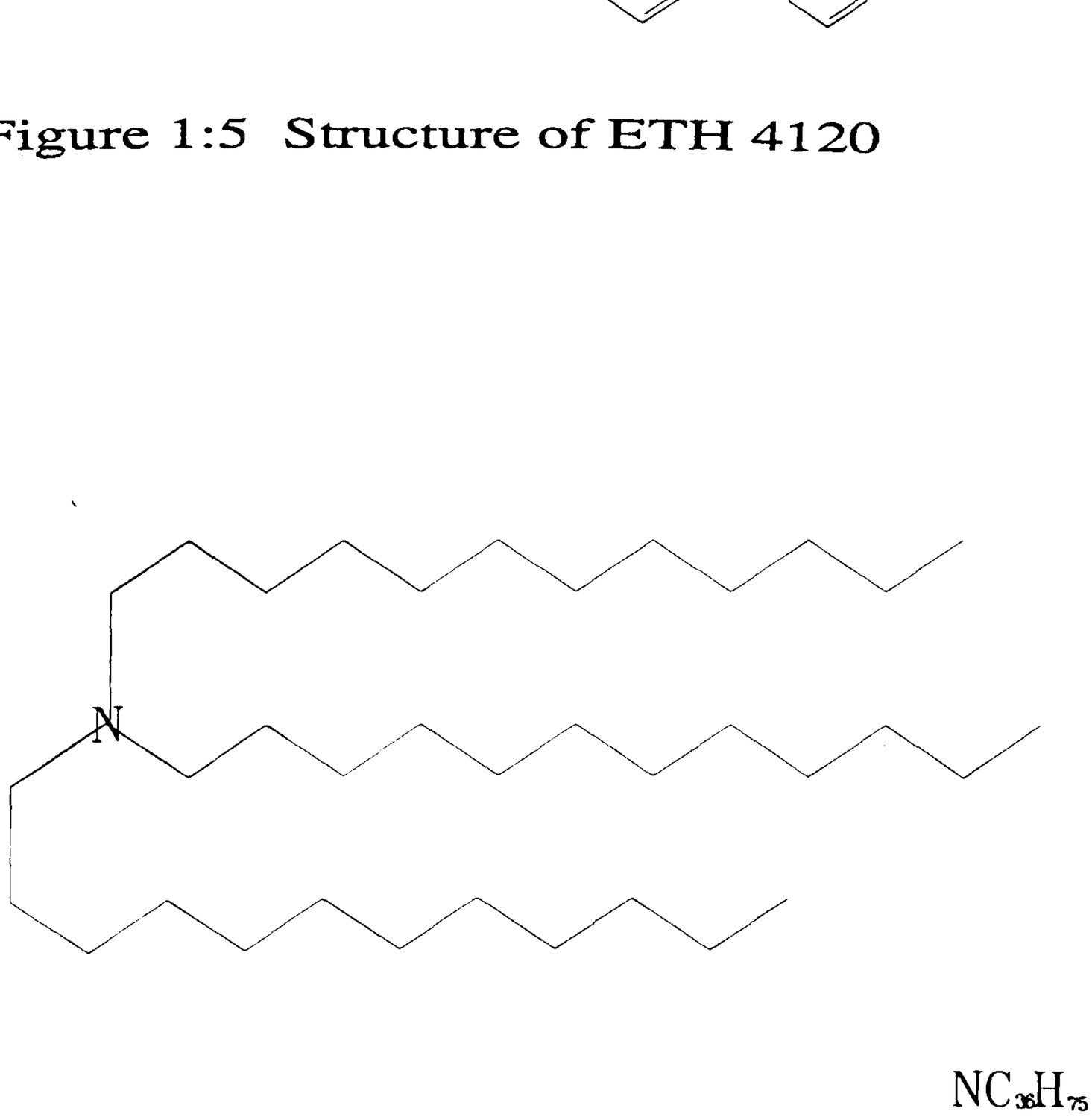

Figure 1:6 Structure of TDDA

discovery of a highly lipophilic sodium selective ionophore, ETH-4120. They stated[58] that lg P must be greater than 15 for the ionophore if the membrane is to be deposited on field effect transistors (FETs). This ionophore, 2, 2',4 -octadecanoyloxymethyl - 1, 2 - phenylenedioxy - N, N, N', N' - tetracyclohexyldiacetamide ($C_{53}H_{88}N_2O_6$) (figure 1:5) was found to be exremely stable and to give membranes with lifetimes of 7 x 10^4 h.

Work here in Newcastle (see Chapter 4.6) used a lipophilic pH sensitive ionophore, tridodecylamine, TDDA (figure 1:6) [59, 60]. As well as high lipophilicity, TDDA has high viscosity and reduced migration with good adhesion to PVC, making it particularly suitable for use with ISFETs.

1.4 Transfer Processes Occurring in Glass Electrodes.

The chief glass forming oxides are SiO_2, B_2O_3, P_2O_5, GeO_2 [61]. Of these, however, only the silicates are sufficiently chemically durable for use in glass electrodes and therefore all glasses used in commercially available glass electrode manufacture contain at least 50% SiO_2 [61].

Silicate glasses exist as random 3D networks [62] as a series of tetrahedral units in which a silicon atom is surrounded by four O atoms, one at each vertice (figure 1:7). Each SiO_2 unit is known as a network former and each alkali oxide as a network modifier. Ion exchange processes occur at the glass surface[63] and it is the presence of these modifiers which allows ion exchange processes to occur. Correctly, glass is never an electrode, but an electrolyte behaving as a barrier between two solutions.

A defect diffusion mechanism is most likely in glasses, as is the case in other solids. The nature of the defect is unknown, but probably due to the mobile interstitial cation. Nicolsky [64, 65] proposed the General Ion Exchange Theory of the glass electrode which expands on the defect diffusion mechanism, taking into account diffusion and phase-boundary

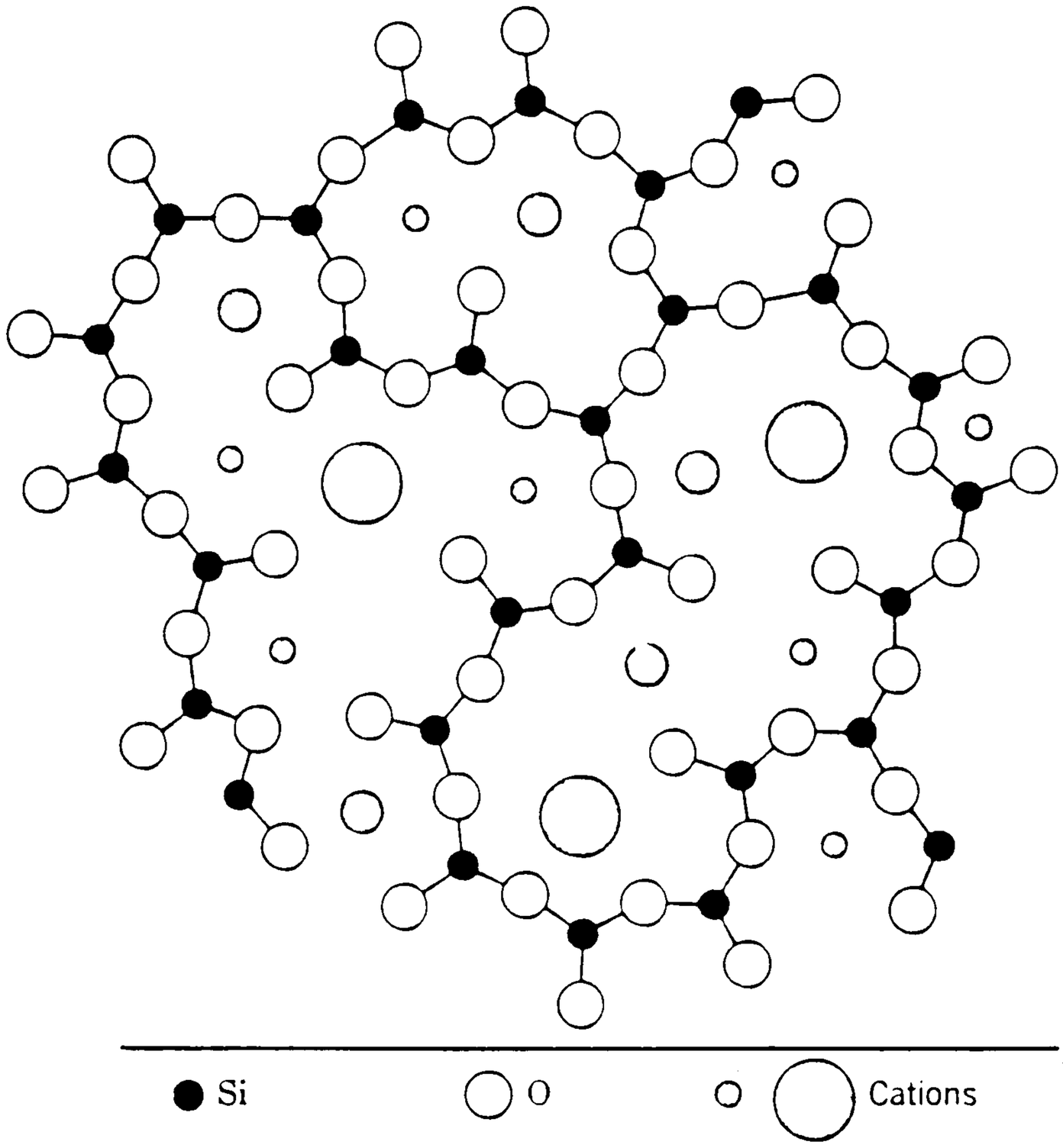

Figure 1:7 Random 3D Network of Silica Glass [62].

potentials. This theory is based on the heterogeneity of ionic bonds in the glass which allow replacement first of weakly bound hydrogen ions, then the more strongly bound protons so that H-M transitions occur, substituting hydrogen ions in the glass by metal ions of the sample solution.

The composition of a particular glass determines its selectivity e.g. NAS 11-18 containing 11% sodium, Na_2O and 18% aluminium, Al_2O_3, which is selective to sodium ions and NAS 27-06 / 27-08 containing 27% Na_2O and 6% / 8% Al_2O_3 which is selective towards to potassium ions. Hughes [66] stated that for good K^+ selective glass electrodes, no K_2O, Al_2O_3 or borates should be present in the glass. A review of glass compositions and their uses may be found elsewhere [67].

It is important that glass electrodes are preconditioned in aqueous solution prior to use. A hydrated layer of 50-1000 Å is formed as Si-O bonds are broken by -OH groups [68]. This layer must be sufficiently thick to prevent H^+ diffusing to the inner boundary layer as this would lead to variations of the potential with continued use. The presence of the hydrated layer increases cation mobility within the glass by *ca.* 10^3, thus improving the rate of ion exchange processes [69].

More detailed discussions of glass electrodes may be found elsewhere [61, 70, 71].

1.5 Classification of Electroactive Membranes.

The materials already described, macrocycles, glass etc. have been classified into three major groups. Membranes formed from these compounds should be able to differentiate amongst ionic species and preferentially respond to only one. Electroactive materials should be relatively insoluble in the sample solution and must, at ambient temperature, be able to conduct electricity by ionic, electronic or defect mechanism and set up (rapidly) an exchange equilibrium or ion exchange process when placed in an electrolyte solution containing the ions of

interest.

1. Glass; the composition of the glass, based on a 3-dimensional SiO_4 network, determines the selectivity. Interstitial ions e.g. Na^+, Ba^{2+}, Cs^+ held by electrostatic fields of neighbouring oxygen atoms can occupy the lattice and affect the selectivity of the electrode [61].

2. Insoluble inorganic salts; e.g.Ag_2S, LaF_3 doped with Eu^{2+}. These reagents must, however, be insoluble above 10^{-6} mol dm^{-3}. Compacted discs and single crystals give better performance than dispersed reagent materials.

3. Long chain ion exchange materials and chelating agents; e.g. alkyl phosphate salts, ring substituted salicylates. These may be charged species, or neutral, and are usually dissolved in plasticized organic polymers of low dielectric constant and high boiling point e.g. poly(vinyl) chloride.

1.6 Ion Selective Devices.

Ion selective electrodes (ISEs) and ion sensitive field effect transistors (ISFETs) are typical direct electrochemical sensors; the activity of the ion (to which the sensor is selectively responsive) is related to a voltage reading on a digital voltmeter. From the Nernst equation,

$$E = \text{constant} \pm (k/z_i) \log a_i \qquad (1.3)$$

where k = the theoretical slope factor (RT/F)ln 10

a_i= the activity of ion i with charge z_i

z_i is positive when ion "i" is a cation and negative if "i" is an anion.

A calibration curve, plotted of voltage *versus* the negative log of activity of concentration for two or more standards, can then be used to determine the activity of the analyte in the sample.

1.7 Classification of Ion Selective Electrodes. [72]

1.7.1. Primary Electrodes.

In homogeneous membranes the active material is in the solid state, either fused and formed, or pressed and machined into pellets or discs e.g. Ag_2S-AgI membranes, polycrystalline halide membranes, or, as in the case of LaF_3 for fluoride determination, a single crystal. For heterogeneous membranes, similar active materials to the homogeneous membranes are used, but now the electroactive material is dispersed by mixing with an inert matrix e.g. hydrophobised carbon, silicone rubber.

Electrodes may be either non-crystalline or crystalline electrodes. In non-crystalline electrodes, the membranes may be liquid, e.g. poly (vinyl) chloride support with charged or uncharged mobile carriers, or of glass with a rigid, fixed site membrane [73].

1.7.2 Sensitized Electrodes.

Gas sensing probes [74] and enzyme electrodes [75-77] are special classes of electrodes and were not used in this work. The former consists of an ISE and suitable reference electrode within the same assembly to form an electrochemical cell, which responds indirectly to the analyte. Similarly, the enzyme electrode is based on a suitably chosen ISE which responds to the product of a reaction involving an immobilized enzyme or substrate.

1:8 Objectives of this Work.

A wide range of applications exists for ISEs and ISFETs and the aim of this work was to show the capability of these devices. In direct potentiometry, the devices respond directly to the ion of interest, the concentration of which may be obtained from a simple pre-determined calibration curve.

Devices may also be used to follow titrations, more specifically auto-titrations. Chapter 4 discusses the experimental requirements of an auto-titrimetric system and describes the development of a volumetric and

coulometric sensor-actuator titration set-up using ISEs as the sensors. As ISEs and ISFETs are well characterised over a large concentration range, very accurate equivalence point determinations can be obtained. In Chapter 5, this property was fully exploited in the re-determination of pK^d_2 for sulphide ions. This value is particularly important in environmental applications; monitoring sulphide emissions and following bacterial activity in lakes.

Chapters 6 and 7 show how electrochemical methods described may be implemented in clinical and industrial work, respectively.

References.

1. Thomson W.
Proc. Roy. Soc. 1875, **A23**, 463,

2. Cremer M.
Z. Biol. 1906, **47**, 562

3. Haber F. & Klemensiewicz Z.
Z. Phsik. Chem. 1909, **67**, 385

4. Hughes W.S.
J. Am. Chem. Soc. 1922, **44**, 2860

5. Horovitz K.
Z.Physik 1923, **115**, 369

6. Horovitz K.
Z. Physik Chem. 1925, **115**, 424

7. Schiller H.
Ann, Physik 1924, **74**, 105

8. Lengyel B. & Blum E.
Trans. Faraday Soc. 1934, **30**, 461

9. Tendeloo H.J.C.
J. Biol. Chem. 1936, **113**, 333

10. Kolthoff H.J.C. & Sanders H.L.
J. Am. Chem. Soc. 1937, **59**, 416

11. Tendeloo H.J.C. & Krips A.
Recl. Trav. Chim. Pays-Bas Belg. 1957, **76**, 703, 946

12. Pungor E. & Hollos-Rokosinyi E.
Acta Chem. Hung. 1961, **27**, 63

13. Covington A.K.
CRC Critical Review in Chemistry, 1974
Ion Selective Electrodes

14. Frant M.S. & Ross J.W.
Science 1966, **154**, 1553

15. Ross J.W.
Science 1967, **156**, 1378

16. Moore C. & Pressman B.C.
Biochem. Biophys. Res. Commun. 1967, **71**, 3862

17. Pederson C.J.
J. Am. Chem. Soc. 1967, **89**, 7017

18. Ammann D., Pretsch E. & Simon W.
Anal. Lett. 1974, **7**, 23

19. Ammann D., Lanter F., Steiner R.A., Schulthess P., Shijo Y. & Simon W.
Anal. Chem. 1981, **53** 2267

20. Ammann D., Morf W.E. Anker P., Meier P.C., Pretsch E. & Simon W.
Ion. Sel. Elec. Rev. 1983, **5**, 3

21. Oesch U., Malinowska E. & Simon W.
Anal. Chem. 1987, **53**, 213

22. "Analysis with Ion Selective Electrodes"
Bailey P.L.
Heyden & Sons Ltd., 1976

23. "Analysis with Ion Selective Electrodes"
Veseley J., Weiss D. & Stulik K.
Ellis Horwood, Chichester 1978

24. "Ion Selective Electrodes"
Koryta K. & Stulik K.
2nd ed. Cambridge University Press, London 1983

25. "Ion Selective Electrodes"
Koryta J.
Cambridge Monographs in Physical Chemistry, 2
Cambridge University Press, London 1975

26. Brockmann H. & Schmidt-Kastner G.
Chem. Ber. 1955, **88**, 57

27. Brockmann H., Springorum M., Traxler G. & Hofer I.
Naturwiss 1963, **50**, 689

28. Shemyakin M.M., Aldanova N.A., Vinogradova E.I. & Feigina M.Yu
Tetrahedron Lett. 1963, 1921

29. Pioda L.A.R. & Simon W.
Chimia 1969, **23**, 72

30. Duax W.L., Hauptman H., Weeks C.M. & Norton D.A.
Science N.Y. 1972, **176**, 911

31. Funck T., Eggers F. & Grell E.
Chimia 1972, **26**, 637

32. Stefanac Z. & Simon W.
Mikrochem. J. 1967, **12**, 125

33. Wipf H.K., Oliver A. & Simon W.
Helv. Chim. Acta 1970, **53**, 1605

34. Armstrong R.D., Covington A.K., Evans G.P. & Handyside T.
Electrochimica Acta 1984, **29**, 1127

35. Armstrong R.D., Lockhart J.C. & Todd M.
Electrochimica Acta 1986, **001**, 31

36. Armstrong R.D. & Todd M.
Electrochimica Acta 1988, **31**, 31.

37. Buck R.P., Toth K., Gray E., Horvai G. & Pungor E.
J. Electroanal. Chem. 1987, **223**, 51

38. Horvai G., Graf E., Toth K., Pungor E. & Buck R.P.
Anal. Chem. 1986, **58**, 2735,

39. Armstrong R.D. & Horvai G.
Electrochimica Acta 1990, **35**, 1

40. Lindner E., Graf E., Niegreisz Z., Toth K., Pungor E. & Buck R.P.
Anal. Chem. 1988, **60**, 295

41. Horvai G., Graf E., Toth K., Pungor E. & Buck R.P.
Anal. Chem. 1986, **58**, 2741

42. Horvai G., Horvath V., Farbas A. & Pungor E.
In press, Talanta

43. Arami M.
Ph.D. Thesis, University of Newcastle-upon-Tyne, 1988

44. Fiedler U. & Ruzicka J.
Anal. Chim. Acta 1973, **67**, 179

45. Wotring V.J., Prince P.K. & Bachas L.G.
Analyst 1991, **116**, 581

46. Lawton R.S. & Yacynych A.M.
Anal. Chim. Acta 1984, **160**, 149

47. Ebdon L., Ellis A.T. & Corfield G.C.
Analyst 1979, **104**, 730

48. LeBlanc O.H. & Grubb W.T.
Anal. Chem. 1976, **48**, 1658

49. Martin C.R. & Freiser H.
Anal. Chem. 1981, **53**, 902

50. Heineman W.R., Wieck H.J. & Yacynych A.M.
Anal. Chem. 1980, **52**, 345

51. Pick J., Toth K., Pungor E., Vasak M. & Simon W.
Anal. Chim. Acta 1973, **64**, 477

52. Oesch U., Ammann D. & Simon W.
Clin. Chem. 1986, **348**, 1448

53. Ammann D., Anker P., Metzger E., Oesch U. & Simon W.
"Ion Measurements in Physiology and Medicine"
ed. Kessler M. *et al.*
Springer-Verlag, Berlin, Heidelberg 1985, pp.102

54. Oesch U., Dinten O., Ammann D. & Simon W.
ref. 53, pp.81

55. Oesch U., Anker P., Ammann D. & Simon W.
In "Ion Selective Electrodes"
ed. Pungor E. & Buzas I.
Akademia Kiado, Budapest 1985, pp. 81

56. Oesch U., Xu A., Brzozka Z., Suter G. & Simon W.
Chimia 1986, **40**, 351

57. Oesch U., Brzozka Z., Xu A., Rusterholz B., Suter G., Pham H.V., Welti D.H., Ammann D., Pretsch E. & Simon W.
Anal. Chem. 1986, **58**, 2285

58. Grehrig G., Rusterholz B. & Simon W.
Anal. Chim. Acta 1990, **233**, 295

59. Oesch U. & Simon W.
"Opportunities of Planar Ion Selective Electrode Membrane Technology"
Transducers 1987, 4th International Conference on Solid State Sensors & Actuators

60. Schulthess P., Shijo E., Pham H.V., Pretsch E., Ammann D., & Simon W.
Anal. Chim. Acta 1981, **181**, 111

61. Isard O.J.
In "Glass Electrodes for Hydrogen and other Cations"
ed. Eisenman G.
Marcel Dekker Inc., New York, 1967
Chap. 3, pp.51

62. Zachariasen W.H.
J. Am. Chem. Soc. 1932, **54**, 3841

63. Nicolsky B.P.
Acta Physicochem. USSR 1937, **1**, 597

64. Nicolsky B.P.
Zh. Fiz. Khim. 1937, **10**, 495

65. Nicolsky B.P.
Zh. Fiz. Khim. 1953, **27**, 724

66. Hughes W.S.
J. Chem. Soc. 1928, pp.491

67. Rechnitz G.A.
Chem. Eng. News 1967, **45**, no. 25, 146

68. Doremus R.H.
Chap. 4, pp.130 of ref. 59

69. Schwabe K. & Suschke H.D.
Angew. Chem. Internat. 1964, **3**, 36
cited in ref. 25, Chap 5

70. "The Glass Electrode"
Dole M.
Wiley, New York 1941

71. "The Glass Electrode"
Eisenman G., Bates R.G., Mattock G. & Friedman S.M.
Wiley Interscience, New York 1966

72. Recommendations for Nomenclature of Ion Selective Electrodes
Pure & Appl. Chem. 1976, **48**, 129

73. Severinghaus J.W. & Bradley A.F.

J. Appl. Pysiol. 1958, **13**, 515

74. Bailey P.L. & Riley M.
Analyst 1975, **100**, 145

75. Clark L.C. & Lyons C.
Ann. N.Y. Acad. Sci. 1962, **102**, 29

76. Hansen E.H. & Ruzicka J.
Anal. Chim. Acta 1974, **72**, 353

77. Guilbault G.G. & Montalvo J.G.
J. Amer. Chem. Soc. 1970, **92**, 2533

CHAPTER TWO

DESCRIPTION OF ION SELECTIVE DEVICES

2.1 Introduction.

A sensor is a device which converts a physical or chemical signal into an optical or electrical form.

Ion selective electrodes (ISEs) and ion sensitive field effect transistors (ISFETs) are typical direct electrochemical sensors which as shown in Chapter 1 respond in accordance with the Nernst equation.

2.2 Cell Design.

The potential of a single electrode cannot be measured, therefore one must consider not the ISE potential, but the potential difference of a cell containing the reference electrode, sample and ISE.

The general electrochemical cell scheme is shown below

Reference Electrode || Sample Solution | ISE

A schematic diagram of the set up is shown in figure 2:1.

2.3 Ion Selective Electrodes.

2.3.1 Electrode Construction.

The construction of an ISE depends on the membrane active material and the use of the electrode e.g. clinical, industrial or fieldwork. A wide range of commercial ISEs is available and several models, specific to different ions, e.g. hydrogen, sulphide were used in this work. These are described in detail where appropriate.

Home made, plasticized PVC electrodes selective to potassium and pH were also used. The potassium electrodes all accomodated a valinomycin ionophore based membrane whereas several different membrane components were used for pH sensing.

Home made electrodes were fabricated in a similar manner to that described by Griffiths, Moody and Thomas [1]. Accurately weighed high molecular weight poly(vinyl chloride) (PVC), plasticizer e.g. dioctyl sebacate (DOS) ionophore and lipophilic anionic salt e.g. potassium tetrachlorophenyl borate were dissolved in freshly distilled tetrahydrofuran (THF) (see Appendix A(i) for details of this distillation).

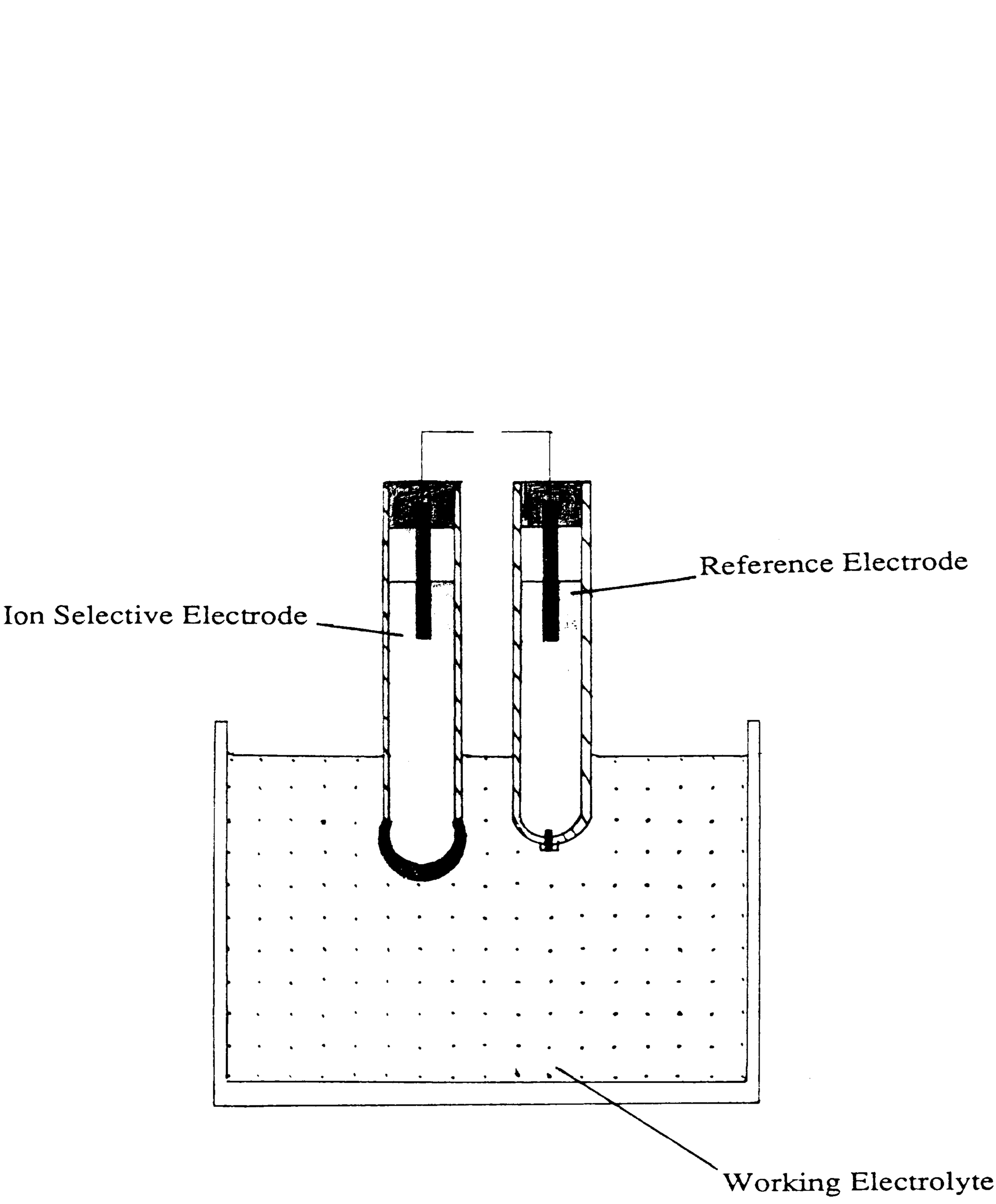

Figure 2:1 Construction of a Two Electrode Electrochemical Cell

In general, 33 wt% PVC, 66 wt% plasticizer and 1 wt% ionophore were used. Minute quantities of salt were taken, *ca*. one tenth of the mass of ionophore used. The mixture was shaken for a minimum of 12 h on a mechanical shaker, (Junka & Kunkel, Ika., Vibrax VXR, supplied by S.H. Scientific, Blyth, Northumberland), before casting the membrane, by pipette to ensure no air bubbles were introduced at this stage, in to a circular PTFE, mould. The diameter of moulds used was chosen such that the thickness of the resulting membrane was *ca*. 1 mm. The THF solvent was allowed to evaporate slowly, taking, approximately, 48 h, after which the PVC membrane was transferred from the mould using tweezers to a PTFE cutting plate where circular membrane discs of *ca*. 8 mm diameter were cut.

The electrode body consisted of a 6 mm glass tube with B9 Quickfit socket. A 3 cm section of 6 mm internal diameter PVC tubing was fixed to the glass tube using PVC cement, formed from PVC granules and THF. The end of the PVC tubing was made even by dipping the tube in THF and rotating the electrode body on a tile. This ensured a flat surface to which the membrane could be adhered. The membrane was attached to the PVC tube using PVC cement and then allowed to dry for 30 min. The seal of the electrode was tested by blowing gently down the electrode body whilst the membrane was dipped in water. If the membrane seal was not airtight, then the membrane was removed, the PVC tube cleaned and the membrane re-fixed before repeating the procedure.

An internal filling solution, containing the species of interest, two-thirds filled the assembly, and an internal silver / silver chloride reference electrode (see section 2.3.2) with B9 cone placed in the electrode body (figure 2:2). The electrode was allowed to condition by dipping the membrane in a solution containing 10^{-2} mol dm^{-3} of the ion to be sensed for 12 h.

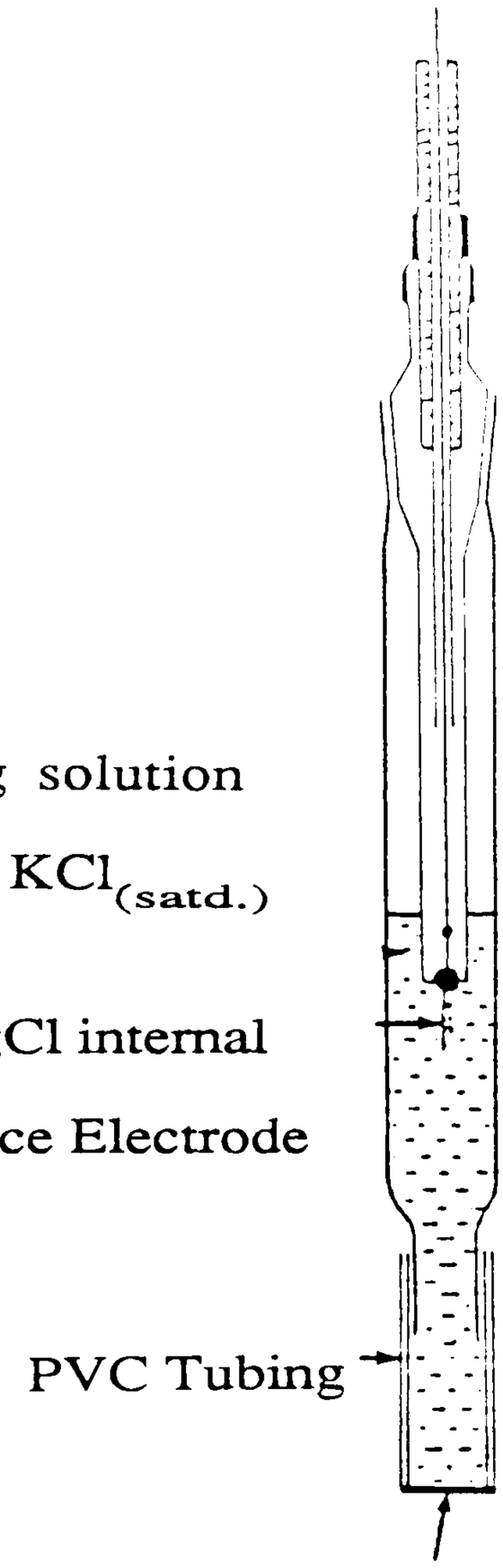

Figure 2:2 Diagram of a Home made PVC Potassium Selective Electrode.

2.3.2 Reference Electrodes [2].

The half cell potential of one electrode, the (external) reference electrode, must be stable and completely insensitive to the species under test. Moreover, it should be possible to prepare easily and reproducibly this electrode and it should be usable over a wide range of conditions. The internal reference electrode provides a stable electrical connection to the inner reference solution and thus to the bulk of the electroactive material.

The most commonly used reference electrodes are the calomel and the silver / silver chloride electrodes both of which are prone to interference by sulphide, iodide and bromide ions. For accurate work, bromide should not exceed 0.005 mol % [3]. The calomel electrode is also affected by the presence of hydroxide ions, as is silver / silver chloride at pH > 10. A drift in the observed response combined with an increase in the resistance of the electrode is normally indicative of interference.

a) Calomel Electrode.

This may be represented by

$$Hg / Hg_2Cl_2 / KCl$$

for which the cell reaction is

$$2\,Hg + 2\,Cl^- \longrightarrow Hg_2Cl_2 + 2\,e^- \qquad (2.1)$$

A saturated potassium chloride solution is normally used and the electrode is referred to as a saturated calomel electrode, SCE. This has a standard potential of +0.244 V at 25 °C [4] and a temperature coefficient of -0.67 mV K^{-1}.

A pool of mercury covered by a layer of calomel (Hg_2Cl_2) is in contact with a reference solution containing chloride ions (usually potassium chloride) and saturated with calomel (figure 2:3). The preparation of calomel electrodes is well documented elsewhere [6]. Calomel electrodes, however, are not stable when miniaturised, currents of

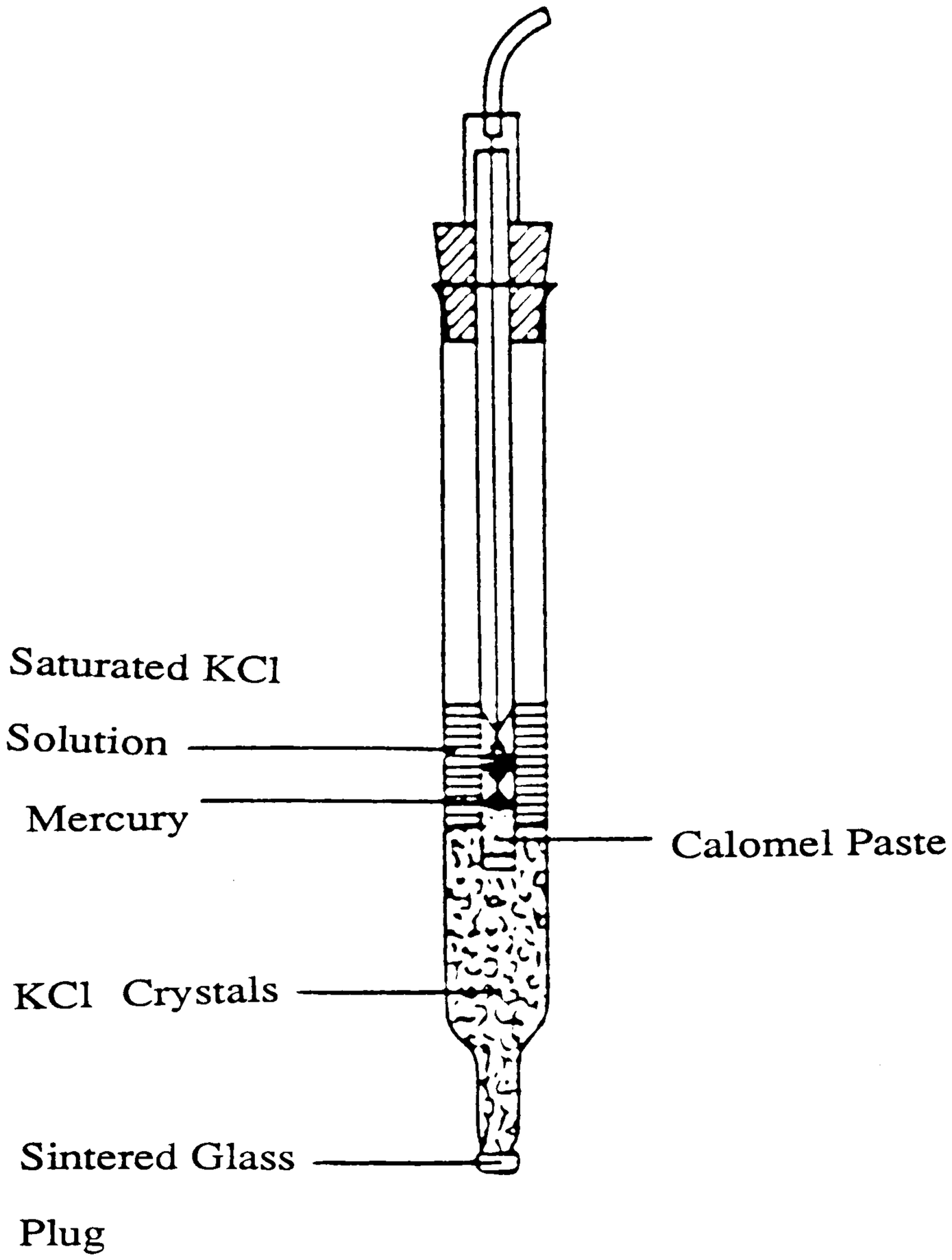

Figure 2:3 Diagram of a Calomel Reference Electrode.

less than 0.5 μA are sufficient to polarise the electrode [6].

b) Silver / Silver Chloride Electrode.

This may be represented by

$$Ag / AgCl / KCl$$

and the half cell reaction as

$$Ag_{(s)} + Cl^- \longrightarrow AgCl + e^- \qquad (2.2)$$

The standard potential of a 3.5 mol dm^{-3} potassium chloride silver / silver chloride electrode is +0.205 V [4] at 25 °C with a temperature coefficient of - 0.73 mV K^{-1}. In its simplest form, this electrode consists of a silver wire or plate coated with silver chloride and in contact with a solution containing chloride ions. It is often used as an internal reference electrode in pH electrodes and ISEs, and in the analysis of foodstuffs as there are no highly toxic chemicals released on damage to the electrode, unlike the calomel and thallium based electrodes. It is more rugged than the calomel electrode and is easy to miniaturise, therefore, it is used extensively in biological applications.

c) Preparation of Thermal Electrolytic Silver / Silver Chloride Electrodes.

For each electrode, a ca. 40 mm strip of platinum wire, fused to a glass tube (100 mm length x 5 mm diameter), was cleaned using

i) concentrated nitric acid

ii) distilled water

iii) acetone

The platinum was then coiled into a small, compact helix and coated with a thin layer of silver oxide and placed in a pre-heated furnace at 450 °C for 40 min. This procedure was repeated three times, allowing the electrode to cool to room temperature between coats, thereby reducing the likelihood of cracks in the silver coating.

The electrodes were chloridised by anodising against a platinum foil cathode of 10 mA for 7-8 min for one electrode (or 12 mA for 8 min for

two electrodes, connected in parallel).

To reduce the bias potential, the completed Ag/AgCl electrodes were placed overnight in 0.05 mol dm^{-3} hydrochloric acid. The potentials of the batch bias potentials were then intercompared and individual electrodes differing from the average potential of the group by > 0.1 mV discarded. Insufficient washing of silver oxide during preparation (see Appendix A(ii)) may lead to a slow electrode response and a high bias potential. This can often be remedied by heating the electrode for 2 h in distilled water at 50 to 60°C.

So, the ISE comprises of an internal reference electrode, Ag/AgCl, internal reference solution, usually KCl for a K^+ selective electrode, and electroactive membrane. The internal reference solution is used to establish a constant potential at the inner surface of the electroactive material and the electrode assembly and also to act as a cation source to saturate the electroactive material with the ion of interest [7].

2.4 Ion Sensitive Field Effect Transistors (ISFETs).

2.4.1 Introduction.

These have developed from ion selective electrodes and solid state integrated circuits, FETs. ISFETs were first reported by Bergveld in 1970 in a short communication [8] and more fully in 1972 [9]. Whilst investigating the use of FETs for determining action potentials in nerve fibres, Bergveld observed response changes to hydrogen ion concentration. A brief discussion is given here of the theory of metal-oxide-semiconductor field effect transistors (MOSFETs) also known as insulated gate field effect transistors (IGFETs), necessary to understand the fundamental ISFET principles.

2.4.2 Insulated Gate Field Effect Transistors (IGFETS).

In a glass ISE, the glass membrane comprising of SiO_2, CaO, Li_2O, typically, is responsible for hydrogen selectivity [10]. By comparison, it is the SiO_2 insulator surface of a FET which responds to pH changes [11].

For an n-type IGFET, the bulk material of the device is lightly doped p-type silicon. Heavily doped n-type silicon (using an arsenic implant) forms the source and drain regions; a cross section of a device is shown in figure 2:4. A thin layer of silicon dioxide lies between the 2 'n' type regions acting as a dielectric between the substrate and an aluminium electrode; this region is known as the **gate.**

If a voltage, V_G, is applied to the gate, positive with respect to the source, then holes are repelled and electrons attracted to the surface, forming an electron conduction layer, or channel, under the gate insulator between the drain and source. As the gate voltage is increased, then the electron density in the conducting layer increases. If a voltage is applied between the source and drain, V_D, then a current, I_D, will flow between the two 'n' regions. The magnitude of this drain current is controlled by V_G, responsible for the electron density in the channel.

Using the site dissociation model [12,13], this selectivity is thought to arise from the equilibrium between surface hydroxyl groups and hydrogen ions in the sample solution. Selectivity to other ions can then be induced by setting down membranes (similar to those for ISEs) over the insulator [14,15]; the device is then referred to as an ISFET.

2.4.3 Charge Distribution State of the IGFET.

Depending on the sign and magnitude of V_G, three different states of charge distribution are possible; inversion, enhancement and depletion.

a) Threshold Voltage and Inversion Layer [16-18].

If the gate voltage applied is sufficiently positive with respect to the bulk, the electron density exceeds the hole density at the semi-conductor surface and an "n-type" inversion is said to have occurred. When this applied voltage is just large enough to bring about inversion, it is defined as the threshold voltage, V_T. This is because a fixed positive charge exists in the oxide even when $V_G = 0$. In order to remove the conductive band, it is necessary to apply a negative potential to the gate.

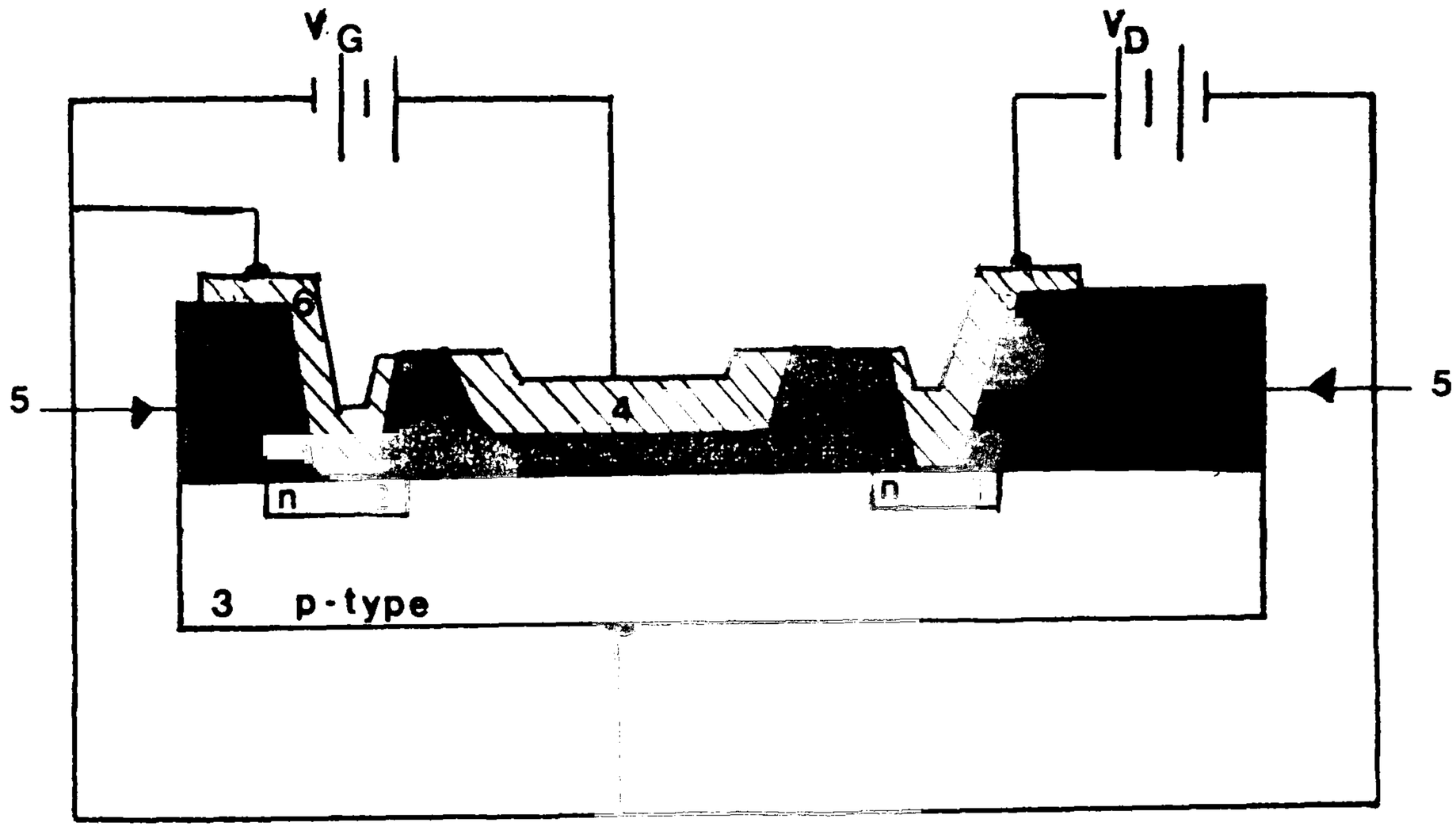

Figure 2:4 Cross Section of an IGFET

1. Drain; heavily-doped n-type.
2. Source; heavily-doped p-type.
3. Lightly-doped p-type silicon substrate.
4. Gate (or in an ISFET, electroactive thin film).
5. Insulator (SiO_2 / Si_3N_4).
6. Metal Contacts.

Beyond V_T, the electron density is controlled by the gate voltage, V_G, and it is this inversion layer which carries the drain-to-source current, I_D. The magnitude of I_D is thus controlled by the electrical resistance of the surface inversion layer and the drain voltage (figure 2:5 a).

b) Enhancement and Depletion Modes.

The enhancement state is produced by an accumulation of positive mobile charge carriers, holes, at the semi-conductor insulator interface, widening the space charge region.

In the depletion mode, the applied positive gate voltage drives the holes away from the surface thus inducing an "n-type" channel to form. The thickness of this layer is dependent on the strength of the field and the characteristics of the doped semi-conductor. The gate voltage may be reduced below zero and this channel isolated. IGFET and ISFET devices are normally depletion devices, an enhancement device requires a positive bias to bring about inversion of the semi-conductor surface (figure 2:5).

c) Saturated and Unsaturated Mode.

When the source and bulk of a semi-conductor are earthed and a positive bias is applied to the drain, a source-to-drain current flows. If the gate voltage is kept constant and the drain voltage increased, the inversion layer decreases until the threshold voltage, V_T, is reached and the device is said to be "saturated". The drain voltage at which the channel just disappears is $V_{D(SAT)}$. Current will flow beyond $V_{D(SAT)}$ but is now due to electrons flowing in the inversion layer and is thus independent of the gate voltage (figure 2:6). In the "saturated" region the drain-to-source voltage, $V_{D,}$ is large with respect to $(V_G - V_T)$ and the drain-to-source current, I_D, is, as shown by Grove [19], expressed as

$$I_D = \mu_n C_O W / L \, [(V_G - V_T) V_D - (V_D)^2 / 2] \quad (2.3)$$

where μ_n = surface carrier mobility

C_o = gate capacitance per unit area

Figure 2:5 Energy Bands in p-type MIS under Various Band Conditions.

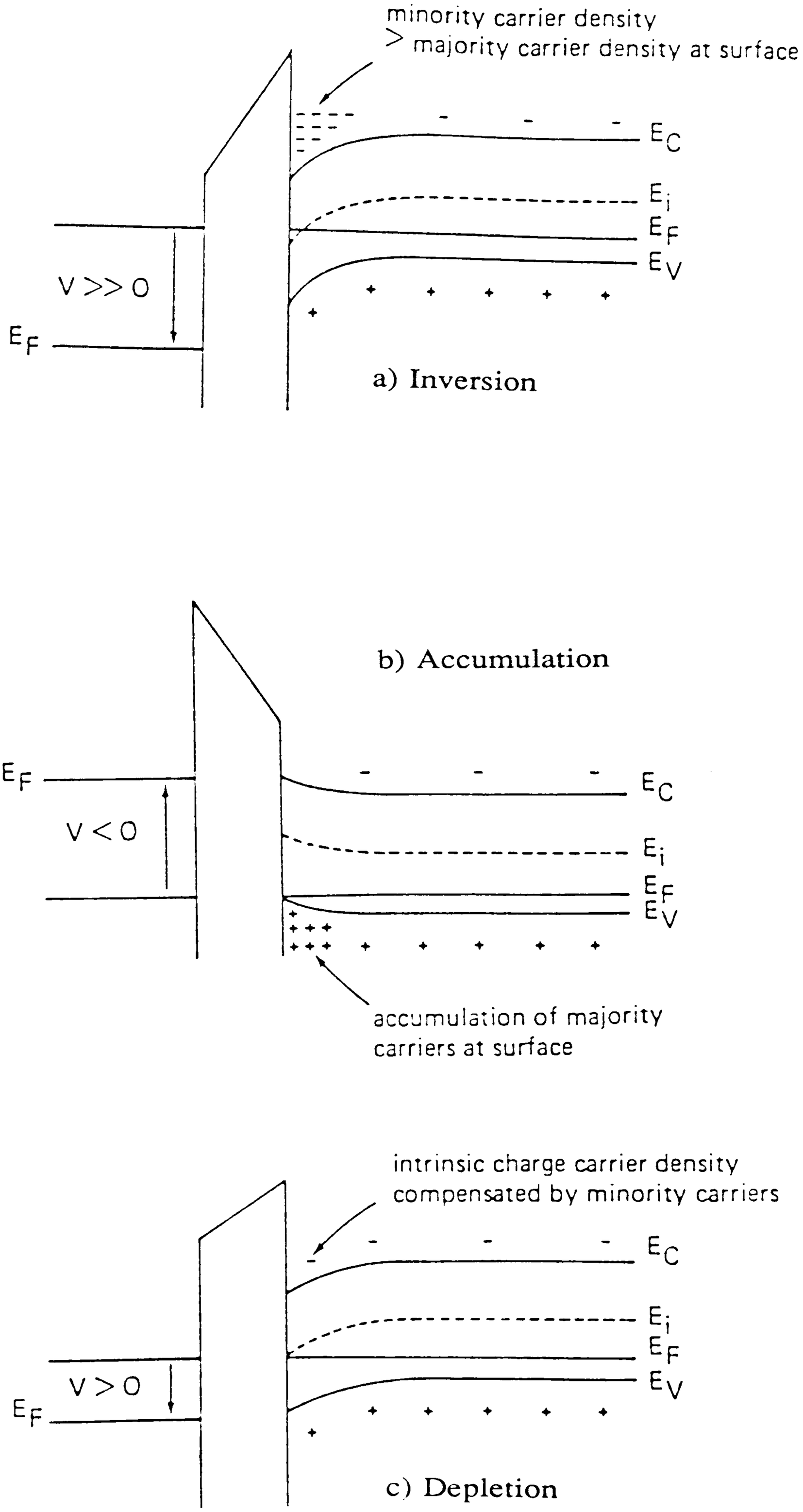

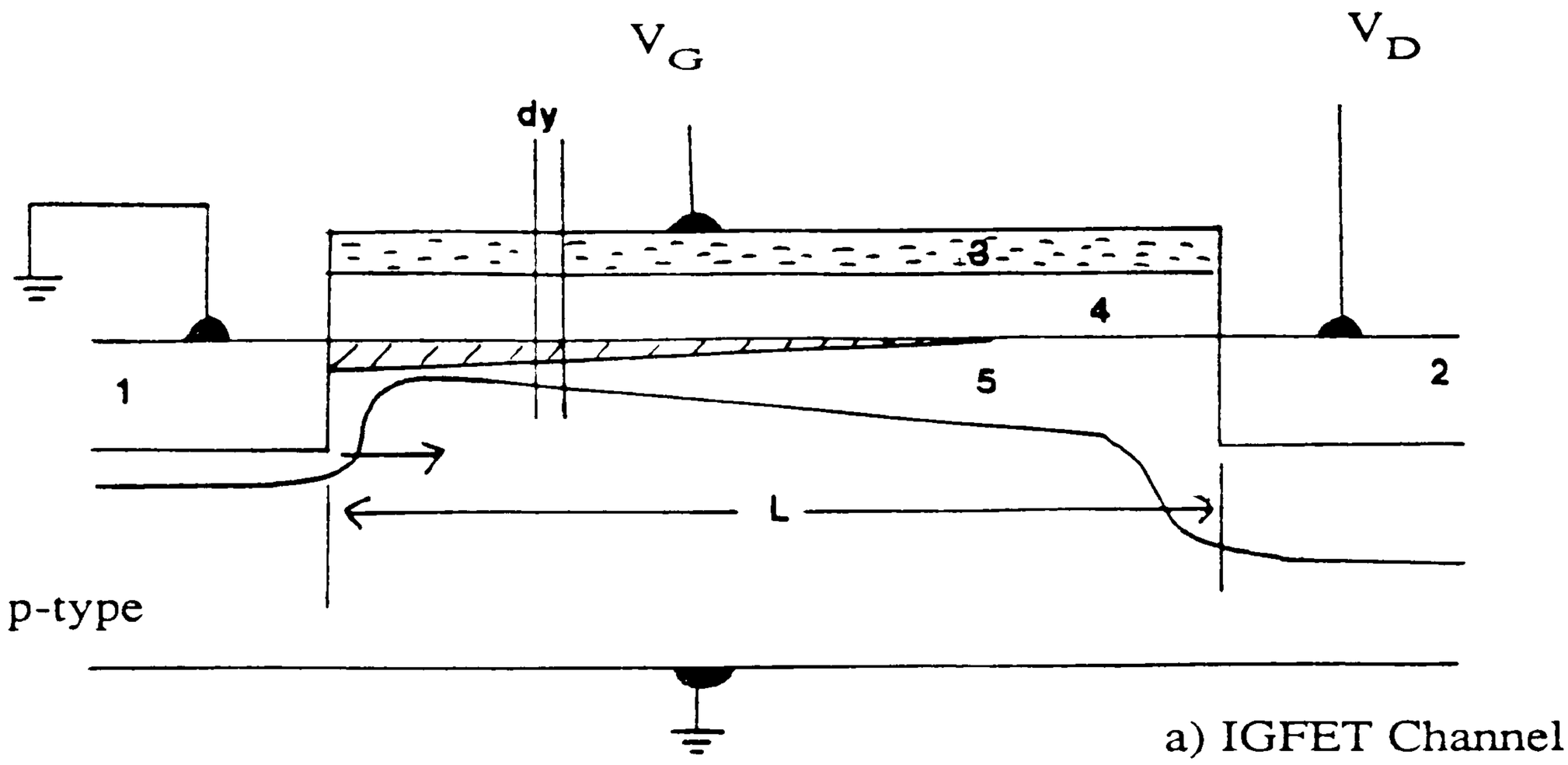

a) IGFET Channel

1. Source, n-type.

2. Drain, p-type.

3. Metal.

4. Insulator.

5. Space Charge.

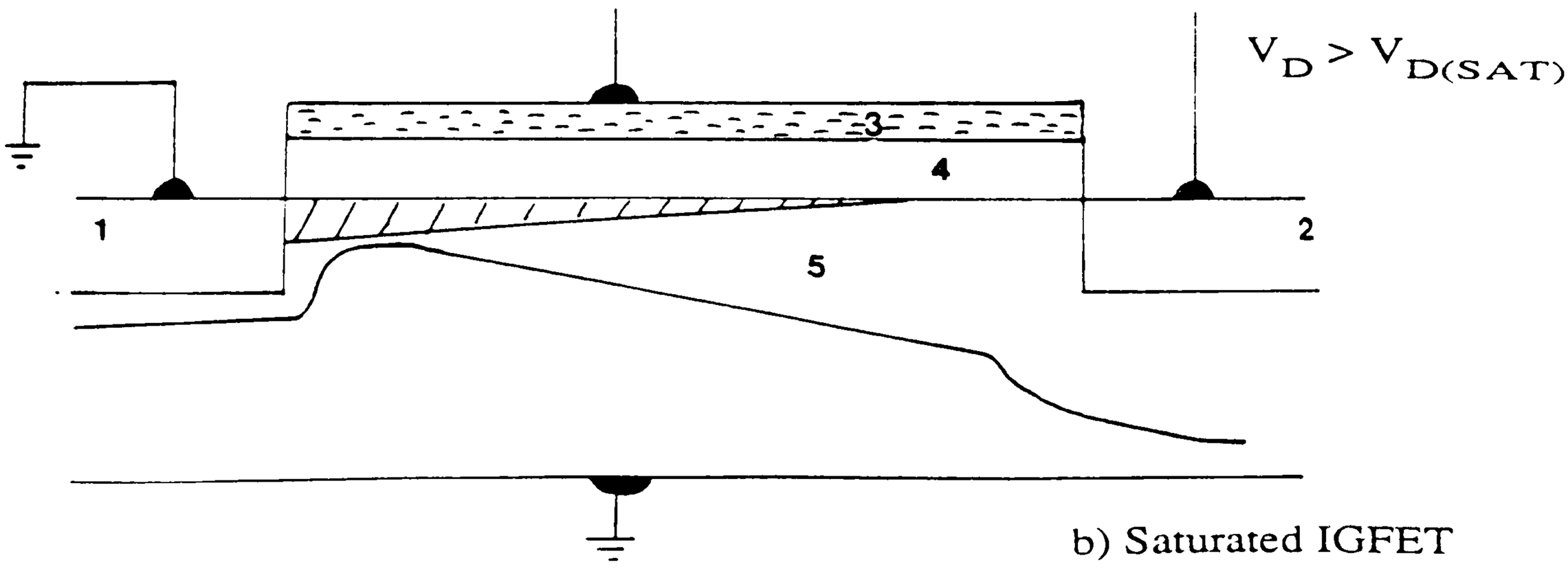

b) Saturated IGFET

Figure 2:6 Unsaturated and Saturated Mode of an IGFET

W = channel width

L = channel length

If the drain-to-source voltage is small compared with (V_G - V_T) then the device is said to be operating in the "unsaturated" region and the drain-to-source current is then given as

$$I_D = \mu_n C_o W / L [(V_G - V_T)^2 / 2] \qquad (2.4)$$

for $V_D > V_{D(SAT)}$

ISFETs are operated in the unsaturated mode.

2.4.4 Construction of ISFETs.

The advantages of ISFETs over ISEs are numerous; small size, potentially low cost mass production, robust, multi-ion sensing and integration of signal processing electronics and therefore compact instrumentation. The semi-conductor devices used in this work, Eμ-146, Eμ-358A, were designed by Dr. A. Sibbald. All chip wafers were provided by Edinburgh Microfabrication Unit.

a) Eμ-146 Chip. (I.C.) (figure 2:7)

This chip, based on the Utah UU03 device [20], was designed initially for catheter-tip type aplications. Electron beam lithography was used to draw the device on the masks prior to processing. The Eμ-146 comprises three ChemFETs and one IGFET on a 2.00 x 1.25 mm die. Each device is n-channel, enhancement mode, fabricated on 75 mm diameter, 14-20 cm p-type wafers with dual dielectric gates; 50 nm thermally grown SiO_2 and 90 nm Si_3N_4 deposited on top at 800 °C by low pressure chemical vapour deposition (LPCVD). The gate dimensions are 20 x 400 μm and it has a "folded" geometry for space efficiency. The metallisation tracks extend as far to the channel as encapsulation permits and a common drain is used to reduce the number of outgoing wires to seven. These devices have been used successfully as simultaneous multi-ion sensing devices by depositing different ion sensitive membranes over each of the gates [21].

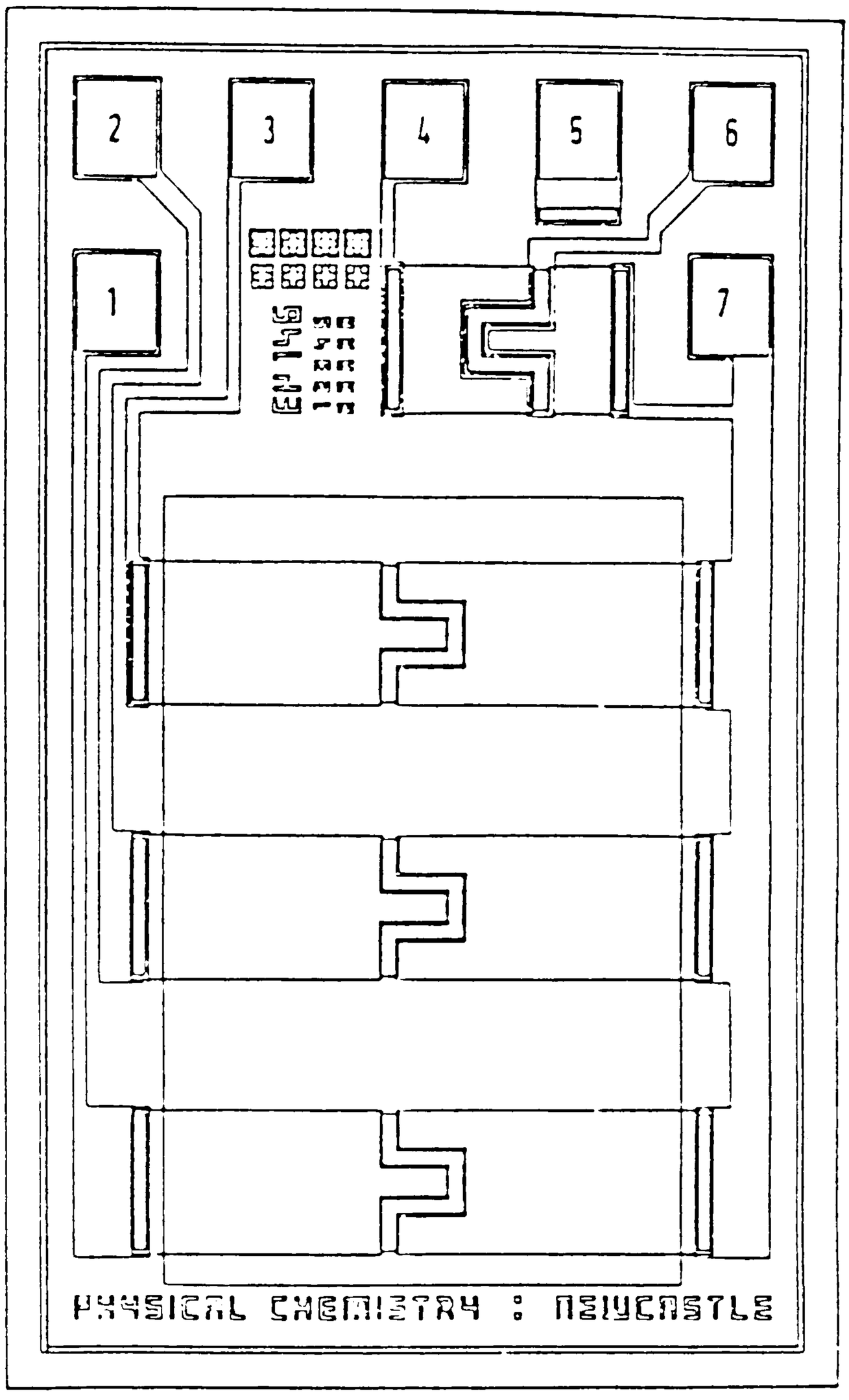

Figure 2:7 Eμ-146 Ion Sensitive Field Effect Transistor.

1. ISFET A Source
2. ISFET B Source
3. ISFET C Source
4. IGFET Source
5. Bulk Connection
6. IGFET Gate
7. Common Drain

b) Eμ-358A (OPTRAN) (figure 2:8)

The Eμ-358A acts as an OPerating chemical TRANsducer in the system, hence the name OPTRAN [22]. This is a single function matched ISFET-IGFET pair connected in a source-coupled dual differential configuration. The output voltages are coupled to a differential / single ended converter and then to one or more d.c. amplifiers so that the ISFET has a non-inverting input.

As with the Eμ-146, the gate dielectric comprises a dual gate. The chips were given n-type channel ion implants (depletion mode). The die size is 2.03 x 2.43 mm with the IGFET positioned along the edge of the upper chip. However, OPTRANs have advantages over conventional, intrinsic FETs. Since the matched reference FET (IGFET) and ChemFET are in the same electriçal and thermal environment, there is very little instability due to reference electrode transient potentials and low thermal sensitivity.

2.4.5 Flow Through Sensors.

For I.C.s in flow through cells, 16 pin DIL ceramic headers (Shinko, SHK-CA-P160035, Dage Intersem Ltd., Buckinghamshire) were used. These headers are compatible with 16 pin DIL socket adaptors (type 103-218, Farnell Electronic Components, Leeds).

2.4.6 Epoxy Encapsulation.

ISFETs must be encapsulated so that only the gate material is exposed to the electrolyte solution and electrical leakage between the gate, source, drain or substrate region is prevented. This stage often determines the lifetime of devices.

The technique now used (see Appendix B) [21] supercedes the original manual method of epoxy application to the devices, with the benefit of greater reliability and extended lifetime.

2.4.7 Membrane Deposition.

After encapsulation, the devices are again ultrasonically cleaned using

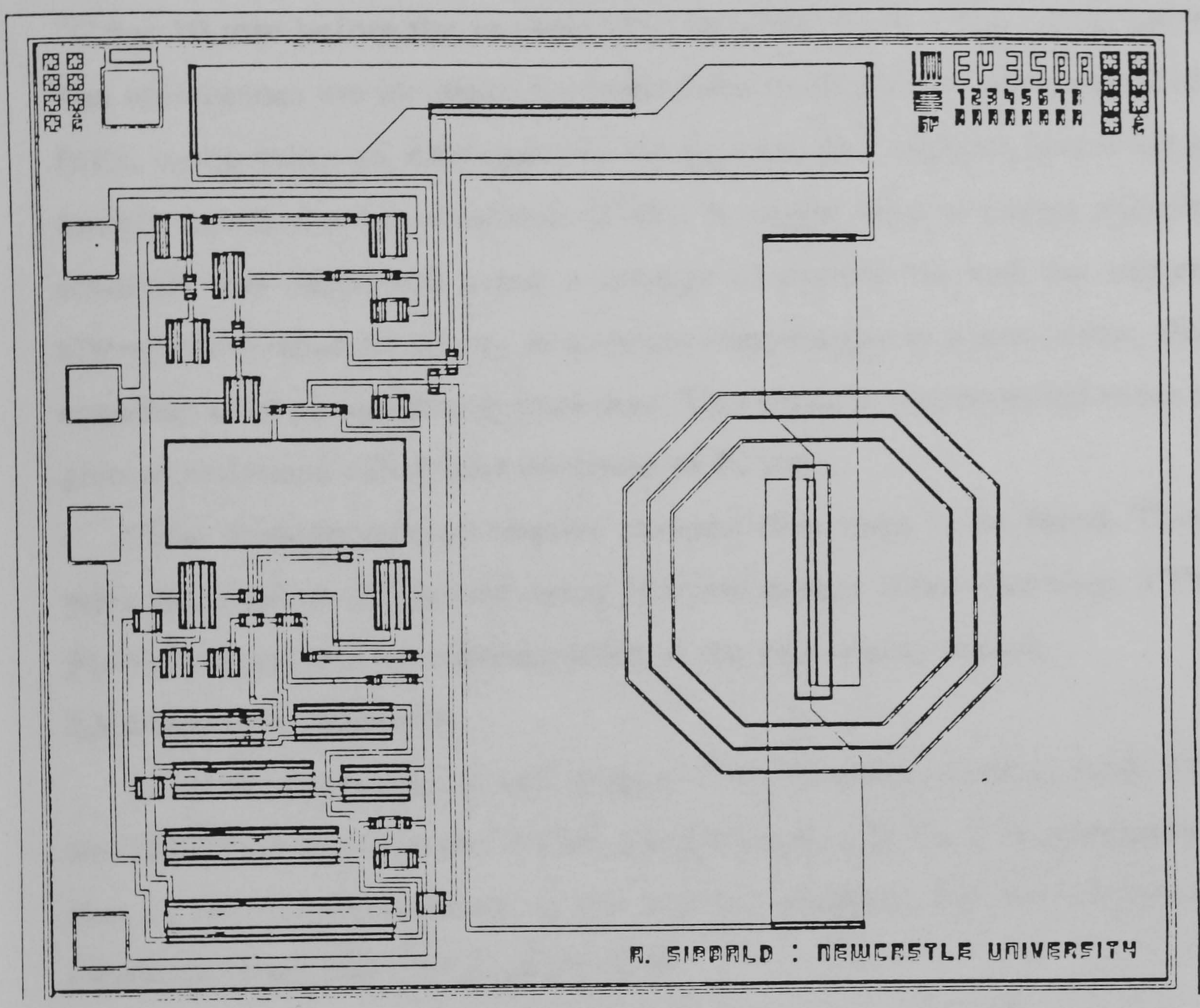

Figure 2:8 Eμ-358A Operational Transducer (OPTRAN)

i) distilled water (x 2)

ii) propan-2-ol

and blown dry with a stream of nitrogen. The I.C.s are oven dried at 100 °C for 10 min before the ion selective membranes are cast on the gates. The membranes are identical in composition to those used for home made ISEs, comprising an electroactive component and support dissolved in freshly distilled tetrahydrofuran (THF). A single drop of doped polymer solution was deposited using a syringe or pipette tip and the solvent allowed to evaporate slowly at ambient temperature in a desiccator, thus ensuring an even membrane thickness. This process was repeated twice to give an estimated membrane thickness of 50 μm.

Flow through sensors require perspex flow caps to be fitted. These were attached to the device using silicone rubber (Dow-Corning, RTV-3145) ensuring that no contamination of the gate region occurs.

2.5 Electrode Response.

In an electrochemical cell (figure 2:1), as stated earlier, both ISEs and ISFETs respond to the determinand according to the Nernst equation; that is for a determinand, i, the Nernst equation for an i-selective electrode (formerly (1.3)), is given as

$$E = \text{constant} \pm (k/z_i) \log a_i \qquad (2.5)$$

z_i is positive when "i" is a cation and negative if "i" is an anion.

Following from the Nernst equation (2.5), E_i, the potential difference determined by the electrode i.e. the cell potential, is the sum of several potentials in the system [23],

$$E = [E_1 + E_2 + E_3 + E_4 + E_5] + E_{LJ} + E_M \qquad (2.6)$$

$$= E_o + E_{LJ} + E_M \qquad (2.7)$$

where E = cell potential

E_o = standard potential of the cell, arising from the reference electrode potentials in the system

$Hg, Hg_2Cl_2 / KCl_{(sat)}$ || salt bridge || sample | membrane |internal solution |AgCl; Ag

E_{LJ} = liquid junction potential

E_M = the membrane potential; the sum of the Donnan potentials (the phase boundary potentials arising from non-uniform distribution of electrically charged species between the two phases) and diffusion potential of the membrane.

Assuming $E_{LJ} \sim 0$ and E_M is dependent on the concentration of analyte present in solution in accordance with

$$E = E_o + (k/z_i) \log a_i \qquad (2.8)$$

For a monovalent cation,

$$E = E_o + 59.16 \log a_i \qquad (2.9)$$

at 25 °C

2.6 Selectivity and Interference.

Ideally, an ISE or ISFET should respond exclusively to the species of interest. However, all sensors are prone to interference; either direct electrochemical interference or chemical interference at the electrode surface [24]. Considering the former of these, the response of a device may deteriorate in the presence of other ions and the Nernst equation must be modified to the simplified Nicolsky-Eisenman equation:

$$E = E_o + (k/z_i) \ln (a_i + K_{ij} (a_j)^{z_i/z_j}) \qquad (2.10)$$

where a_j = activity of the interfering species in the sample

k_{ij}= selectivity coefficient of the electrode

K_{ij} is the selectivity coefficient of the electrode for the primary ion, i, with respect to the interferent, j.

Selectivity coefficients depend upon the composition of the membrane, varying widely from one type to another [25], therefore one should use literature values merely as a guide to the extent of interference by a particular species. k_{ij} may take values ranging from zero (i.e. no interference) to greater than unity (i.e. the electrode responds more strongly to the interferent than to the primary species).

2.7 Methods of Determining K_{ij}.

The following assumptions are made when determining K_{ij};

i) the ion exchange equilibrium for the primary ion and the interferent is sufficiently rapid

ii) there is the same composition in the bulk and at the membrane surface.

2.7.1 Separate Solution Method.

Measurements are made in discrete solutions containing only one of the ions i, j, both of the same charge. Then for $a_i = a_j = 0.1$ mol dm^{-3}

$$E_i - E_j = + k \log (K_{ij} a_i / a_j)$$

reducing to

$$E_{0.1} = + k \log K_{ij} \qquad (2.11)$$

where E_i = potential in the solution containing i only

E_j = potential in the solution containing j only

Using this method, both ions must give the same slope, k, also a shift in E_o (equation (2.9)) is often observed on transfering the electrode between solutions [26], therefore mixed solution methods are preferred.

2.7.2 Mixed Solution Method.

a) Constant Interferent Concentration.

The concentration ratio of interferent, j, is increased until the electrode no longer responds to the primary ion; a plot of potential difference vs pa_i gives a horizontal slope. With no interferent present, a

Nernstian slope (RT/zF) ln10 is observed and so between these two limits the graph is curved (figure 2:9) [27]. By extrapolation of the constant potential to the extended Nernstian slope, $a_{i(j)}$ may be determined from which k_{ij} can be calculated;

$$\Delta E = E_{i(j)} - E_i$$

$$= k \log (a_i + K_{ij}(a_j)) / a_i \qquad (2.12)$$

and when $\Delta E = 0$, this reduces to

$$K_{ij} = a_{i(j)} / a_i \qquad (2.13)$$

b) Constant Primary Ion Concentration.

Alternatively, the concentration of the primary ion is kept constant and the interferent ion concentration varied. A calibration graph is plotted for the interferent ion only and then repeated with the addition of a fixed high concentration of primary ion.

In this work, method a) was used to determine selectivity coefficients.

2.8 Response Limits.

Many definitions of detection limits for ISEs have been proposed. The practical limit of detection in this work is that recommended by IUPAC [28] which defines the detection limit as the activity or concentration of the primary ion "i" at which the electrode potential deviates by $18/z_i$ mV from the extrapolation of the linear portion of the graph [28] (figure 2:10).

The detection limit depends both on the properties of the electrode, e.g. finite solubility of membrane material in the sample solution, and on the conditions of measurements e.g. temperature and presence of interfering species which cannot be removed from the sample background. The limit of detection for each electrode determines its measuring range. It is important that the conditions of measurements are stated.

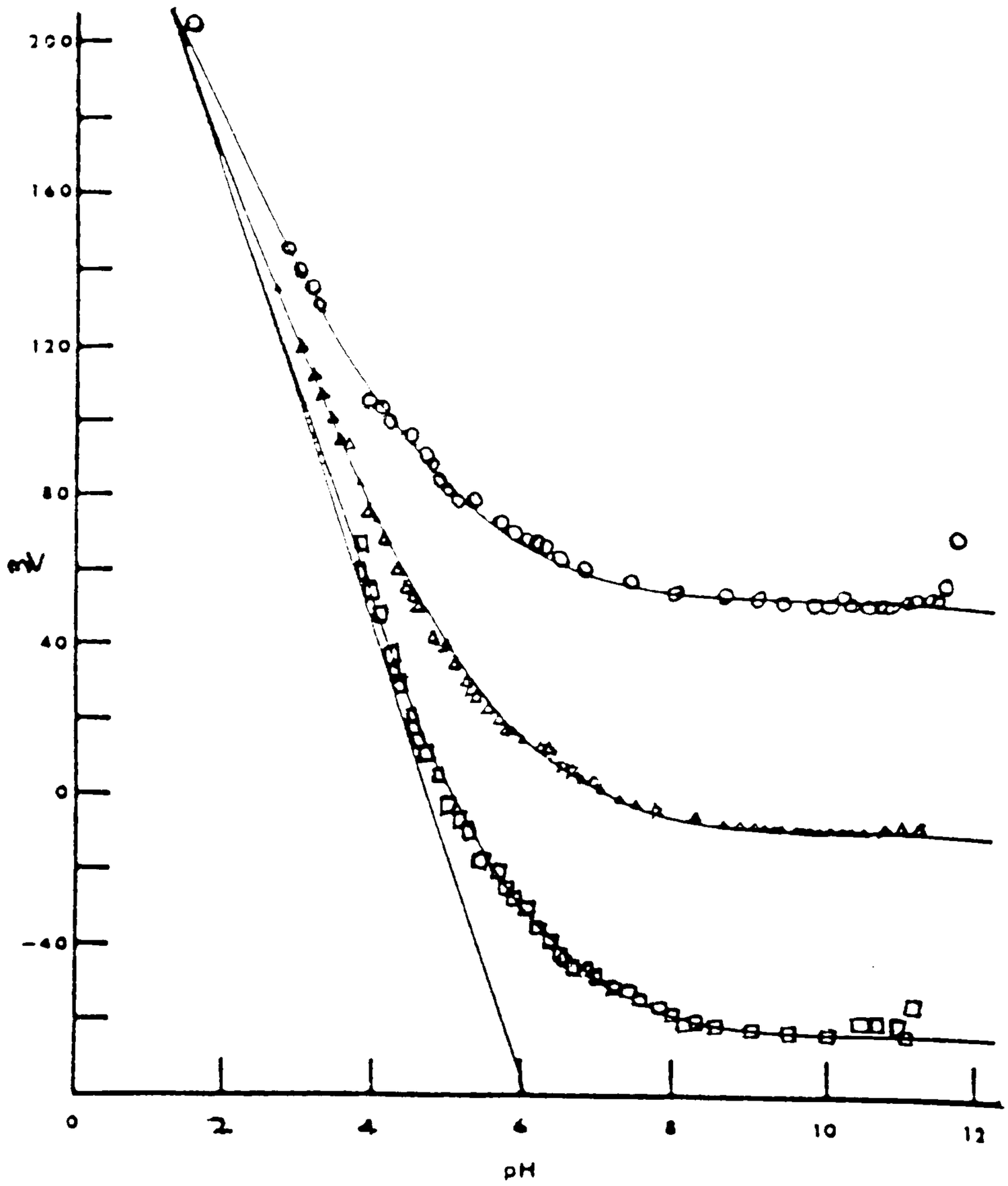

Figure 2:9 Graphical Method used to Determine the Selectivity of an H^+ Selective Membrane[27].

- o 0.7 mol dm^{-3} Na^+
- Δ 0.07 mol dm^{-3} Na^+
- □ 0.007 mol dm^{-3} Na^+

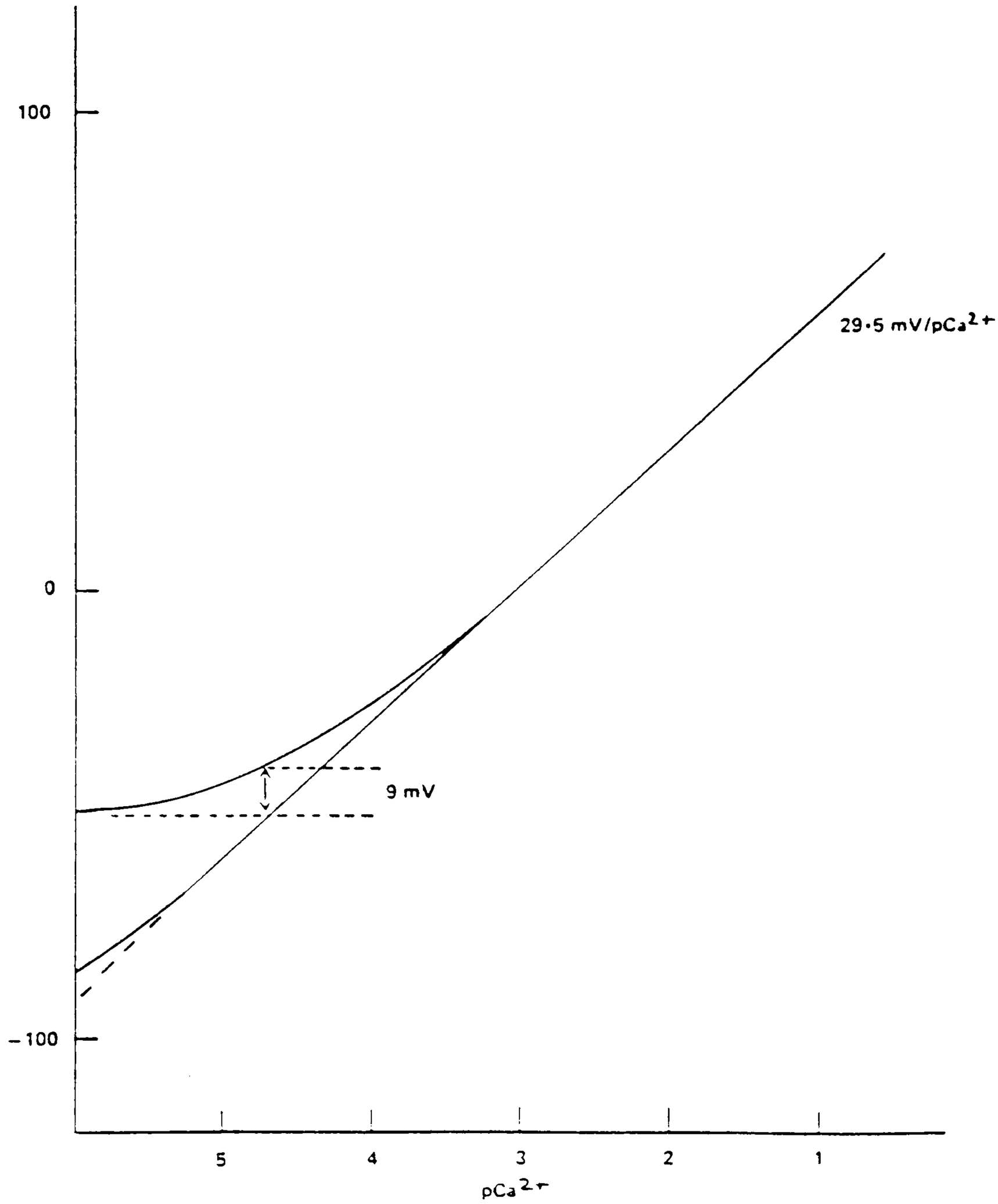

Figure 2:10 Graphical Method of Determining the Response Limits of an Ion Selective Electrode [28].

2.9 Response Time.

IUPAC [29] defines this as the time taken for the potential at the cell containing the electrode (or ISFET) to reach a value 1 mV from the final equilibrium potential after a supposedly instantaneous change in the determinand activity.

On stating response time for an electrode, it is critical that experimental conditions such as stirring rate, pretreatment of the electrode, initial and final concentrations and the method by which concentration change was produced are noted.

In general, the response time depends upon the membrane type, the rate of change of solution activity and the presence of interferents.

2.10 Liquid Junction Potentials.

In the derivation of equation (2.9), the liquid junction potential, E_{LJ}, was taken as zero. However, this is never the case. When two electrolyte solutions of different composition are brought into contact, a potential develops at the interface due to the unequal distribution of ions across the boundary arising from the difference in migration rates.

The liquid junction potential may be calculated, making certain assumptions, from mobilities of the ions involved. The junction potential is affected by the geometry of the junction; this is influenced by the leakage rate (of outward flowing filling solution into the sample) and determines the speed at which E_{LJ} is established. An in-depth review of factors affecting liquid junction is given elsewhere [30]. The junction potential may be reduced by use of an equitransferent (e.g. KCl) salt bridge between the test and reference solutions [31]. If the total mobilities of all ions in the bridge solution are nullified,

$$\sum_i z_i c_i u_i = 0 \qquad (2.14)$$

where z_i = charge on ion, i

c_i = concentration of ion, i

u_i = mobility of ion, i

then the solution is said to be equitransferent. If this is not possible, E_{LJ} can be minimised by using a bridge solution almost identical to that of the analyte.

References.

1. Griffiths J., Moody G.J. & Thomas J.D.R.
Analyst 1972, **97**, 420

2. "Ion Selective Electrodes"
ed. Durst R.A.
Proceedings of a meeting held at NBS, Gaithersburg, Maryland
Dept. of Commerce, NBS Special Publication 314, 1969

3. "Determination of pH: Theory and Practice"
Bates R.G.
2nd ed. J.Wiley, New York 1973

4. "Standard Potentials in Aqueous Solutions"
ed. Bard A.J., Parsons R. & Jordan J.
Marcel Dekker Inc., New York & Basle 1985

5. "Electrochemistry"
Reiger P.H.
Prentice-Hall International, Inc., New Jersey 1987, Chapter 1

6. Hills J.G. & Ives J.G.
J.Chem. Soc. 1951, 311

7. "Ion Selective Electrodes"
ed. Covington A.K.
Vol. 1, 1979
CRC Press, Boca Raton, Florida

8. Bergveld P.
IEEE Trans. Biomed. Eng. 1970, **BME-17**, 70

9. Bergveld P.
IEEE Trans. Biomed Eng. 1972, **BME-19**, 342

10. Nicolsky B.P., Shultz M.M., Belijustin A.A. & Lev A.A.
In "Glass Electrodes for Hydrogen and other Cations"
ed Eisenman G.
Marcel Dekker Inc., New York 1967
Chapter 6

11. Moss S.D., Smith J.B., Comte P.A., Johnson C.C. & Astle L.
J. Bioeng. 1976, **1**, 11

12. Bousse L., de Rooij N.F. & Bergveld P.
IEEE Trans. on Electron Devices 1983, **30**, 1263

13. Bousse L. & Bergveld P.
Sensors and Actuators 1984, **6**, 65

14. Van der Spiegel J., Lauks I., Chan P. & Babic D.
Sens. and Act. 1983, **4**, 291

15. Moss S.D., Janata J., Johnson C.C.
Anal. Chem. 1975, **47**, 2238

16. Blackburn G.F.
In " Implantable Sensors for Closed-Loop Prosthetic Systems."

ed. Ko W.H.
Futura Publ. Co. Inc. 1985, Chap. 8

17. Sibbald A.
Ph.D. Thesis, Univ. of Newcastle-upon-Tyne, 1982

18. Covington A.K. & Sibbald A.
Phil. Trans. Roy. Soc. Lond. 1987, **316**, 31

19. Grove A.S.
"Physics and Technology of Semiconductor Devices"
J. Wiley & Son, New York, 1967

20. Janata J. & Huber R.J.
In "Ion Selective Electrodes in Analytical Chemistry"
ed. Freiser H., Plenum Press, New York, 1980, Chap. 3

21. Sibbald A., Whalley P.D. & Covington A.K.
Anal. Chim. Acta 1984, **159**, 47

22. Sibbald A.
Sensors and Actuators 1985, **7**, 23

23. Moody G.J. & Thomas J.D.R.
Talanta 1972, **19**, 623

24. Morf W.E.
"The Principles of Ion Selective Electrodes and of Membrane Transport"
Elsevier, New York, 1981, Chap. 1

25. Pungor E., Toth K. & Hrabeczy-Pall A.
Pure & Appl. Chem. 1979, **51**, 1980

26. Rechnitz G.A., Kress M.R. & Zamochnick S.B.
Anal. Chem. 1969, **41**, 1203

27. Buck R.P., Boles J.H., Porter R.D. & Margolis J.A.
Anal. Chem. 1974, **46**, 255

28. "Ion Selective Electrodes"
Covington A.K.
CRC Critical Reviews in Analytical Chemistry 1974 pp. 335
CRC Press, Boca Raton, Florida

29. Lindner E., Toth K. & Pungor E.
Pure & Appl. Chem. 1986, **58**, 469

30. Covington A.K. & Rebelo M.J.F.
Ion Selective Electrode Rev., 1988, **5**, 93

31. Grove-Rasmussen K.V.
Acta Chem. Scand. 1948, **2**, 937

CHAPTER THREE

INSTRUMENTATION AND CALIBRATION METHODS

3.1 Introduction.

This chapter deals with experimental features common to all studies carried out, and apparatus used in potentiometric measurements and methods of calibration.

3.2 Buffer Amplifiers.

The membrane resistance of ISEs is very high, of the order of 10^{10} Ω. It was therefore necessary for high impedance instruments to be designed for general laboratory use. The input impedance of the buffer amplifier should be greater than that between the test solution and the ISE, and the impedance of the insulation between the test solution and the ground should be more than 100 times greater than that between the reference solution and ground [1]. A schematic of this system is shown in figure 3:1 and a circuit diagram for the single impedance buffer amplifiers, manufactured in the Department of Chemistry workshops, University of Newcastle-upon-Tyne is shown in figure 3:2.

In a single impedance buffer amplifier, as shown in Chapter 2, the membrane potential is dependent on the concentration of the primary ion, interferents (the extent of which depends on the selectivity coefficient) and activity effects e.g. changes in activity of the primary ion arising from changes in concentration of other ions. The latter may be avoided by working at high ionic strength i.e by addition of an ionic strength adjustor (ISA) e.g. TISAB (Total Ionic Strength Adjustment Buffer).

The liquid junction potential, E_{LJ}, is often neglected in studies, but this also depends on the composition and activity, I, of the analyte as well as the geometry of the junction. It is possible to remove the liquid junction potential using a differential amplifier, two ISEs are used, one acting as the reference electrode and the other as an ISE. Several conditions must be met when using this system. For example, if the fluoride ISE is used as the reference electrode (ISE 2) then the activity of fluoride must be kept constant, though not necessarily high, in calibration solutions. and this must also be present in the sample.

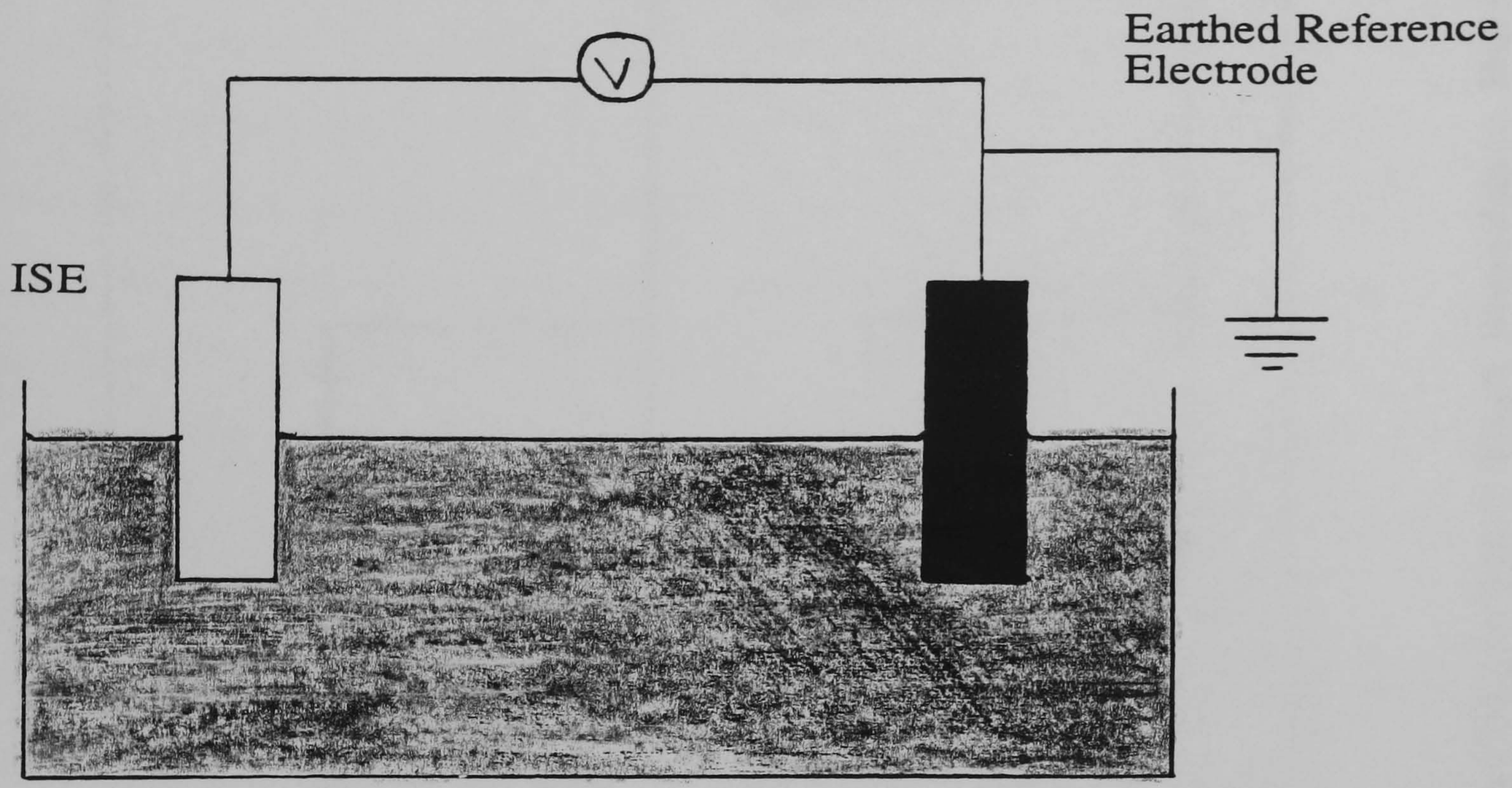

Figure 3:1 Schematic of a Single Input High Impedance Buffer Amplifier.

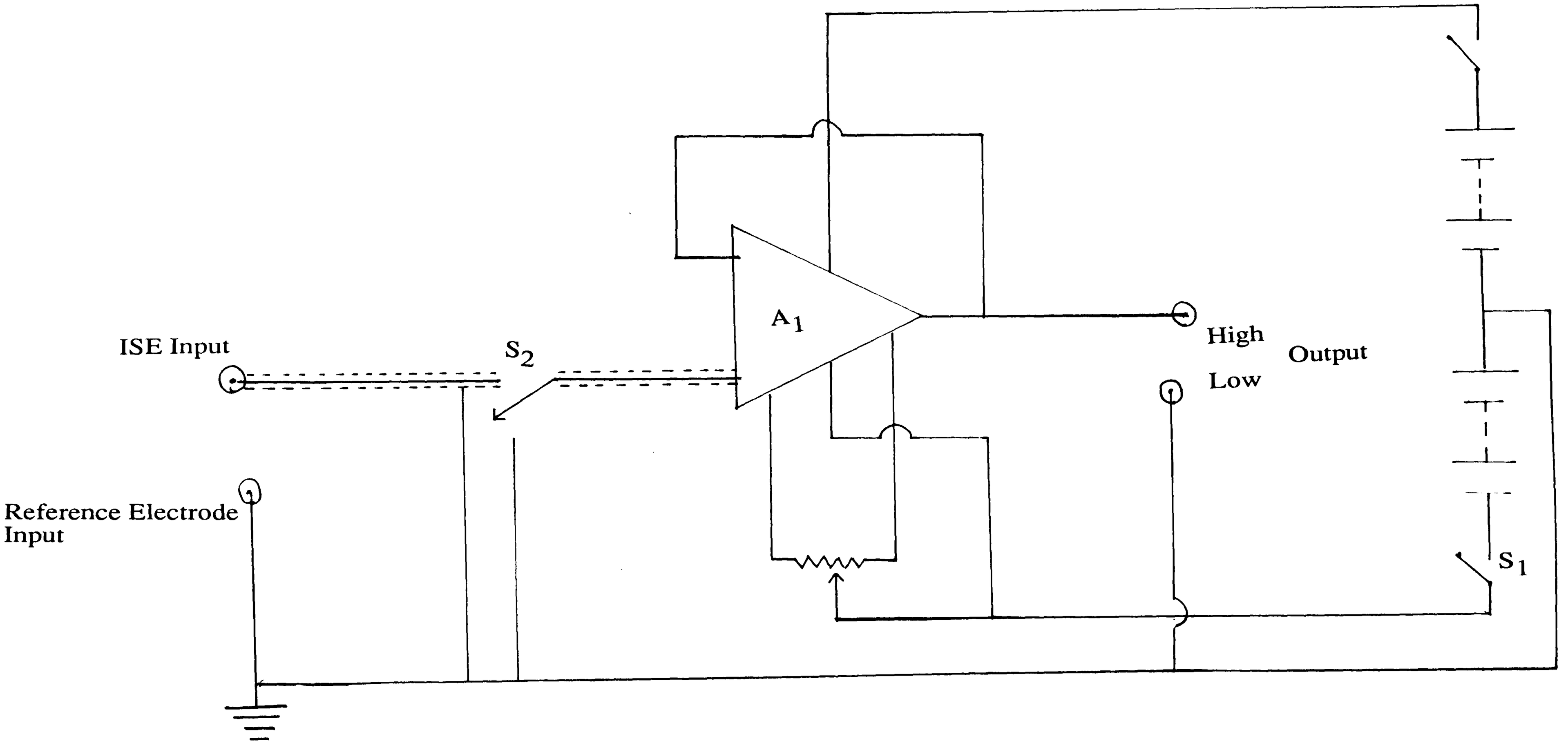

Figure 3:2 Circuit Diagram of a Single Input High Impedance Buffer Amplifier.

Obviously, it is important that the reference ISE is chosen carefully, ensuring there is no interference with the sample or sensing electrode; a schematic of this set up is shown in figure 3:3. Since two high impedance electrodes are now in operation, the buffer amplifier must be designed with dual high impedance circuitry, this is shown in figure 3:4.

High impedance devices are very susceptible to electrostatic pick-up [2] and therefore it was necessary for good shielding of electrode systems; covering electrode leads with aluminium foil, spraying meters with static eliminators and ensuring the operator does not wear nylon or woolen clothing. Where feasible, experiments were carried out in a Faraday cage, thereby electrically isolating the system.

The amplifier included a controlable offset so that it was possible to make measurements over a large range. Battery operated devices were used to remedy problems associated with mains spiking and noise.

For fieldwork, a very compact, water-proofed buffer amplifier was built.

3.3 ISFET Operation.

The low impedance of ISFETs means they do not require high impedance buffer amplifiers. Application of an electric field (irrespective of source) to the surface of a semi-conductor enhances or depletes the density of mobile charge carriers, as shown in Chapter 2; that is, the solution / electroactive gate potential difference is functionally related to the activity, a, of the sensed ion, i. As the drain current, I_D, is dependent on the external applied voltage, V_G, it is possible to characterise the devices in terms of I_D / V_G .

3.3.1 Methods of Measurement.

There are two main methods used;

i) Constant Applied Gate Voltage, V_G.

All externally applied voltages are held constant, by means of an operational amplifier, and the change in drain current, I_D, reflects the

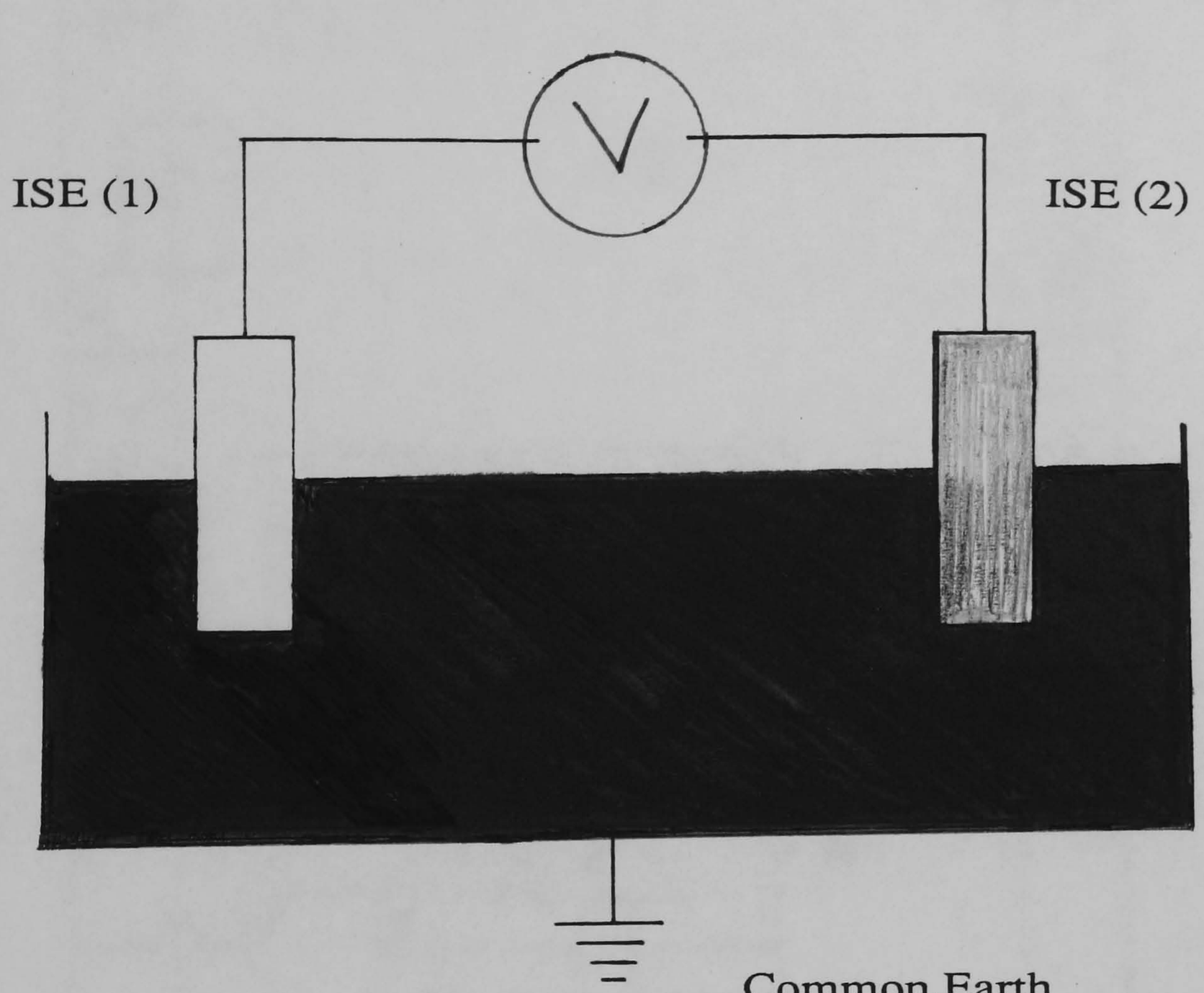

Figure 3:3 Schematic of a Dual Input High Impedance Buffer Amplifier.

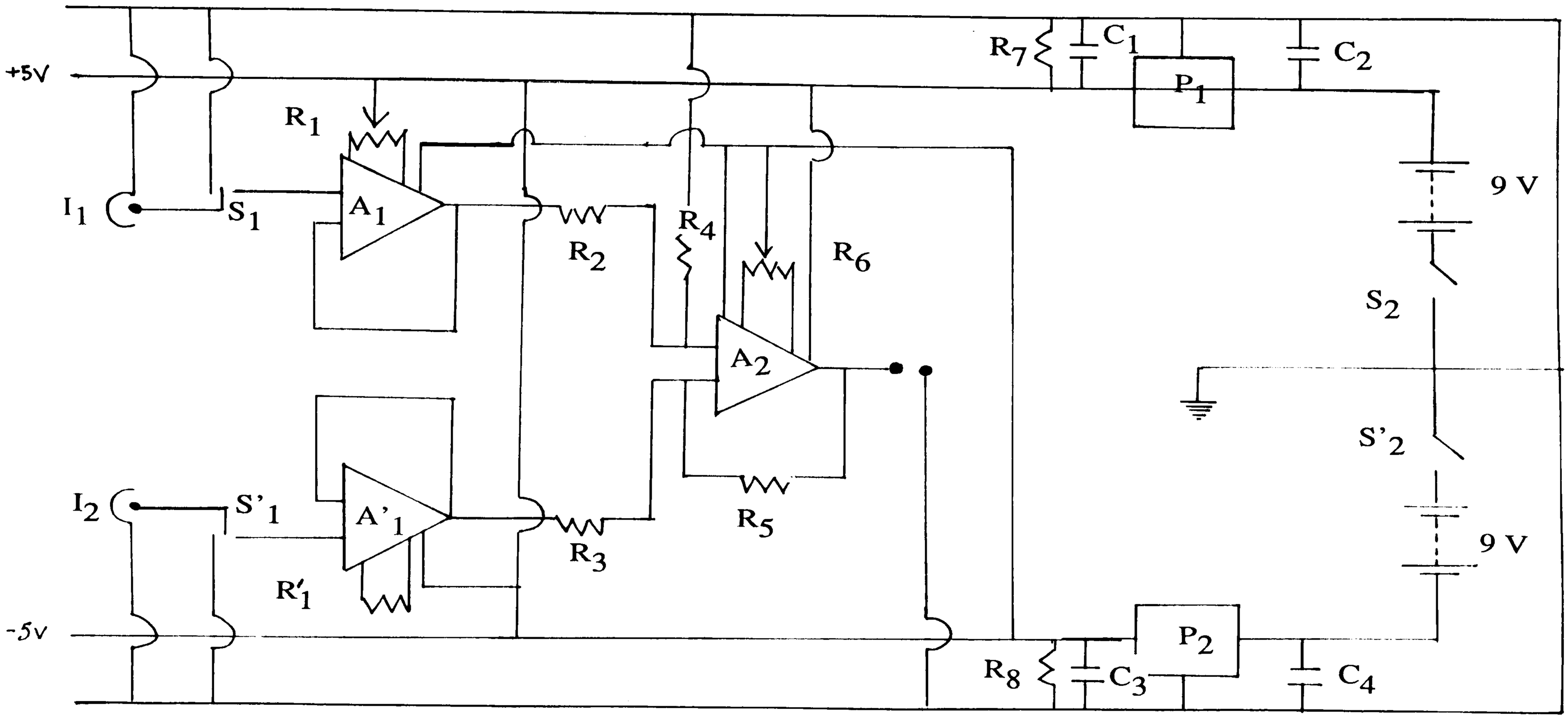

Figure 3:4 Circuit Diagram of a Dual Input High Impedance Buffer Amplifier.

Annotation for Figure 3:4.

The Circuit Diagram for a Double High Impedance Input Differential Amplifier.

I_1, I_2	Two high impedance inputs
S_1, S'_1	Double pole double throw toggle switch
S_2, S'_2	Double pole single throw toggle switch
A_1, A'_1	High performance dual F.E.T. amplifier (R.S. Component no. 305-939)
A_2	High performance single F.E.T. amplifier (R.S. Component no. 305-945)
P_1	Fixed Voltage - 100 MA regulator (R.S. Component 78L05, output voltage +5 V (+5%))
P_2	Fixed Voltage - 100 MA regulator (as above)
$R_1 = R_2$	20-turn cermet trimmer, 10 KΩ
$R_2 = R_3 = R_4 = R_5$	10 KΩ (matched to < 1%)
R_6	20-turn cermet trimmer, 10 KΩ
$R_7 = R_8$	4.7 KΩ
$C_1 = C_3$	0.47×10^{-6} Farad capacitor
$C_2 = C_4$	0.22×10^{-6} Farad capacitor

change in ionic activity of the analyte (figure 3:5).

$$V_{OUT} = I_D \times R_{SET} \qquad (3.1)$$

where R_{SET} is the magnitude of a calibration resistor.

ii) Constant Drain Current, I_D.

The device drain current is held at a constant, preset value (100 μA for Eμ-146 devices) by means of a negative feedback loop (figure 3:6), (chemically induced potential changes are offset by an opposing potential using an operational amplifier). The observed voltage is now a function of the activity of the sensed ion (Nernst relationship) and the readout is obtained directly in mV.

The latter mode of operation was used for all ISFET studies.

In the case of OPTRANs, Eμ-358A, circuitry is integrated onto the chip. The set up for operation of these devices is shown in figure 3:7.

3.4 Display of Signal.

The buffer amplifier, or constant current source, was connected to a digital voltmeter (Thandar TM451 multimeter) with precision of 0.1 μV and to a Y / t chart recorder (Linseis 0.5.80L flat-bed, multirange recorder) fitted with back-off facilities and incorporating a suitable capacitor across the input to smooth the signal.

3.5 Thermal Effects.

It can be seen from the Nernst equation, $E = \text{constant} + k \ln a_i$, where k is a function of temperature ($k = RT/F$), that the potential difference is proportional to temperature. However, ISEs are not Nernstian over the whole temperature or concentration range. The thermal sensitivity of the reference electrode system (the internal reference electrode and the liquid junction potential) and the activity of species in the analyte solution are temperature dependent, thus making temperature compensation difficult. If it is impossible to carry out all experiments at the same temperature, plotting a calibration curve of potential difference *versus* temperature

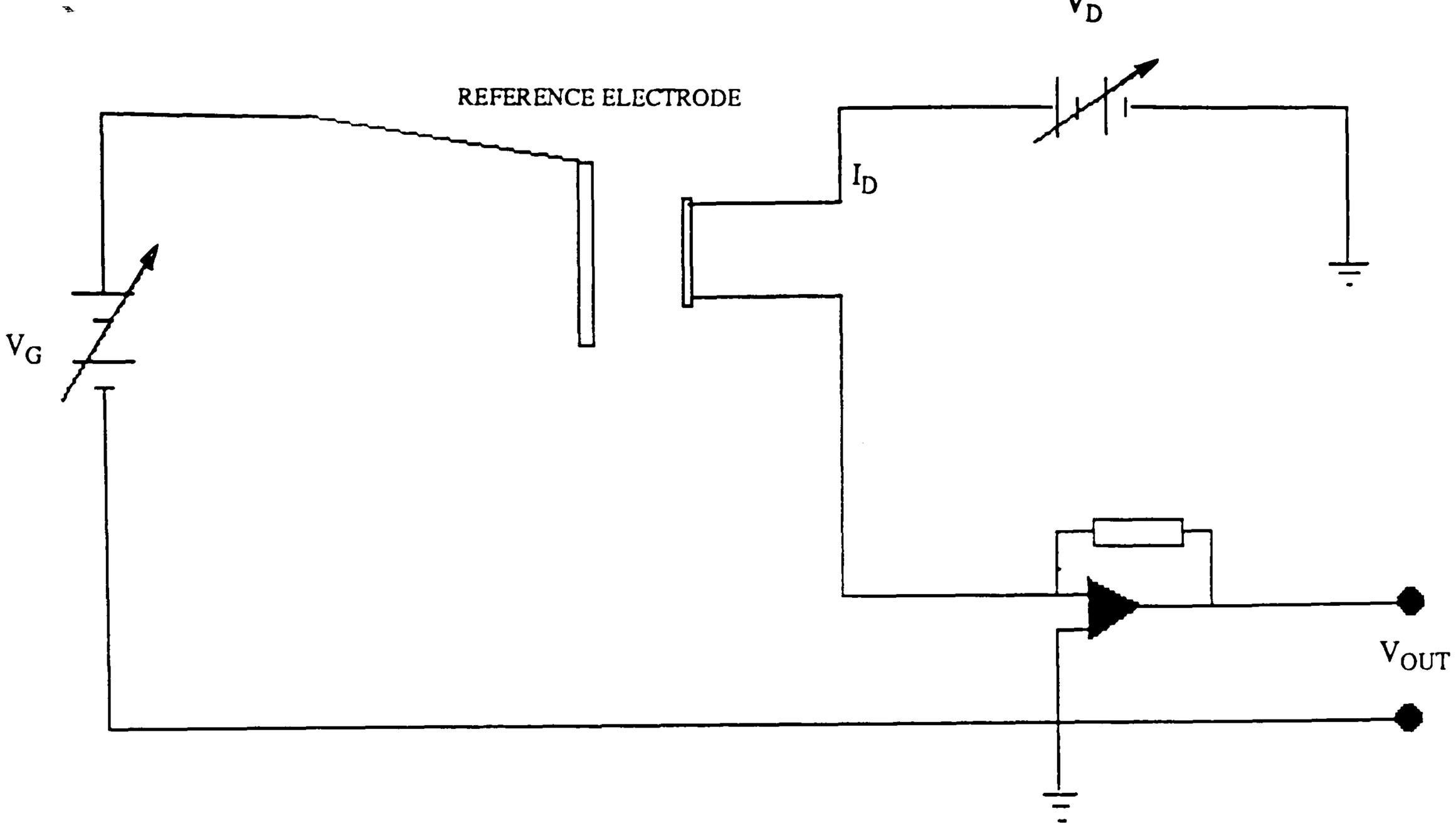

Figure 3:5 Measurement of Device Drain Current (I_D) using Fixed Gate Voltage (V_G) Method.

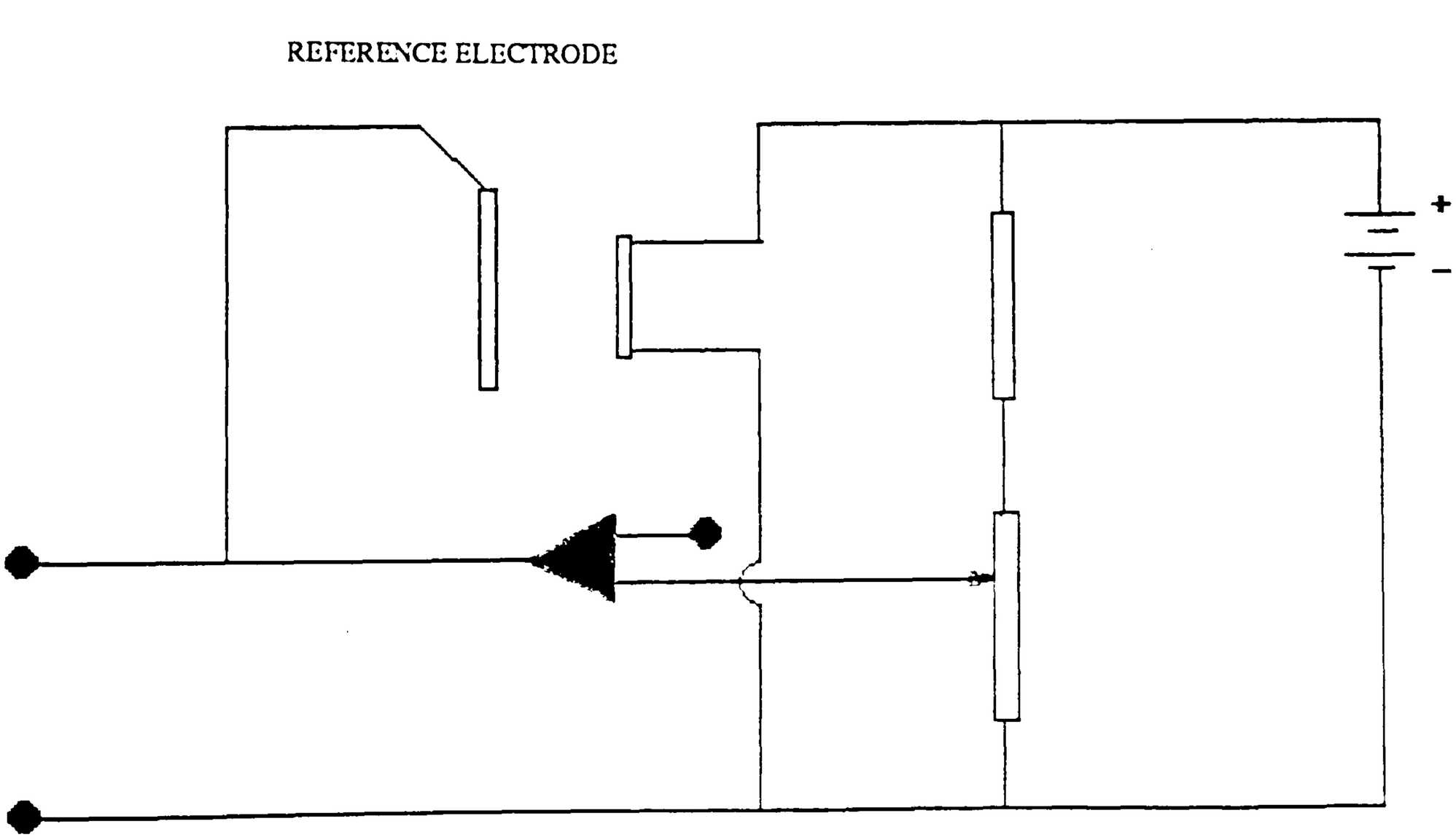

Figure 3:6 Measurement of Device Drain Current (I_D) using Fixed Drain Current Method.

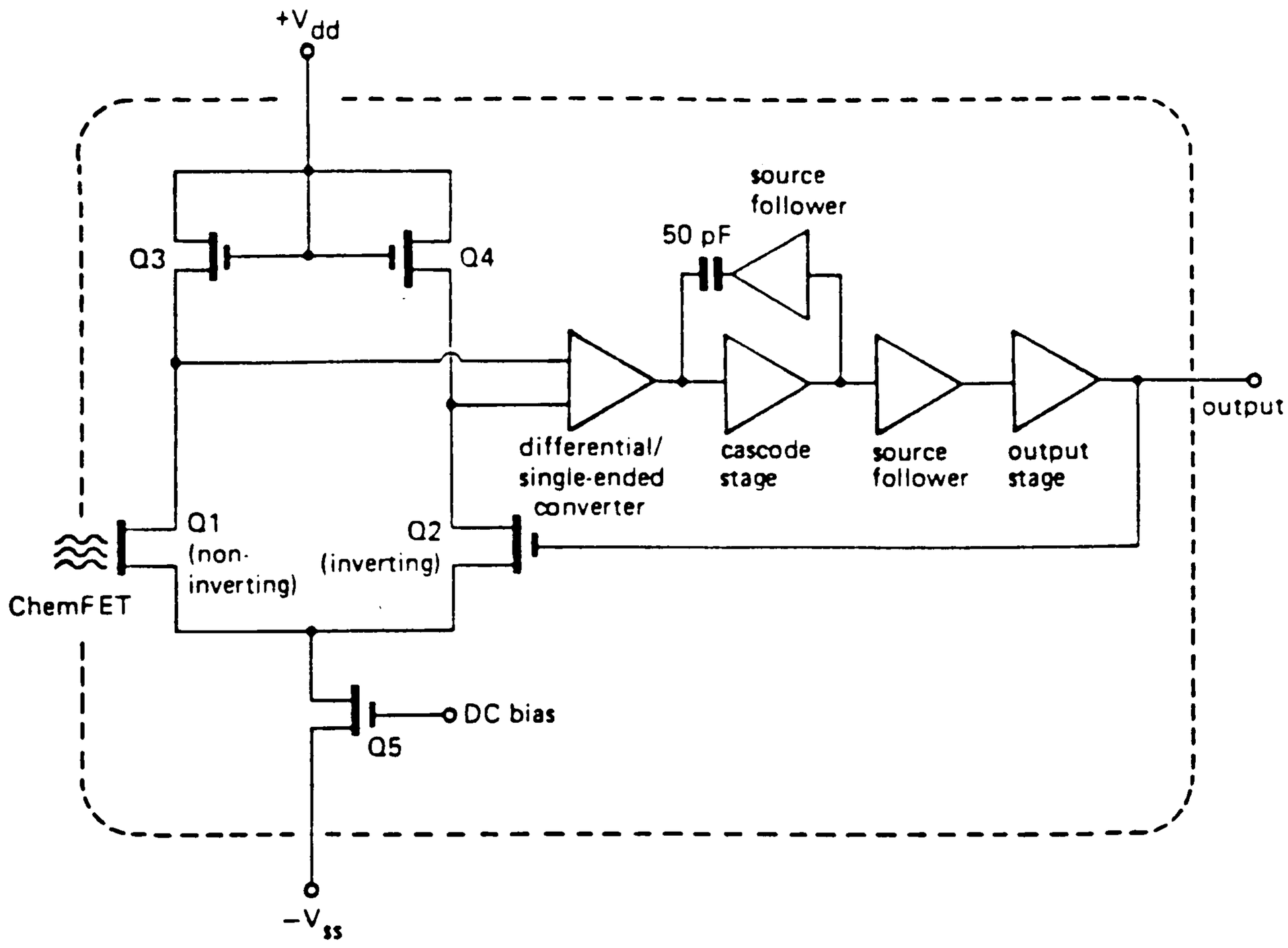

Figure 3:7 Block Diagram of an Eμ-358A Operational Transducer.

with a standard solution gives an indication of the compensating factor required.

In order to reduce the effect of temperature, several precautions may be taken [4];

i) use a thermostatted water bath (depends on the system)

ii) carry out experiments in an air thermostatted environment, serving also as a Faraday cage

iii) prepare chemically stable solutions > 10^{-5} mol dm^{-3} several hours prior to use to ensure thermal equilibrium.

3.5.1 Thermal Characteristics of FETs.

The thermal sensitivity of ISFETs is not completely understood, though well documented [5]. The thermal characteristics of a device are intrinsic to a particular chip, not wafer, affecting the voltage threshold and the mobility of the charge carriers. There is, however, an athermal locus in the I_D / V_G characteristics plot at which I_D value the thermal effects are almost self-cancelling [6]. The easiest method of determining this value is to run an I_D / V_G characteristics plot at two accurately known temperatures, encompassing the normal working temperature, e.g. 20 °C and 40 °C. The I_D at the intersection of the two curves is the I_D athermal value and should be used for further work (figure 3:8).

3.6 Effect of Stirring.

Although many stirring methods are available, a magnetic stirrer (Tecam MS1) was used throughout in this work. Stirring causes motion of solutions up to a distance of 6 x 10^{-5} cm from the electrode [7]. It is necessary to reduce deposition of analyte components on to the membrane surface and to prevent desorbed membrane materials remaining in the surface region, which result in inaccurate potential values. Fast stirring rates increase the speed of response by minimising the width of laminar diffusion film at the membrane [8].

The mechanical action of the stirrer can, however, lead to noise and a

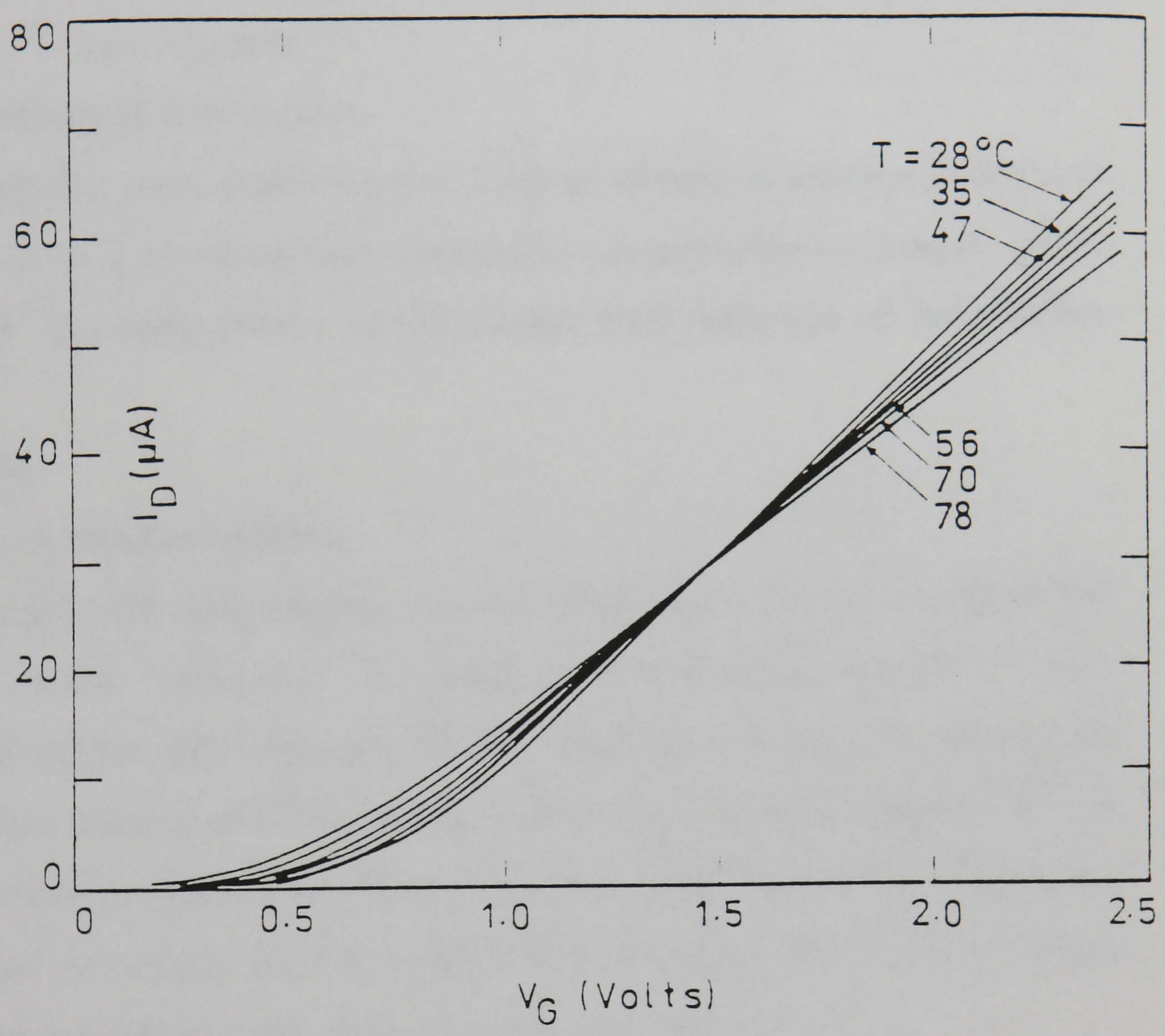

Figure 3:8 The ISFET Drain Current Thermal Sensitivity.

Determination of the Athermal Locus.

"shift" in the observed potential as well as an increased gaseous exchange between the sample and the atmosphere. A warming effect, arising from the stirring motor, can be reduced by clamping the analyte cell slightly above the magnetic stirring plate. When making measurements in suspensions, the rotating magnetic field of the stirrer bar may lead to erroneous readings, therefore the stirrer must be stopped prior to making observations [9] (see Chapter 7).

3.7 Pretreatment of Electrodes.

All electrodes were conditioned by pretreatment in dilute solutions of the sample, or in a standard very similar in composition to sample, prior to use as this has been shown to reduce the time response of membranes [10].

3.8 Dip Tests.

3.8.1 Beaker to Beaker Method.

Preliminary ISE calibrations were carried out with solutions in the range 10^{-6} to 10^{-1} mol dm^{-3} of analyte. It has been stated [11] that solutions of high ionic strength do not require stirring. However, all solutions were stirred as S-shaped responses have been reported [12] in lower concentration solutions. Serial analyses was carried out from least to most dilute solutions as ISE responses have been shown to be faster when the concentration jump occurs in this direction [13].

The beaker to beaker method is quick and simple and it was possible to reject a faulty electrode immediately. All dip measurements experience a delay of response on account of disturbance (make / break) of the electronic circuit; this effect is significantly more important than that of stirring as the electric shock experienced by the electrode can delay measurements for several minutes [14]. For electrodes with slow responses, dip tests are preferable over flow methods [15].

3.8.2 Standard Addition Technique [16].

Standard addition techniques overcome difficulties associated with

differences in matrices of the sample and standard solution. This is a very simple method, eliminating problems associated with breaking the electronic circuit, though stirring effects are still a problem.

A known volume of sample is added to the standard, or *vice-versa*, and the corresponding change in potential difference noted. Using this method, it is necessary to know the Nernst response of the electrode. Alternatively, aliquots of accurately known volume of sample are added to the standard, from which a calibration curve may be plotted (taking into account the dilution factor with each increment in volume).

Where possible, analyses were carried out using flow methods in preference to dip tests.

3.9 Flow Methods.

3.9.1 Response Times.

Obviously, it is necessary to know the response time of an electrode if it is to be used in a flow system. As there is such a range of response times for ISEs, from 10^{-3} s [17] to several hours [18], the parameters of the flow system must be chosen accordingly.

The response time of the electrodes, using both dip and flow methods, is influenced by many features; the presence of interferent [8], the age of the electrode [19] and the thickness of the diffusion layer at the membrane surface [20].

Morf *et al.* [21] stated that the surface layer of the membrane surface should be minimized; in dip tests this is implemented by using a fast stirring rate. In flow systems, however, as fresh solution is continually presented to the membrane, there is less chance of deposition of samples / interferents on the membrane surface.

Interferents have a marked effect on the response time of electrodes [20] and cannot be determined from the selectivity coefficient. Fleet [20] suggested that the response time increases as the atomic weight of the interferent.

In studies with glass electrodes, Nagy *et al.* [22] showed that a fast flow rate reduced the diffusion layer thickness and therefore increased the response time. The flow rates used by Nagy were, typically, 30 ml min^{-1}, 20 ml min^{-1}. These are much faster than the flow rates used in this work, typically 4 ml min^{-1}.

3.9.2 Dip Methods *versus* Flow Methods.

Using the information presented above, it is therefore possible to see that flow methods have many advantages over dip tests;

i) the membrane is continually in contact with fresh solution

ii) as the test solution is moving, only a small diffusion layer can form at the membrane surface, therefore there should be a faster time response by the electrode

iii) the reference electrode is downstream of the sensor, therefore no compounds leach from the reference electrode and interfere with the ISE

iv) serial analyses is very simple to carry out

v) on-line analyses is very simple.

The basis of all continuous flow systems is a very reproducible flow rate provided by a peristaltic pump; the age, length and internal diameter of the tubing affect the delivery time. The peristaltic pumps used in this work were mounted by the Chemistry Workshop, University of Newcastle-upon-Tyne. A variable D.C. power supply, stabilised, of 4 - 12 V, 1 A, with motor (ESCAP) was used to drive a 4 roller peristaltic pump mounted in a die cast box. Pump tubing of a range of internal diameters (i.d.) was used, but most often ca. 1 mm. A summary of the most common flow techniques available is now given.

3.9.3 Conventional Continuous Flow Methods [23].

Widely used in chemical analyzers in hospitals, these rely on an air-segmented carrier stream. Originally, bubbles were regarded as necessary to prevent excess sample dispersion, promote turbulent mixing, scrub the

walls of the tubing between samples, thus preventing cross-contamination. However, these claims are not justified and there are distinct disadvantages in using air-segmented techniques. These drawbacks are;

i) a pulsating flowing stream is observed

ii) at fast sampling rates it is necessary to control the bubble size (difficult)

iii) it is necessary to debubble the solution before entering the ISE detector cell.

For these reasons, unsegmented flow systems have been used.

3.10 Unsegmented Flow Techniques.

3.10.1 Flow Injection Analysis. (FIA). [24]

A precise volume is introduced into an unsegmented carrier stream. As there are no bubbles, a higher rate of analysis (100-300 h^{-1}) is possible [25] with enhanced response times (less than 1 min between sample injections).

Although FIA was not used, from results of reliability studies of the constant volume dilution technique (see section 3.12), it would seem practical to consider this technique for routine calibration and analysis. Injecting a known volume of sample into a carrier stream of standard, a variation of the standard addition technique may be carried out. The set-up and shut-down of the FIA method are very rapid and the only complexity of the system is the injection device.

3.11 Flow Cells.

3.11.1 Introduction.

In order to substantiate claims that flow methods provide more accurate information than dip tests when used with ISEs, a small, perspex flow cell was made, based on the Orion model (figure 3:9) [26]. The response time and stability of response were observed for an ISE fitted with this flow cell. Two other designs were also used; these are discussed

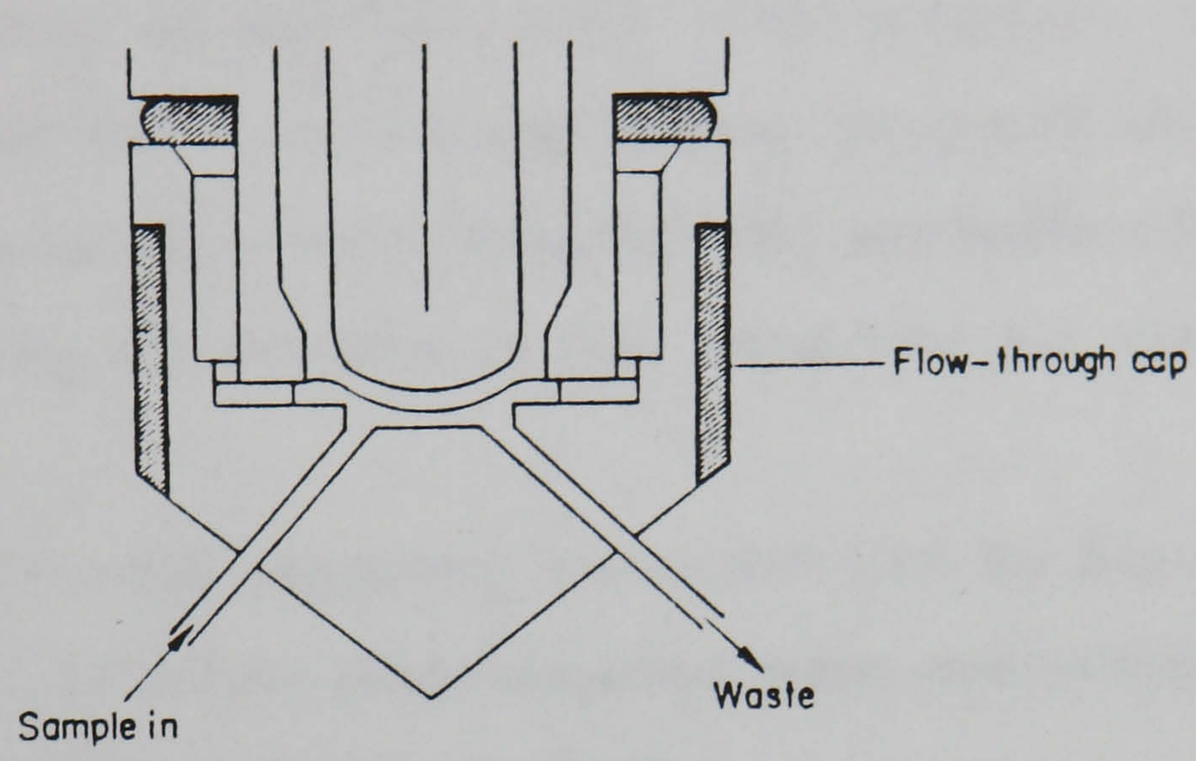

Figure 3:9 The Orion type Flow Cap.

in the following section.

3.11.2 Experimental.

An iodide ISE (Radelkis Type OH-8533), pre-soaked for 6 h in 10^{-3} mol dm^{-3} potassium iodide and a glass electrode (Russell CE77L) were used for the investigation of the flow cells. Test solutions in the range 10^{-1} to 10^{-5} mol dm^{-3} potassium iodide (prepared by serial dilution) were used in conjuction with the iodide ISE and buffers B2, B4, B7 [27] (see Appendix C) devised as test solutions for the glass electrode.

Glycine and TRIS (buffer reagents) were provided by Sigma and Research Organic Inc., all other reagents used were analytical grade (Analar) supplied by BDH Chemicals Ltd., Poole.

The potential difference between solutions was measured against a calomel reference electrode (Russell CE711), placed downstream of the sensing device, and the signal displayed via a buffer amplifier on a digital voltmeter. A Y / t chart recorder was used to monitor the stability of response with time. Using the "Orion"-type flow cell (figure 3:9) each solution was pumped, in turn, across the ISE membrane.

3.11.3 Results

As the Orion type flow cell is small and can therefore be flushed rapidly, the sampling rate was increased and greater demands could be imposed on this system than those using larger flow cells. This cell was, therefore, used for analyses of a batch of fertilizer solutions (Chapter 7). A series of fertilizer suspensions was analysed on-line, with a minimum of time between introduction of each sample in order to appraise the possible sample load of the system. To ensure no sampling errors were present, analysis of samples was repeated in a random order.

Good, reproducible results were obtained using this flow cell, however, there is still a small dead space incorporated into this cell design which inevitably leads to slight carry-over errors. Normally in

glass electrode flow systems, solution remains trapped above the electrode's glass bulb; a new perspex flow cell was designed which minimizes this effect (figure 3:10). This new design exposes only the sensing region, i.e. the lower portion of the bulb, to solution. The cell is in two parts; the upper section is attached to the stem of the electrode and blocks off the upper portion of the bulb. The lower, removable section of the cell has a hemispherical cavity which surrounds the bulb, this portion incorporates the inlet and outlet for solution flow. The two portions are screwed together, and a rubber 'O' ring ensures an air tight seal. A similar design, in one piece, was designed for the iodide ISE (figure 3:11), however, since the iodide ISE is cylindrical and has a flat sensitive membrane, a one piece cell, with rubber 'O' ring to ensure a good seal, is sufficient to ensure good solution flow.

Experiments using these flow cells showed good response times and stability compared with dip tests, and in tests for the iodide ISE the new design proved to be better than the Orion-type flow cell for on-line serial analysis.

3.11.4 Conclusion.

The new, small miniature flow cells described are suitable for rapid, on-line analysis. By reducing the dead space in the cells, errors associated with carry-over are minimized. There are distinct problems associated with the design of mini flow cells for use with bulb shaped electrodes; this two piece cell has overcome many of these problems, in particular those due to carry-over.

3.12 Constant Volume Dilution.

3.12.1 Introduction.

The constant volume dilution technique (CVD) first introduced by Horvai *et al.* [28] in 1976 has been widely used as a calibration method. It is a very simple method in which the concentration, c, of an ion, i, with time, in a constant volume, stirred, flow through cell can be described by

Figure 3:10 The Novel Two Piece, Glass Electrode Flow Cell.

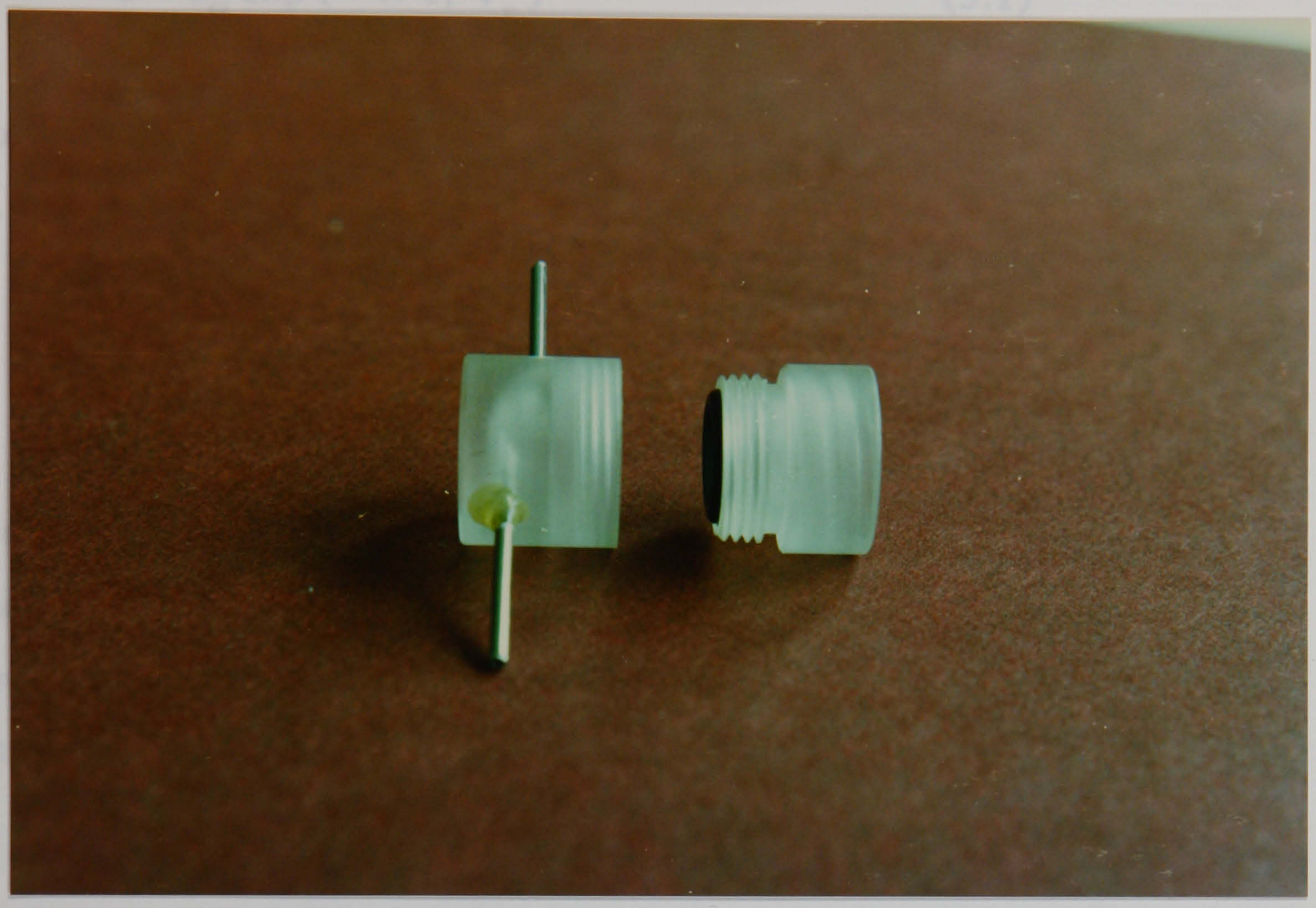

Figure 3:11 The Iodide Electrode Flow Cap.

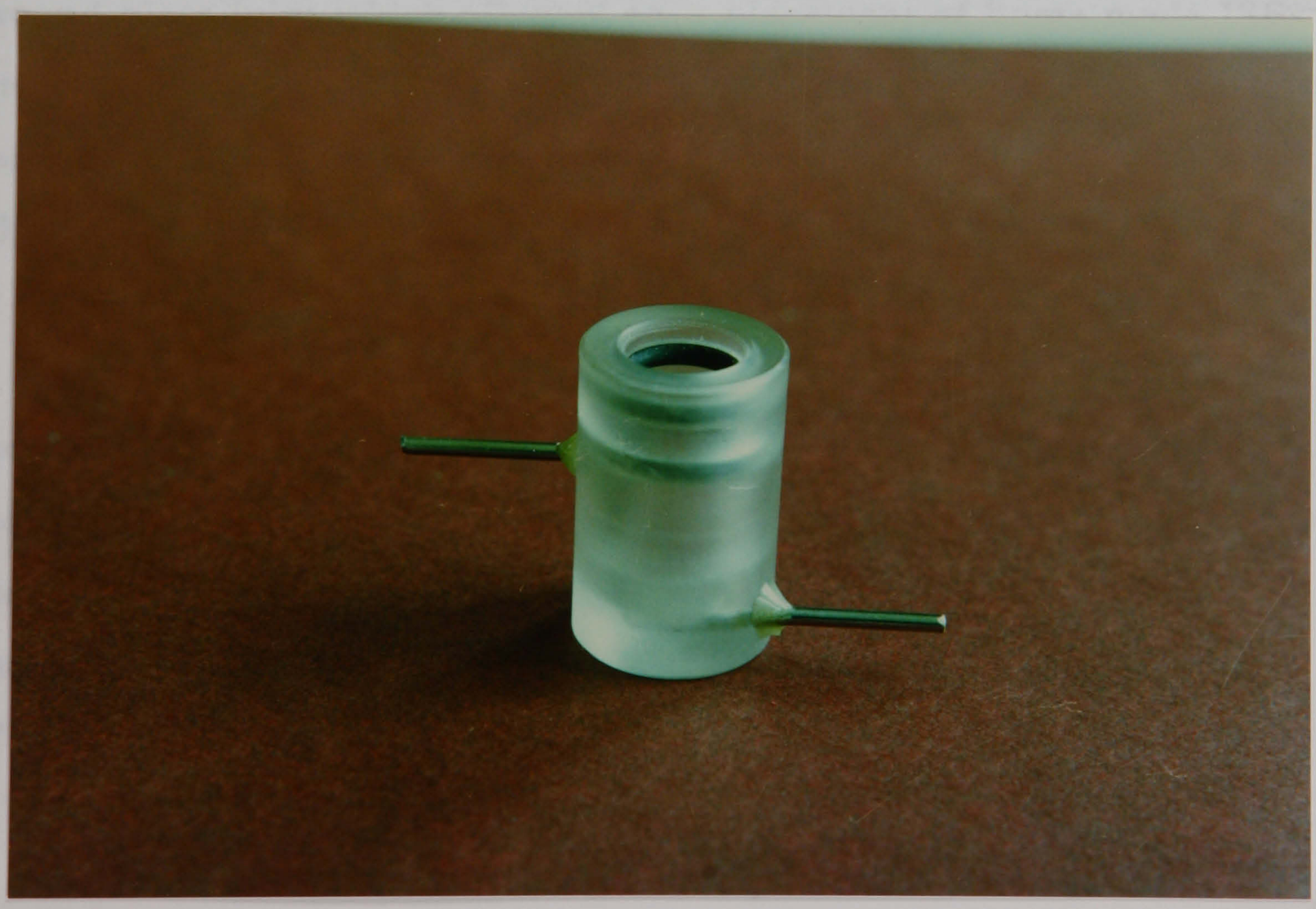

$$c = c_o \exp (- W t / V_r) \qquad (3.1)$$

where c_o = initial concentration of the solution

W = flow rate of the diluent

t = time from start of dilution

V_r = volume of the dilution vessel

An 'i' sensitive ISE is placed in the CVD vessel containing a known concentration of the primary ion 'i'. The solution is then diluted at a known flow rate and the potential response of the 'i' sensitive ISE *versus* a reference electrode measured, which can be recorded on a Y / t chart recorder. The units conventionally used are given,

$$1 \text{ min} = (h / \text{mm} \,.\, V_r / \text{ml}) / (2.303 \, W / \text{ml min}^{-1}) \quad \text{mm} \qquad (3.2)$$

where h = mm equivalent on the chart recorder

The CVD vessel was made from a water jacketed glass tube with B19 ground glass joint which allowed easy placement of home made ISEs fitted with a B19 socket. Commercial electrodes were sealed into place using drilled PTFE stoppers, paraffin wax ensured an air / water-tight seal (figure 3:12). The system can be used with ISFETs by placing the ISFET at the outlet of the stoppered cell.

It is important, however, following directly from equation (3.1), that the values of experimental parameters are chosen carefully when using this method. That is, the magnitudes of the volume of the dilution vessel used, the flow rate of solution and the stirring rate within the dilution cell should be carefully considered. Tests were carried out to assess the impact of altering these parameters.

3.12.2 Experimental.

In order to determine the accuracy of the CVD method, the concentration of analyte in the vessel during dilution was measured using an alternative analytical technique. The apparatus was set up as for a

Figure 3:12 The Constant Volume Dilution Cell with Home made ISE.

conventional CVD experiment, replacing the electrochemical detector with a spectrophotometric detector (figure 3:13). Using a form of detection other than ISE or ISFET it was therefore possible to assign the difference between the observed (spectrophotometric) and expected (calculated) concentrations to assumptions made in equation (3.1) and not to the electrochemical detector. A specially designed flow through spectrophotometric cell was used in this assembly (figure 3:14). The cell was a 1 cm width glass cell with B5 ground glass joints. A 10 cm length of glass capillary tube connected the flow cell to the dilution system.

A UV-vis spectrophotometer (Unicam SP1800 Ultraviolet spectrophotometer) was used to follow the change in concentration of analyte, 0.1 mol dm^{-3} chromium (III) nitrate (BDH Ltd.). A wavelength of 410 nm,was found from a spectrum scan (figure 3:15) to be the maximum absorbance peak.

Potassium dichromate solutions (BDH Ltd.), a standard solution used in spectrophotometry, was used to repeat tests carried out using chromium (III) ions. If slightly less than 100% absorbance had been obtained initially (using chromium (III)), then this would have greatly affected readings at lower concentrations. A very strong, sharp peak observed at 350 nm (figure 3:16) was used as λ_{max} for dilution studies. 10^{-4} mol dm^{-3} dichromate solution was used as the initial solution and the sensitivity of the spectrophotometer adjusted to a more sensitive scale (0 - 0.5). More concentrated, e.g. 10^{-3} mol dm^{-3}, dichromate solutions were completely off-scale, even using the least sensitive absorbance scale.

To ensure that Beer's Law was obeyed by the chromiuim (III) and dichromate solutions, calibrations were carried out with solutions in the ranges 10^{-1} - 10^{-5} mol dm^{-3} and 10^{-4} - 10^{-6} mol dm^{-3}, respectively.

Experiments were also carried out using a dual monitoring system; potentiometrically with an iodide ISE *versus* a saturated calomel reference electrode and spectrophotometrically. Now the analyte used was an

Figure 3:13 The Constant Volume Dilution System with Spectrophotometric Detector.

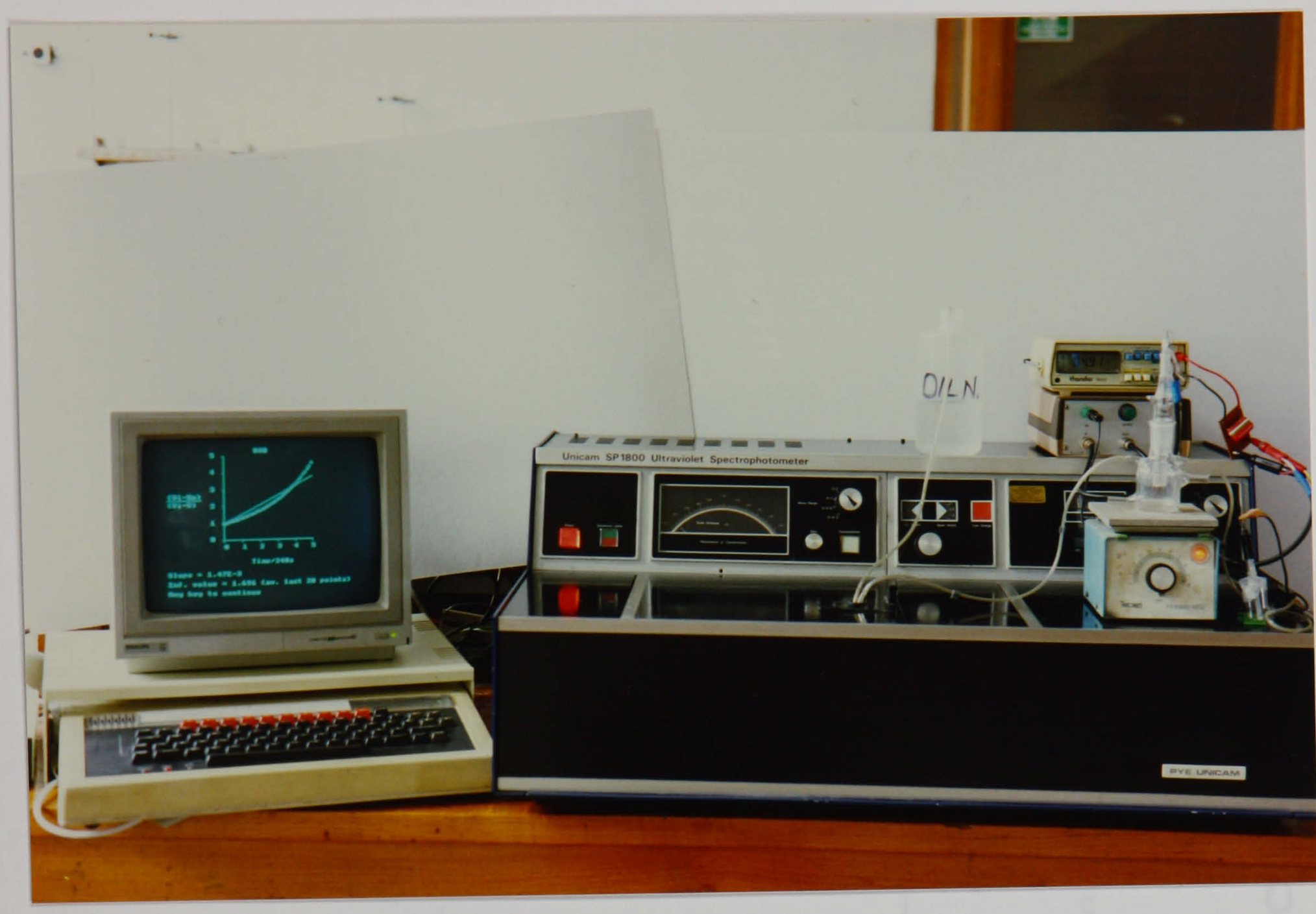

Figure 3:14 The Flow Through Spectrophotometric Cell.

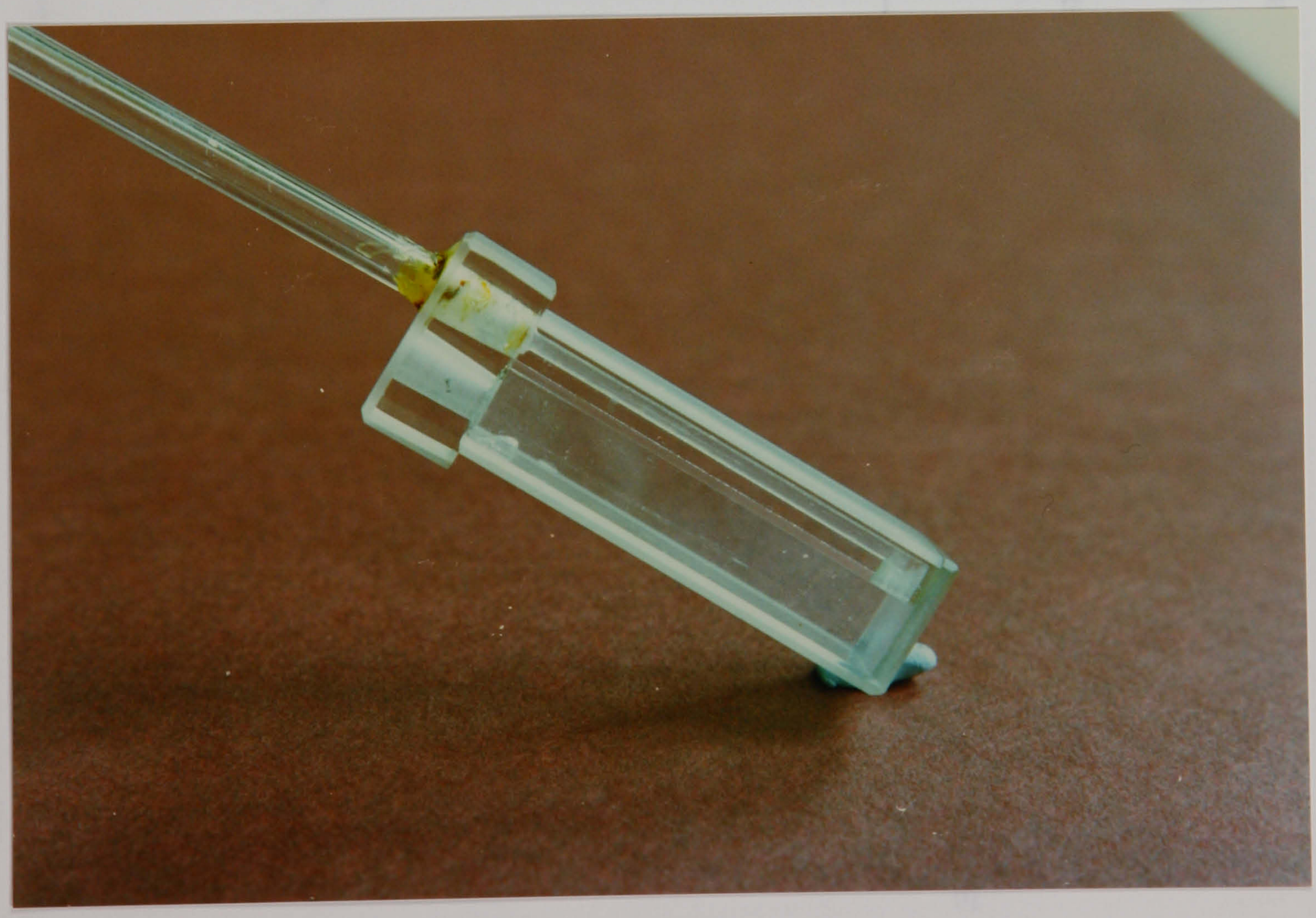

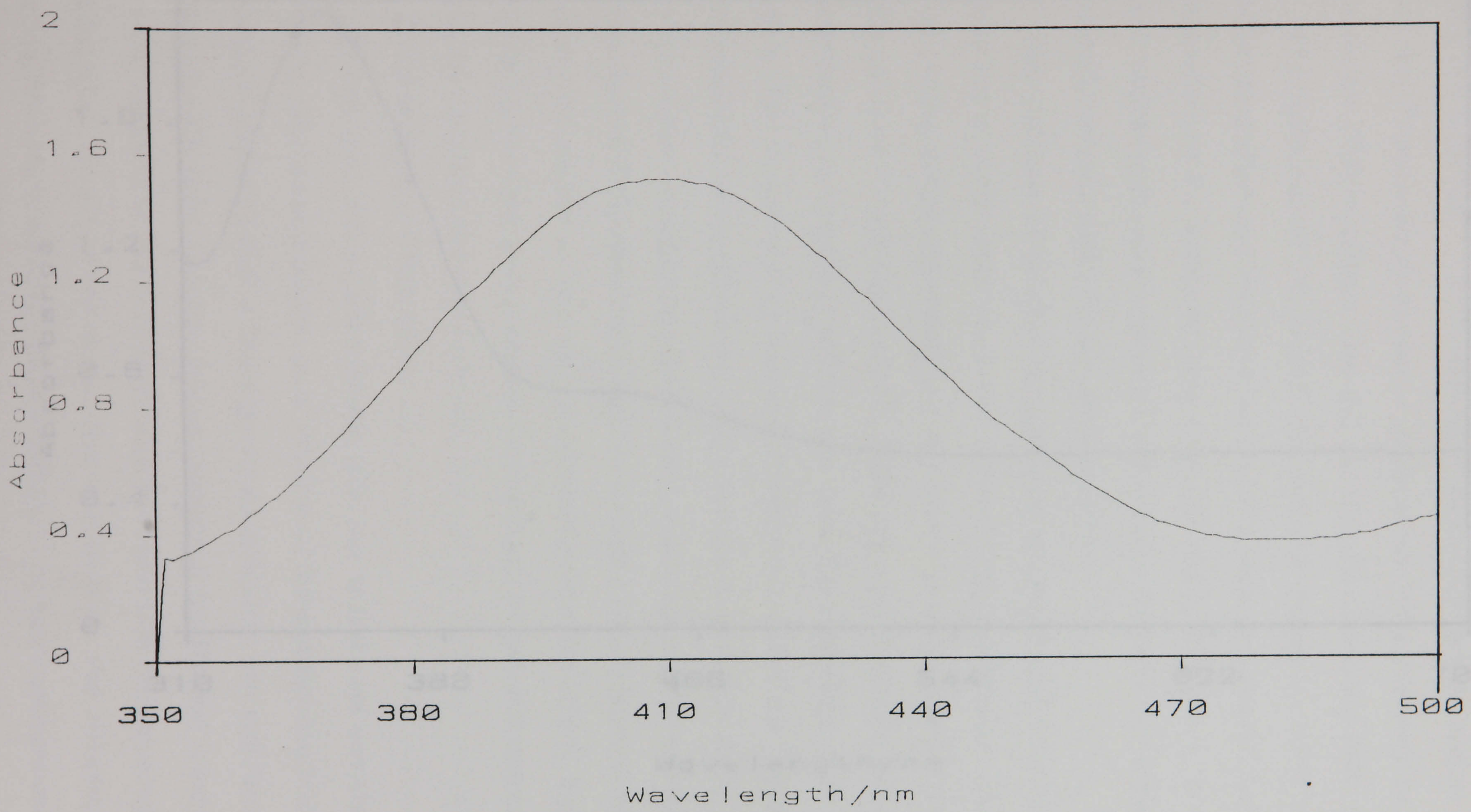

Figure 3:15 Spectrum Scan to obtain λ_{max} for Chromium (III) Solutions.

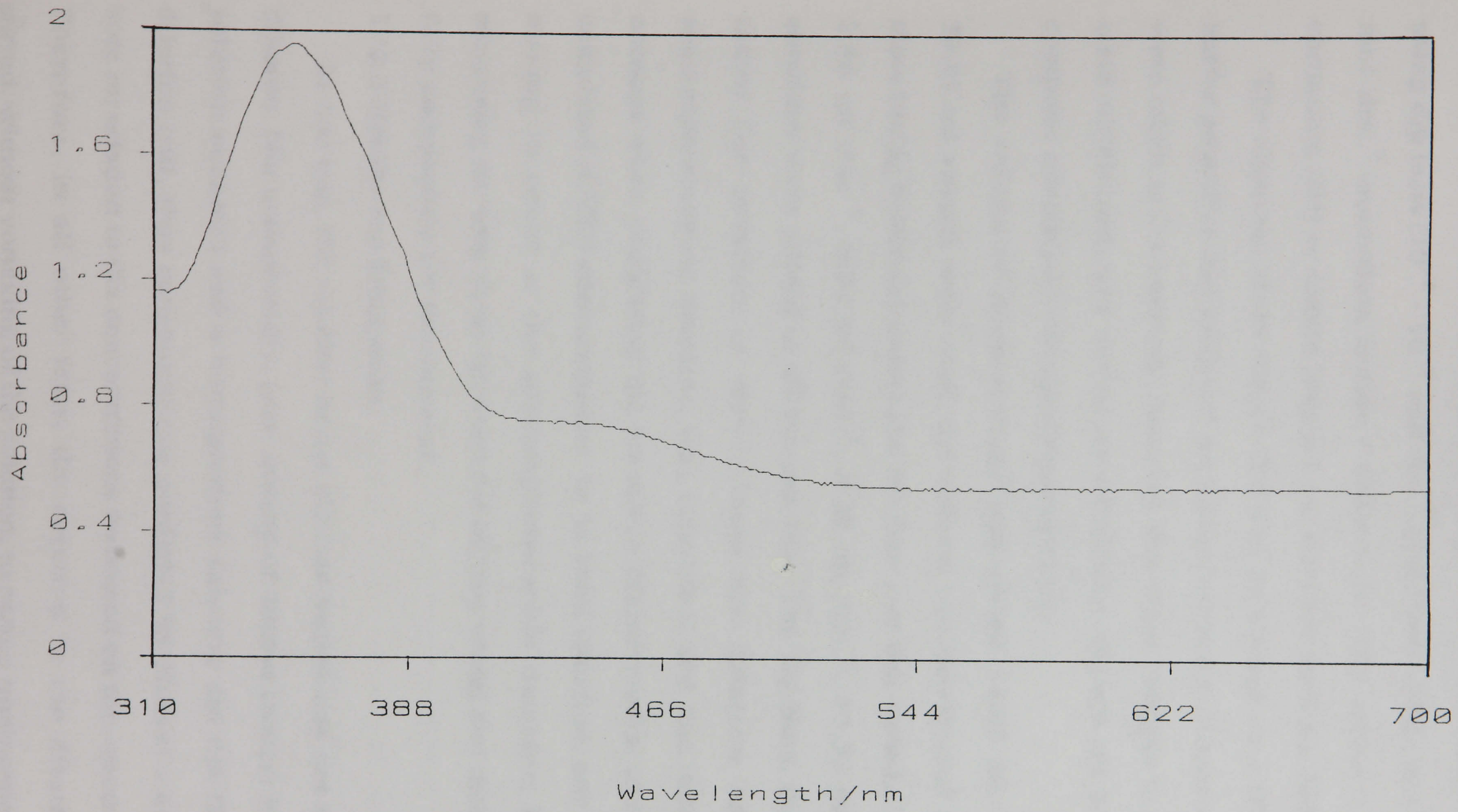

Figure 3:16 Spectrum Scan to obtain λ_{max} for Dichromate Solution

equimolar solution of 5 x 10^{-2} mol dm^{-3} chromium (III) nitrate and potassium iodide (BDH Ltd.). The iodide ISE was calibrated prior to use, using dip tests (10^{-1} - 10^{-5} mol dm^{-3} potassium iodide and in 10^{-1} - 10^{-5} mol dm^{-3} potassium iodide / chromium (III) nitrate) to show that chromium (III) or nitrate ions did not interfere with the ISE.

The response of the iodide ISE was monitored on a DVM through a buffer amplifier and recorded on a chart recorder. Absorbance readings were taken at 2 s intervals, ensuring that rapid changes in concentration were monitored, and stored as a function of time on a BBC Master computer interfaced to the spectrophotometer.

The volume of dilution vessel was varied, 14.65 ml, 32.50 ml and 39.55 ml vessels were used; the volume was determined accurately by mass (using deionised water) and the flow rate was varied, 2.21 ml min^{-1}, 2.86 ml min^{-1}, 6.82 ml min^{-1}, 8.20 ml min^{-1}, 13.33 ml min^{-1}. The solutions were stirred in all but one test. The lag-time, that is the time taken for solution to travel from the dilution vessel to the spectrophotometric detector, was measured, and this delay taken into account when comparing the measured (experimental absorbance) and calculated (CVD) concentrations. In an ideal situation, one would prefer mixing to occur at the spectrophotometric detector, however, by measuring the time delay between the mixing vessel and detector, one can fully compensate for this interval.

3.12.3 Results and Discussion.

In one test, the solution in the dilution vessel was not stirred during dilution. Not unexpectedly, poor mixing of diluent (water) with the initial solution occurred and a homogeneous solution did not flow from the dilution cell, thus concentrations predicted by Horvai's equation (3.1) bore no relation to the concentrations measured on the spectrophotometer. Therefore, in all other tests, the solution in the dilution cell was stirred, without vortexing of the solution, to ensure homogeneous mixing.

When a fast flow rate was used, 8.20 ml min^{-1}, it was more difficult to follow the absorbance during dilution and the ion selective electrode had difficulty in following the dilution, this is shown in figure 3:17. Also, the disparity of values (observed *versus* expected) increased.

The decrease in absorbance of chromium (III) during dilution is shown in figure 3:18. The flow rate during this experiment was 6.98 ml min^{-1} and the volume of the dilution vessel 32.50 ml. As the solution became more dilute, the ratio of observed / theoretical concentration decreased.

Using a slower flow rate, 2.21 ml min^{-1}, with the same dilution vessel (figure 3:19), a similar trend was observed although now the discrepancy between the spectrometric and predicted concentrations was much smaller than during fast flow experiments.

A smaller dilution vessel, 14.59 ml, was used at diluent flow rates of 6.98 ml min^{-1} and 2.87 ml min^{-1}; the absorbance neasurements made during dilution are shown in figure 3:20, 3:21. Once again there was a large disparity between expected and observed values. Due to drifting potentials below 10^{-5} / 10^{-6} mol dm^{-3}, at which concentrations stirring is a much more influential parameter, and the difficulty in obtaining absorbances on this spectrometer at lower concentrations, dichromate was not used in further investigations, though its use had substantiated arguments that there are flaws in the CVD technique.

From figure 3:22, one can see that the disparity of the calculated and experimental (spectrophotometric) concentrations was much greater when a fast flow rate of dilution was used; equation 3:1 predicts a more rapid dilution rate than was observed with the spectrometer. This lag in the spectrophotometric results was believed to be due to inefficient mixing of the diluent with the initial solution. In effect, there is a large dead space in the dilution vessel, the volume of which depends on the flow rate used; this is shown schematically in figure 3:23. Horvai's equation (3:1) does not take dead space into account, but assumes homogeneous

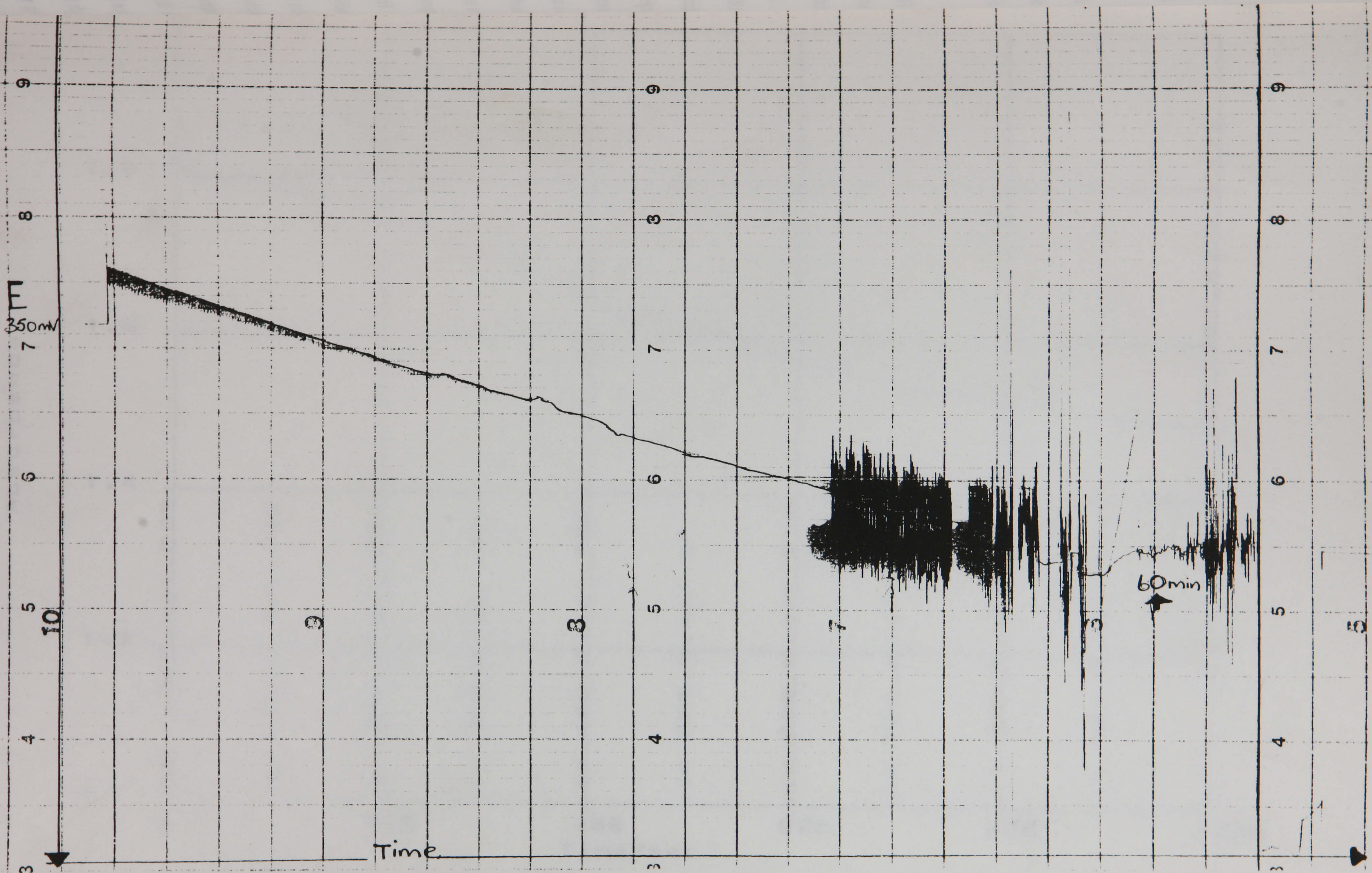

Figure 3:17 Chart Recorder Trace showing Response of the Iodide ISE during CVD Experiment with fast (> 10 ml min^{-1}) Flow Rate.

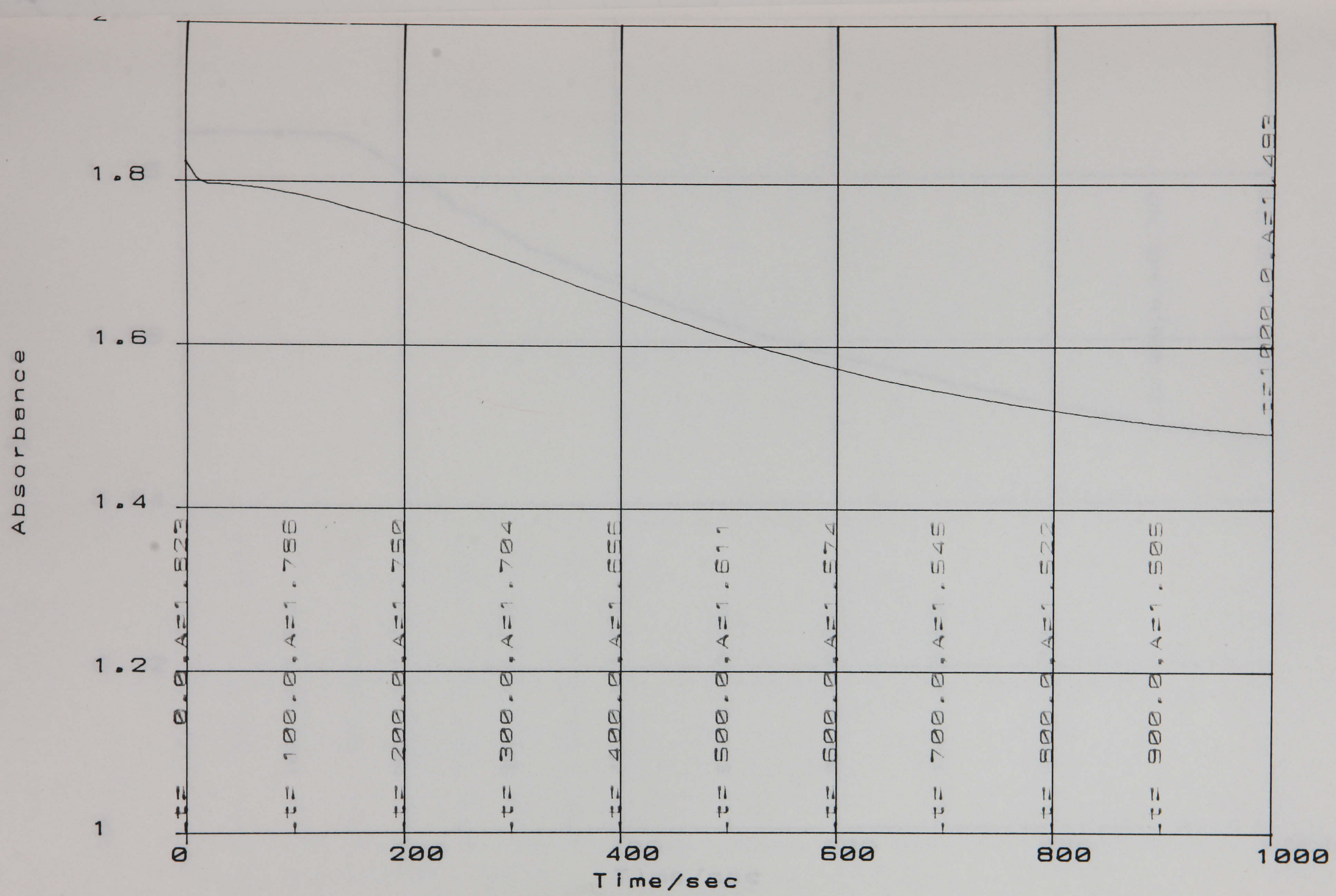

Figure 3:18 Decrease in Absorbance of Cr (III) during CVD Experiment.

Flow Rate = 6.98 ml min^{-1}
Volume of Dilution Vessel = 32.50 ml

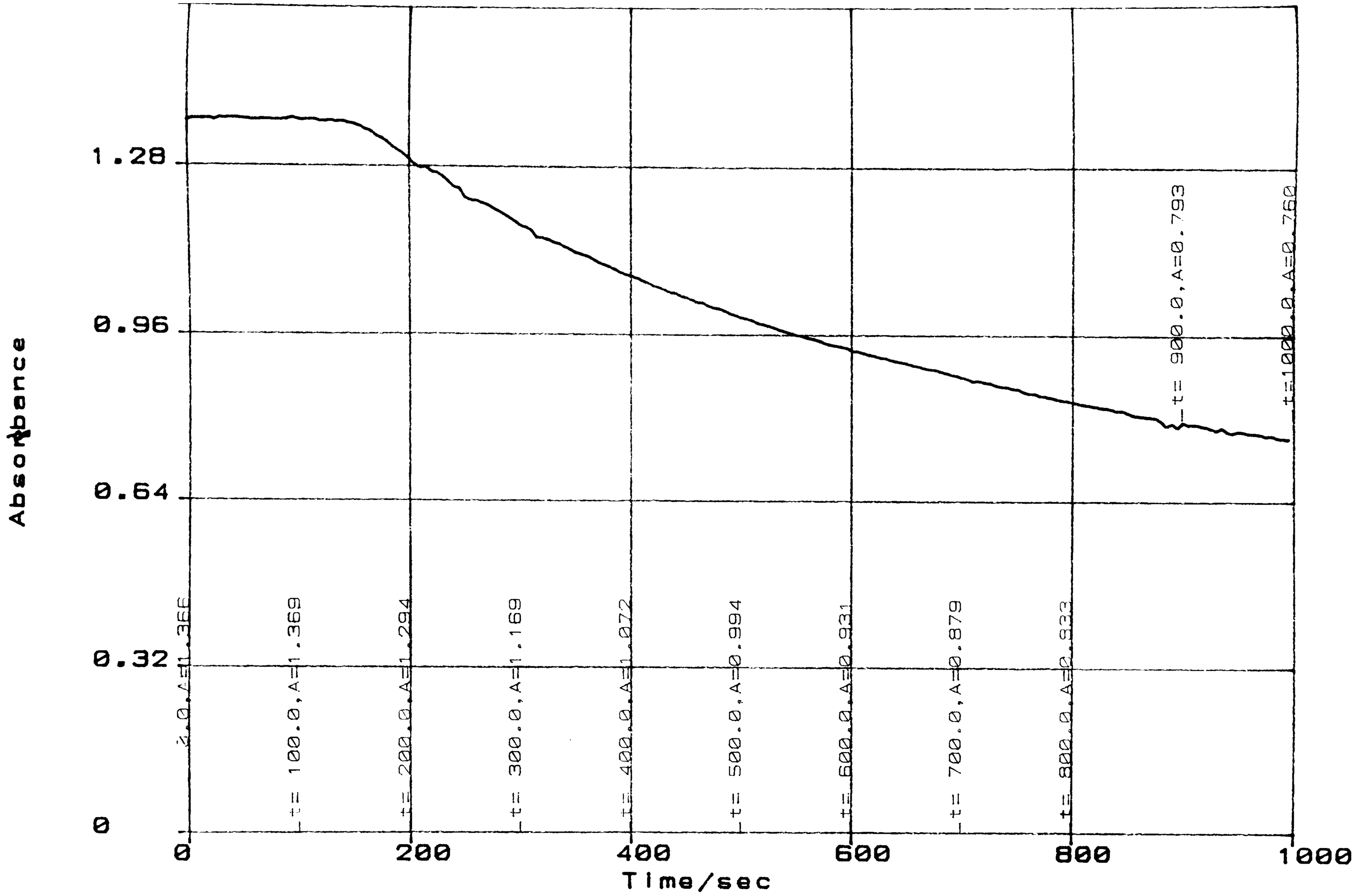

Figure 3:19 Decrease in Absorbance of Cr (III) during CVD Experiment.

Flow Rate = 2.21 ml min^{-1}
Volume of Dilution Vessel = 32.50 ml

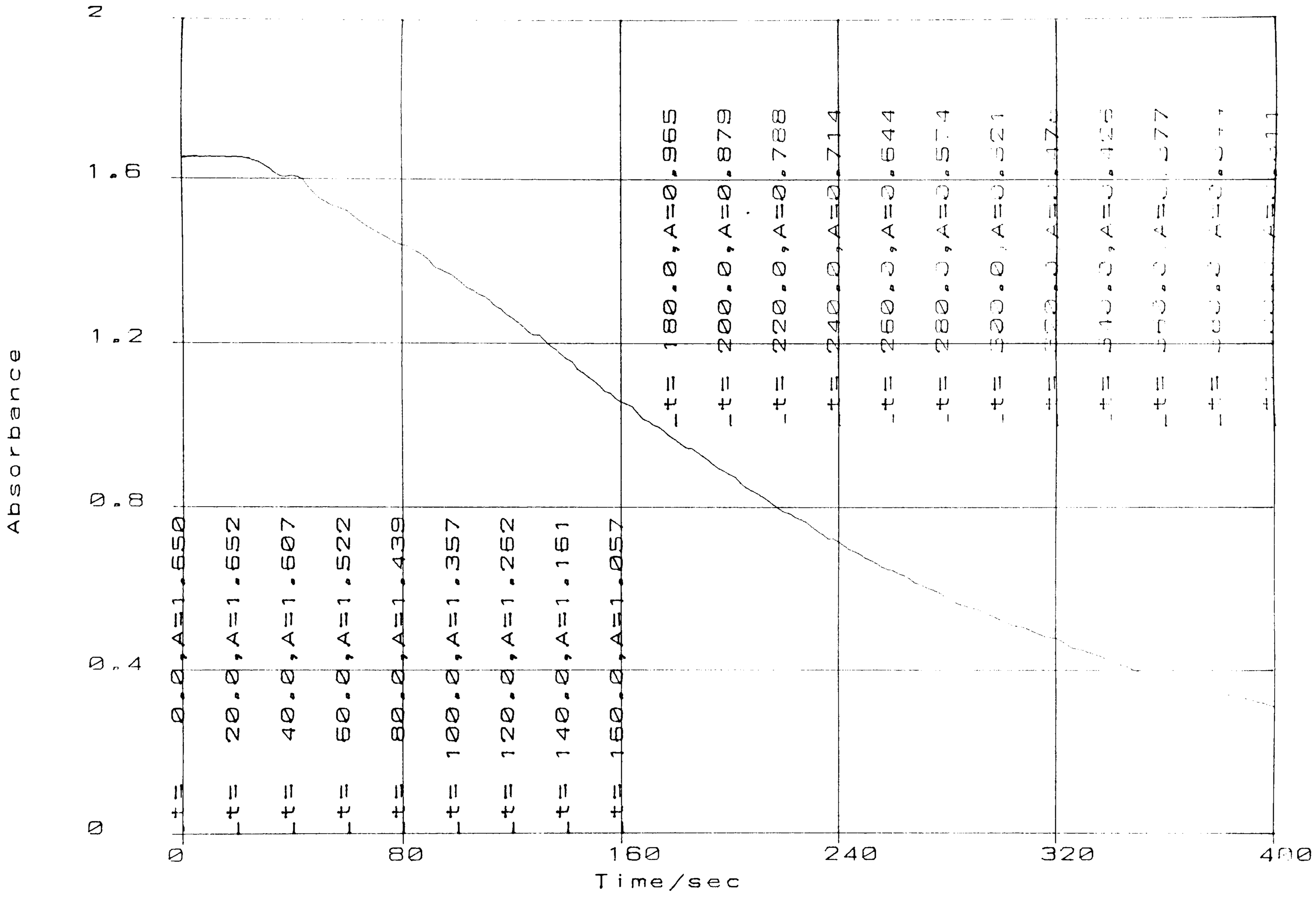

Figure 3:20 Decrease in Absorbance of Cr (III) during CVD Experiment.

Flow Rate = 6.98 ml min^{-1}
Volume of Dilution Vessel = 14.59 ml

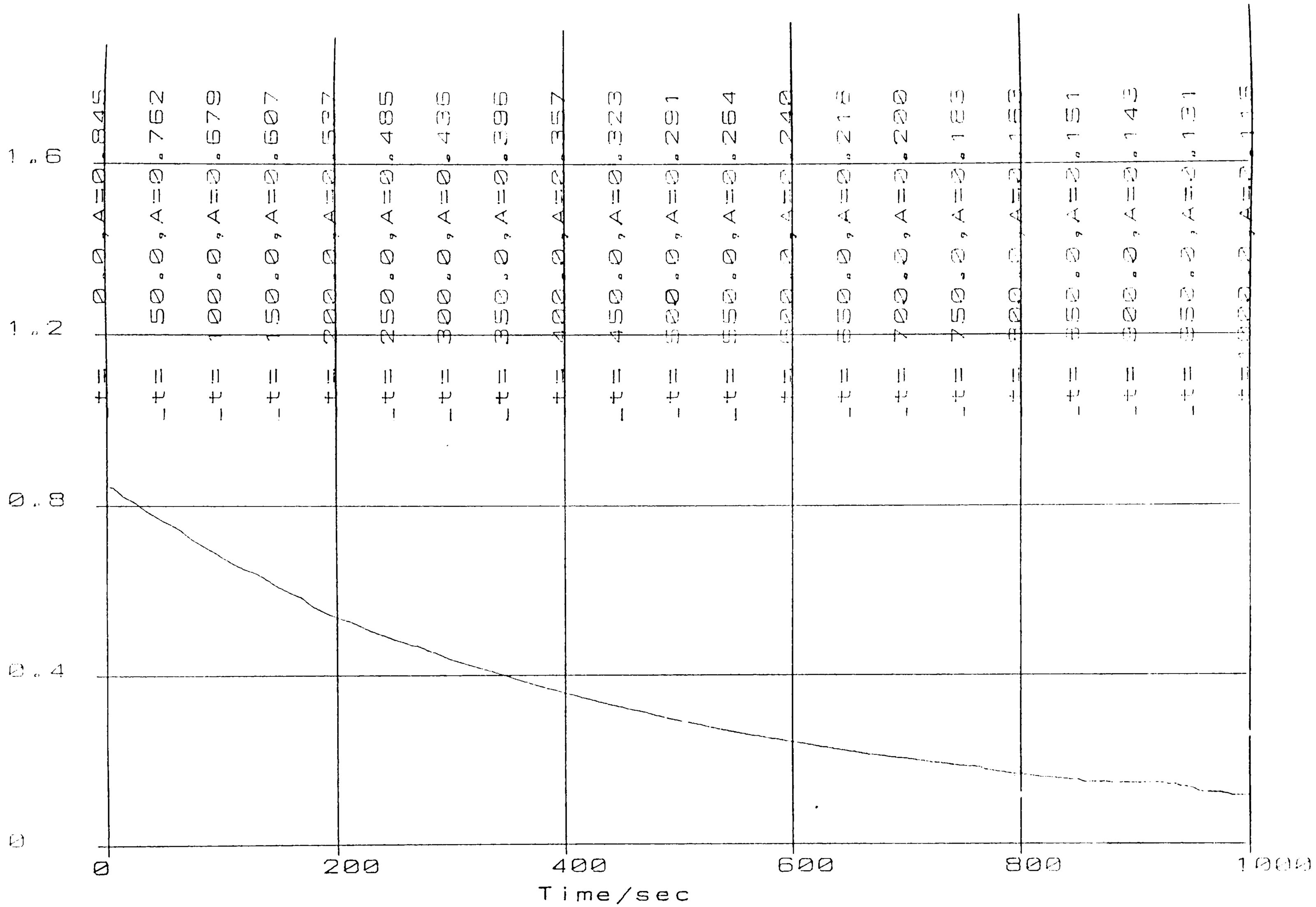

Figure 3:21 Decrease in Absorbance of Cr (III) during CVD Experiment.

Flow Rate = 2.87 ml min^{-1}

Volume of Dilution Vessel = 14.59 ml min^{-1}

Figure 3:22

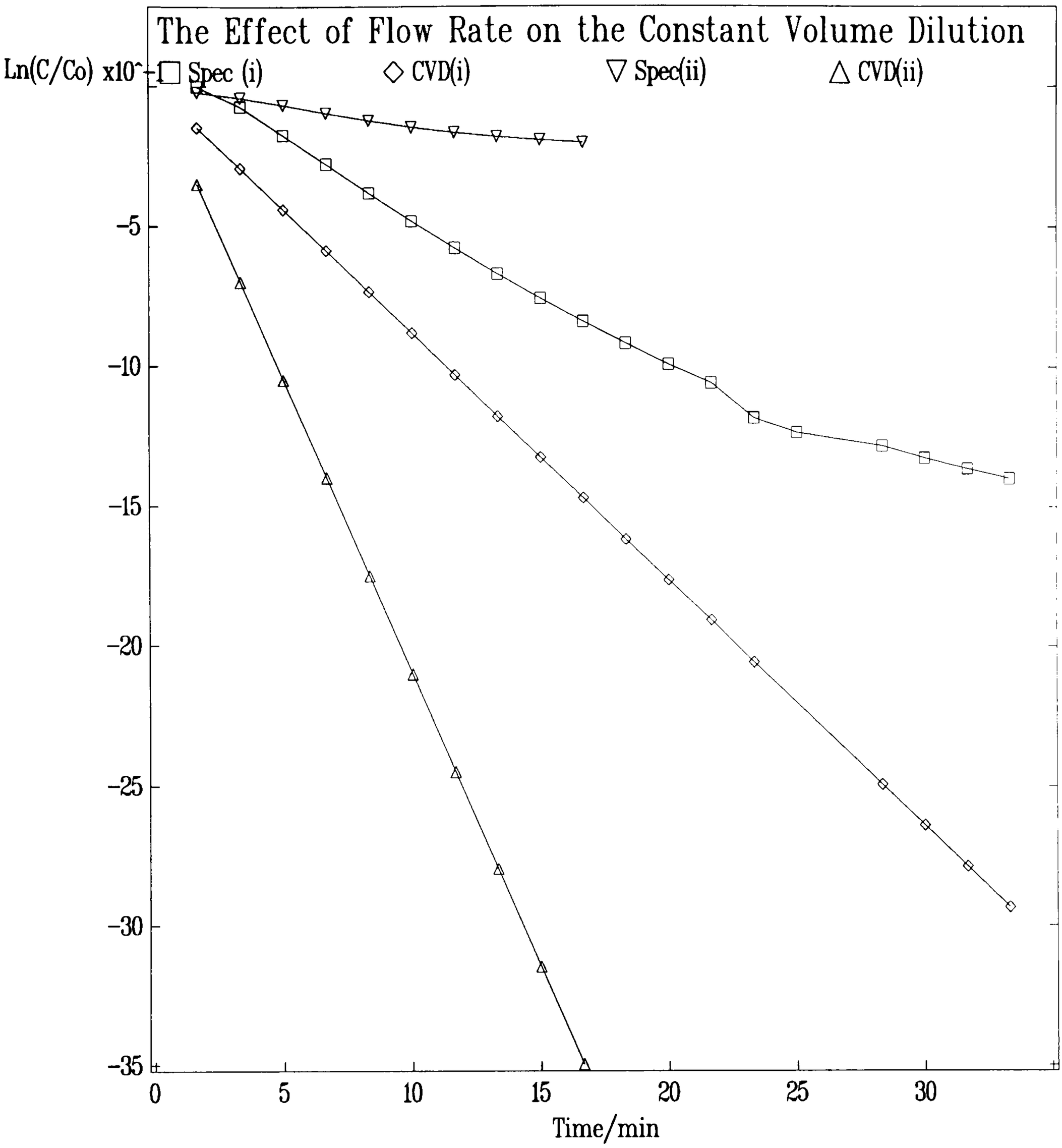

Volume of the Dilution Vessel = 32.50 ml

Flow rate (i) = 6.98 ml min^{-1}

Flow rate (ii) = 2.86 ml min^{-1}

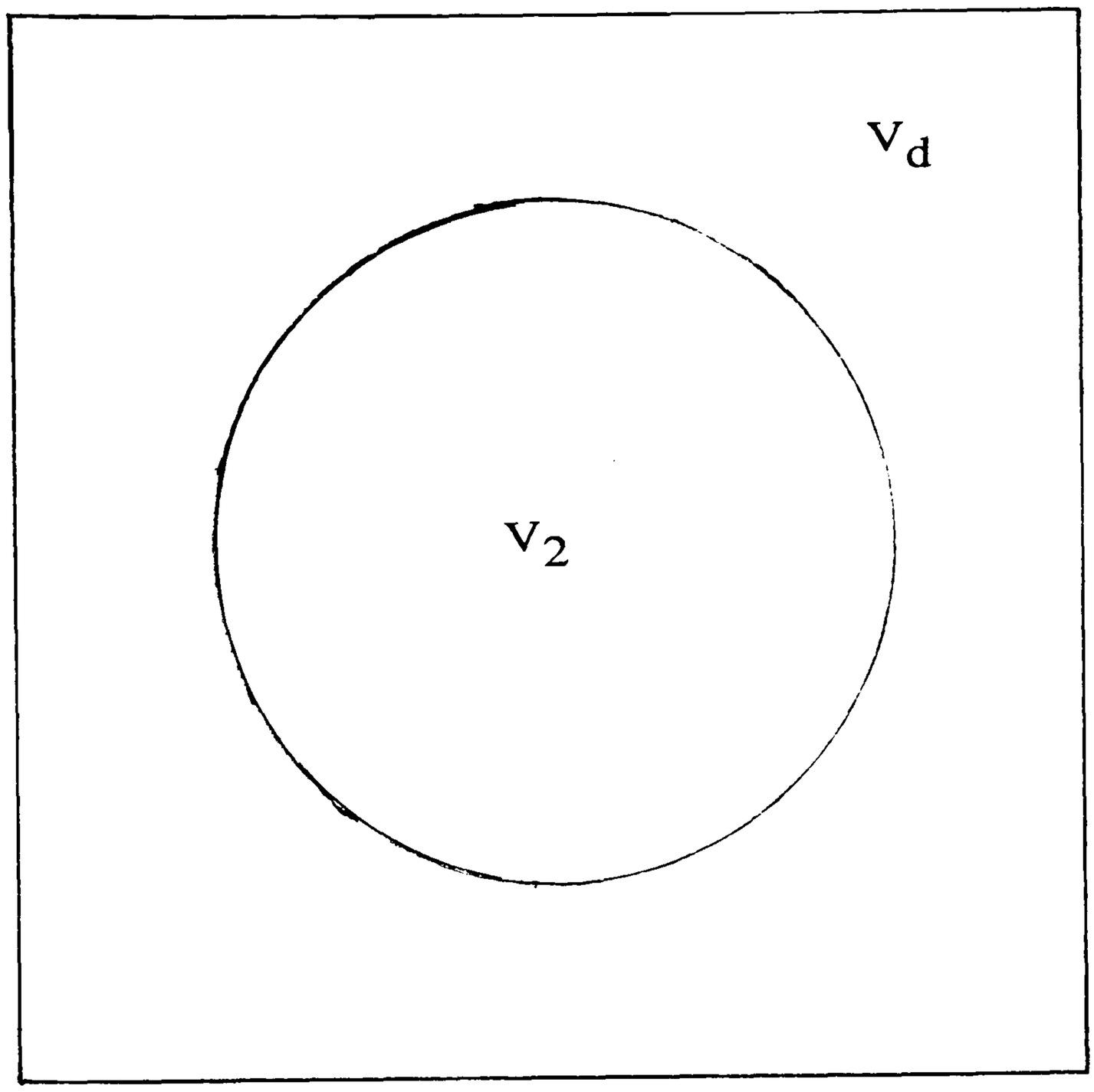

Figure 3:23 Schematic showing the Dead Space remaining in the Flow Cell during Dilution.

$$V_r = V_d + V_2$$

where V_r = total volume of the dilution vessel

V_d = dead space in the cell

V_2 = volume of the cell swept out during dilution

If the total volume of the cell is swept out during dilution, then equation 3:1 holds, that is

$$c = c_0 \exp(-Wt / V_r)$$

If the dead space in the cell is constant throughout the experiment, and there are no other parameters to consider, then equation 3:1 is modified to

$$c = c_0 \exp[-Wt / (V_r - V_2)]$$

In both cases, first order kinetics will be obeyed for the whole reaction (dilution). However, since first order kinetics were not obeyed, this model is too simple to explain the experimental results obtained.

solutions in the dilution vessel at all times.

Since reasonably straight line graphs were observed for ln (c / c_o) *versus* time, t, (figure 3:22) one can see that first order kinetics were approximately obeyed throughout the dilutions. At faster flow rates, a tailing off of the experimental curves was observed (figure 3:24) which corresponds to a deviation from first order kinetics. From these studies, we can see, as expected, that the 'observed', experimental and predicted rate constants are best matched using slow flow rates, *ca*. 2.5 ml min^{-1}. The gradient of the line, for each line plotted, gives the rate constant for the reaction (dilution). It is not, however, possible to determine the dead volume in the cell. A model based solely on two defined regions, effective volume and dead volume is too simple.

Determinations of selectivity coefficients using the mixed solution method method, keeping the concentration of primary ion constant (see section 2:7) can still be made with the constant volume dilution method. There will be an error in the determined c_j value, that is, the concentration of secondary ion, j, when the ISE fails to respond to the primary ion, i, due to the error in calibrating the time axis on the recorder. The CVD method predicts the dilution to have proceded further than it actually has, therefore the "cut off" concentration used to determine the selectivity coefficient, k_{ij}, is less than the experimental "cut off" concentration. For example, in Chapter 6, the potassium selective DOS membrane was found to have a $k_{K+,Ca2+}$ of 4.44×10^{-4}, that is calcium does not interfere to a very great extent. However, as CVD techniques were used to calibrate the Nernst response of the ISE and to determine k_{ij}, then there is an error in the time (concentration) axis, so that the cut off point of 4.44×10^{-5} mol dm^{-3} is most likely 8.88×10^{-4} mol dm^{-3}, giving a $k_{K+,Ca2+}$ value of 8.88×10^{-3}.

3.12.4 Conclusion.

Smaller dilution vessels gave the best results. Slower flow rates also

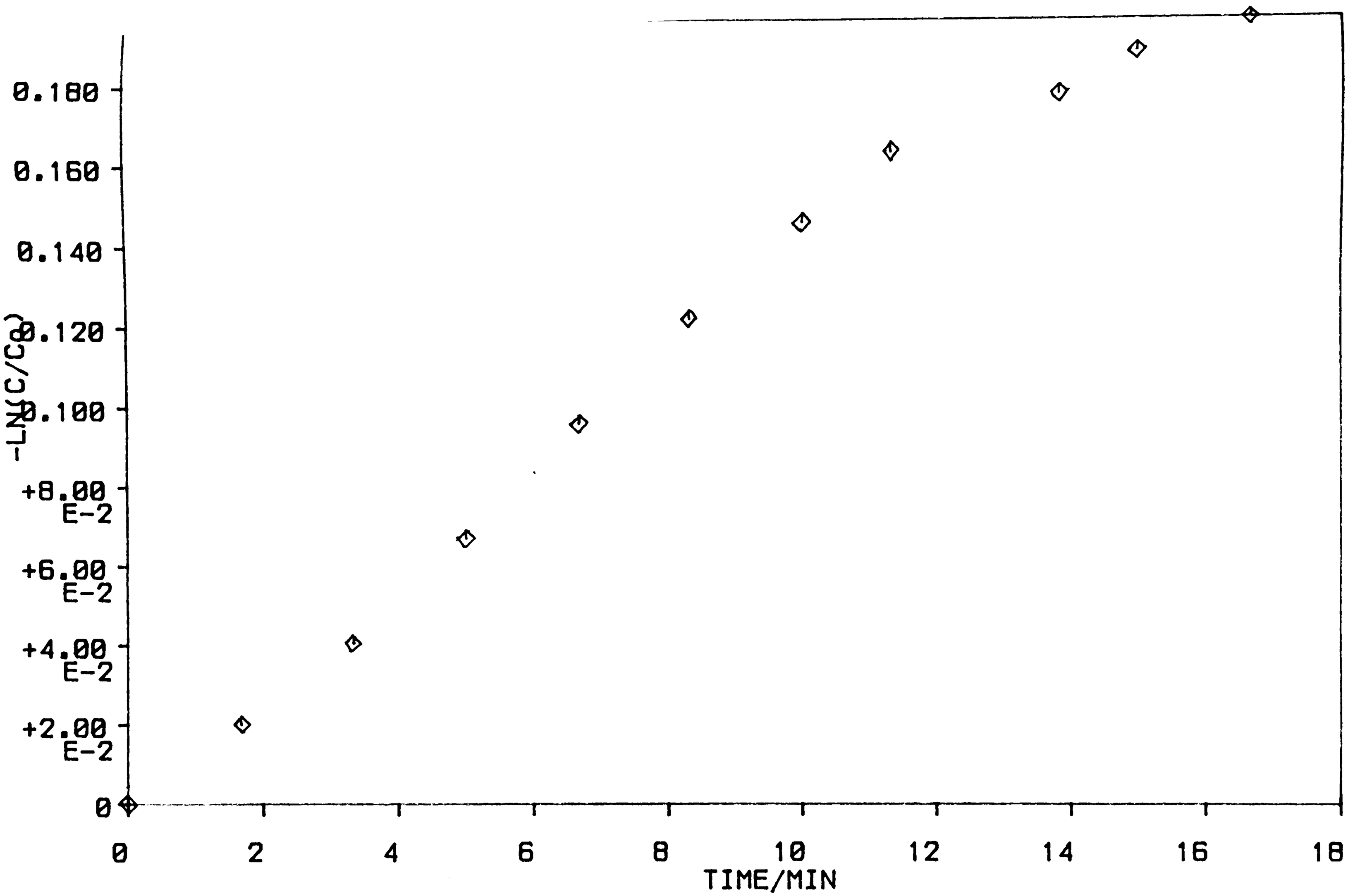

Figure 3:24 To show the deviation from first order kinetics at faster flow rates.

Flow rate = 6.98 ml min^{-1}

ensured good mixing could occur; flow rates of < 2.5 ml min^{-1} are suggested.

Using the dual detector system, the iodide ISE had difficulty in following the experiment when fast dilution rates were used (figure 3:17) leading to non-uniform mixing, hence very noisy response. This is because at faster flow rates the response time of the ISE is not sufficiently fast to allow the ISE to respond to the rapidly changing solution concentration.

The overall reaction (dilution), determined spectrophotometrically, approximately follows first order kinetics, except at low concentrations or very fast flow rates and the rate constants for these reactions can be obtained directly from a plot of $-\ln (c / c_o)$ *versus* time, t. The predicted and experimental rate constants are more similar at slower flow rates, here, 2.86 ml min^{-1}.

It is possible to use CVD techniques in the determination of selectivity coefficients if small dilution vessels and slow flow rates are used. In future work using this method, the volume of the dilution cell and, more importantly, the flow rate should be reported. Summarising, the CVD method is an attractive technique, simple to use and readily automated, however the technique must be used with caution.

References.

1. "Specifications for Laboratory pH Meters."
   B.S. 3145 ,1978

2. "Chemical Sensors" Chapter 1
   ed. Edmonds T.
   Glasgow, Blackie 1987

3. Friedman S.M.
   In "Glass Electrodes for Hydrogen and Other Cations."
   ed. Eisenman G.
   Marcel Dekker, New York 1967

4. Burton R.P.
   In "Ion Selective Electrodes" Vol II, Chapter 2
   ed. Covington A.K.
   CRC Press, Boca Ratan, Florida 1979

5. Sibbald A., Whalley P.D. & Covington A.K.
   Anal. Chim. Acta 1984, **159**, 47

6. Bergveld P. & Sibbald A.
   In "Analytical and Biomedical Applications of Ion Selective Field Effect Transistors" Chapter 9
   Wilson & Wilson's Analytical Chemistry. Vol XXIII
   ed. Svehla G.
   Elsevier Science Publishers, Oxford 1988

7. "Instrumental Methods in Electrochemistry" Chapter 16
   ed. Delahey P.
   Interscience Publishers, J. Wiley & Sons, New York 1954

8. Marcovic P.L. & Osburn J.O.
   Am. Inst. Chem. Eng. J. 1973, **19**, 504

9. Mattock G. & Band D.M.
   Chapter 16 of ref.3

10. Morf W.E., Lindner E. & Simon W.
    Anal. Chem., 1975, **47**, 1596

11. Whalley P.D.
    Ph.D. Thesis, University of Newcastle-upon-Tyne 1982

12. Papacostas S.
    Ph.D. Thesis, University of Newcastle-upon-Tyne 1985

13. Toth K., Gavaller I. & Pungor E.
    Anal. Chim. Acta 1971, **52**, 131

14. Johansson G., Karlberg G. & Wikby A.
    Talanta 1975, **22**, 953

15. Pungor E., Nagy G. & Toth K.
    Chapter 4 of ref. 4

16. Rechnitz J. & Kugler G.C.
    Anal. Chem. 1967, **39**, 1682

17. Blaedel W.J. & Dinwiddie D.E.
Anal. Chem. 1975, **47**, 1070

18. Shatkay A.
Anal. Chem. 1976, **48**, 1039

19. Morf W.E., Lindner E. & Simon W.
Anal. Chem. 1975, **47**, 1596

20. Fleet B., Ryan T.H. & Brand M.J.D.
Anal. Chem. 1874, **46**, 12

21. Morf W.E.
"The Principles of Ion Selective Electrodes and of Membrane Transport" Vol II
Elsevier Scientific Publishing Co., Oxford 1981

22. Nagy G., Feher Z.S. & Pungor E.
Anal. Chim. Acta 1970, **52**, 47

23. Skeggs L.T.
An. J. Clin. Pathol., 1957, **28**, 311

24. Ruzicka J. & Hansen E.H.
Anal. Chim. Acta 1984, **161**, 1

25. Hansen E.H., Krug F.K., Ghose K.A. & Ruzicka J.
Analyst 1977, **102**, 74

26. Bailey P.L.
"Analysis with Ion Selective Electrodes" Chapter 9
Heydon & Son Ltd., London 1976

27. Covington A.K. & Ferra M.I.A.
Anal. Chem. 1977, **49**, 1363

28. Horvai G., Toth K. & Pungor E.
Anal. Chim. Acta 1976, **82**, 45

CHAPTER FOUR

DEVELOPMENT OF A SENSOR-ACTUATOR TITRATION SYSTEM

4.1 Introduction.

A coulometric procedure is defined as the theory and practice of any analytical procedure that depends on Faraday's laws of electrochemical equivalence [1, 2]. Coulometry involves the measurement of coulombs (A s) required for reaction. The technique is based on the electrolytic reduction or oxidation of the analyte to a new oxidation state and can be used in the absolute mode so that only a single reference standard, the Faraday, F, need be used for a range of samples.

4.2 Historical.

In 1833, Michael Faraday [1] stated that " *for a constant quantity of electricity, whatever the decomposing conductor may be, whether water, saline solutions, acids, fused bodies etc., the amount of electrochemical action is also a constant quantity i.e. would always be equivalent to a standard chemical effect founded upon ordinary chemical affinity* ". This led to "*the law of constant electro-chemical action*" whereby "*the chemical power of a current of electricity is proportional to the absolute quantity of electricity which passes.*"

From these emerged Faraday's two laws of electrolysis [2-4]

$$m = Izt \qquad (4.1)$$

where m = mass of species liberated in grams

I = current in Amperes

t = time in seconds

z = "*electrochemical equivalent*" of the material liberated, now replaced by relative molecular mass, M_r and number of electrons, n, transferred in the reaction.

which gives

$$m = (ItM_r) / zF \qquad (4.2)$$

where F = Faraday constant

Q = number of coulombs required in the reaction

$$Q = It \qquad (4.3)$$

more often expressed as

$$Q = I \int dt \qquad (4.4)$$

As a corollary to this, in the late 50's, the coulomb was considered as a primary standard for analytical procedures [5,6] due to the accuracy (and simplicity) of the measurements. However, the coulomb was not made a primary standard, but is still maintained as a means of standardising analytical methods.

The first application of coulometric analytical methods was reported by Grower in 1917 [7]. He determined the total quantity of tin on tinned copper wire by measuring the charge required to remove tin and alloy from the wire; this was later repeated by Cambell and Thomas [8].

The wide application of coulometric titrations was first appreciated by Szebelledy and Somogyi [9, 10] who determined thiocyanate using coulometrically produced bromine from aqueous bromide ions. However, their apparatus was cumbersome and their method was not appreciated by other workers for another ten years [11, 12].

4.3 Background.

As coulometry is an absolute method, it requires only one-time calibration. The titrant is generated in-situ, therefore one can dispense with primary standards and standardizing reagents thus there is no storage of chemicals, obviously an advantage for labile reagents. The total charge required to carry out an electrolysis can be determined using equation (4.4).

The sample solution requires no dilution and the technique is therefore suitable for ultra(micro) analysis. The method depends on 100% current efficiency, i.e. the reaction must be exclusive, which relies on correct choice of supporting electrolyte (see later), no side reactions e.g. no continuous Faradaic current due to electrolysis of the solvent or

impurities present in solution such as dissolved gases (giving rise to impurity Faradaic currents) and the correct cell geometry (see section 4.4.5), as well as the nature and previous use of the the generating electrodes. These may be cleaned before use to remove passivating surface films e.g. silver bromide and platinum oxide on silver and platinum anodes respectively. It is possible to test the current efficiency of a cell by running a blank prior to titration. Current efficiency is defined by

$$\% \text{ Current Efficiency} = I_s / (I_s + I_B + I_{IMP}) \times 100 \quad (4.5)$$

$$= I_S / I_T \times 100 \quad (4.6)$$

where I_s = sample current

I_B = electrolysis current of the solvent

I_{IMP} = electrolysis current of impurities in solution

I_T = total current passed

Combining these advantages with ease of automation and coulometry is seen to be a convenient and accurate means of analysis. Several reviews are available discussing the development and application of coulometry [13 -24].

The feasibility of using ion sensitive field effect transisitors (ISFETs) in rapid acid-base volumetric titrations was identified by Bos, Bergveld and Van-Blaauw [25] which rapidly lead to the application of a micro-processor controlled [26-28] coulometric method of hydroxyl generation. The Netherlands group further explored the possibilities of coulometry and designed a chemical sensor-actuator [28, 29] with improved stability by means of a feedback information loop [30], which enabled the pH of a solution to be kept at a constant pH by generation of hydrogen or hydroxide ions, as required. Gold electrodes were responsible for the hydroxyl generation and pH-sensitive ISFETs were used for end point determination of sub-microlitre titrations. The system was adapted

for use as a CO_2 sensor [30] and for enzyme studies [31].

This work has extensive applications in studies requiring very accurate measurements of concentrations of small, micro-litre, samples e.g. in clinical chemistry. Also, in clinical chemistry it is not the total concentration of an element which is important but the **available** ionized species. Spectroscopic methods, normally used in clinical work, measure the total concentration of a given element, providing information of limited importance.

pH is one of the most precisely measured parameters. Very small variations in pH may have dramatic effects; normal human blood pH lies in the range 7.36 - 7.44 [32]; outside pH 7.0 - 7.8, death ensues rapidly [33]. Aspects of clinical chemistry are discussed more fully in Chapter 6. It is important that the indicator electrode or ISFET is not prone to drift or signal fluctuation; a variation of 1 mV in output signal is equivalent to 4 % concentration error for univalent ions and to 8 % variation divalent ions, therefore, frequent recalibration is necessary to overcome longterm drift problems [34]. However, as stated earlier, using a sensor-actuator system any variation from a pre-defined pH value can be compensated for by addition of coulometrically produced hydrogen or hydroxide ions (depending on the current direction) by hydrolysis of water according to

$$2\ H_2O \rightarrow 4\ H^+ + O_2 + 4\ e^- \qquad (4.7)$$

$$2\ H_2O + 2\ e^- \rightarrow 2\ OH^- + H_2 \qquad (4.8)$$

The sensor-actuator system may be used to control the progress of coulometric titrations to obtain accurate end point determinations.

The aim of the Newcastle work was to design a similar system for in-situ coulometric titration of microlitre samples using a constant current source, altering the magnitude of each charge impulse by controlling the duration of each pulse. Initial work was carried out using ion selective

electrodes, ISEs, with the aim of optimizing the titrimetric system before introducing ISFETs for end point determinations. During development of the sensor-actuator system, the field effect of the generating electrodes was found to vary using different indicator electrodes and cell arrangements and a study of this phenomenon was carried out. An appraisal of the titration systems used is included.

4.4 Design and Development of Apparatus.

4.4.1 General Cell Features.

The ohmic resistance of the cell must be as low as possible and, as stated above, the current efficiency 100%. The ratio of working electrode area to cell volume should be large, the current density as low as possible on the generating electrode, and there should be efficient agitation of the solution to ensure complete mixing of reagents [35]. The salt bridge or reference electrode should be close to the inert working electrode, the product at the counter electrode must not interfere with the titration reaction and the detector e.g. indicator electrodes, must be placed to give rapid response. Details of these are discussed in the following sections.

4.4.2 Cell Design.

A large working electrode to cell volume ratio is required to minimize the ohmic drop. The cell, therefore, should be sufficiently large to house all equipment; electrodes, generating and indicator electrodes where applicable, gas inlet and outlet (to provide an inert gas blanket), and to allow efficient agitation of the solution [36].

Usually, a two compartment cell is used (see figure 4:1). The auxiliary electrode is immersed in supporting electrolyte in a side arm, separated by a frit or plug (see 4.4.3). The cell should be gas tight. Numerous designs have been used [37-44]. However, for this work, using an unstirred system, a very simple design is adequate. Altering the cell geometry does not affect the time constants for charging or relaxation of the capacitive double layer as the geometric capacitance, C_g, is much smaller than the

Figure 4:1 Two Compartment Cells used in Coulometric Analyses.

capacitance of the double layer, C_d.

4.4.3 Separators.

These are most often used when gases are produced at the auxiliary electrode. The separator is usually a sintered glass diaphragm; the optimum porosity of the glass is determined by balancing two factors. The coarser the porosity the smaller the electrical resistance but also the greater the leakage rate and rate of diffusion; a dye may be used to study the diffusion rate. An agar plug [45] or ion exchange membrane [46, 47] may also be used. Studies carried out by Lakshminarayanaih [48], to investigate the diffusional and viscous flow in cells, showed that dialysis tubing acted as a more effective barrier than glass filters against hydrodynamic flow. The length of the tube connecting the auxiliary compartment is also important; if it is short, there is a more profound effect [35].

4.4.4 Depolarizers.

These are reagents added to the electrolyte to prevent undesirable electrode reactions occuring e.g. Bergveld et al. [26] used quinhydrone (1:1 hydro p-benzoquinone / hydroquinone). The reaction

$$\text{p-benzoquinone} + 2\ H^+ \rightleftharpoons \text{hydroquinone}$$

occurs at a lower redox potential than hydrogen formation [49] and thus suppresses gas evolution. However, it should be noted that hydroquinone is a weak acid and in very alkaline solutions the pH may be affected.

4.4.5 The Working Electrode.

In most electrochemical processes, the working electrode has as small a surface area as possible in order to minimize the bulk concentration. Coulometric techniques, however, require the surface area to solution volume ratio to be as large as possible, maintaining a low current density, and ensuring that there is little change in the resistance during reaction, hence foil or gauze electrodes are preferred. In order to reduce noise in the measuring and electrical circuits, the electrodes should be rigid.

A range of materials has been investigated for electrode production. Industrial anodes, ca. 1900, were made of gas carbon which were slowly consumed. Wax impregnated carbon graphite [50, 51], carbon paste [52], pyrolytic carbon and glassy carbon [53] electrodes have all been used. Carbon electrodes have the advantage of low background currents in potentiostatic determinations and are important for microanalysis.

Platinum, gold and palladium electrodes can all be operated in anodic mode. Most often used is platinum, despite a thin oxide film which forms at high potential [49] (the value of which is pH dependent), which is detrimental to electrode performance. Gold is readily attacked and will also form an oxide film, though different in nature to that in platinum. However, gold is also susceptible to attack by chloride and cyanide ions.

The activity of the pure metals at low currents is [54]

$$Pd > Pt = Au > Ag$$

These materials can also be used for cathode construction, though platinum and mercury are most commonly used. Mercury is extremely effective at low potentials due to the high overpotential of hydrogen on mercury.

As the working electrode is inert, within a certain potential range e.g. 0 - 0.8 V for platinum, the equilibrium position of the reaction is not influenced by the material used, however, the rate is affected.

4.4.6 The Auxiliary Electrode.

As stated earlier, the auxiliary electrode may be immersed directly in the sample solution providing the product at this electrode does not interfere with the titration reaction. However, this is only the case when an irreversible single step reaction occurs at the working electrode. In general, it is better to use a separate cell or separating diaphragm or to introduce a depolarizer to prevent generation of interferents.

The auxiliary electrode should be positioned to ensure uniform current density across the working electrode - deviation from this leads to a

variation in the potential difference across the working electrode, which in turn can give rise to areas of inactivity or production of side reagents on this electrode. A silver anode auxiliary electrode may have a silver error, that is slight solubility of the electrode which can coat the platinum cathode [55]. Using a separator or depolarizing agent the effect of this dissolution may be suppressed.

4.4.7 Supporting Electrolyte.

This must be very similar to the working electrolyte. In a flow system it is possible to use the supporting electrolyte to remove unwanted side-products, however, there is then also the possible loss of working electrolyte and sample by converse migration.

Ions must migrate between the working and auxiliary compartments; this is Faradaic conductance and is necessary for current to flow, only neutral species do not migrate. All ions in the system contribute to the Faradaic current, the extent to which they do so is determined by their concentration, mobility, magnitude of charge, the electrode polarity and the sign of the charge. This process can mean loss of the required species from the auxiliary compartment and, therefore, in order to reduce this effect, the following precautions may be taken:

1. the supporting electrolyte should be neutral (i.e. no migration) or of the correct sign i.e. cationic species for reduction, anionic for oxidation.
2. the supporting electrolyte should be comparable with the working electrolyte and therefore unnoticeable
3. the products at the auxiliary electrode should not interfere
4. both electrolytes (working and supporting) should be swamped with a high concentration of "inert" ions thereby reducing the transport number of the sample and by-product species.

4.4.8 Stirring.

Bergveld *et al.* [26] did not use stirred sample solutions but relied on

diffusion controlled processes for reaction on the ISFET gate. In the present work, solutions were agitated, enforcing convectional mass transport processes rather than diffusion processes to control the rate of reaction.

Stirring of the working electrolyte should be efficient without being vigorous as this leads to cavitation, loss of the sample and exposure of the electrode. The auxiliary electrolyte is not usually stirred, unless the junctions are well immobilised, as electrolytes from the auxiliary compartment (and the salt bridge) are sucked into the working compartments.

The most common forms of agitation are:

1. magnetic stirrer - Lindberg [35] showed that the efficiency of stirring was not affected by the bar size or stirring rate.
2. gas stirring [56] - although generally insufficient on its own
3. ultrasonic stirring [56]
4. vibrating electrode [57]
5. thermal convection electrode [58].

Measurements are made after a predefined time delay to ensure good mixing and a homogeneous solution is assumed in all cases.

4.4.9 Detectors.

As in volumetric titrimetry, a range of detectors may be used for coulometric titrimetry. These include colorimetric and spectrophotometric techniques, however, in this work, as with other workers [59-61], a potentiometric detector was used, an ion selective electrode versus a reference electrode.

a) The Indicator Electrode.

In amperostatic methods, the indicator electrode should preferably be outside the generating field but close to the working electrode, thereby ensuring rapid end point determination. Current lines of the generating electrode pair affect the indicator electrode leading to an error signal

dependent on the cell geometry and the electrodes [62].

b) The Reference Electrode.

A calomel, or silver / silver chloride, double junction reference electrode is most commonly used, though Herrmann *et al.* [63] expressed concern at the use of a calomel reference due to the higher impedance of these electrodes making them susceptible to power line frequency noise. They suggested using a coupled reference electrode system combining a platinum wire reference electrode with the calomel reference electrode. In pulsed operation, only the low impedance wire reference electrode operates, acting as a noise filter.

No current should be carried by the reference electrode as this leads to polarization and therefore a potential shift.

4.4.10 Atmospheric Gases.

i) Removal of Dissolved Oxygen.

The presence of oxygen during anodic processes is not usually a problem, though deoxygenation is advised. For cathodic processes oxygen removal is a necessity to prevent interference due to oxygen reduction. In aqueous media in contact with air, 2×10^{-4} mol dm^{-3} of dissolved oxygen exists; this can be reduced to 10^{-5} mol dm^{-3} by bubbling oxygen free nitrogen through the solution, and to 2×10^{-6} mol dm^{-3} by boiling and cooling with a nitrogen flow. This latter method was used here for oxygen and carbon dioxide removal (see following section). Only by purifying nitrogen gas through a scrubber e.g. hot copper or chromium (II) sulphate can the concentration of dissolved oxygen be further reduced, to less than 10^{-6} mol dm^{-3}.

ii) Removal of Dissolved Carbon Dioxide.

It is always stated in the literature that carbon dioxide must be removed for all but the most uncritical acid-base determinations. The general method for removing dissolved carbon dioxide is

a) boil distilled water, in a conical flask, for ca. 30 min

b) cool in ice, with bubbling nitrogen, until cold

c) stopper flask containing water under a nitrogen blanket.

Complete removal of carbon dioxide is impossible at pH greater than 7.5. In order to obtain 100 % current efficiency, degassed solutions are recommended.

4.4.11 Constant Current Systems.

As stated earlier, the system was designed to operate in constant current mode, which is one of the most precise analytical techniques [64]. Using sophisticated potentiostats, a precision of 1 in 10^6 is possible [40], but imprecision of international standards [40, 65] limit reliability to ~ 10 ppm. The accuracy of the method is dependent on 100 % current efficiency, as discussed in 4.3.

The value of charge, Q, can be obtained by integrating the current over experimental time (equation (4.4)) or conversely by ensuring there is no fluctuation in the current and thus calculating directly the charge passed from equation (4.3). To ensure no variation in current, e.g. due to mains modulation or changes in resistance, a feedback loop from the input to a resistor may be utilised which compensates for signal variation.

4.4.12 Pulse Generation.

It is preferable to use a charge step method with pulses of constant current applied to the cell for short duration (0.1 - 1.0 μsec). Since the pulses are short and the corresponding charge injection is small, only charging of the double layer will occur, with negligible charge transfer reaction. Pulsed systems also allow accurate end point determinations by preventing overshoot of the end point.

A major advantage of pulse injection systems is that measurements are made at open circuit i.e. when no external current flows, hence the ohmic drop of the cell is unimportant and it should be possible to make measurements in solutions of high resistance. In reality, if the solution does have a very high ohmic resistance, then more time is required to

deliver charge. A time delay between charge injection and measuring allows discharge of the capacitive double layer, hence there is little competition between Faradaic and non-Faradaic processes.

The shape of the pulse is not important (e.g. square, saw-tooth, sinusoidal) and the pulse is commonly produced by discharging a small capacitor across the electrochemical cell. The capacitance of the double layer is never lower than that required to produce the impulse, therefore all charge goes to the cell. However, the charge injection causes the electrode potential to shift from its original value, E_i, to a new value, E_q, and

$$E_q - E_i = \Delta q / C_d \qquad (4.9)$$

where q = the charge pulse applied, in coulombs

C_d = the capacitance of the double layer

The charge decays through Faradaic impedance and the potential relaxes to E_q. If it is not possible for E_q to decay through Faradaic discharge, Faradaic current, I_F, will not flow and the double layer remains charged i.e. the electrode is polarized.

A disadvantage of the pulsed system is the high voltage across the cell as the pulse is delivered which can overload the amplifier; it is therefore important that an amplifier is chosen with this constraint in mind.

4.4.13 Computer Control.

By the mid 60's, the large quantites of raw data produced by chemical techniques, such as mass spectrometry and gas chromatography, prompted the development of more powerful computers. Data acquisition and charge or titrant delivery could be controlled by the same micro-computer [66, 67]; Lauer *et al.* [66] showed how this could be used for chronocoulometry. Stephens *et al.* [68] first reported computerized data collection for a controlled potential system and Jaycox *et al.* [69] showed the capabilities of extending this to a controlled current system. Other designs allowed electronically controlled titrations to be carried out [70,

71].

Early designs in the 60's used a passive interface. Although the computer could obtain information about the experiment, human intervention was necessary to make a decision as to the next action, which the computer would then implement (see figure 4:2). This was improved in the 70's [72, 73, 22] (figure 4:3) and early 80's [74, 75] when active interfaces were designed (figure 4:4). Now the behaviour of the experiment influenced the (preprogrammed) response of the computer. A preprogrammed number of pulses, which, in turn, controlled volume or charge, could be added to the titrant and after a pause of 3 s, the pH / mV signal could be read before addition of another aliquot. The computer stopped the titration either after a given number of pulses or when there was no increment in the (pH or mV) / volume added ratio against a preset value. Martin and Freiser [73] even created a new high level language, CONVERS, specifically to control volumetric titrations with a Mettler DV10 auto-burette.

These systems did not vary the volume added as the equivalence point was neared. In a manual titration, the operator reduces titrant delivery by dropwise addition, and may also increase the time between subsequent aliquots. The sensor actuator system uses computer control to read the mV signal and the value of this reading determines whether there is any dimunition (or increase) in the charge added, dictated by the software. This was the principle developed for the set up designed here,

The coulometric current used was supplied in two different forms. A continuous generating current derived from an coulometric auto-titrator and using pulse generating systems.

4.5 Experimental.

4.5.1 Reagents.

Analytical grade reagents were used throughout. The NBS standard buffers [76] and "Good" buffers [77] were prepared using Sigma

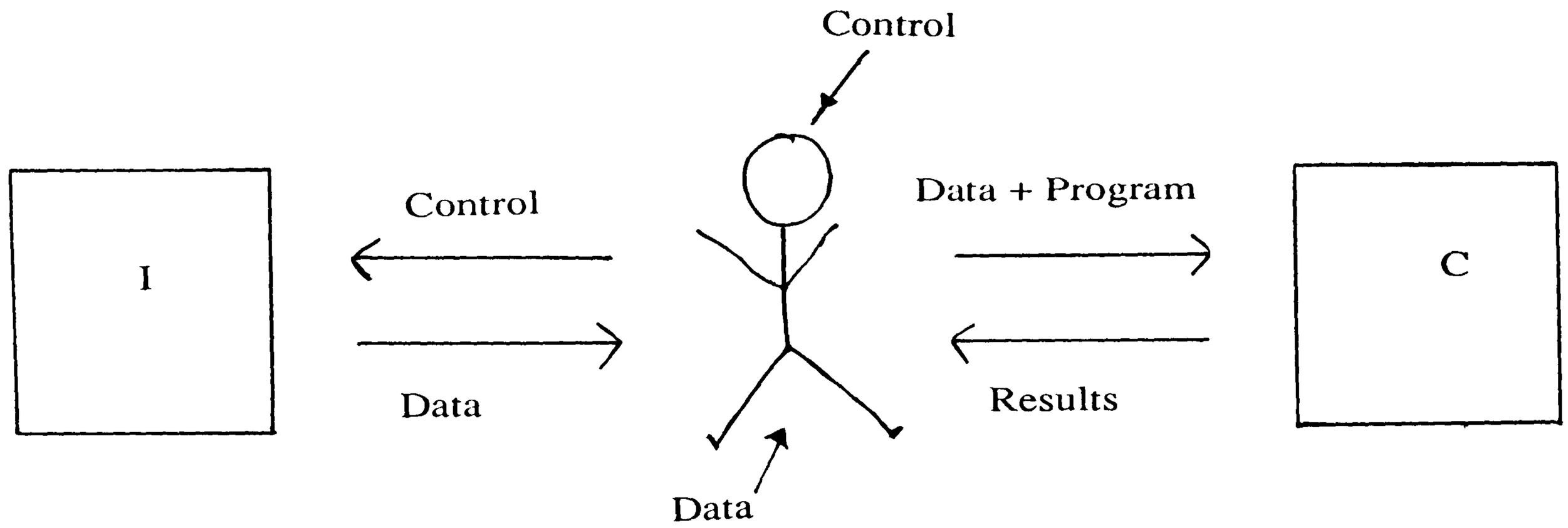

Figure 4:2 An Off-line (Human) Interface *ca*. 1960.

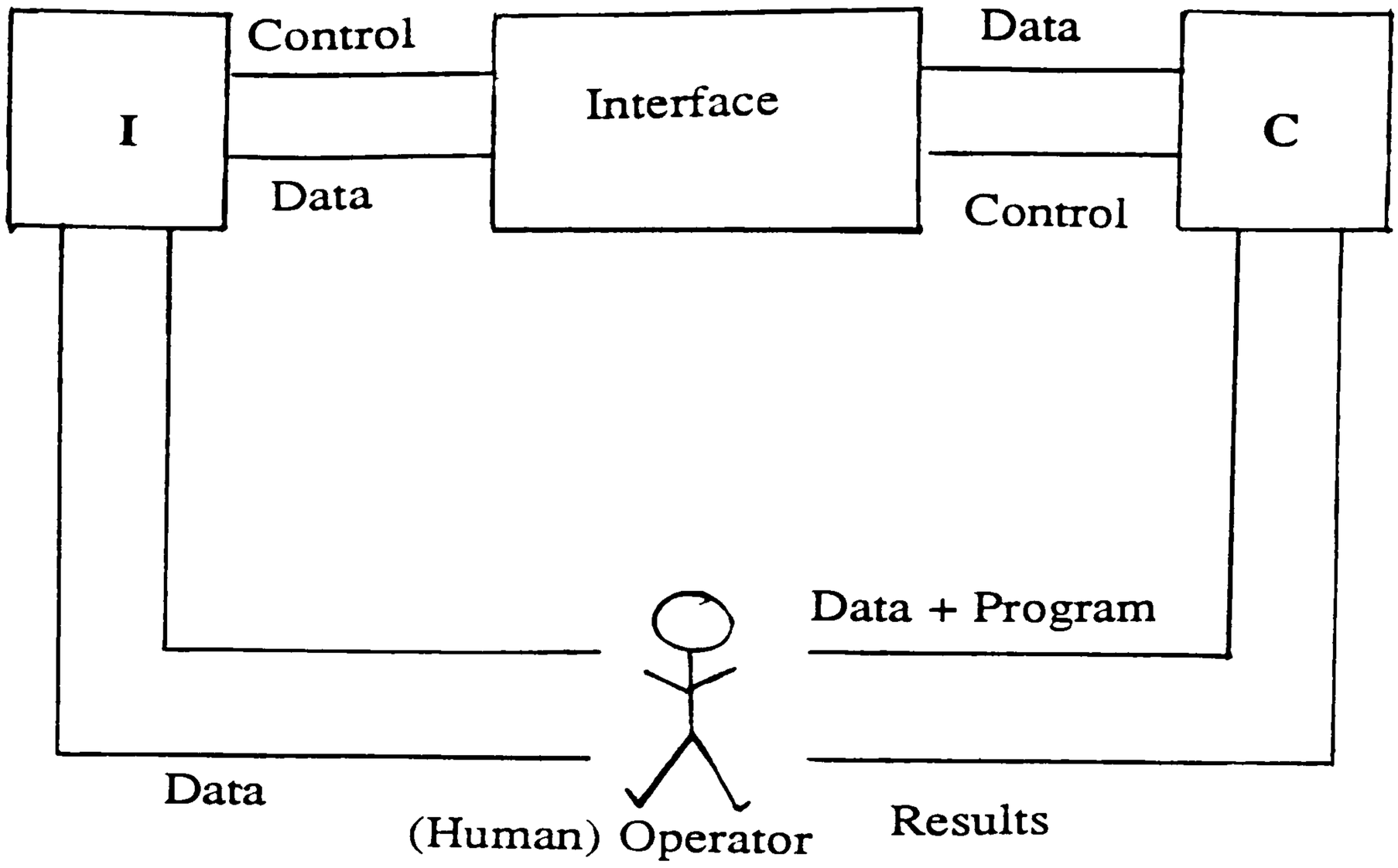

Figure 4:3 On-line (Electronic) Interface Design *ca.* late 1970's, 1980's

Totally automatic system but still requires some operator interaction.

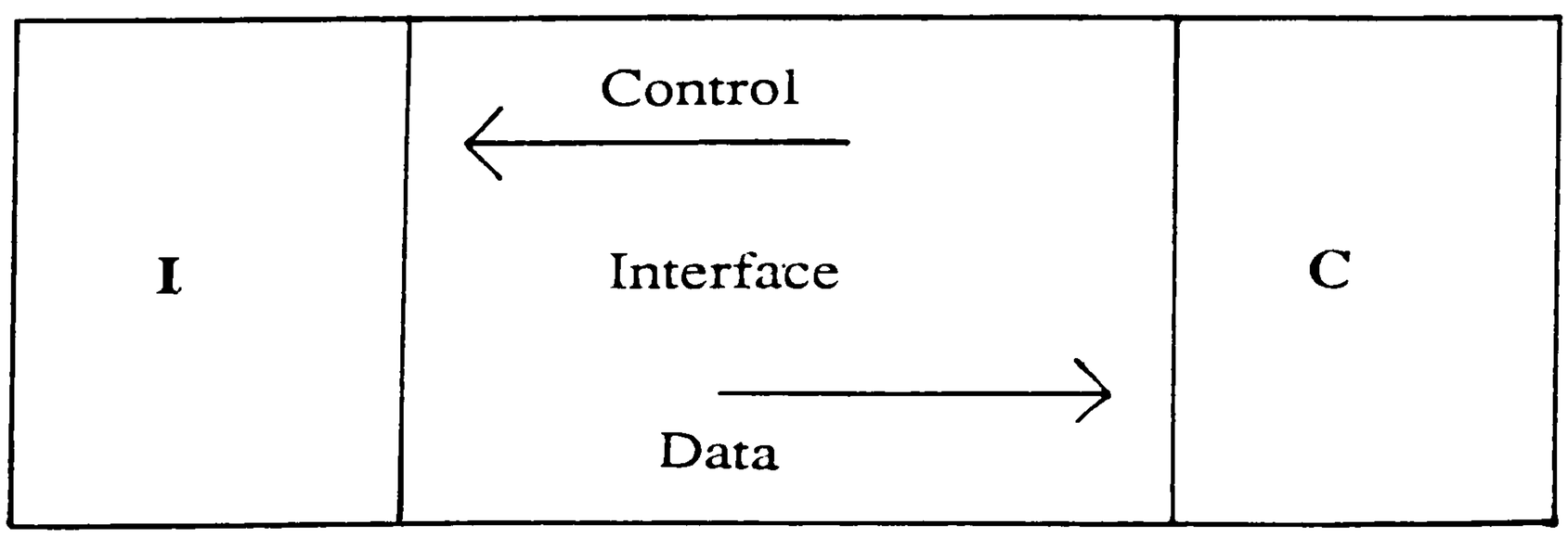

Figure 4:4 In-line **Active** Interface *ca.* 1980's

Intelligent capability, therefore no operator required.

Biochemical Buffer Reagents (see Appendix C). The home-made ISE was prepared using Fluka (Fluka AG, CH-9470, Buchs, Switzerland) reagents designed specifically for ISEs. All other chemicals were supplied by BDH Chemicals Ltd.

4.5.2 Apparatus.

Initial work was carried out using a commercially available auto-titrator, OH-407 Universal Recording Titrator, manufactured by Radelkis, (Budapest) and supplied by EDT, (London) (figure 4:5). The instrument could be operated at a range of generating currents with the option of running titrations to a preset endpoint value only or beyond, that is in 'over-titration' mode. Curves could be examined as primary and first derivative plots; the latter allowing closer examination of equivalence points. Features of this instrument are discussed elsewhere [78].

However, although this system provided a good insight into practicalities of coulometry e.g. cell design and application (see Chapter 5), it could not be easily adapted to fit the constraints of a sensor-actuator system. A major drawback of the titrator was its method of supplying a continuous current to the generating electrodes. Advantages of using a pulsed system were discussed earlier (4.4.12). A resume of experiments carried out with this titrator now follows.

4.6 Method.

10^{-1} - 10^{-5} mol dm^{-3} hydrochloric acid (50 µl) in 10^{-1} mol dm^{-3} potassium bromide (10 ml or 20 ml) was titrated, initially using the EDT titrator with generating currents of 6.4 mA and 12.9 mA using platinum sheet cathode (surface area 1.59 cm^2) and silver rod anode. Titrations were plotted as "over-titrations" and as "end point" determinations; that is, the generating current was interrupted when the end point was reached, thus allowing series analyses to be carried out. These plots were recorded as primary and first derivative curves.

Observations were made on the effect of using degassed solutions,

1. Current Generator
2. Titration Cell
3. Generator Electrode Pair
4. Automatic Burette
5. Titrant Delivery
6. Selector for type of titration
7. Indicator Electrode Pair
8. Measuring Amplifier
9. Function Switch
10, Control Unit
11. Display (μC supplied)
12. Chart recorder

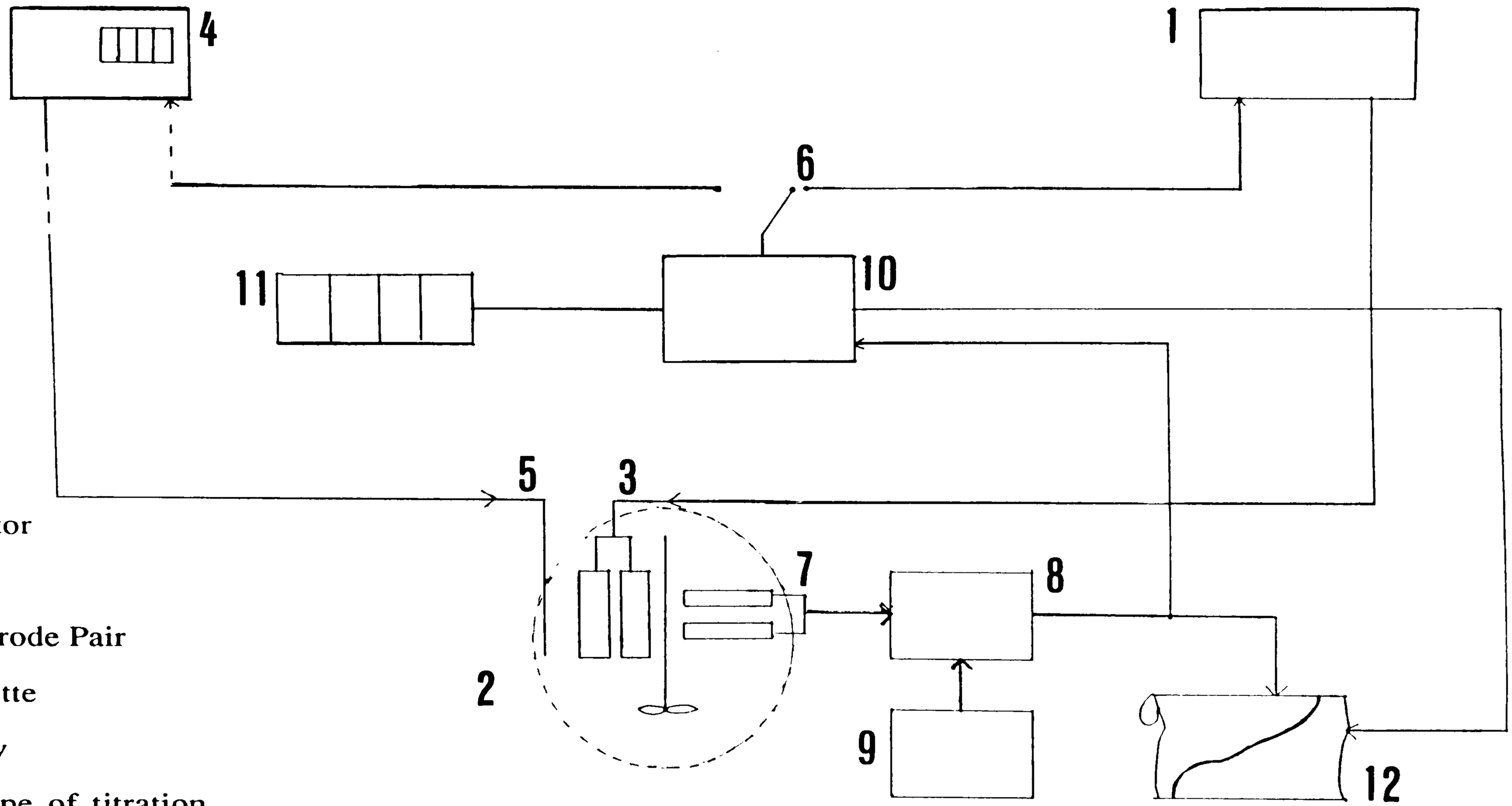

Figure 4:5 Schematic Representation of the Radelkis OH-407 Auto-titrator.

purging with nitrogen to inhibit carbon dioxide dissolution, the relative positions of electrodes in the cell, the type of stirrer used and the use of a mains smoother.

The latter experiments were necessary to investigate claims by others [79] regarding interference with the indicator electrode by the generating electrodes.

The experiments were repeated using various other electrodes;

Russell combination electrodes nos. 1, 2, 3, 4, 5 (type CE7L)

RS combination electrode

Russell glass electrodes, no. 1, 2, 3, 4 versus a calomel reference electrode (3.5 mol dm^{-3} potassium chloride)

home made PVC pH electrode* versus calomel reference electrode (" " filling solution)

* The composition of home made pH PVC electrode is given below;

1 wt % tri-n-dodecylamine (TDDA) (ionophore) [80]

0.08 wt % potassium tetrakis-chlorophenyl borate (salt)

33 wt % high molecular weight PVC (inert support)

66 wt % ETH 2041

(3,3',4,4'tetra-n-undecyl benzophenonetetracarboxylate) (plasticizer)[61]

The plasticizer used, more commonly known as ETH 2041, also discussed in Chapter 6, was used because of its high lipophilicity and impermeability to carbon dioxide. Simon's group also proposed [82] that the ionophore should have high lipophilicity as well as good selectivity (here pH selectivity). The advantages of TDDA were discussed in Chapter 1, most important is the ionophore's high lipophilicity which prevents preferential leaching from the membrane by body fluid components. Although this work is to be extended to ISFETs which have a pH sensitive silicon nitride gate, and silicon nitride does not contribute to thrombi formation as suspected [83], the behaviour of this membrane was examined. Some workers [84] use a hydrogel over the gate of the ISFET to

"improve blood compatibility", it is possible that the TDDA / PVC membrane could be used in the same way.

The internal filling solution, of pH 5.6, used was

1.0 mol dm^{-3} citric acid

2.73 mol dm^{-3} sodium hydroxide

0.01 mol dm^{-3} sodium chloride

The pH range and selectivity of this electrode were examined to determine the effect, if any, of lithium, sodium and potassium on the membrane. The following solutions were used to characterise the nembrane;

a) a background of 60 mM Li^+ in citrate buffer

60 mM lithium hydroxide

6.6 mM citric acid

11.4 mM boric acid

b) a background of 140 mM Na^+ in TRIS buffer

10 mM sodium hydroxide

130 mM sodium chloride

10 mM TRIS (tris (hydroxymethyl)amine methane)

c) 200 mM K^+ background in TRIS buffer

190 mM potassium chloride

10 mM potassium hydroxide

10 mM TRIS

Having determined the parameters required with respect to cell design and experimental, an intermediate system was developed before the sensor actuator system was set up in order to examine theories regarding open-circuit measuring, accuracy of pulses supplied etc.

A pulse generator, with timer accurate to 0.1 % of 10 seconds and an accurately measured variable current was manufactured by the electronics workshop of the Chemistry Dept., University of Newcastle-upon-Tyne. This was used in conjuction with a Chemical Electronics Co. potentiostat,

type TR 70 (figure 4:6). This system provided a square wave pulse to the cell and was used as an intermediate system to examine the improvement in end point determination using a pulsed system. No quantative experiments were made with this system.

4.7 Designing the Sensor-Actuator System.

The sensor actuator system was controlled by a BBC-Master computer to which a pulse control was connected via the user port. This is an 8-bit input / output port containing 8 lines; on each line a binary digit can be set to input or output data from the computer. By setting, or "poking", lines high (1=5 V) or low (0=0 V), the user port can be made to fulfill a range of conditions. The initialising or set up procedure PROCINIT (line 60) states the addresses and values of the low order (J% at FEC8) and high order counters (K% at FEC9) (see Appendix D for programme listing).

To obtain a pulse, PROCPULS (line 310) is called up. Both counters are initially set high, line 320 and then one is set low, line 340, which latches the counter and starts ADC (analogue to digital conversion) for the selected channel, "translating" the analogue voltages to a signal which can be understood by the operator. In essence, the user port acts as the central connector, transferring information from the experiment to the computer. A 1 MHz BUS parallel input / output device, i.e. an IEEE port, is then used to transfer binary coded information between the computer and the disc and printer, as selected, units. A block diagram of this is shown in figures 4:7, 4:8.

The pulse control was designed originally to supply charge, this was later adapted so that the option of volumetric titrations was possible. In both cases an external pulse signal source was used. For coulometric procedures, this could provide currents up to 100 mA with respect to earth in steps of 1/4000. The duration of the impulse was controlled by the computer's internal timer (a countdown system) so that pulses of 1/16000 s to a maximum of 1 s could be applied. In volumetric titrations,

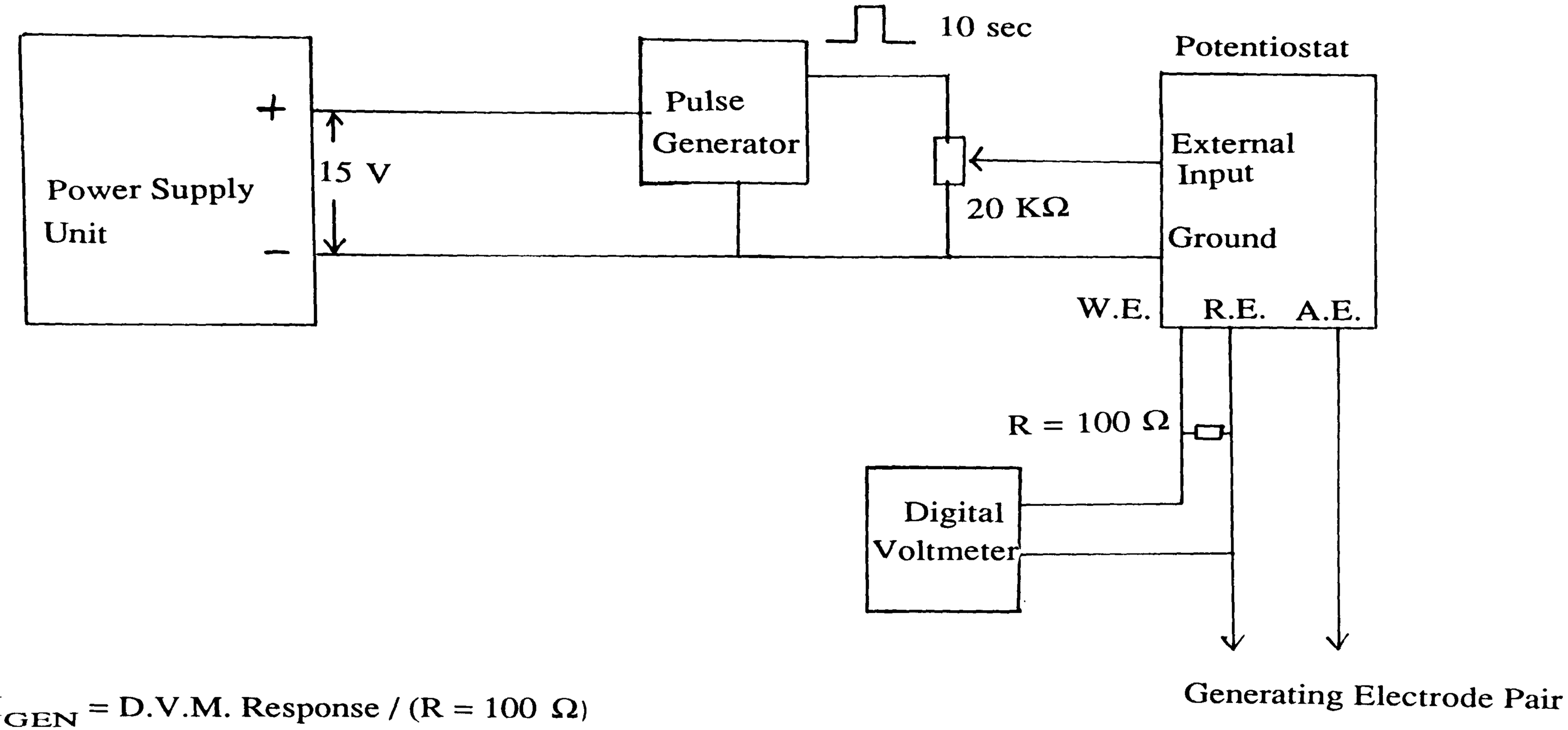

I_{GEN} = D.V.M. Response / (R = 100 Ω)

Figure 4:6 Schematic of the Intermediate Pulse Generation System.

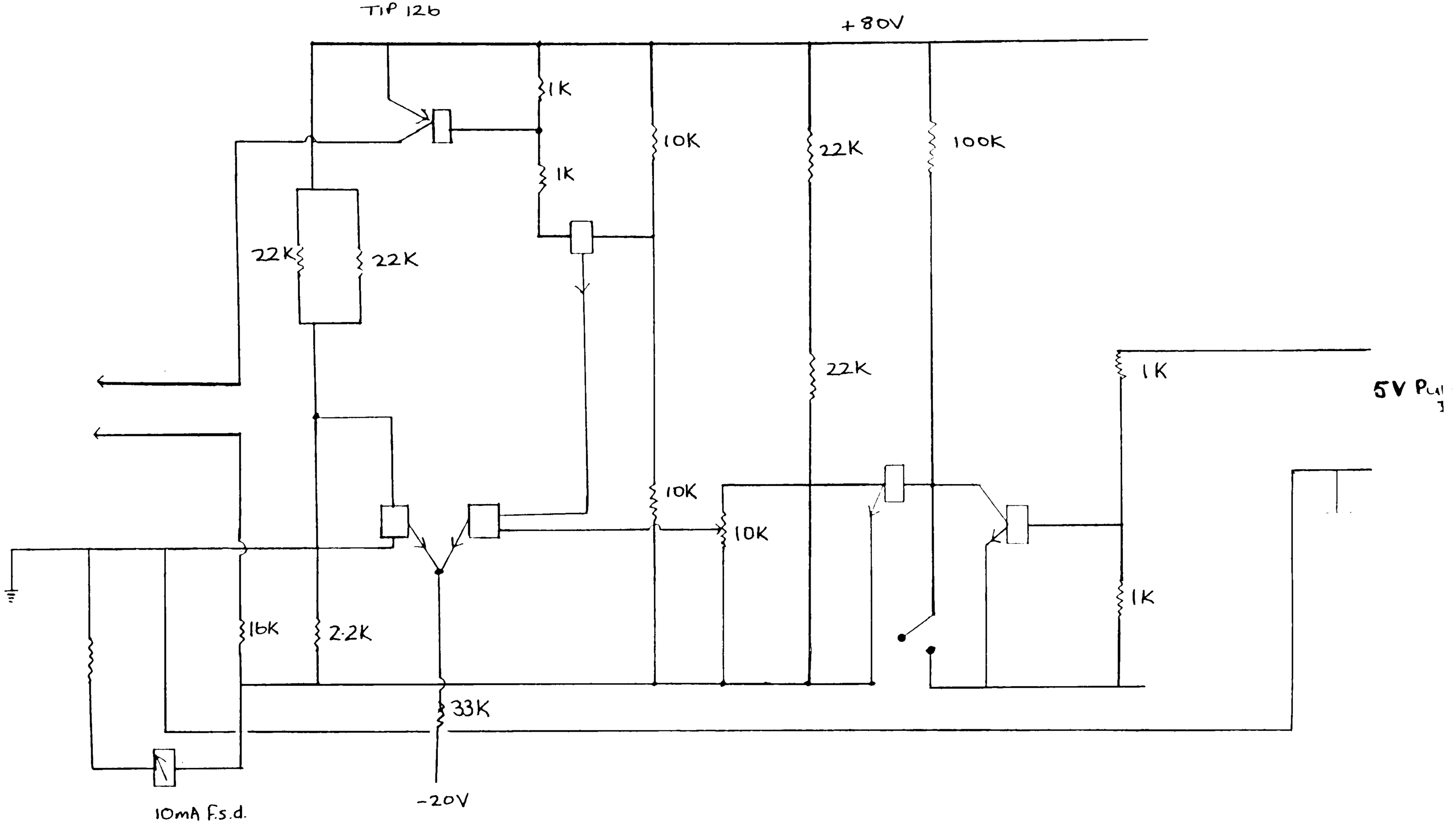

Figure 4:7 Circuit Diagram for the Constant Current / Pulse Generation System.

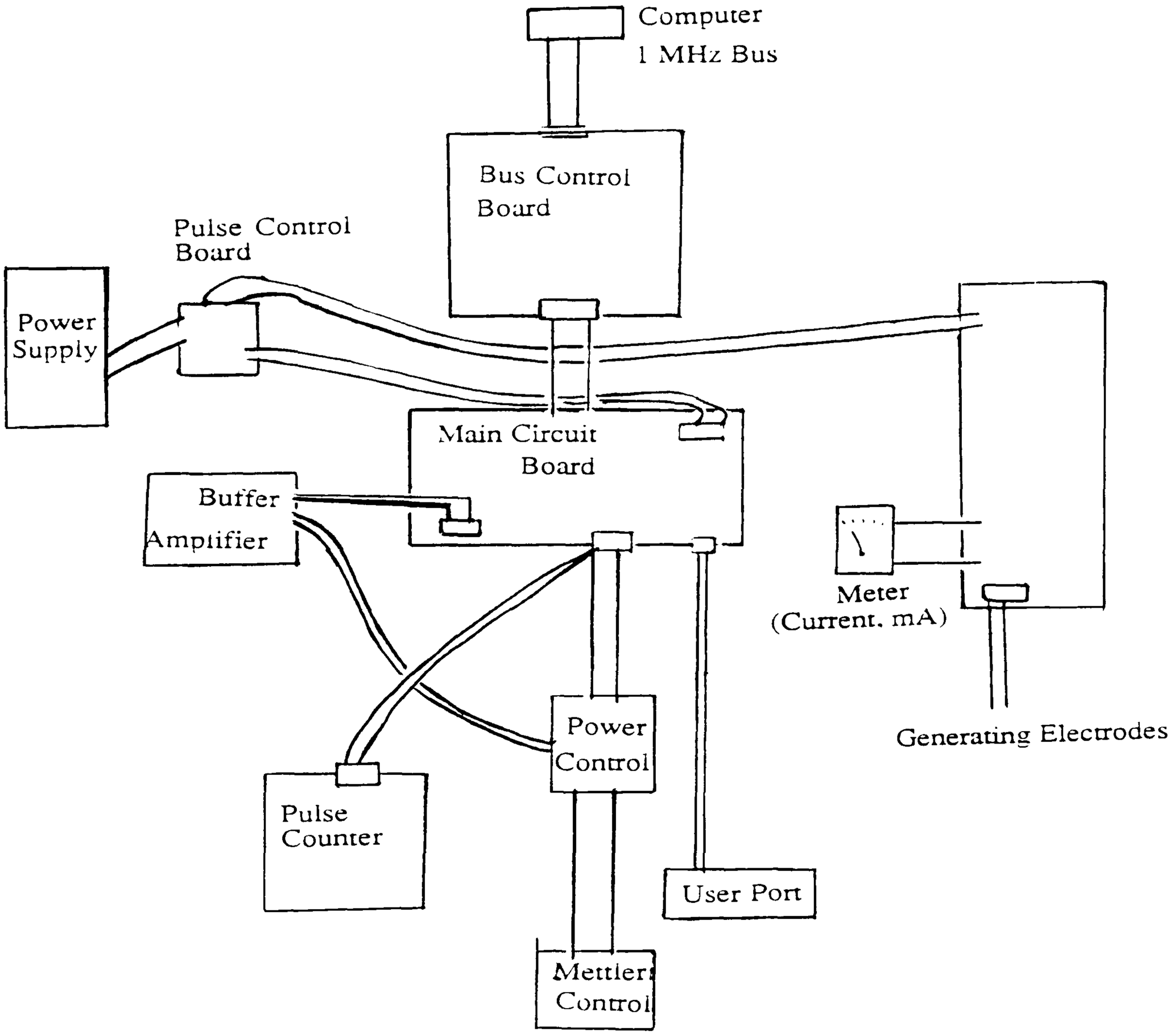

Figure 4:8 Schematic Representation of the Sensor Actuator System.

the pulse source was interfaced to the external trigger of a Mettler DV11 titrator, and in the same manner, delivery of reagent could be altered by adjusting the number of pulses.

In order to isolate the charge impulse and the measuring hardware, an optocoupler (RS 6N139) was fitted and a large 50 kΩ resistor was used to prevent blowing the transistor. During operation, a potential of 50 V was maintained between the generating electrodes.

After the pulses were delivered, a preset time was allowed for re-equilibration, i.e. Faradaic discharge, before a reading in mV (converted to pH) was made at open circuit by calling up PROCRADC. By comparing this with the previous voltage reading, made immediately before the pulse was applied, the difference ΔV between subsequent readings determined the duration of the next pulse, held at constant current. This allows accurate determination of the equivalence point, since in this range the rate of change of ΔV with charge, Q, is greatest and thus shorter charge impulses are injected. By recording the variation of the slope of the curve i.e. the second derivative of the titration, the equivalence point can accurately be determined as the curve reaches a point of inflection. The titration can be programmed to halt or to continue to find another equivalence point.

The initial operating programme was developed from a system devised for volumetric auto-titration using a Mettler DV11, operated by the Rockwell AIM 65, interfaced to an R6522 VIA (Versatile Interface Adapter) and thus to MTS (Michigan Terminal Systems) mainframe. Here, a non- linear least squares programme, SUPERQUAD [85], read the titration data into a file which was then used to determine the formation constants for the metal ion under test and various known ligands. Other, similar programs are available to operate on titration data to obtain information with respect to formation constants e.g. SCOGS2, DALSFEK [86-89].

Experimental work was carried out with this system to obtain familiarity with the set up. The AIM 65 set up is now obsolete, hence the need to develop a new system allowing volumetric titrations to be carried out. The AIM 65 was programmed to deliver a constant, preset, volume of aliquots i.e. the volume could not be reduced near the end point. Also, the AIM 65 programme had the disadvantage of using an assembler code as well as BASIC for operation. Although machine code is very fast, since it is a low level language, it is certainly not user friendly, and also has the drawback of requiring an assembler or compiler. High level languages, such as BASIC, allow large blocks of machine code to be replaced by single statements and although not as concise as more mathematically orientated languages, e.g. FORTRAN, ALGOL, BASIC is sufficiently fast enough for this work and much less intimidating for the operator.

As SUPERQUAD requires a constant aliquot to be added throughout an experiment, the complexity of a sensor actuator system was not required, therefore, the set up was programmed with an option to operate as a standard auto-titrator.

At present, the BBC-Master computer stores all titration data on floppy disc, which can then be sent to an IBM computer using a conversion programme [90, 91]. The sensor-actuator system will eventually be installed on an IBM system, allowing direct treatment of results (e.g. with SUPERQUAD), therefore development of a better conversion programme was not undertaken. The only proviso is correct format of input data, as SUPERQUAD is written in FORTRAN.

4.8 Results and Discussion.

4.8.1 Experimental Details.

Several features have arisen from this work; the respective orientation of the electrodes was found to be extremely important, as was stirring. Carrying out titrations in decarboxylated / deoxygenated solutions in a nitrogen atmosphere did not significantly improve titrations in trial runs,

compared with those without precautions against aeration. However, due to the small samples used in experiments, 50 µl, compared to the larger aliquots taken for trial runs, 0.5 ml or greater, this precaution was maintained. Atmospheric carbon dioxide interference is a greater problem for basic solutions, in these instances bubbling nitrogen through decarboxylated / deoxygenated solutions is of the utmost importance (see Chapter 5).

The results of selectivity tests carried out for the TDDA / PVC electrode showed that the membrane exhibited very little or no interference from lithium, sodium or potassium and TDDA is therefore suitable for use in clinical work with ISFETs.

Using a two compartment cell, with separation of the generating electrodes by a ground glass frit, gave repeatable, less noisy electrode responses than when a single compartment cell was used. This was the case for all titration systems used (see figures 4:9 - 4:11).

The relative positions of the electrodes were varied in order to determine the orientation least susceptible to noise. Using a single compartment cell, the most stable response was observed when the indicator electrode (s) were placed near to the working electrode but not between the generating electrode pair (figure 4:12), as this led to severe noise, making accurate determination of the end point difficult.

The "paddle"-stirrer supplied by Radelkis with their titrator, was found to be inefficient; using dropwise additions of permanganate to the vessel and observing the time required for complete homogeneity, poor mixing was observed and a more effective magnetic stirrer was used in further work.

The extent of the interference effect of the generating electrode pair varied with different electrodes. Table 4:1 shows that not all electrodes experienced an interference effect, for example the Radelkis and RS combination electrodes.

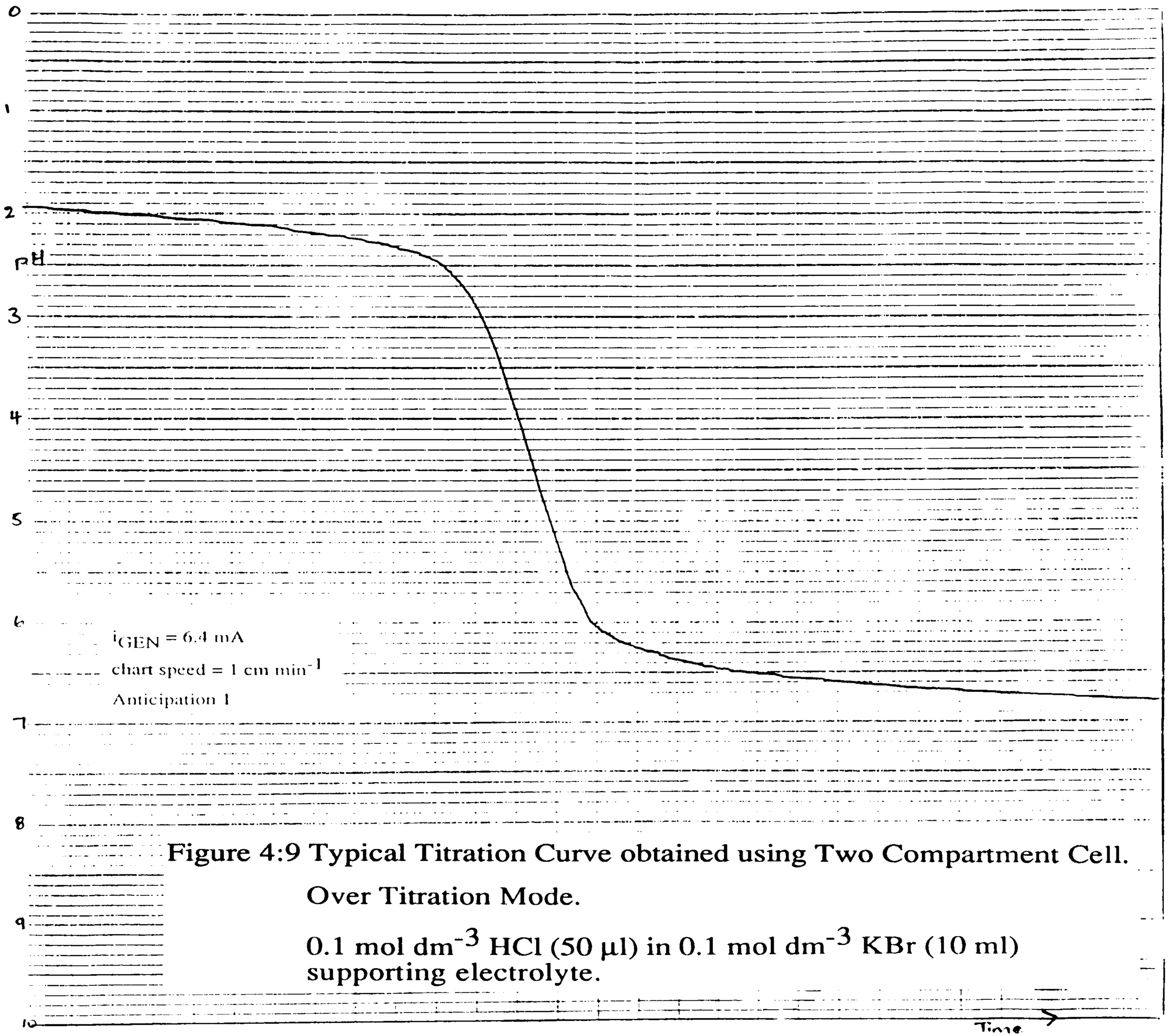

Figure 4:9 Typical Titration Curve obtained using Two Compartment Cell. Over Titration Mode.

0.1 mol dm^{-3} HCl (50 µl) in 0.1 mol dm^{-3} KBr (10 ml) supporting electrolyte.

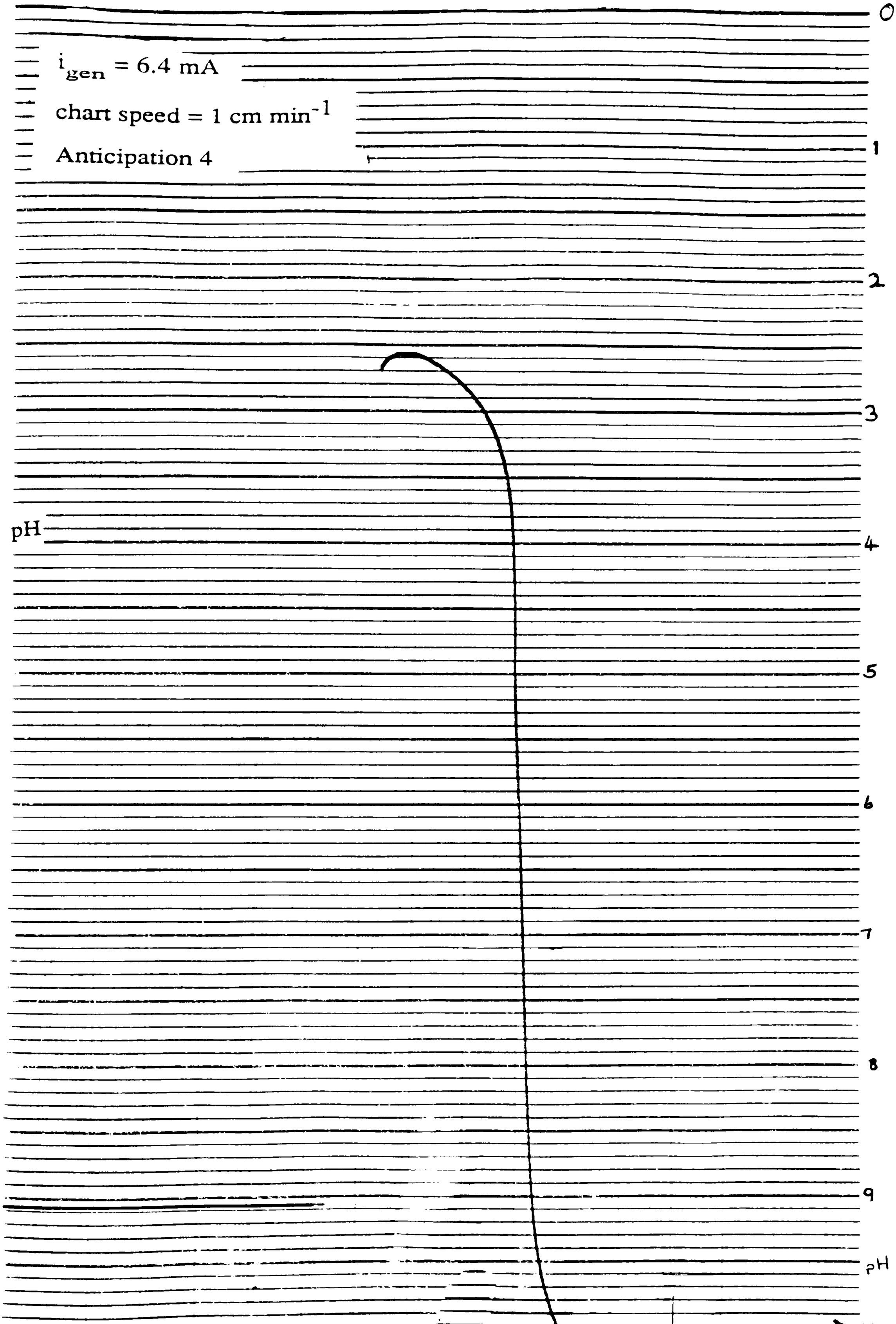

Figure 4:10 Example of a Titration Curve obtained using a Two Compartment Cell (end point determination).

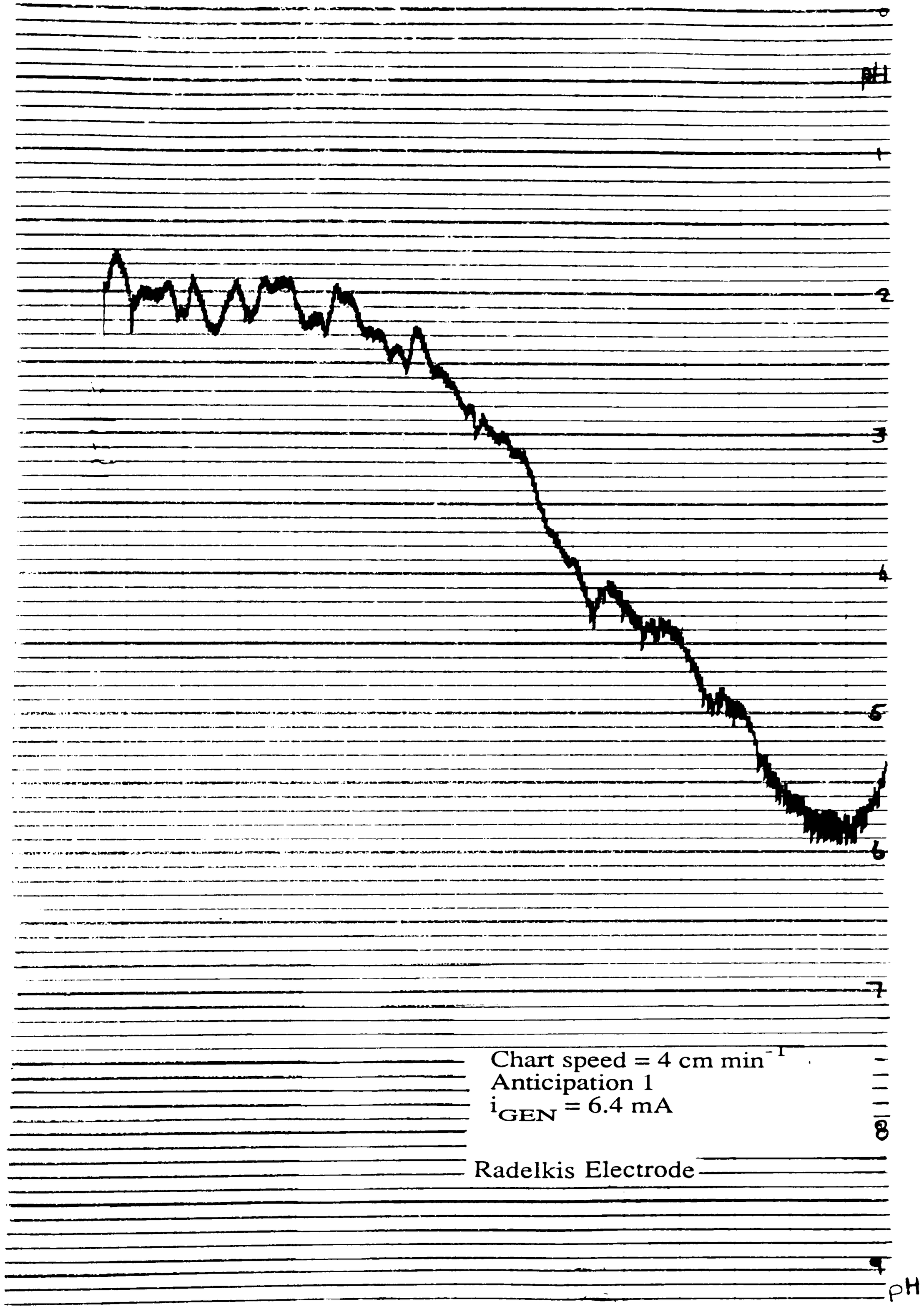

Figure 4:11 Typical Titration Curve obtained using a Single Compartment Cell. Over titration mode.

0.1 mol dm^{-3} HCl (50 µl) in 0.1 mol dm^{-3} KBr (10 ml) supporting

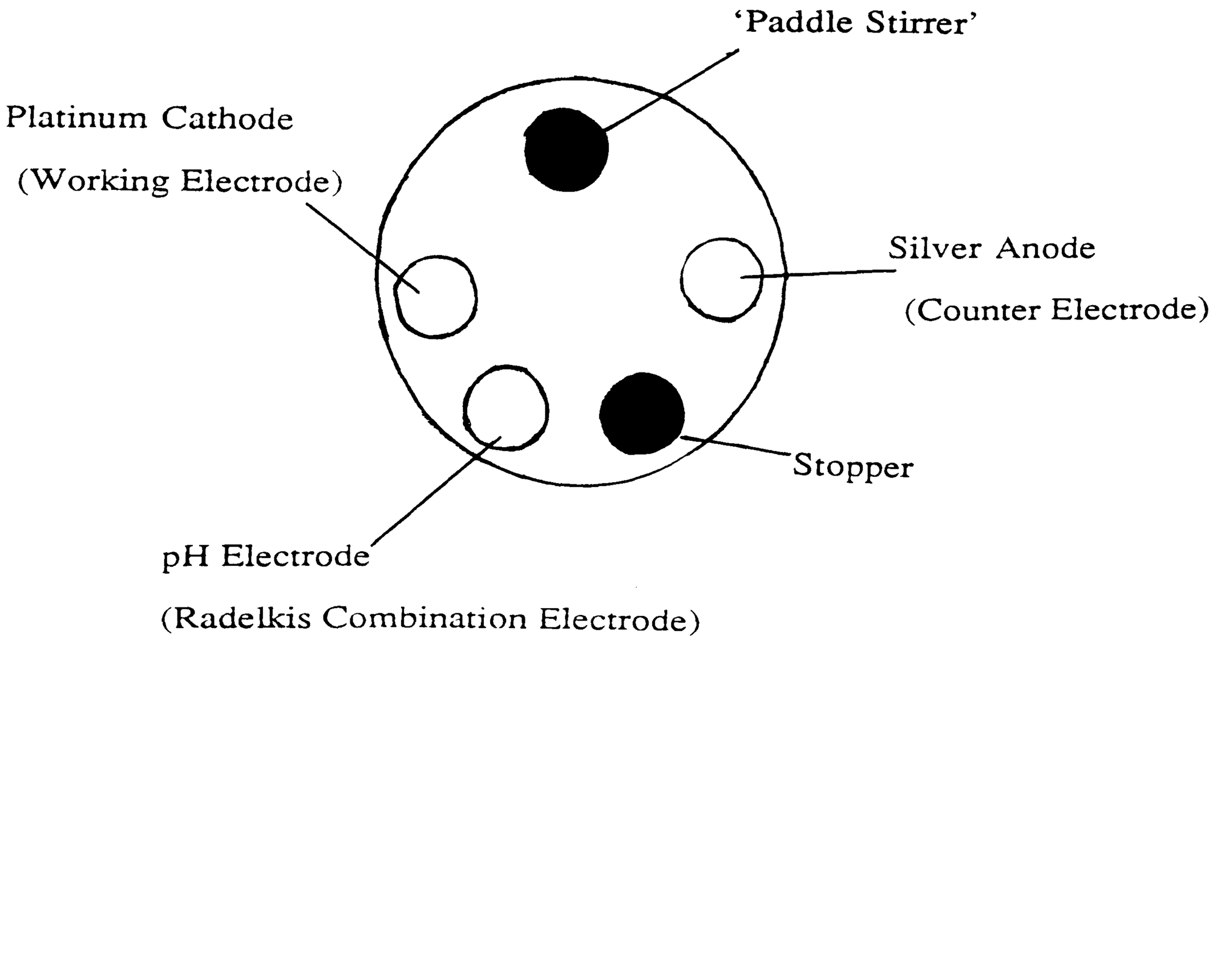

Figure 4:12 Electrode Orientation giving Least Interference by the Generating Electrode on the Indicator Electrode Pair.

Out of five Russell combination electrodes tested, three showed a shift in the original potential, E_i, to a new value, E_q. The size of the error signal increased with magnitude of the generating current. Considering electrode (a), a jump from +234 mV to +90 mV was observed when the generating electrodes were placed in solution. Two of the four Russell glass electrodes also showed anomalous behaviour, as did the home-made PVC / TDDA electrode which had an (E_q -E_i) value of -80 mV in B2 buffer solution and an increased signal to noise ratio. The direction of the polarization was, not unexpectedly, in the same direction for all electrodes (see figure 4:13).

Table 4:1 To Show those Indicator Electrode(s) Affected by the Generating Electrode Pair.

Type of electrode	Interference?	Label
Radelkis combination	No	a
Russell combination	Yes	b
RS combination	No	c
Russell G.E., no.1	Yes	d
Russell G.E., no.2	Yes	e
Russell G.E., no.3	No	f
Russell G.E., no.4	No	g
TDDA PVC pH Electrode[#]	Yes	h

[#] suitable for pH 2 - 8 only

The original design of the pulse system also showed this polarization effect, but this was found to be due to an electrical design fault. The early system did not include floating generating electrodes, but was a single ended system and current was therefore able to flow to earth through the 10 Ω resistor (A), a low impedance route to earth. Correcting this flaw, no polarization of electrodes was observed using the pulsed

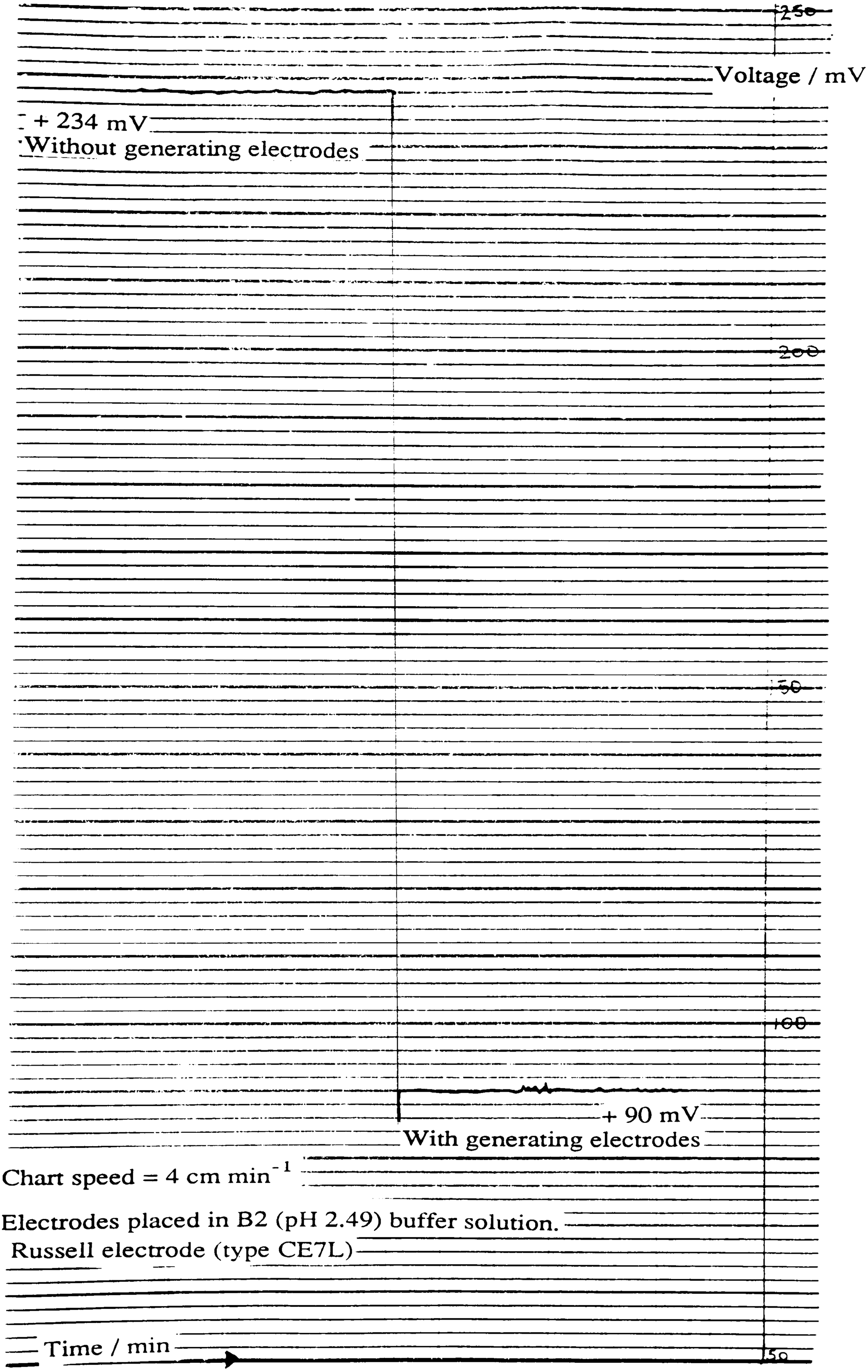

Figure 4:13 Polarization / Interference on the Indicator Electrodes observed on Introduction of Generating Electrodes.

system. However, this does call into question the apparatus used by Radelkis, unless they were able to include some significant design parameters in construction of the indicator electrode.

Several attempts were made to try to eliminate noise problems, including using a mains smoother which did not improve the situation. It was found that the whole laboratory was connected to the same mains line, and thus the noise, at least, could be due to interference effects from other instrumentation.

The EDT titrator and intermediate pulsing system were therefore moved to a side laboratory where the mains line carried minor equipment only, and the previous titrations were repeated. Noise problems were eliminated and the electrostatic field of the generating electrodes was not a problem. Although the EDT apparatus had been returned to the manufacturers for repair between these two experimental periods, experiments carried out in the main laboratory immediately after return of the instrument still showed mains interference.

The resistance or impedance of the electrodes was considered to be responsible for the variation in response of different electrodes, though this explanation seems insufficient for different electrodes of the same type. The impedance of the Russell (CE7L) and Radelkis (OH-8513) electrodes (figure 4:14) was measured.

4.8.2 A.C. Impedance Studies.

In A.C. Impedance techniques, a sinusoidal potential wave, V, is applied across an electrochemical cell between the reference electrode and the working electrode, causing a sinusoidal current, I, to flow. Generally, the potential wave applied has an amplitude less than 5 mV so that i) the system is not disturbed too far from equilibrium and ii) the I / V relationship is almost proportional over the whole perturbation range.

However, there may be a phase difference between the induced current and the potential wave, which is a vector quantity and may be described by

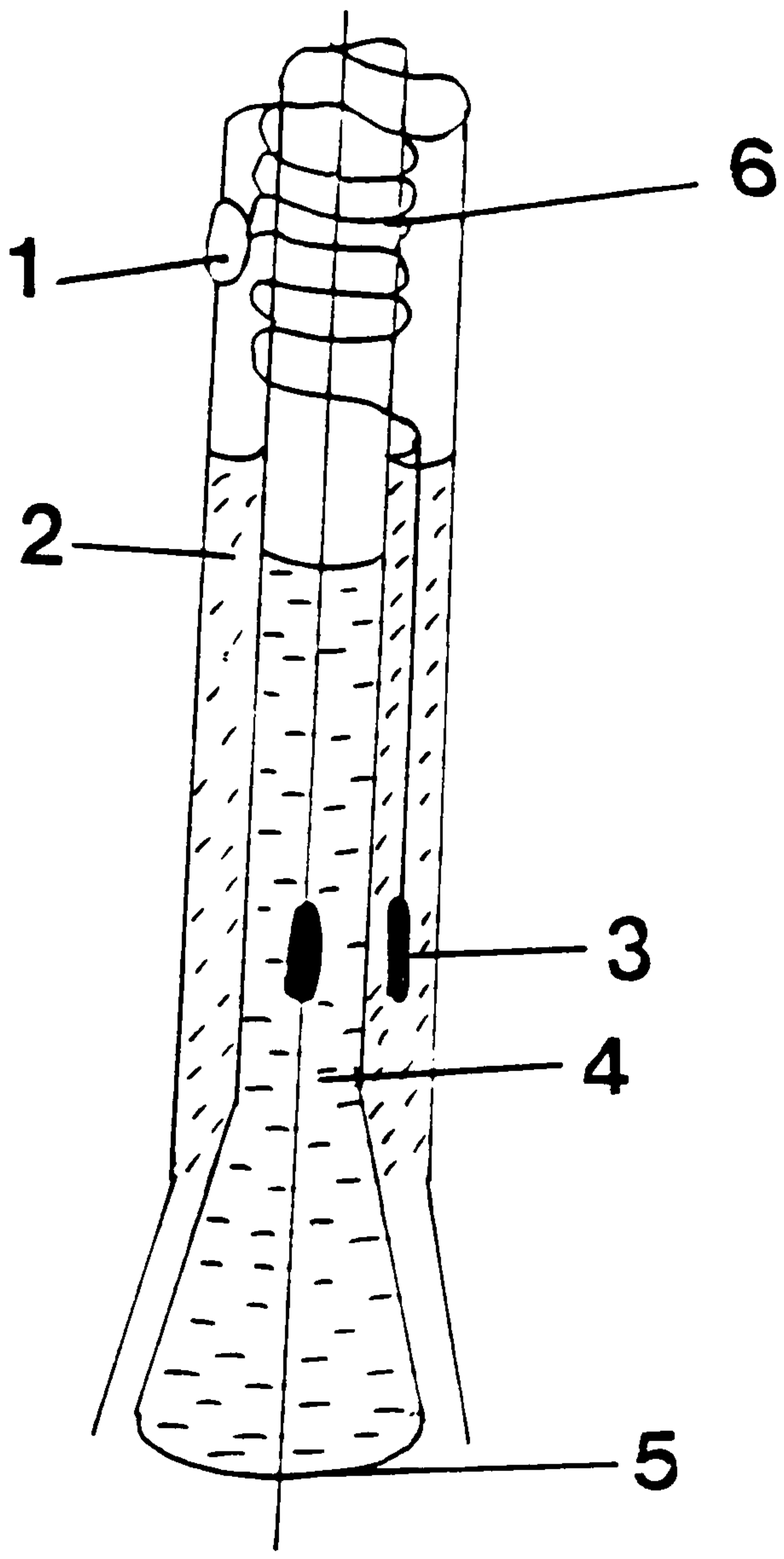

Figure 4:14 a) Radelkis OH-8513

The Diaphragmless pH Sensitive

Electrode.

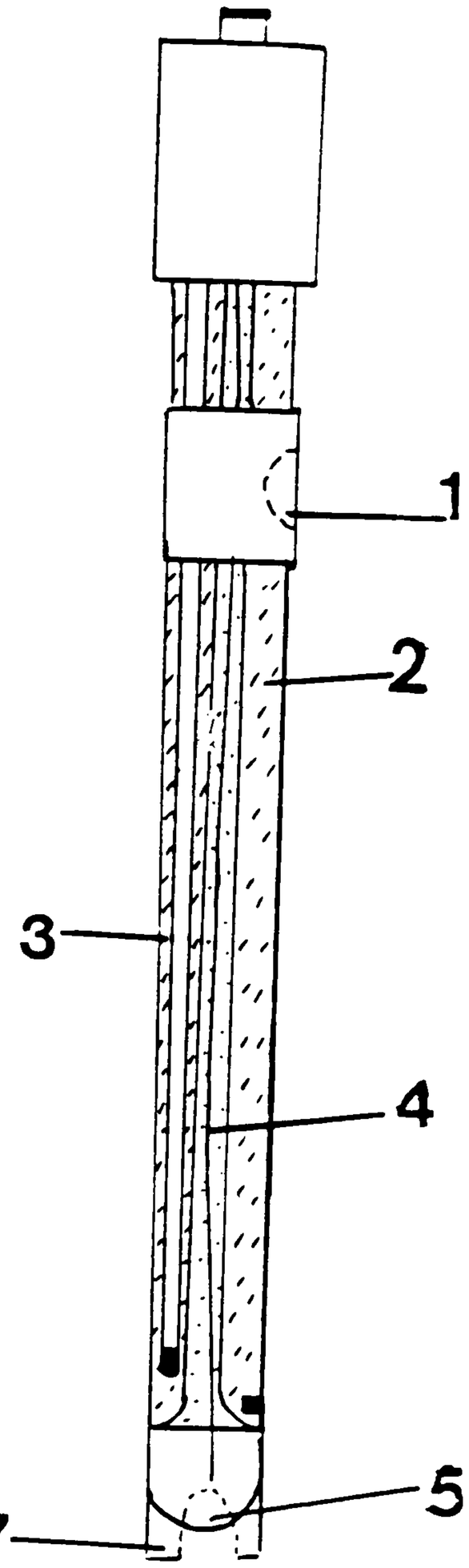

Figure 4:14 b) Russell CE7L

The General Purpose Plastic Bodied

Combined pH / Reference Cell.

1. Filling hole of the reference electrode solution.
2. Solution compartment of the reference electrode.
3. Ag /AgCl reference element of the reference electrode.
4. Ag / AgCl reference element of the indicator electrode.
5. pH sensitive glass membrane.
6. Shielding spiral.
7. Detachable protective skirt

size, z, and direction, θ, or as a point in a complex plane. As the frequency changes, so also does the position in the complex plane. The current **in** phase gives information with respect to the **real** resistance, associated with the resistance of the working electrode, the **out** of phase current gives information with respect to the **imaginary** resistance, or capacitance.

For this work, a three electrode system was used [92] with two silver / silver chloride electrodes, one as reference electrode and the other as counter electrode, and using the test electrode as working electrode. 1.0 mol dm^{-3} potassium chloride calibration reagent was used as working electrolyte and the electrodes were assembled in a watertight PTFE cell as shown in figure 4:15. A 5 mV amplitude sinusoidal potential was applied between the test electrode and the counter electrode over a range of 10^{5} - 10^{-1} Hz supplied by a Solartron 1186 electrochemical interface and a Solartron 1174 frequency response analyser (FRA) measured the current response of the test electrode. The system was run by an Apple IIe microprocessor with Solartron 1186 Electrochemical Interface, acting as a potentiostat connecting the FRA, the cell and the microprocessor [93] (figure 4:16).

Results of the A.C. impedance experiments are shown in Tables 4:2, 4:3, Figures 4:17 - 4:20. The Russell electrode showed capacitance of 100 pF and the Radelkis electrode 140 pF. For the D.C. resistance of these electrodes, values of 5.14×10^{4} Ω and 4.80×10^{5} Ω were determined for the Russell and Radelkis electrodes respectively. It is possible that the higher resistance of the Radelkis electrode allows less current to flow through it, therefore, in the presence of an electric field, i.e. with the generating electrodes, Radelkis electrodes are less prone to electrical disturbances. It is evident that Radelkis have overcome problems associated with electrical interference / noise, and state as much in their literature, so this may be a possible explanation. Alternatively, the very

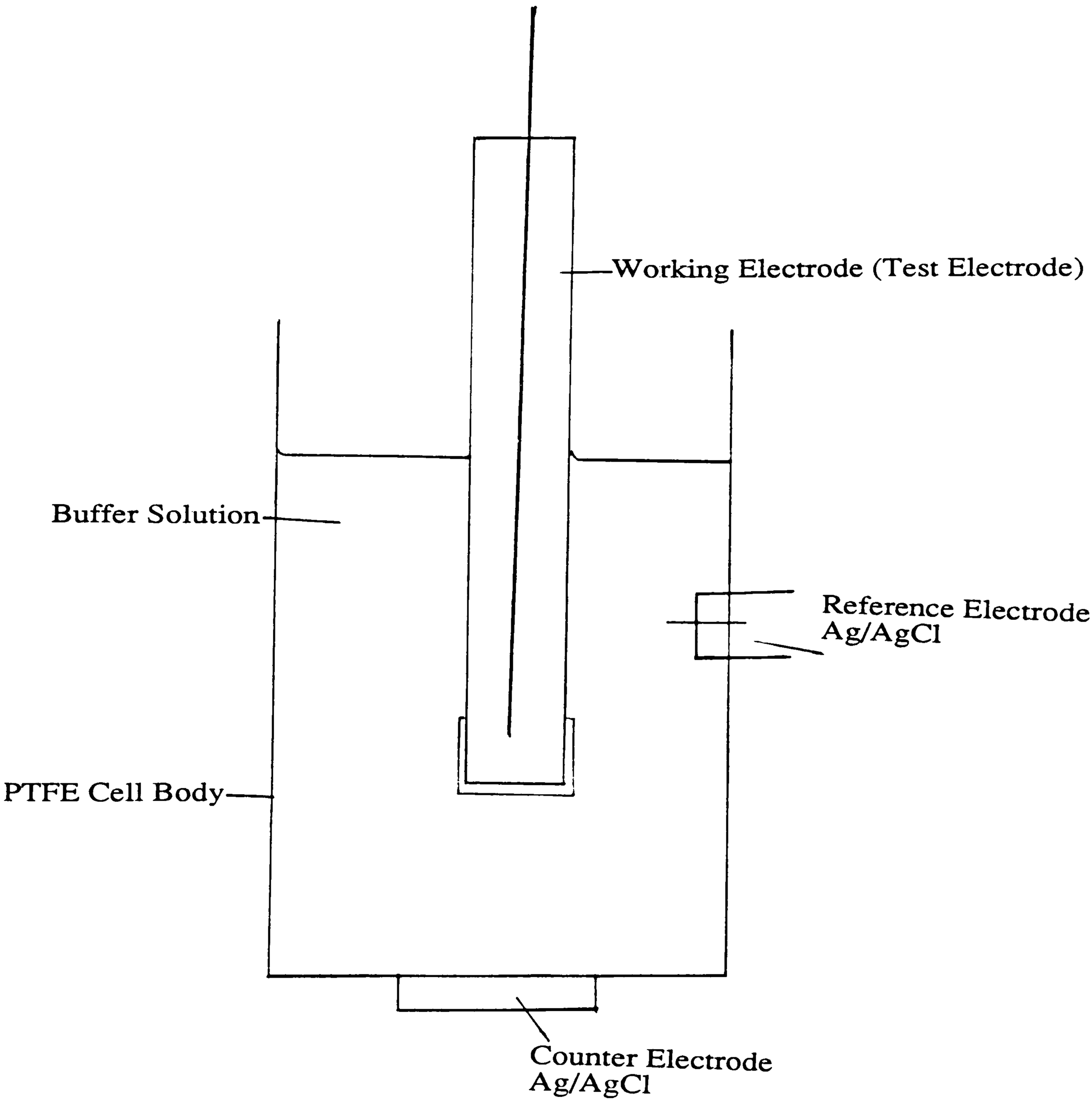

Figure 4:15 The Three Electrode Cell used for A.C. Impedance Measurements.

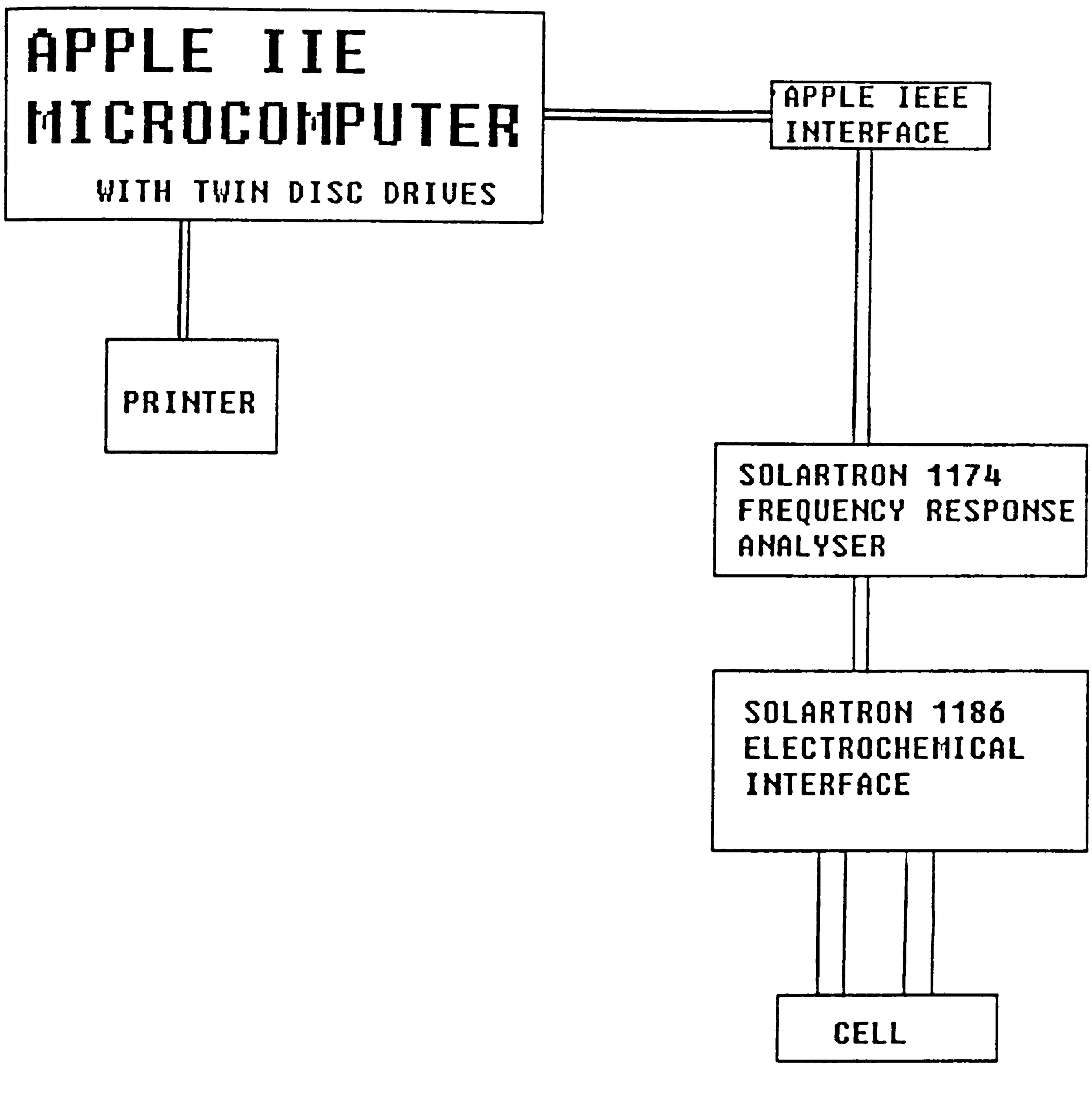

Figure 4:16 Schematic of the A.C. Impedance Measuring System.

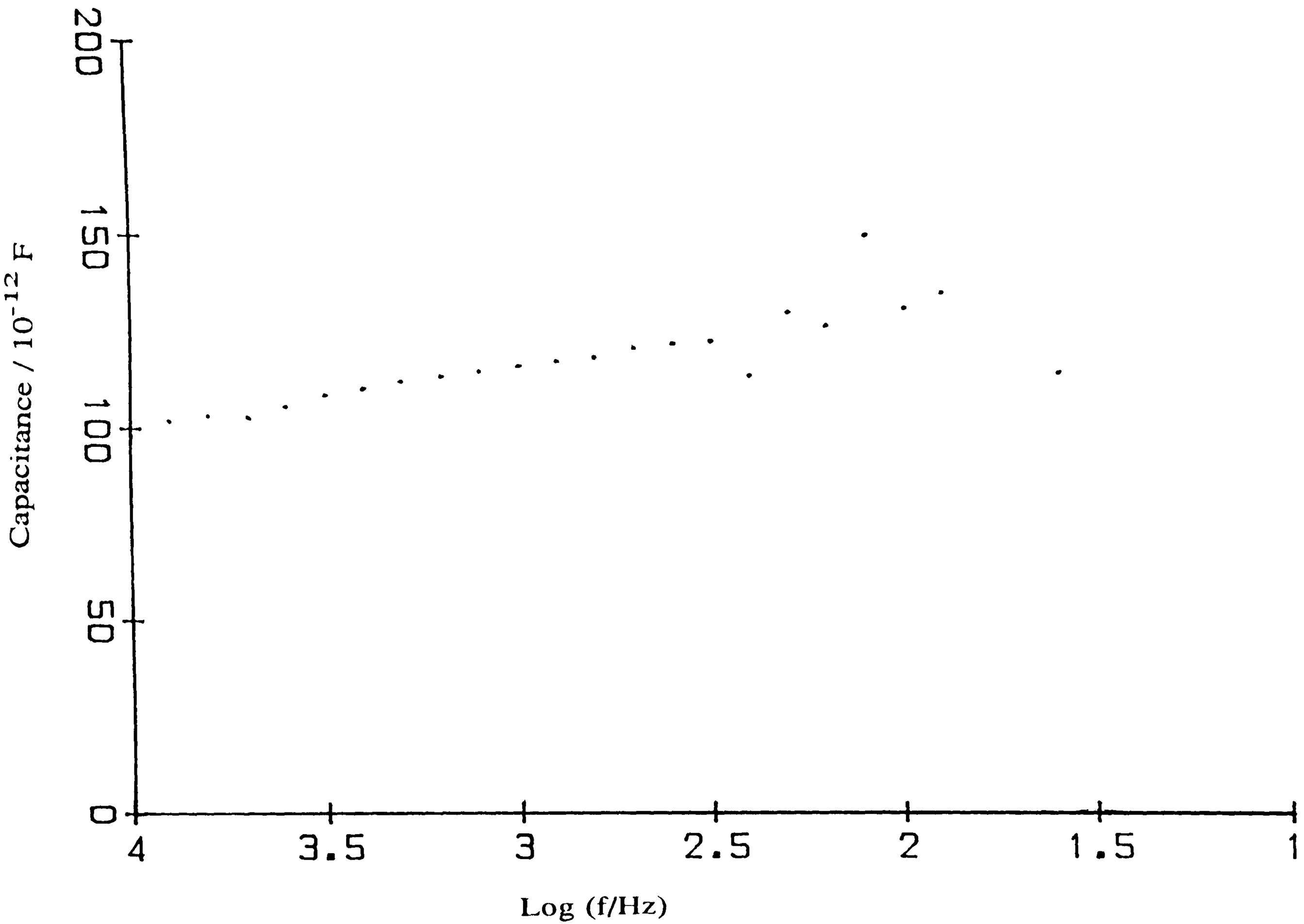

Figure 4:17 A.C. Impedance Results for the Russell (CE7L) Electrode.

"Imaginary" Resistance.

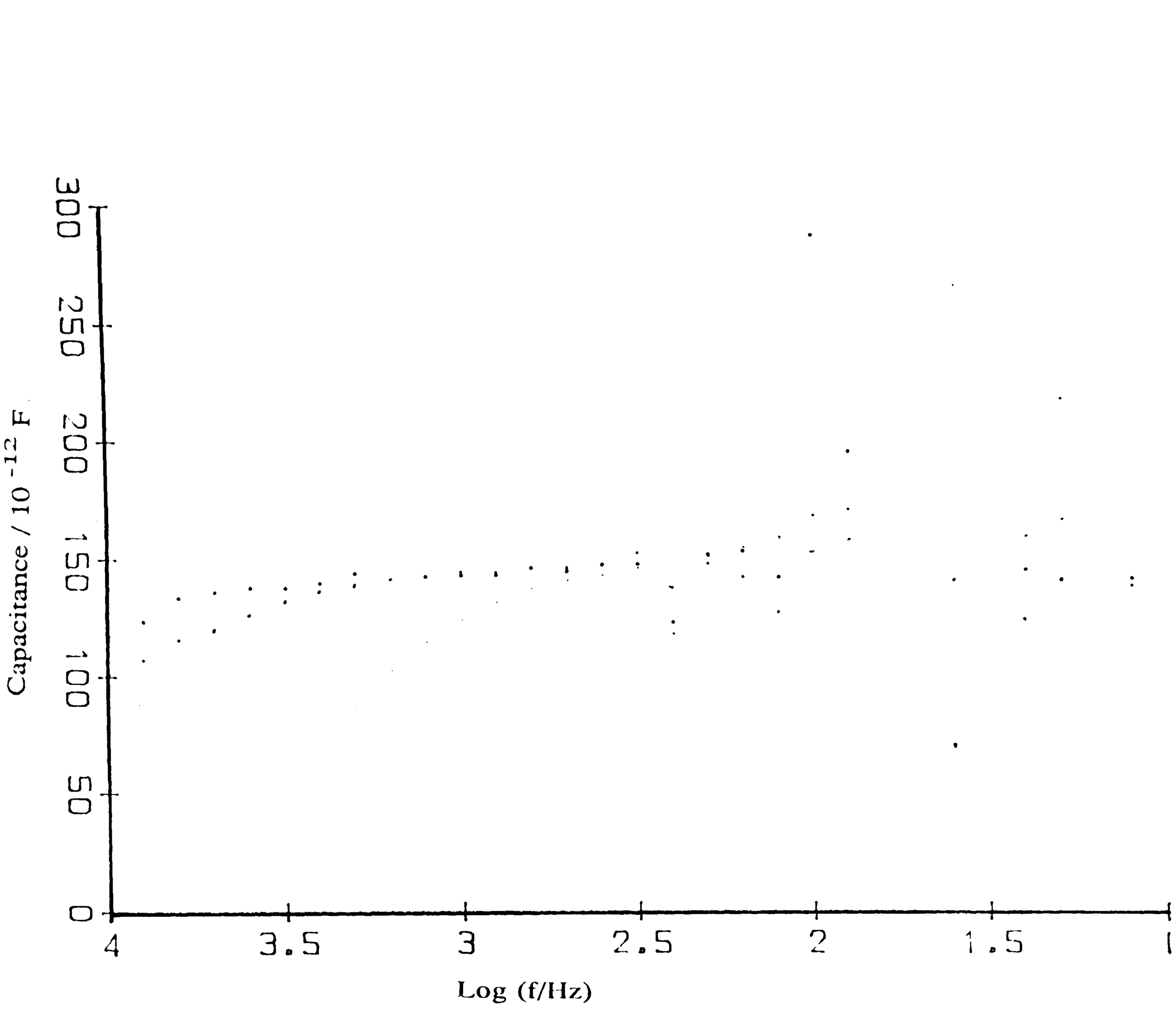

Figure 4:18 A.C. Impedance Results for the Radelkis Electrode (OH 8513 Electrode. "Imaginary" Resistance.

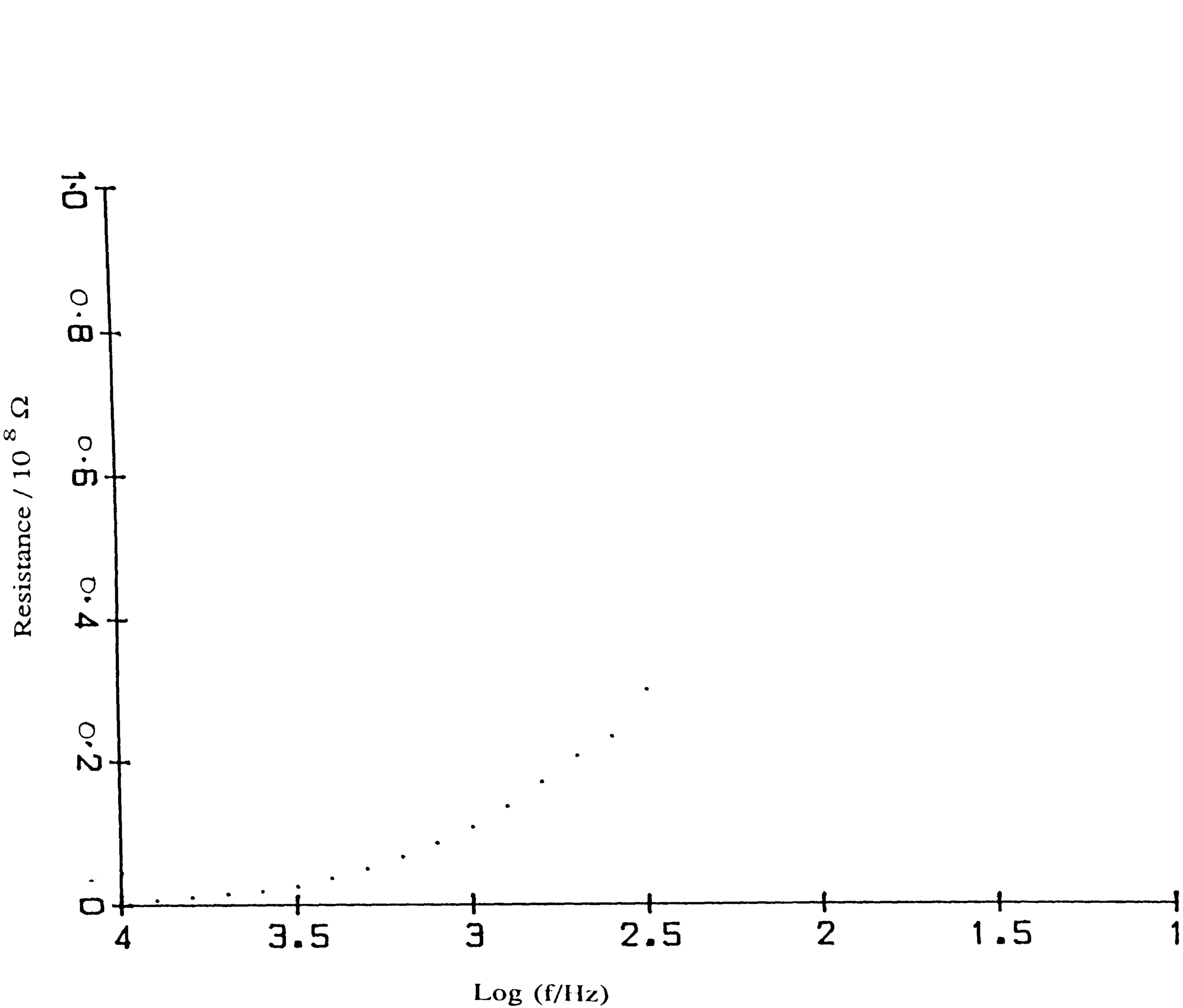

Figure 4:19 A.C. Impedance Results for the Russell (CE7L) Electrode.

"Real" Resistance.

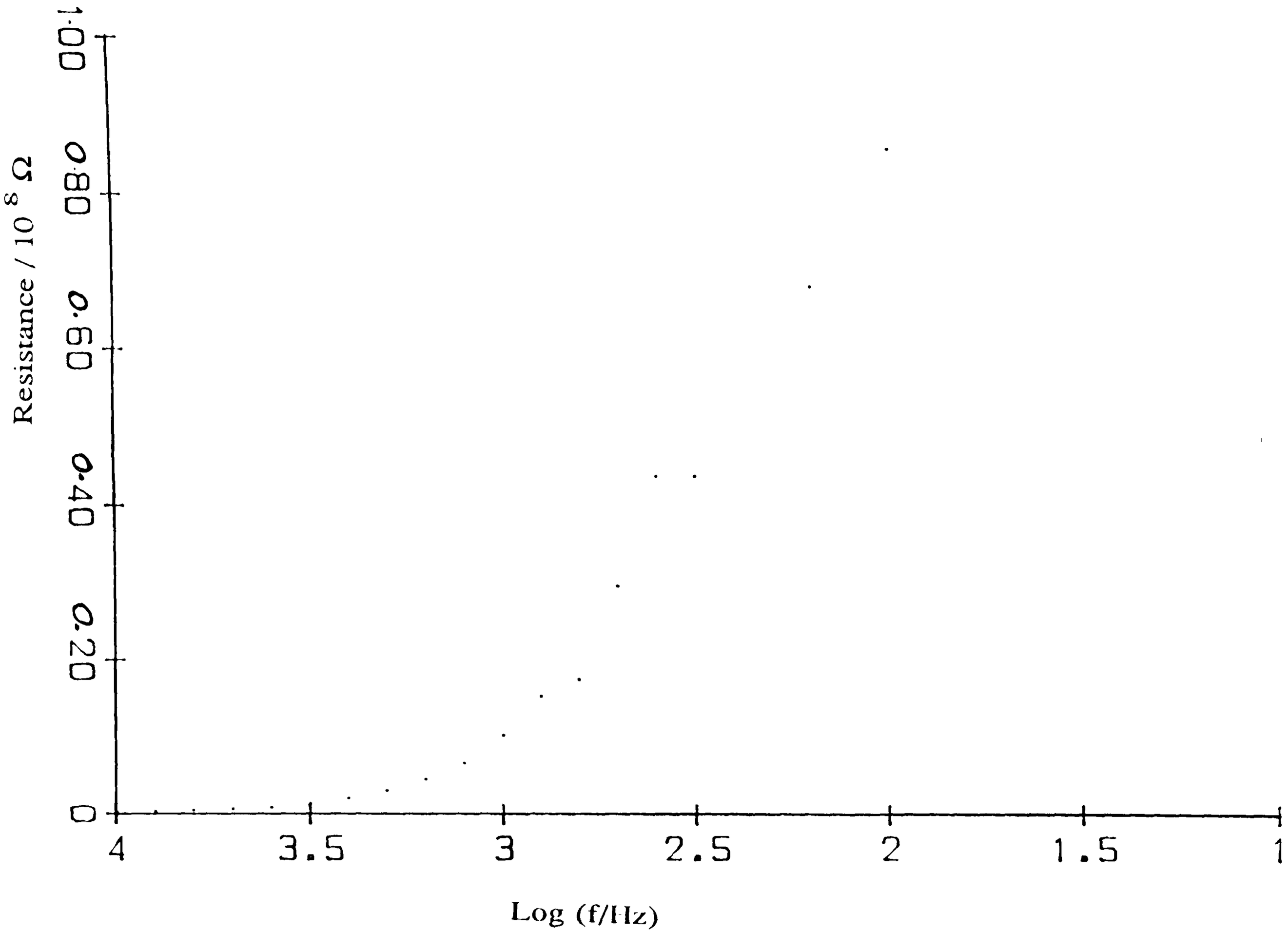

Figure 4:20 A.C. Impedance Results for the Radelkis (OH 8513) Electrode. "Real" Resistance.

flat membrane used by Radelkis compared with the glass bulb used by Russell may suggest the explanation lies in the capacitance effect.

Table 4:2 Results of Impedance Studies for the Russell Electrode (CE7L).

Frequency / Hz	Z'/ Ω x 10^4	Z''/ Ω
1.000E+05	5.10	-3.62E+03
7.936E+04	5.09	4.03E+03
6.305E+04	5.10	1.16E+04
5.004E+04	5.09	2.00E+04
3.975E+04	5.09	2.93E+04
3.155E+04	5.10	4.05E+04
2.506E+04	5.13	5.35E+04
1.991E+04	5.15	6.95E+04
1.580E+04	5.17	8.95E+04
1.255E+04	5.21	1.13E+05
9.964E+03	5.22	1.44E+05
7.936E+03	5.21	2.32E+05
6.305E+03	5.27	2.32E+05
5.004E+03	6.11	2.97E+05
3.975E+03	7.14	3.65E+05
3.155E+03	7.96	4.50E+05
2.506E+03	8.67	5.62E+05
1.991E+03	9.69	6.98E+05
1.580E+03	11.3	8.73E+05
1.255E+03	13.5	1.08E+06
9.964E+02	16.7	1.35E+06
7.936E+02	20.4	1.68E+06
6.305E+02	25.4	2.09E+06
5.004E+02	31.9	2.58E+06
3.975E+02	44.0	3.21E+06
3.155E+02	53.9	4.03E+06
2.506E+02	-6.14	5.58E+06
1.991E+02	91.1	5.99E+06
1.580E+02	176	7.51E+06
1.255E+02	169	8.06E+06
9.964E+01	396	1.06E+07
7.936E+01	183	1.45E+07
6.305E+01	119	-1.80E+06
3.975E+01	1172	2.03E+07
3.155E+01	1320	-1.52E+07

D.C. Resistance ~ 5.14 x 10^4 Ω

The values between the dashed lines are those plotted in Figures 4:17, 4:19.

Table 4:3 Results of Impedance Studies for the Radelkis Electrode (OH-8513).

Frequency / Hz	Z'/ Ω x 10^5	Z''/ Ω x 10^5
1.000E+05	9.82	-7.23
7.936E+04	8.78	-6.69
6.305E+04	7.77	-6.08
5.004E+04	6.81	-5.36
3.975E+04	6.00	-4.58
3.155E+04	5.37	-3.78
2.506E+04	4.90	-2.99
1.991E+04	4.56	-2.26
1.580E+04	4.30	-1.56
1.255E+04	4.12	-0.905
9.964E+03	3.96	-0.214
7.936E+03	3.90	0.622
6.305E+03	4.29	1.40
5.004E+03	4.58	1.72
3.975E+03	4.53	2.27
3.155E+03	4.49	3.04
2.506E+03	4.47	4.01
1.991E+03	4.49	5.18
1.580E+03	4.53	6.63
1.255E+02	4.59	8.44
9.964E+02	4.68	10.6
7.936E+02	4.77	13.3
6.305E+02	4.92	16.7
5.004E+02	5.26	21.0
3.975E+02	5.49	26.5
3.155E+02	5.66	33.1
2.506E+02	14.5	48.8
1.991E+02	7.84	51.1
1.580E+02	10.4	62.6
1.255E+02	18.2	74.3
9.964E+01	15.1	101.0
7.936E+01	31.9	116.0

D.C. Resistance ~ 4.80 x 10^4 Ω

The values between the dashed lines are those plotted in Figures 4:18, 4:20.

4.8.3 Using SUPERQUAD.

The following section explains how an auto-titration system, delivering small, accurately measured aliquots (or charge pulses) may be used in conjunction with SUPERQUAD to determine the β formation constants for metal-ligand complexes.

The β constants can be expressed by

$$\beta_{mlh} = \{ [M_m L_l H_h] / [M]^m [L]^l [H]^h \} A_H^h \qquad (4.10)$$

where m, l are positive integers or zero

h is positive for protonated species, negative for hydroxo complexes or zero

$[M_m L_l H_h]$ is the concentration of the complexed species

[M] is the concentration of uncomplexed metal

[L] is the concentration of uncomplexed ligand

A_H is the measured proton activity

The analytical concentration of M, L, H at any point during a complexometric titration may be given by the series of mass balance equations

$$T_M = [M] + {}^j\Sigma_{\mu=1} \beta_{mlh} [M]^m [L]^l [H]^h \qquad (4.11)$$

$$T_L = [L] + {}^j\Sigma_{m=1} \beta_{mlh} [M]^m [L]]^l [H]^h \qquad (4.12)$$

$$T_H = [H] + {}^j\Sigma_{m=1} \beta_{mlh} [M]^m [L]^l [H]^h + A_H / f - (K_w / A_H^h) \qquad (4.13)$$

where T_M, T_L, T_H are the analytical concentrations of M, L, H, respectively, and can be determined from the original concentration of test solutions taken.

f is the activity coefficient for H^+

K_w is the dissociation constant of water

A_H is obtained from potentiometric titration

Other workers [94] have used SUPERQUAD to evaluate the formation and dissociation constants of the 'Good' buffers [77], which are used in clinical studies. Good [77] calculated approximate values for the dissociation constants; knowing the metal binding constants, one can introduce a correction factor on introduction of metal salts to compensate for metal complexation. Kataky [94] determined these complexation properties for a range of 'Good' buffers, MOPS, HEPES, TES, BES with metal cations, Na^+, K^+, Ca^{2+}, titrating with base and analysing the data using SUPERQUAD.

The buffers MOPS, HEPES etc. are zwitterionic; the unprotonated form (h=1) is considered as LH^+. The β formation constants for 1:1 metal complexes can be calculated from the following equations

$$L^- + H^+ \text{ ==== } LH^+ \qquad (4.14)$$

$$K_{a2} = [LH^+] / [L^-] A_{H+} \qquad (4.15)$$

$$\beta_{0,1,1}$$

$$LH^+ + H^+ \text{ ==== } LH_2^+ \qquad (4.16)$$

$$K_{a1} = [LH_2^+] / [LH^+] A^- \qquad (4.17)$$

$$\beta_{0,1,2}$$

$$LH^+ + M \text{ ==== } MLH^+ \qquad (4.18)$$

$$K_{MLH+} = [MLH^+] / [M] [LH^+] \qquad (4.19)$$

$$\beta_{1,1,1}$$

$$LH_2^+ + M \text{ ==== } MLH_2^+ \qquad (4.20)$$

$$K_{MLH2+} = [MLH_2^+] / [M] [LH_2^+] \qquad (4.21)$$

$$\beta_{1,1,2}$$

Using this information, a header file, shown in Table 4:5, may be set

up in SUPERQUAD. The value in the 'KEY' column denotes whether log β is a constant (0), to be refined (1) or to be ignored initially and refined during the second refinement (-1); the file shows β for MLH_2^+ and MLH^+ to be refined Further details regarding the set up of SUPERQUAD files may be obtained in the 'HELP' and 'Setting up SUPERQUAD' documentation (see Appendices E(i), (ii)).

Table 4:5 SUPERQUAD Header File for Calcium / MOPS Complexometric Titration.

log β	m	l	h	KEY
-11.57	1	0	-1	0
-24.17	1	0	-2	0
7.8	1	1	1	1
11.6	1	1	2	1
7.42	0	1	1	0
10.42	0	1	2	0
-13.62	0	0	-1	0

4.8.4 Titration Results.

Accurate end point determinations were obtained using the sensor-actuator system. The data obtained were read directly into a curve plotting programme, this programme to be incorporated into the titration programme as an available option, allowing rapid visual appraisal of the experiment; figure 4:21 shows a representative titration curve. For the relevant titrations, data were transferred, on disc, to determine the β formation constants of various metal / ligand species, as described in the previous section. Chapter 5 describes in detail the application of SUPERQUAD.

As stated earlier, this titration set up is soon to be developed on-line, and was, therefore, treated as a prototype. In the revised system,

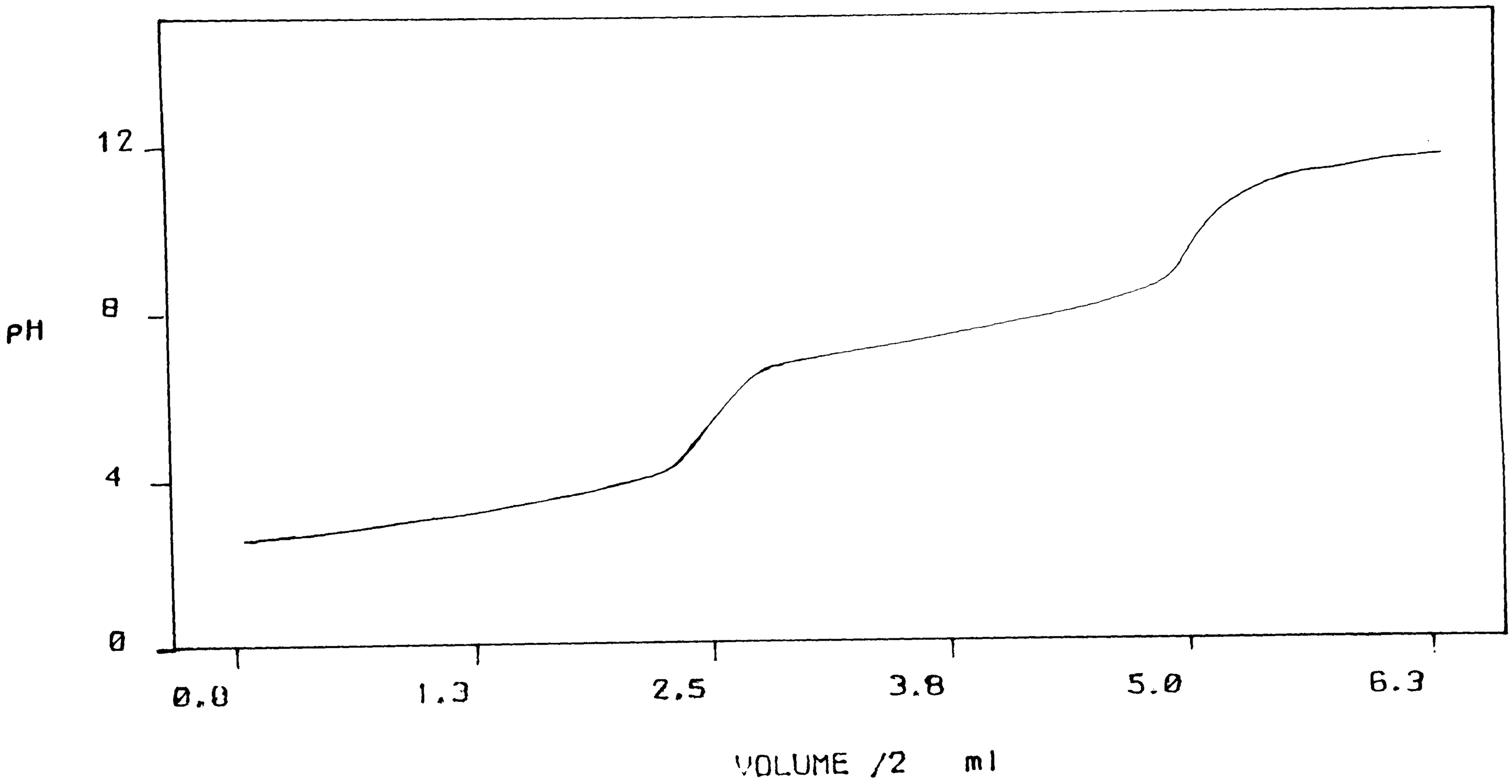

Figure 4:21 Typical Titration Curve using the Sensor Actuator System.

data will be fed directly into a curve fitting programme and can be read directly into SUPERQUAD, if required. At the present time, however, titration data are stored on disc and manipulated, as necessary, at a later date.

4.9 Conclusions.

Having fully appraised the EDT coulometric auto-titrator, it can be concluded that although this system was suitable for continuous current applications (see Chapter 5) it could not be adopted to a sensor-actuator system.

Most electrodes were susceptible to interference from the electric field of the generating electrode pair and it is therefore recommended that a two compartment cell is used and that the orientation of electrodes in the cell is chosen so that the indicator electrode is placed near the working electrode but not between the generating electrode pair (figure 4:12).

The Radelkis electrode, OH-8513, was not susceptible to this interference. This may be due to the high resistance of the Radelkis electrode or possibly due to the flat glass membrane. Disturbingly, only two out of four of the Russell, CE7L, electrodes were prone to interference from the generating electrodes. One would expect all of the electrodes to behave in the same manner. This discrepancy may be due to a variation in age of electrodes, affecting the resistance of the membrane. A.C. Impedance tests could be carried out to evaluate this feature.

For very accurate end point determinations in volumetric or coulometric titrations, the developed sensor-actuator system was found to be far superior to the EDT system. Results here show this system in auto-titration mode, as required by SUPERQUAD, however the system functions well in actuator mode. This set up acted as the fore-runner to a more complex system which is being developed on-line, and has allowed many of the teething problems to be solved.

References.

1. Faraday M.
Phil. Trans. 1833, 505
cited in ref. 17

2. Faraday M.
Phil. Trans. 1834, 732
cited in ref. 17

3. Faraday M.
Phil. Trans. 1834, 747
cited in ref. 17

4. Faraday M.
Phil. Trans. 1834, 821
cited in ref. 17

5. "Experimental Research in Electrochemistry"
ed. Taylor R. & Taylor J.E.
London 1839, Vol I

6. Tutundzic P.S.
Anal. Chim. Acta 1958, **18**, 60

7. Grower G.G.
Proc. Amer. Soc. Testing Material 1917, **17**, 129

8. Cambell W.E. & Thomas U.B.
Nature 1938, **142**, 253

9. Szebelledy L. & Smogy Z.
Fresenius Z. Anal. Chem. 1938, **112**, 313, 323, 332, 358, 391, 395, 400

10. Szabadvary F. "History of Analytical Chemistry"
Pergamon Press, New York, 1966 pp. 316 - 317

11. Briglio A. Jr., Brockman J.A., Schlinger W. & Shaffer P.A. Jr.
U.S. Dept. of Commerce Office of Publication Board
O.S.R.D. Report 1945, 6047, PB 5925
cited in ref. 12

12. Shaffer P.A. Jr., Briglio A. Jr. & Brockman J.A. Jr.
Anal. Chem. 1948, **20**, 1008

13. Deford D. & Miller J.W.
Coulometric Analysis in " Treatise on Analytical Chemistry"
Kolthoff I.M., Ewing P.J., Sendell S.B. eds.
Part I, Vol 4, pp. 2475 - 2531
Interscience Publishing Co., New York 1963

14. Milner G.W.C.
"The Principles and Applications of Polarography"
Chap. 1, 2, 8
Longmans, Green & Co. Ltd., London 1957

15. "Coulometric Analysis"
Abresch K. & Classen I. (English Translation)
Chapman & Hall Ltd., London 1961

16. "Polarography."
2nd ed. Kolthoff I.M. & Lingane J.W.
Vol. I Theoretical Principles . Instrumentation and Technique.
Chap. XVI, XVII
Interscience Publishers Inc., New York 1952

17. "Comprehensive Analytical Chemistry"
ed. Wilson C.L. & Wilson D.W.
Vol. IID "Coulometric Analysis."
Elsevier Scientific Publ. Co., Amsterdam 1975

18. Lingane J.J.
"Electroanalytical Chemistry"
Interscience Publishers Inc., New York 1953

19. Davis D.G.
Anal. Chem. 1974, **46**, 21R

20. Tackett S.L.
Chem. Technol. 1972, **2**, 734

21. Specialist Periodical Reports
"Electrochemistry" Vol 3 p.232
ed. G.J. Hills
The Chemical Society, London

22. Ewing G.W.
A.C.S. Symposium Series 1989, **390**, 402
"Electrochemistry, Past and Present"
Chapter 27 "Colometric Titrimetry"

23. "Coulometry at Controlled Current"
in " New Instrumental Methods in Electrochemistry"
ed. Delahey P.
Interscience Publ. Inc., New York 1954
Chapter 14

24. Meites L.
"Controlled Potential Electrolysis"
in "Physical Methods of Organic Chemistry"
ed A Weissberger Vol I, Part IV, Chapter XLIX, pp.3281

25. Bos M., Bergveld P. & van Veen Blauuw A.M.W.
Anal. Chim. Acta 1979, **109**, 145

26. Bergveld P., van der Schoot B.H. & Onckiewicz J.H.L.
Anal. Chim. Acta 1983, **151**, 143

27. van der Schoot B.H. & Bergveld P.
Sensors & Actuators 1985, **8**, 11

28. van der Schoot B.H. & Bergveld P.
Proc 2nd meeting on Chemical Sensors, Bordeaux, France, 1986
pp. 665

29. van der Schoot B.H.
Ph.D. Thesis, Twente Univ. of Technology, 1986

30. van der Schoot B.H. & Bergveld P.
Sensors & Actuators 1988, **13**, 251

31. van der Schoot B.H. & Bergveld P.
Anal. Chim. ACta 1987, **199**, 157

32. Willatts S.M.
"Lecture Notes on Fluid and Electrolyte Balance"
Blackwell Scientific Publications, Oxford, London
2nd ed., 1987

33. Worth H.G.J.
Analyst 1988, **113**, 374

34. Simon W., Morf W.E. & Ammann D.
Mikrochem J. 1987, **36**, 3

35. Lindberg J.
J. Electroanal. Chem. 1972, **40**, 265

36. Bard A.J. & Santhanan K.V.S.
in "Electroanalytical Chemistry" Vol. IV, Chapter 3, ed. Bard A.J.
Marcel Dekker, New York 1970

37. Bishop E.
Mikrochim. Acta 1956, 619

38. Janata J. & Mark H.B.
Anal. Chem 1967, **39**, 1896

39. Atkinson G.F. & Shaw J.H.
J. Chem. Educ. 1969, **46**, 387

40. Clem R.G., Jakob F., Anderberg D.H. & Orlas L.D.
Anal. Chem. 1971, **43**, 1398

41. Nakamura K., Kuboyama K., Ono K. & Kawada K.,
Mikrochim. Acta 1972, **3**, 353

42. Ruttinger H.H. & Spohn U.
Anal. Chim. Acta 1987, **202**, 75

43. Lingane J.J.
J. Amer. Chem. Soc. 1945, **67**, 1916

44. Smith W.H. & Bard A.J.
J. Amer. Chem. Soc. 1975, **97**, 5203

45. Cooper F.A. & Quayle J.C.
Analyst 1966, **91**, 363

46. Pearson R.G. & Piethe L.H.
J. Amer. Chem. Soc. 1954, **76**, 3087

47. Eisner U. & Mark H.B.
Talanta 1964, **16**,27

48. Lakshminaarayanaih N.
In "Transport Phenomena in Membranes"
Academic Press, New York 1969 pp. 319 - 325
cited in ref. 35

49. "Standard Potentials in Aqueous Solutions"
Bard A.J., Parsons R., Jordan J. (ed.)
Marcel Dekker Inc., New York & Basle 1985
Chapter 10 (Hg), 12 (Pt)

50. Elving P.J. & Krivis A.F.
Anal. Chem. 1958, **30**, 1645

51. Elving P.J. & Smith D.L.
Anal. Chem. 1960, **32**, 1849

52. Adams R.N.
Anal. Chem. 1958, **30**, 1576

53. Yoshimori T., Arakawa M. & Takeuchi T.
Talanta 1965, **12**, 147

54. Giner J., Parry J.M. & Swette L.
Abstr. paper 154th meeting Amer. Chem. Soc., Sept, 1967, pp. L15

55. Bishop E. & Riley M.
Analyst 1973, **98**, 416

56. Bard A.J.
Anal. Chem. 1963, **11**, 191

57. Facsko G.
Rev. Roum. Chim. 1966, **11**, 191

58. Ducret L. & Cornet C.
J. Electroanal. Chem. 1966, **11**, 317

59. Epstein J., Sober H.A. & Silver S.D.
Anal. Chem. 1947, **19**, 625

60. Bishop E. & Short G.D.
Analyst 1964, **89**, 587

61. Reis B.F., Godinho O.E.S., Aleixo L.M. & Rohwedder J.J.R.
Anal. Chim. Acta 1989, **22**, 379

62. Sease J.W., Niemann C. & Swift E.H.
Anal. Chem. 1947, **19**, 197

63. Herrmann Cal.C., Perrault G.G. & Pilla A.A.
Anal. Chem. 1968, **40**, 1173

64. Marinenko G. & Taylor J.K.
Anal. Chem. 1968, **40**, 1645

65. Ho P.P.L. & Marsh M.M.
Anal. Chem. 1963, **35**, 618

66. Lauer G., Abel R. & Anson F.C.
Anal. Chem. 1967, **39**, 765

67. van Leeuwen H.P.
Electrochimica Acta 1978, **23**, 207

68. Stephens F.B., Jakob F., Rigdon L.P. & Harrar J.E.

Anal. Chem. 1970, **42**, 764

69. Jaycox L.B. & Curran D.J.
Anal. Chem. 1976, **48**, 10

70. Kelley M.T., Jones H.C. & Fisher D.J.
Anal. Chem. 1959, **31**, 488

71. Kelley M.T., Jones H.C. & Fisher D.J.
Anal. Chem. 1959, **31**, 956

72. Earle W.E. & Fletcher K.S.
Chem. Instrum. 1976, **1**, 101

73. Martin C.R. & Freiser H.
Anal. Chem. 1979, **51**, 803

74. Smit J.C. & Smit H.C.
Anal. Chim. Acta 1982, **143**, 45

75. Smit J.C., Smit H.C. & Hannema U.
Anal. Chim. Acta 1982, **143**, 79

76. Covington A.K. & Ferra M.I.A.
Anal. Chem. 1977, **49**, 1363

77. Good N.E., Winget D.G., Winter W. & Connolly T.M.
Biochemistry 1960, **5**, 467

78. Radelkis Handbook for Operation of the EDT-401 Autotitrator
Radelkis, Budapest

79. Private Communication with Dr. Henry Hudson, Deakin Univ.,
Waurn Ponds, Victoria, Australia

80. Oesch U., Xu A., Brzozka Z., Suter G. & Simon W.
Chimia 1986, **40**, 351

81. Oesch U., Anker P., Ammann D. & Simon W.
"Ion Selective Electrodes"
ed. Pungor E. & Buzas I.
Akademia Kiado, Budapest, 1985, pp.81

82. Ammann D., Anker P., Metzger E., Oesch U. & Simon W.
"Ion Measurements in Physiology and Medicine"
ed. Kessler M.
Springer-Verlag, Berlin, Heidelberg 1985, pp.102

83. Matsuo T., Esashi M., Nakajimi H. & Shoji S.
"Implantable Sensors for Closed Loop Prosthetic Systems"
ed. Ko W.H.
Futura, Mount Kisco, New York 1985, Chap. 9

84. Shimada K., Yano M., Shibatani K., Komoto Y., Esashi M. & Matsuo T.
Med. & Biol. Eng. & Computing 1980, **18**, 741

85. Gans P., Sabatini A. & Vacca A.
J.Chem. Soc. Dalton Trans. 1985, pp.1195

86. Sayce I.G.

Talanta 1968, **15**, 1397

87. Sabatini A. & Vacca A.
J. Chem. Soc. Dalton Trans. 1972, 1693

88. Alcock R.M., Hartley F.R. & Rogers D.E.
J. Chem. Soc. Dalton Trans. 1978, **115**

89. Perrin D.D. & Stunzi M.
"Computational Methods for the Determination of Binding Constants"
ed. Leggett D.J.
Plenum Press, New York, London 1985 Chap.4

90. Hill B
Beebug April 1988 pp. 59

91. Hill B.
Beebug May 1988 pp. 58

92. Evans G.P.
Ph. D. Thesis, University of Newcastle-upon-Tyne 1985

93. Churchouse S.
Ph. D. Thesis, University of Newcastle-upon-Tyne 1985

94. Kataky R.
Ph. D. Thesis, University of Newcastle-upon-Tyne 1988

CHAPTER FIVE

DETERMINATION OF pK_2^d FOR HYDROGEN SULPHIDE

5.1 Introduction.

The values of pK_1^d, pK_2^d of hydrogen sulphide are important in industrial processes, e.g. in the paper and the oil industry [1], in environmental and health science e.g. water pollution control [2, 3]. In geochemical processes, in order to predict the behaviour of naturally occurring hydrogen sulphide in pore water and anoxic basins in biological processes [4], it is necessary to know the stability relationship of metal oxides and sulphides under various conditions. The behaviour of biological sulphate-reducing bacteria may be monitored using a sulphide ion selective electrode [5, 6].

Speciation is dependent on environment e.g. pH and temperature, and these studies will lead to an understanding of hydrothermal processes [7-9]. The presence of dissolved hydrogen sulphide, is an important indicator of the redox character of ground water, which affects the molarity of metal and non-metal species in this medium [10-12]. Knowing the preferred conditions for sulphide formation is of critical importance in the oil-drilling industry, enabling the formation of pockets of gaseous hydrogen sulphide to be predicted [13].

Also, in sewage and industrial effluents, in freshwater and sea water [14, 15], measurements of pH and dissolved sulphide concentration give information about the quantity of hydrogen sulphide present. Since the rate of escape of sulphides to the atmosphere is almost proportional to the bulk concentration of hydrogen sulphide [2], then this method of dual monitoring of sulphide and pH can be used as a means of determining sulphide content. This procedure relies on a knowledge of the dissociation constants.

Meyers [16], in a poor review of values for pK_2^d of H_2S, states that earlier values of pK_2^d of 12-14 are much too low and gives a 'new' value of 19 ± 2, more in line with periodic trends (Table 5:1). He suggests that, like O^{2-}, S^{2-} should not be regarded as a component of aqueous solution. Meyers attributed the large discrepancy in published pK_2^d values to the

presence of polysulphides formed by incomplete removal of dissolved oxygen and not considered by early workers.

Table 5:1 Periodic Trends

Comparison of the Group VIA Acid Dissociation Constants in Water.

Acid	pK_1^d	pK_2^d	$pK_1^d - pK_2^d$
H_2O	15.7	36*	20*
H_2S	7.0	19#	12
H_2Se	3.6	15.0	11.4
H_2Te	2.6	11.0	8.0

* Latimer W.M. [17]

\# Meyers R.J. [16]

Spectrophotometric techniques such as Raman[18], UV-absorption [19], and colorimetry [20], conductance methods [21], as well as potentiometric methods [22], have been used in the determination of pK_2^d. In the work described here, electrochemical methods were used and results obtained compared with other methods.

5.2 Hydrolysis of Hydrogen Sulphide.

The hydrolysis of hydrogen sulphide is governed by the following equations [23];

$$H_2O + S^{2-} \overset{K_{h1}}{\rightleftharpoons} HS^- + OH^- \qquad (5.1)$$

$$H_2O + HS^- \overset{K_{h2}}{\rightleftharpoons} H_2S + OH^- \qquad (5.2)$$

where the hydrolysis equilibrium constants, K_{h1}, K_{h2} are given by

$$K_{h1} = K_w / K_2^{\,d} = 2.773 \qquad (\mu=0.1) \qquad (5.3)$$

$$K_{h2} = K_w / K_1^{\,d} = 0.628 \times 10^{-7} \quad (\mu=0.1) \quad (5.4)$$

where μ is ionic strength

$K_1^{\,d}$, $K_2^{\,d}$ are the acid dissociation constants for the sulphide species

K_w is the auto protolysis of water given by

$$K_w = [H^+][OH^-]/[H_2O] \qquad (5.5)$$

for the hydrolysis of water

$$H^+ + OH^- \longrightarrow H_2O \qquad (5.6)$$

The total concentration of sulphide present at any pH is the sum of the sulphide and bisulphide ions present, given by

$$[S^{2-}] = f_{S2-}\,[S^{2-}]_{TOT} / \{1+ ([H^+] / K_2^{\,d})\} \qquad (5.7)$$

$$[HS^-] = f_{HS^-}[S^{2-}]_{TOT} / \{1+([H^+]/K_1^{\,d}) + (K_2^{\,d}/[H^+])\} \quad (5.8)$$

$$[H_2S] = f_{H2S}[S^{2-}]_{TOT} / \{(1+(K_1^{\,d}/[H^+]) + (K_1^{\,d}K_2^{\,d}/[H^+])\} \qquad (5.9)$$

where $[S^{2-}]$, $[HS^-]$, $[H_2S]$ = sulphide ion, bisulphide ion, hydrogen sulphide concentration, respectively

$[S^{2-}]_{TOT}$ = total sulphide concentration

f_{S2-} = activity coefficient of the sulphide ion

In alkaline solutions, only the first hydrolysis step (equation (5.1)) is important, so $K_1^{\,d}$ is negligible, and

$$[S^{2-}] = f_{S2-}[S^{2-}]_{TOT} / \{\ 1 + ([H^+] /K_2^{\,d})\} \qquad (5.8)$$

It can be seen, from equation (5.8) that, if there is a constant concentration of total sulphide species and the ionic strength does not change, then the activity of sulphide, S^{2-}, increases with pH. Above pH 12, it is assumed that most of the total sulphide present existed as the sulphide S^{2-} ion. Below pH 12, the total sulphide concentration is the sum of the sulphide and bisulphide, HS^-, concentrations [24]. An earlier worker [25] found that below pH 10, less than 10 % of total sulphide species present existed as the sulphide ion. This is substantiated by Umezawa *et al.* [26].

Simplifying equation (5.8),since $([H^+]/ K_2^d) >> 1$ and at constant ionic strength, μ, the value for $[H^+]$ may be inserted into the Nernst equation for sulphide ions,

$$E = \text{constant} - 0.0296 \log [S^{2-}] \qquad (5.10)$$

giving $$E = \text{constant} - 0.0296\ pH \qquad (5.11)$$

which is a relationship between pH values and potential difference for a given concentration of sulphide ions. Crombie *et al.* [27] stated that due to this relationship of hydrogen ions and sulphide ions, it was necessary to monitor only pH during titration of sulphide solutions. Hseu and Rechnitz [23] simultaneously monitored pH and sulphide ion concentration during volumetric titrations with hydrochloric acid (0.05 mol dm^{-3}) (figure 5:1).

The aim of this research was to carry out titrations of sodium sulphide solutions, monitoring the hydrogen ion and sulphide ion concentrations simultaneously, as did Hseu and Rechnitz, but using a coulometric titrator and taking steps to prevent sample oxidation.

5.3 Review of Previous Spectroscopic Work.

Giggenbach [28] measured the UV / vis spectra of 0.434 mol dm^{-3} solutions of hydrogen sulphide as a function of sodium hydroxide concentration over the range 5.7 to 15.2 mol dm^{-3} at 43600 cm^{-1},

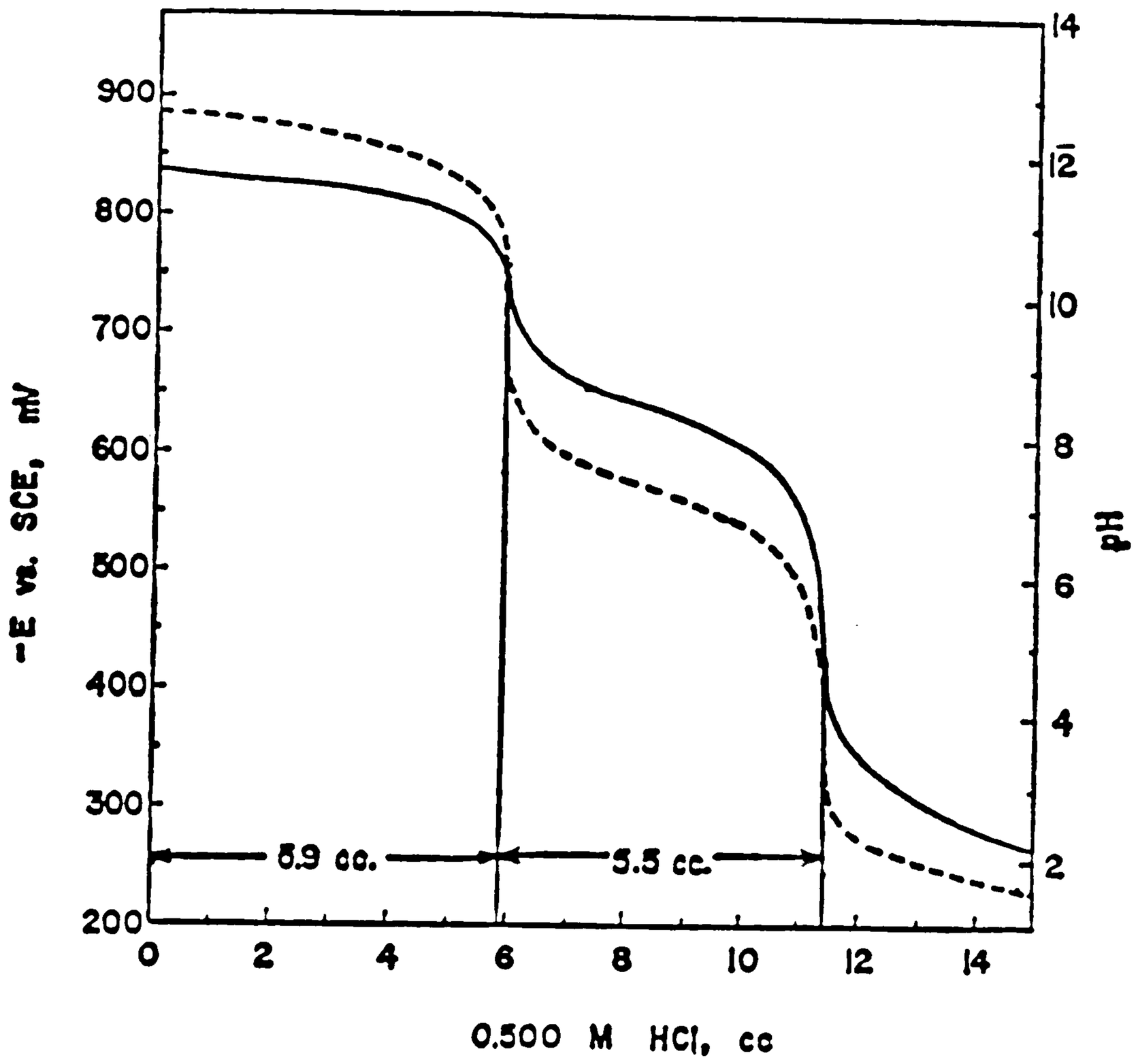

Figure 5:1 Simultaneous pH and Sulphide Monitoring during Volumetric Titration of Sodium Sulphide (5.0×10^{-2}) with Hydrochloric Acid [23].

assigning this band to bisulphide ions (Table 5:2). Precautions were taken to exclude oxygen and in highly alkaline solutions, 5.7 to 18.2 mol dm^{-3} sodium hydroxide, Giggenbach calculated K_2^d to be 17.1± 0.1.

Table 5:2 UV Absorption Band Assignments for Sulphide Species.

BAND cm^{-1}	163000	16800	25000	27750	27700	31000	40000	43500	43600
AUTHOR									
Ellis & Golding 1959 [28]	-	-	-	-	-	-	-	HS^-	-
Blandamer *et al.* 1964 [35]	-	-	-	-	S^{2-}	-	-	S^{2-}	-
Ellis & Milestone 1967 [9]	-	-	-	-	S^{2-}	-	-	-	HS^-
Giggenbach 1971 [29-31]	-	S_2^-	S_4^{2-}	polysulphides				S^{2-}	HS^-
Ellis & Giggenbach 1971 [34]	-	-	-	S_n^{2-} or SO_4^{2-}	-	-	S^{2-}	-	HS^-
Clark & Cobbold 1978 [32]	-	-	S_2^-	-	-	-	-	-	-
Cotton *et al.* 1976 [33]	S_3^-	-	-	-	-	-	-	-	-

Ellis and Golding [29], who did not exclude atmospheric oxygen and carbon dioxide, also observed a band in this region, at 43500 cm^{-1}, which they assigned to the bisulphide ion. Subsequent work carried out by

16800 cm^{-1} - 31000 cm^{-1}. Giggenbach showed the hypersulphide ion (S_2^-) to be responsible for the 16800 cm^{-1} band and the tetrasulphide band (S_4^{2-}) for the 25000 cm^{-1} band. He studied the formation and rearrangement of polysulphides and dissociation to polysulphide radicals as a function of temperature and pH and showed that most polysulphides are unstable above pH 8 and thiosulphate ions may be formed. Only S_2^{2-} and S_3^{2-} are stable in aqueous solution with absorption bands at 25000 cm^{-1}, 16300 cm^{-1} respectively [33, 34].

In concentrated alkaline conditions, 5 mol dm^{-3}, Ellis and Giggenbach [34] observed a shoulder at 40000 cm^{-1} on the major peak of 43500 cm^{-1}. This band was found to form in the presence of hydroxide ions and was attributed to sulphide ions, rather than to complexes containing sulphide or bisulphide ions, from the back reaction of equation (5.1),

$$SH^- + OH^- \rightleftharpoons S^{2-} + H_2O \qquad (5.1)$$

They, therefore, dismissed the claims by Blandamer *et al.* [36], who observed a weak absorption band at 27700 cm^{-1} which had been assigned to sulphide ions, substantiating this argument by comparing the spectra of chloride and sulphide species, and iodide and bisulphide species (Table 5:3, 5:4). Following group trends, one would expect sulphide ions to have an absorption maximum < 35000 cm^{-1}. Ellis and Giggenbach, again, explained this absorption to polysulphide formation.

Table 5:3 Comparison of the UV Absorption of Chloride and Sulphide Ions, in Aqueous [36].

Chloride		Sulphide	
Species	Wavenumber max. / cm^{-1}	Species	Wavenumber max. / cm^{-1}
Water	55200	Water	27750
CsCl	58350	BaS	30820
RbCl	58980	SrS	38100
KCl	61394	CaS	41950

Table 5:4 Comparison of UV Absorption of Iodide and Bisulphide Ions in Various Solvents (20 °C).

Solvent	Wavenumber ν_{max} / cm^{-1}	
	Bisulphide	Iodide
water, 1 atm	43500 [29]	44200 [37, 38]
water, 345 atm	43850	44400 [39]
4 mol dm^{-3} $KF_{(aq)}$	-	45085 [40]
6 mol dm^{-3} $KF_{(aq)}$	44650	-
Methyl Cyanide 0.175, 0.1587 mol fraction water	41750	41980 [41]
Methyl Cyanide 0.311, 0.35 mol fraction water	44700	45100 [42]

Below 5 mol dm^{-3}, the 40000 cm^{-1} band could not be produced, and below 8 mol dm^{-3} sulphide ion, concentrations could not be measured

reliably due to the equilibria:

$$S^{2-} + H_2O \underset{K_{h1}}{\overset{-K_{h1}}{\rightleftharpoons}} SH^- + OH^- \qquad -K_{h1} \sim 1 \qquad (5.12)$$

hence highly alkaline solutions were used. Experimental values were extrapolated from high to low ionic strengths from

$$K_2{}^d = K_w / K_{h1} = (K_w K_e) / a_w \qquad (5.13)$$

where K_w is the autoprotolysis constant for water (0.96×10^{-14} at 24 °C)

and $a_w = [H_2O]\, f_{H2O}$

$[H_2O]$ = analytical concentration of water

f_{H2O} = activity coefficient of water for concentrated sodium hydroxide solution

and $K_e = \{([S^{2-}]a_w) / [SH^-][OH^-]\}\ \{f_{S2-} / (f_{HS-}\, f_{OH-})\}$ (5.14)

leading to the modified form

$$K_e = K'_e\, f\pm \qquad (5.15)$$

where $K'_e = [S^{2-}]\ a_w / [SH^-]\ [OH-]$, the modified experimental concentration coefficient

$$f\pm = f_{s2-} / (f_{HS-}\, f_{OH-})$$

a_w was included in K'_e as Giggenbach expected f± to be less sensitive to changes in ionic strength of solution.

All workers are in agreement that the bisulphide ion is observed at 43500 - 43600 cm^{-1}; it is the assignation of a band to the sulphide ion which is the cause of concern.

Equation (5.15) was used by Meyer *et al.* [18]. They used Raman spectroscopy (excitation with 488.0 nm blue line) to observe the H - S stretch in solutions of of 0.6 mol dm^{-3} sodium sulphide in 8.9 mol dm^{-3} to 20 mol dm^{-3} sodium hydroxide. From a 'bisulphide' calibration curve (no details are given of the calibrant) obtained immediately prior to experiments, they found that the principal species in deoxygenated

solutions was the bisulphide ion. No peaks were observed due to polysulphide or thiosulphate.

It can be seen, therefore, that early workers [9, 21] did not appreciate the detrimental effect of atmospheric oxygen and carbon dioxide. Thus the dissociation constants for hydrogen sulphide were erroneously calculated as a result of incorrect band identification in spectrometric work.

Also, independently, two groups [18, 29] using different spectrophotometric techniques, have shown the bisulphide ion to be the principal species present in strong alkaline solution. Both state that the sulphide ion should not be considered a primary species but as an intermediate. From equation (5.13), it therefore follows that pK_2^d must necessarily be greater than pK_w (0.96×10^{-14} at 24 °C). These data are supported by periodic trends; a large pK_2^d is necessary in order for the inductive effect due to formal charge ($pK_2^d - pK_1^d$) to be in line with periodic trends.

Branch and Calvin [43] predicted that a difference of 12.3 between pK_1^d and pK_2^d for a weak acid in which the negative charge resulting from the first dissociation step is localised on the same atom to which the second proton is bonded. This was certainly found [44] to be the case for H_2Se and a high value for pK_2^d of hydrogen sulphide (17 to 19) would thus be consistent with other group VIA dihydrogen compounds [45].

Licht carried out a number of studies in highly alkaline conditions, 17.5 mol dm^{-3} potassium hydroxide, to obtain pK_2^d [46-49]. All but the last of these four reports used potentiometric techniques. A glass electrode *versus* calomel reference electrode was used to measure pH in solutions of potassium sulphide and potassium hydrogen sulphide titrated with potassium hydroxide over a range of concentrations. The results were used to solve a series of mass balance equations. From these studies, Licht calculated pK_2^d as 17.6 ± 0.3.

However, there are many flaws in the argument presented by Licht. Much of the analyses of the work is based on studies carried out by Kielland [50] and Picknett [51]. Kielland calculated the individual ion activity coefficients, using an arbitary basis [52, 53], and Picknett used Kielland's values in the three constant form of the Debye-Huckel equation and assumed a linear 1 mV dec^{-1} change in the liquid junction potential with potassium salt concentration. Licht used Kielland's values for the ion size parameters in calculating single ion activity coefficients from a form of the Debye-Huckel equation up to $\mu = 0.2$. Picknett's calculation of liquid junction potentials is fallacious, as pointed out by Covington [54].

Also, Licht dismisses the importance of a 23 mV shift in the glass electrode stability and has assumed steady state for the readings he has taken, when in actuality the plots he included in his paper clearly indicate a variation of ~10 mV. The variation observed, Licht assigned to alkaline error of the glass electrode. In order to substantiate any of Licht's findings, it would be necessary to repeat his work using a mercury / mercury oxide reference electrode which is stable in strongly alkaline solutions.

Licht's most recent publication [49] describes differential densometry as a means of calculating the dissociation constant. However, again, Licht has over-simplified the model and has not taken into account the interaction of aqueous species which vary with concentration, or that density of solutions containing isolated species may be significantly different from that of solutions in mixed equilibrated systems. The conclusion Licht drew from his flawed work was that there are negligible amounts of free sulphide present in metal sulphide systems except in very extreme alkaline conditions. Stephens and Cobble proposed this in 1971 [55] and suggested that the sulphide species existed as a more complex species, or that the hydration sphere was less tightly bound than is predicted by the charge density.

An interesting paper was presented by Schoonen and Barnes [56] who extrapolated the thermodynamic data for the dissociation of polysulphides to include hydrogen sulphide. Figure 5:2 shows pK^d *versus* reciprocal chain length, n, and using this 1/n dependence, a value of 18.51 ± 0.56 was determined for pK_2^d. They further expanded their argument to include the weak acid theory [43] (figure 5:3) and again, as did Meyers[16], obtained a large value, 18.57 for pK_2^d. However, this argument is based on limited information which may be subject to systematic error in the determination of pK_2^d, and also assumes that there is no interaction between the end groups of polysulphides which influence pK_n^d [57]. Obviously, when two bonding sites of protons are close together in a molecule, as in hydrogen sulphide and smaller polysulphides, then the negative charge left at one site strongly inhibits the dissociation of the second proton by electrostatic attraction. As n increases, so also does the separation and hence the degree of interaction decreases.

5.4 Experimental.

5.4.1 Reagents.

Sulphide solutions, 1.0 mol dm^{-3} to 10^{-5} mol dm^{-3} were prepared from sodium sulphide nonahydrate by serial dilution and degassed deionised water. Due to the deliquescent nature of sodium sulphide nonahydrate, there must be some error introduced into the concentration of the stock solution and this should be standardisised before preparing a series of standards. see experimental considerations section.

To the solutions was added sulphide anti-oxidant buffer, SAOB, [58] in a 1:1 v/v ratio [59] with the sample. The composition of SAOB used was in accordance with that used by another worker at Newcastle [25] recommended by Orion Inc. [60] (Appendix F (i)). The presence of SAOB maintains a high pH and high ionic strength, therefore establishing a fixed fraction of total sulphide with constant activity coefficient.

Tri-butyl phosphine (TBP) in 1:50 v/v ratio was used by Millero [61]

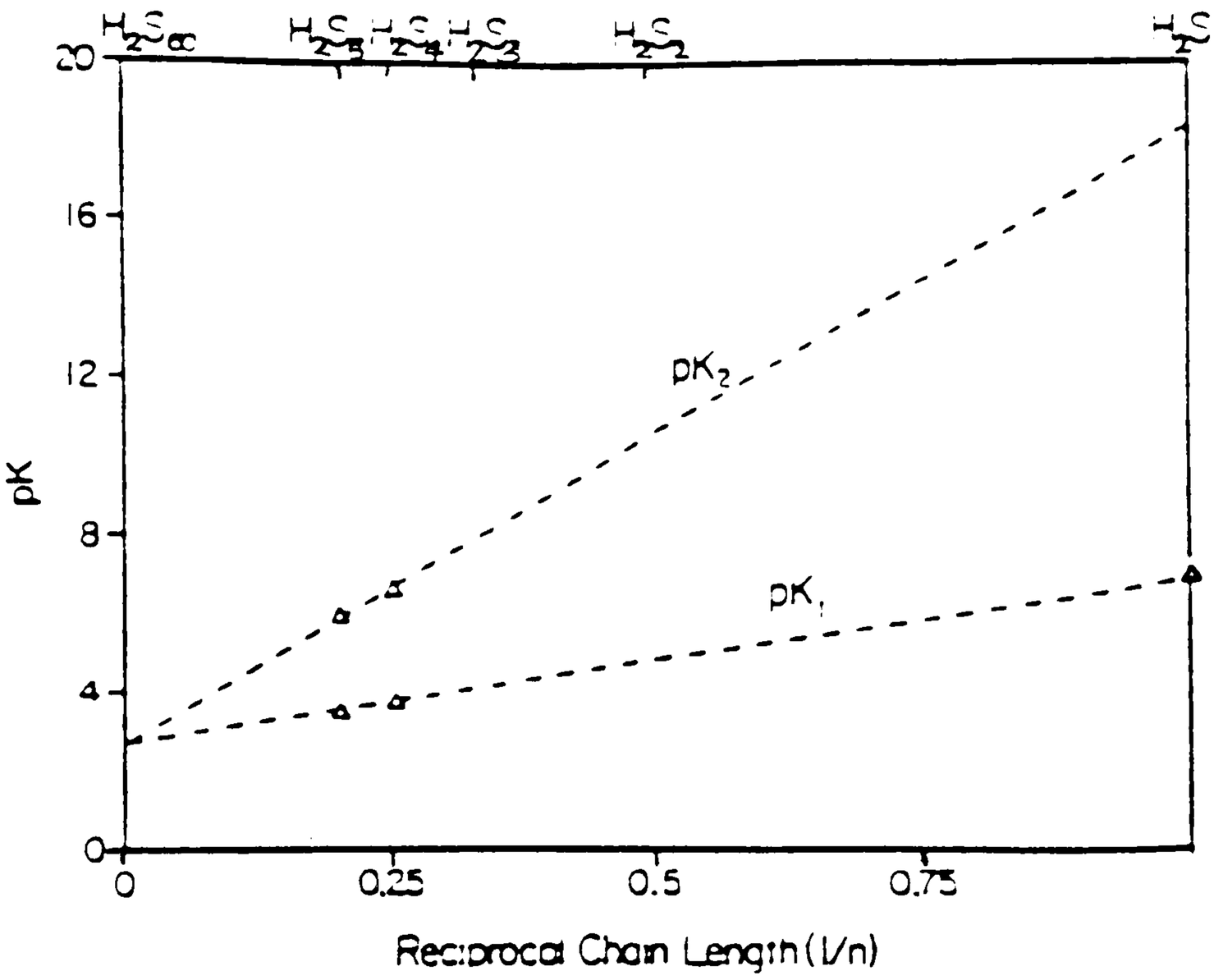

Figure 5:2 Dissociation Constants of H_sS and Polysulphides[56].

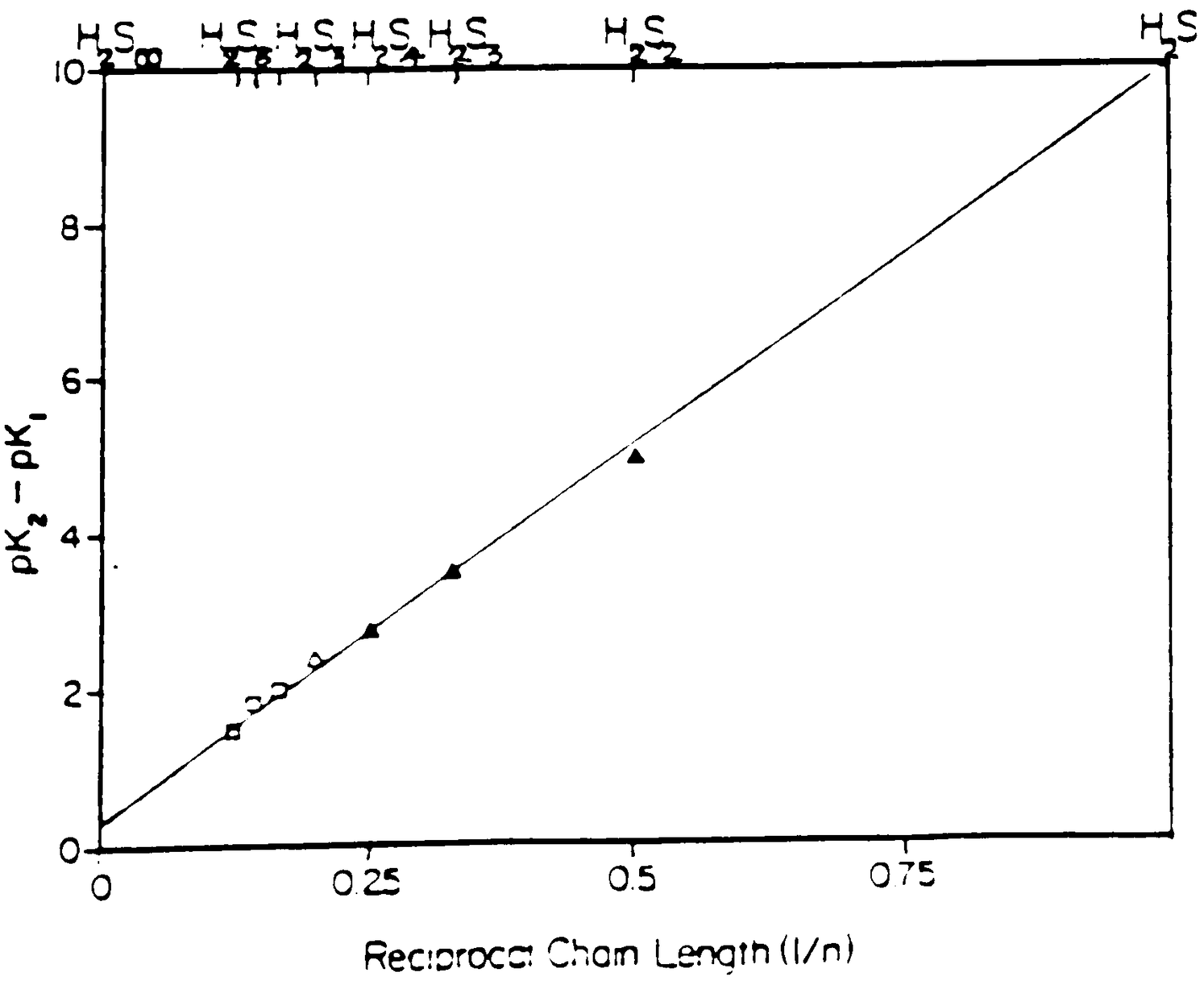

Figure 5:3 Difference between First and Second Dissociation Constants of the Polysulphides[56].

in order to reduce the formation of polysulphides in the solution and on the membrane surface. TBP is used industrially in organic solvents to prevent polysulphide formation but has not been widely used in aqueous solution [62]. TBP is highly toxic and although this was used in preliminary work [63], use of it was discontinued when Millero was unable to produce data supporting the use of this reagent [64] and when calibration curves in work at Newcastle did not show any problems associated with polysulphides.

Potassium chloride (10^{-1} mol dm^{-3}, 10 ml) was used as supporting electrolyte during titration. All solutions were stored under a nitrogen blanket to reduce aerial oxidation.

5.4.2 Experimental Set-up.

Titrations were carried out coulometrically to reduce sample manipulation and thus minimise atmospheric sulphide oxidation and exclude carbon dioxide uptake. End point determinations were made using a sulphide ISE and a glass electrode against separate external reference electrodes.

A Radelkis sulphide ISE (type OH-8523) was used. The electrode was conditioned by presoaking in sodium sulphide (10^{-3} mol dm^{-3}) for ca. 48 h, renewing the solution after 24 h. The sulphide concentration was determined using this ISE *versus* a double junction calomel reference electrode (saturated potassium chloride, 1.0 mol dm^{-3} potassium nitrate). Single junction calomel reference electrodes are not suitable for measurement of sulphides, as insoluble sulphide species may interfere with the liquid junction and the calomel, causing variation in the liquid junction potential. These electrodes were connected to a high impedance buffer amplifier, the output displayed on a Thandar digital voltmeter and recorded on a Linseis chart recorder.

The pH of the system was monitored using a Russell glass electrode *versus* double junction calomel reference electrode (as discussed in

Chapter 4). The electrodes were connected to the titrator unit, EDT OH-407, as described in Chapter 4, which recorded the pH during titration. Radelkis platinum sheet generating electrodes with surface area 1.58 cm^2 (type OH-8583) were used with a generating current of 6.4 mA.

The electrodes were assembled in a 25 ml glass cell with air-tight PTFE lid. Orientation of the electrodes was found to be important; the auxiliary electrode was placed in a separate side-arm, as described in Chapter 4, dipped in common electrolyte. Figure 5:4 shows the relative positions of the electrodes, which led to the least interference. The cell (figure 5:5) was purged with nitrogen prior to experiments and a nitrogen flow maintained over the sample during titration. The solutions were stirred using a Teflon stirrer bar.

5.5 Calibration of Electrodes.

5.5.1 Experimental.

The sulphide ISE was calibrated in sulphide solutions prepared with degassed water and SAOB in the air-tight cell, under nitrogen. In order to substantiate claims that using both degassed water and SAOB are necessary, calibration solutions were also carried out on sulphide solutions without these reagents. A range of solutions containing TBP was also examined.

The pH electrodes were calibrated using buffers B7 and B11 (see Appendix C), prepared with degassed water. Buffer solutions were also stored under nitrogen.

5.5.2 Calibration Results.

The calibration results of sulphide solutions under various conditions are shown in Tables 5:5 - 5:7 and figures 5:6, 5:7. It was proved, as anticipated, that it was necessary to prepare all solutions with degassed water and to store them under a nitrogen blanket. Those solutions prepared without safeguards to preclude aerial oxidation gave a non-linear mV dec^{-1} response to sulphide.

The slope of calibrations without SAOB, although super-Nernstian,

Figure 5:4 Orientation of the Electrodes in the Cell Assembly.

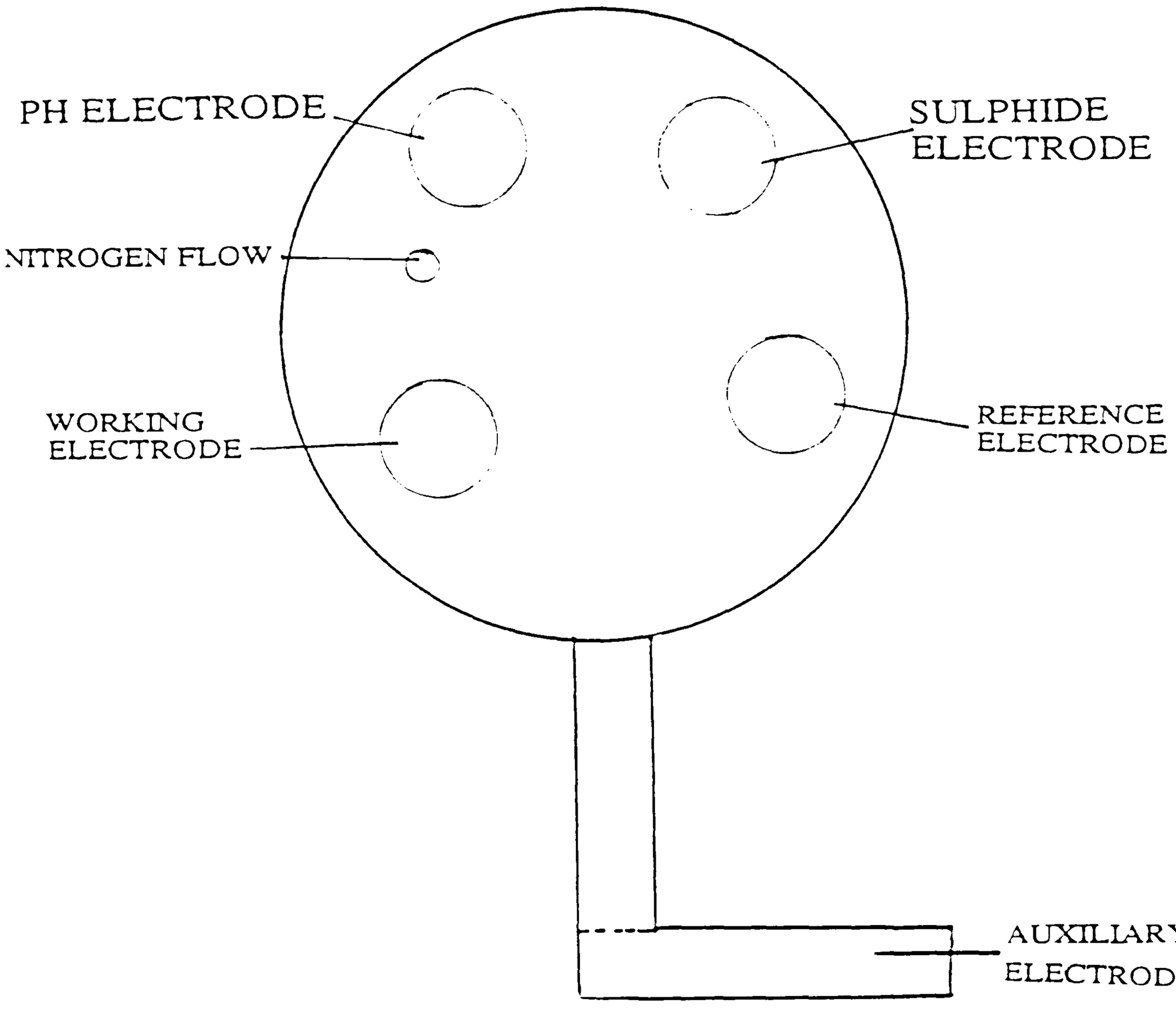

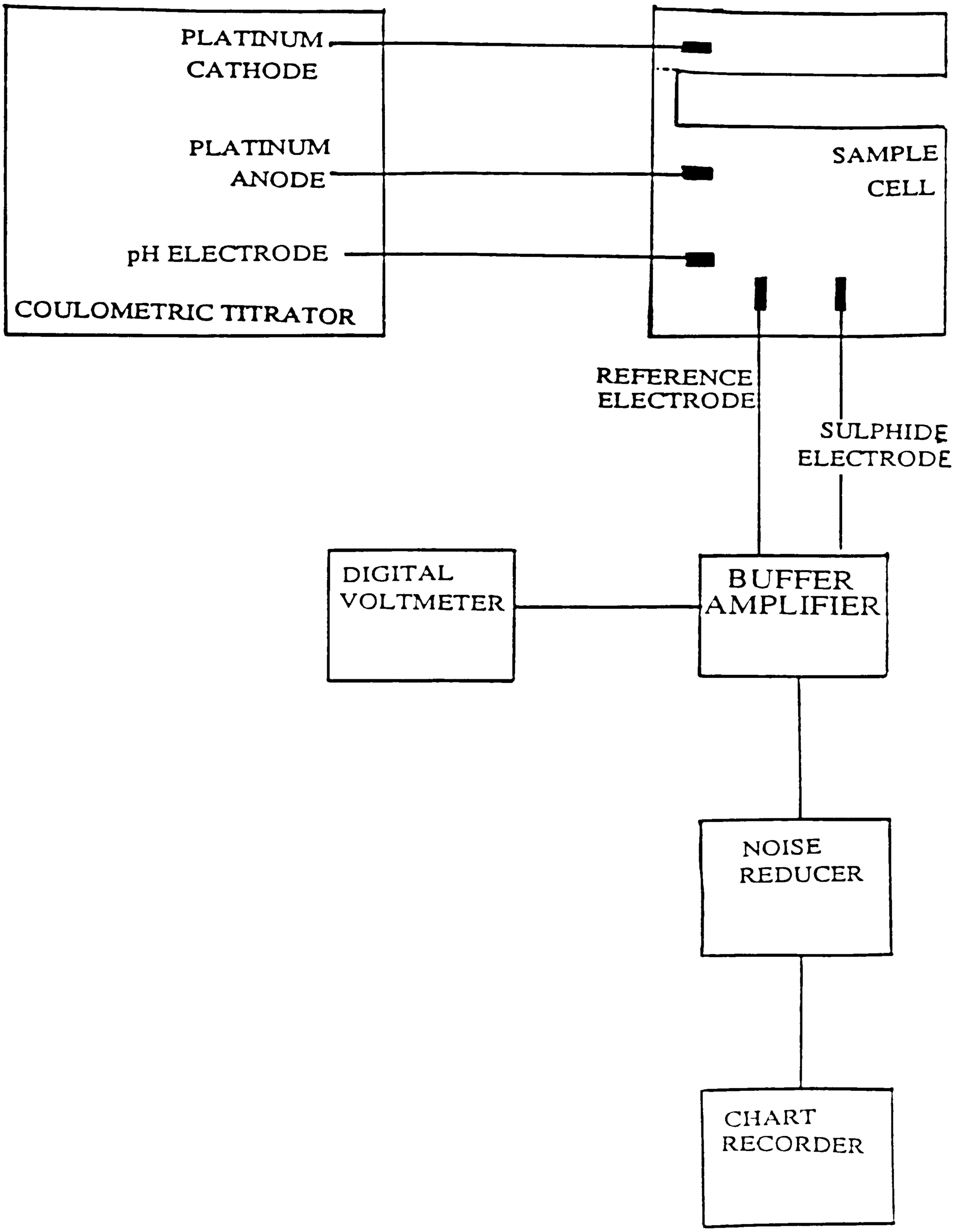

Figure 5:5 Block Diagram of the Coulometric Auto-titration System for Simultaneous Sulphide and pH Determination.

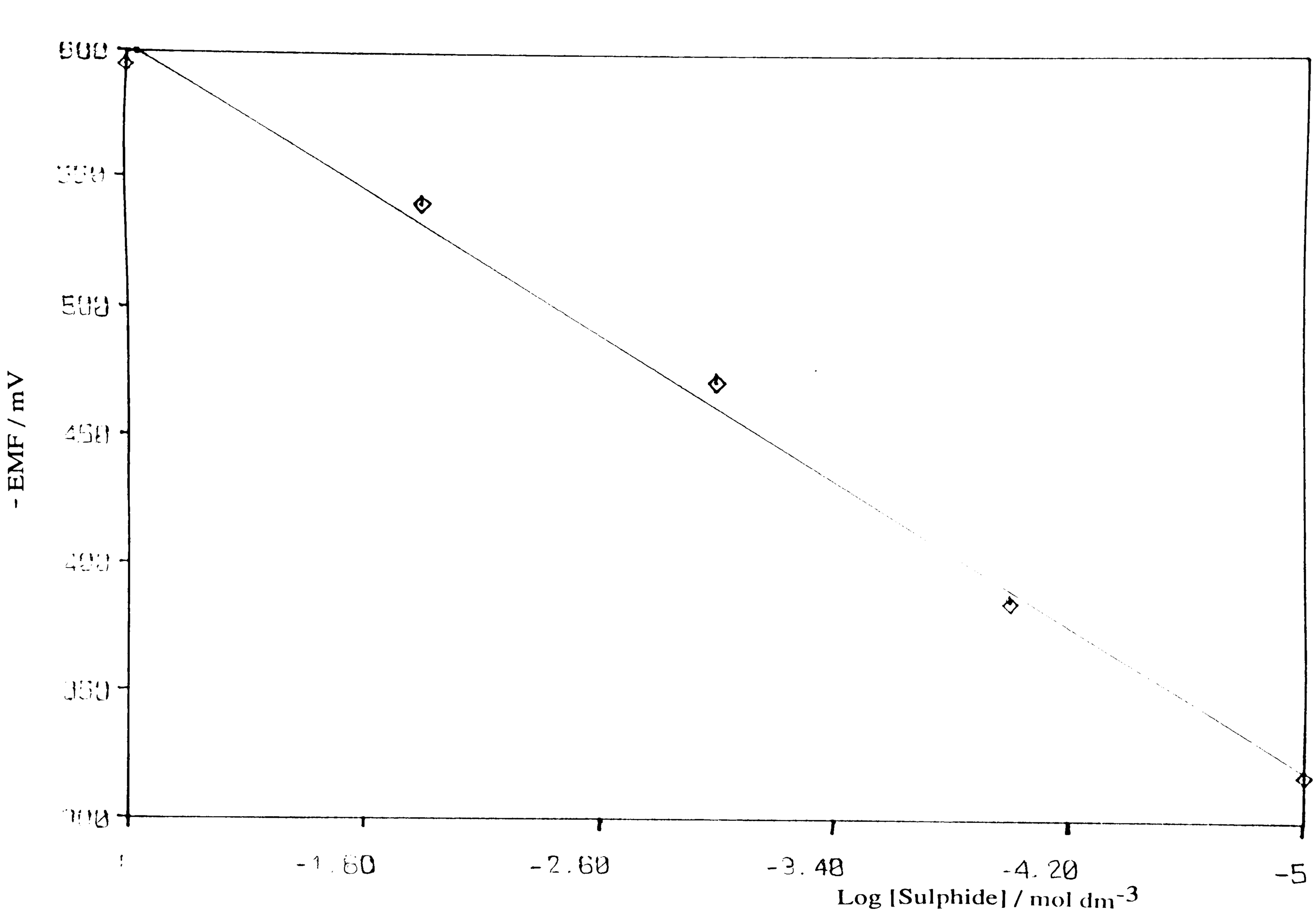

Figure 5:6 Sulphide ISE Calibration Curve; No SAOB Present

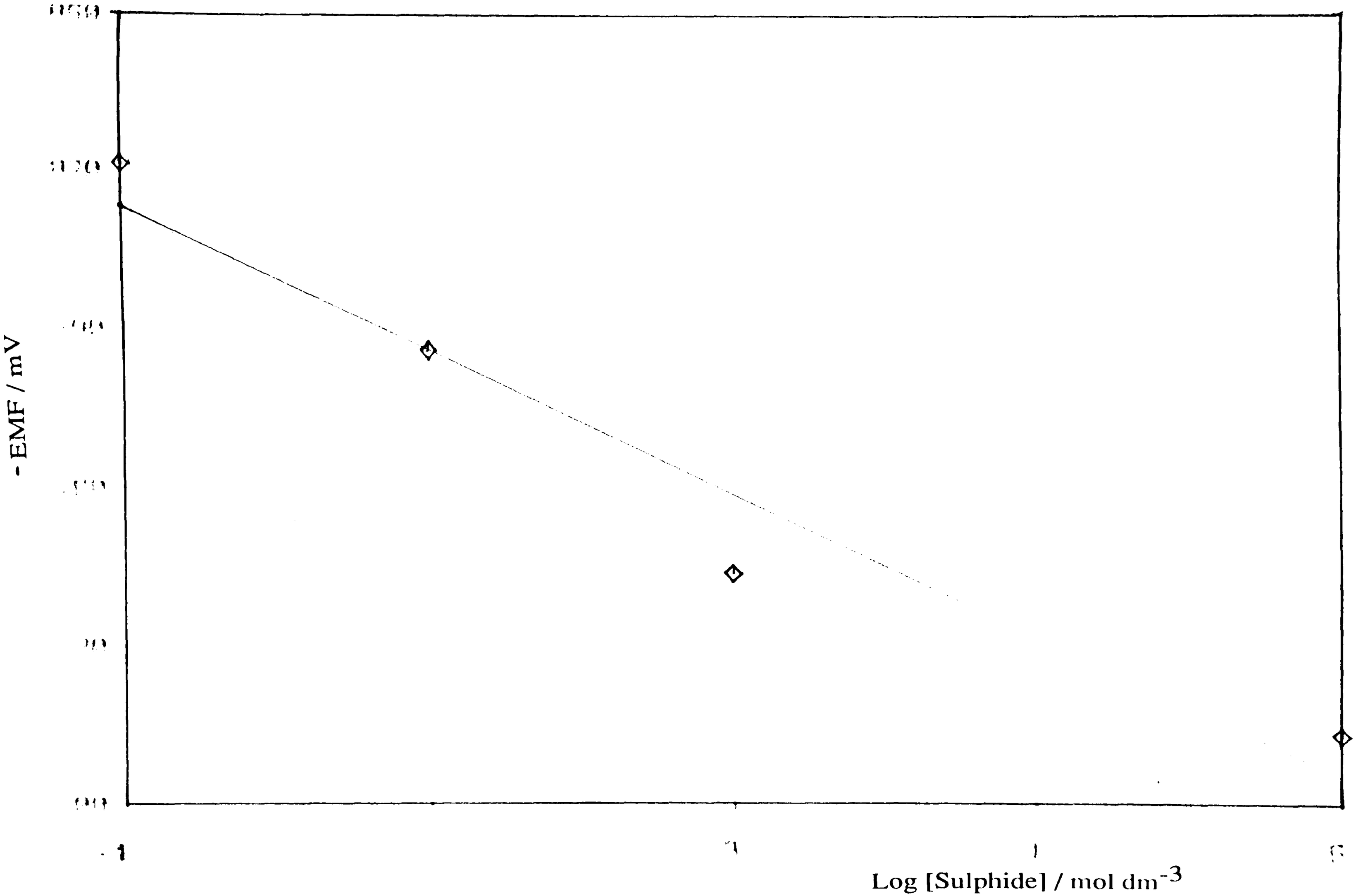

Figure 5:7 Sulphide ISE Calibration Curve; SAOB Present

70.5 mV dec^{-1} and 65.5 mV dec^{-1}, were more typical of a univalent ion, suggesting that oxidation by dissolved oxygen had occurred to produce the bisulphide ion. When SAOB was added to calibration solutions, 26.7 mV dec^{-1}, 27.0 mV dec^{-1} slopes were observed, showing that sulphide ions were the dominant species. Below 10^{-5} mol dm^{-3}, a super-Nernstian response was seen, suggesting that at low concentrations it was more difficult to preclude oxidation. This agrees with findings by Vesely *et al.* [65] and Ruzicka *et al.* [66] who obtained ca. 30 mV dec^{-1} slope to 10^{-6} mol dm^{-3}, after which a more positive potential, i.e. a greater sulphide ion concentration, was observed than expected.

The pH of the calibration solution was measured and shown, not unexpectedly, to be greater than 12 in solutions containing SAOB. In those solutions without SAOB, the pH value decreased from 12 at 10^{-1} mol dm^{-3} to 7.4 at 10^{-5} mol dm^{-3}. This, and the slopes, verified claims that at pH > 12 sulphide ion is the most abundant species. Crombie *et al.* [27] studied the change of Nernst slope with pH and obtained similar results. They[27] also noted a 10^{-6} mol dm^{-3} limit of detection for sulphide, below this concentration sulphide oxidation took place. Also, as shown by equations (5.10), (5.11), at a constant pH (at constant ionic strength) one can determine the sulphide ion concentration.

Preliminary work carried out using TBP, without SAOB, showed that there was a ca. 60 mV dec^{-1} slope, but in solutions with TBP and SAOB a 30 mV dec^{-1} slope was found. No significant improvement in stability or response time was observed in the presence of TBP, despite reports to the contrary [61], therefore due to the serious health hazards involved with this reagent, TBP was not used further.

70.5 mV dec^{-1} and 65.5 mV dec^{-1}, were more typical of a univalent ion, suggesting that oxidation by dissolved oxygen had occurred to produce the bisulphide ion. When SAOB was added to calibration solutions, 26.7 mV dec^{-1}, 27.0 mV dec^{-1} slopes were observed, showing that sulphide ions were the dominant species. Below 10^{-5} mol dm^{-3}, a super-Nernstian response was seen, suggesting that at low concentrations it was more difficult to preclude oxidation. This agrees with findings by Vesely *et al.* [65] and Ruzicka *et al.* [66] who obtained ca. 30 mV dec^{-1} slope to 10^{-6} mol dm^{-3}, after which a more positive potential, i.e. a greater sulphide ion concentration, was observed than expected.

The pH of the calibration solution was measured and shown, not unexpectedly, to be greater than 12 in solutions containing SAOB. In those solutions without SAOB, the pH value decreased from 12 at 10^{-1} mol dm^{-3} to 7.4 at 10^{-5} mol dm^{-3}. This, and the slopes, verified claims that at pH > 12 sulphide ion is the most abundant species. Crombie *et al.* [27] studied the change of Nernst slope with pH and obtained similar results. They[27] also noted a 10^{-6} mol dm^{-3} limit of detection for sulphide, below this concentration sulphide oxidation took place. Also, as shown by equations (5.10), (5.11), at a constant pH (at constant ionic strength) one can determine the sulphide ion concentration.

Preliminary work carried out using TBP, without SAOB, showed that there was a ca. 60 mV dec^{-1} slope, but in solutions with TBP and SAOB a 30 mV dec^{-1} slope was found. No significant improvement in stability or response time was observed in the presence of TBP, despite reports to the contrary [61], therefore due to the serious health hazards involved with this reagent, TBP was not used further.

Table 5:5 Calibration of ISE using Sulphide Solutions Prepared without Degassed Water or SAOB.

$[S^{2-}]$ mol dm^{-3}	Potential Difference /mV	ΔV mV
10^{-1}	-815	
		+66
10^{-2}	-749	
		+111
10^{-3}	-638	
		+299
10^{-4}	-349	
		-17
10^{-5}	-366	

Slope, not applicable.

Table 5:6 Calibration of ISE using Sulphide Solutions Prepared with Degassed Water but no SAOB.

$[S^{2-}]$ mol dm^{-3}	pH	Potential Difference/ mV	ΔV mV
10^{-1}	12.0	-594.3	
			+54.9
10^{-2}	11.3	-539.4	
			+68.8
10^{-3}	8.9	-470.6	
			+84.8
10^{-4}	8.1	-385.8	
			+67.4
10^{-5}	7.4	-318.4	

Slope = 70.54 mV dec^{-1}

Table 5:7 Calibration of ISE using Sulphide Solutions Prepared with Degassed Water and Containing SAOB.

$[S^{2-}]$ mol dm^{-3}	pH	Potential Difference /mV	ΔV mV
10^{-1}	12.30	-588.8	
			+25.3
10^{-2}	12.32	-563.5	
			+28.6
10^{-3}	12.40	-543.9	
			+25.5
10^{-4}	12.60	-509.4	
			-55.7
10^{-5}	12.52	-553.7	
SAOB only	12.30	-491.6	

Slope = 26.68 mV dec^{-1}

5.6 Coulometric Titrations.

5.6.1 Experimental.

Solutions of sodium sulphide, 50 µl, of 10^{-1}, 10^{-2} mol dm^{-3} and SAOB, 50 µl, in potassium chloride (10 ml, 10^{-1} mol dm^{-3}) as supporting electrolyte, were titrated against coulometrically produced hydrogen ions. Titrations were repeated for 10^{-1} mol dm^{-3} sodium sulphide solutions, replacing SAOB with 10^{-1} and 5 x 10^{-2} mol dm^{-3}sodium hydroxide, in order to observe the effect of SAOB on titrations. Table 5:8 shows the composition of each sample tested. The pH and sulphide concentrations were calculated at the equivalence points from calibration curves obtained immediately prior to titration.

Table 5:8 Composition of Samples Used

Sample Name	$[S^{2-}]$ mol dm^{-3}	SAOB or [NaOH] mol dm^{-3}	titratable moles in vessel
1	10^{-1}	10^{-1}	1.5×10^{-5}
2	10^{-1}	SAOB	1.1×10^{-4}
3	10^{-1}	SAOB	1.1×10^{-4}
4	10^{-1}	10^{-1}	1.5×10^{-5}
5	10^{-1}	5×10^{-2}	1.25×10^{-5}
6	10^{-2}	SAOB	1.05×10^{-5}

where titratable moles is the total number of moles, sulphide ions + hydroxide ions, available for titration with hydrogen ions

5.6.2 Titration Results.

Chart recorder tracings for titration of 10^{-1} mol dm^{-3} sodium sulphide with 10^{-1} mol dm^{-3} sodium hydroxide as ionic strength adjustor and 10^{-1} mol dm^{-3} sodium sulphide with SAOB (samples 1 and 2) are shown in figures 5:8, 5:9. These typify the titration curves obtained for the sulphide electrode curves (a), and glass electrode, curves (b). The profile of curves obtained for each sample tested was similar. From the curves, the end points were estimated and compared with those values obtained by Hseu and Rechnitz [23], see Tables 5:9, 5:10. One cannot correlate exactly the voltage values as different ionic strengths and liquid junction potentials, exist between samples, however, generally the values agree well.

Hseu and Rechnitz [23] stated that more titrant was required to reach the first end point than required to go from the first to second end point due to initial titration of excess hydroxide ions. They explained this as the excess hydroxide ions formed by loss of hydrogen sulphide (through hydrolysis) on initially dissolving sodium sulphide, therefore, the

Figure 5:8 Chart Recorder Tracings for Titration of Sample 1

(10^{-1} mol dm^{-3} $Na_2S.9H_2O$ + 10^{-1} mol dm^{-3} NaOH)

a) Sulphide

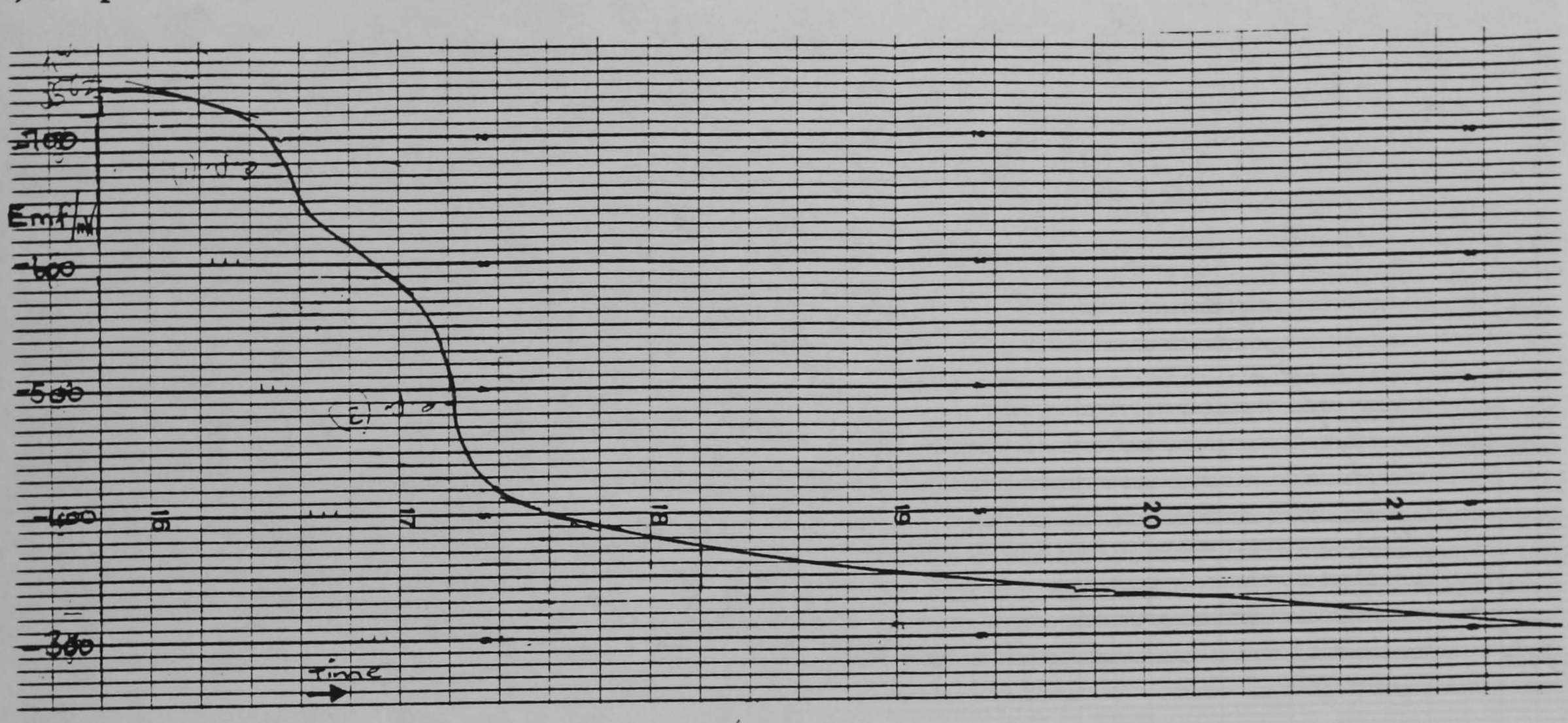

b) pH

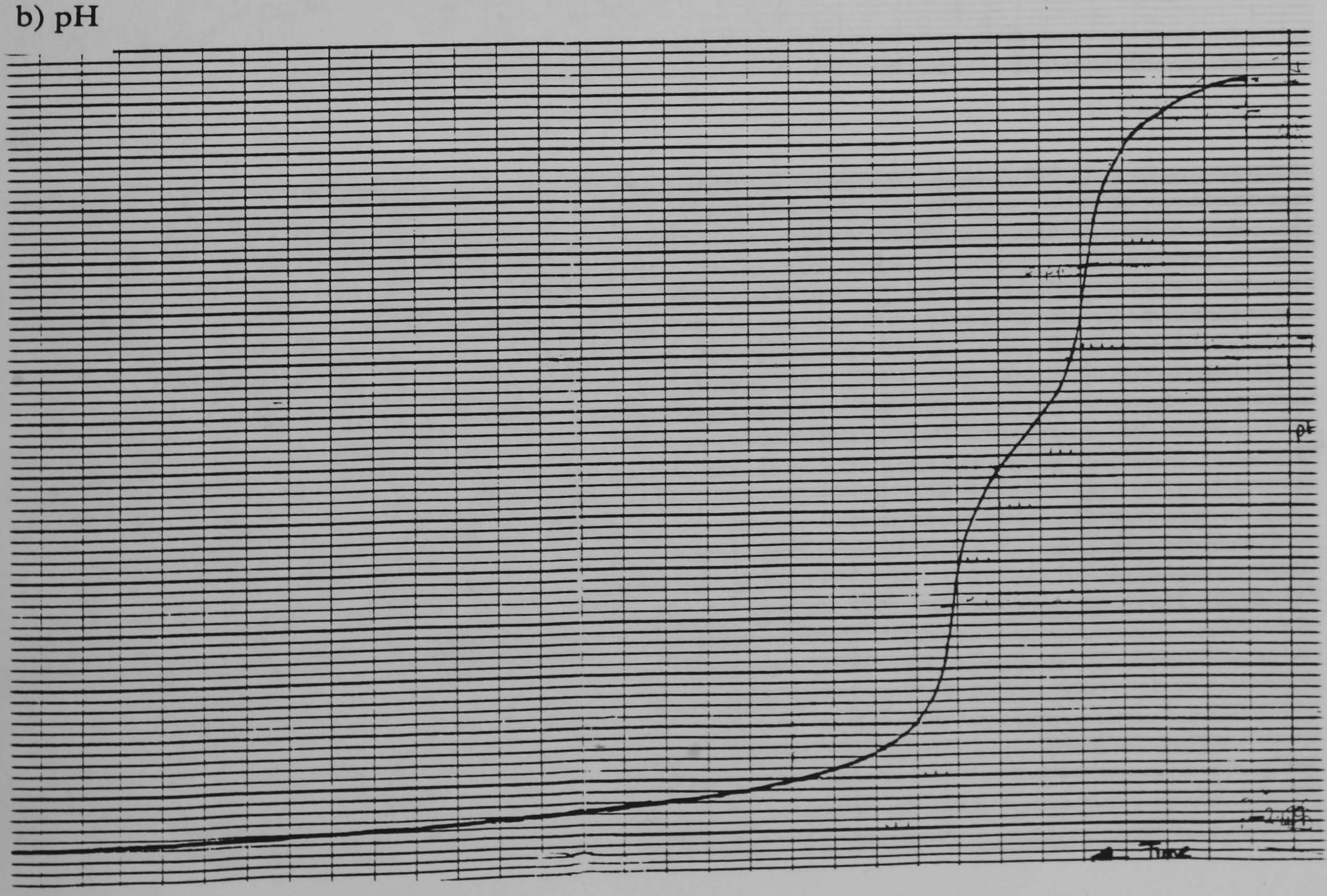

Figure 5:9 Chart Recorder Tracings for Titration of Sample 2

(10^{-1} mol dm^{-3} $Na_2S.9H_2O$ + SAOB)

a) Sulphide

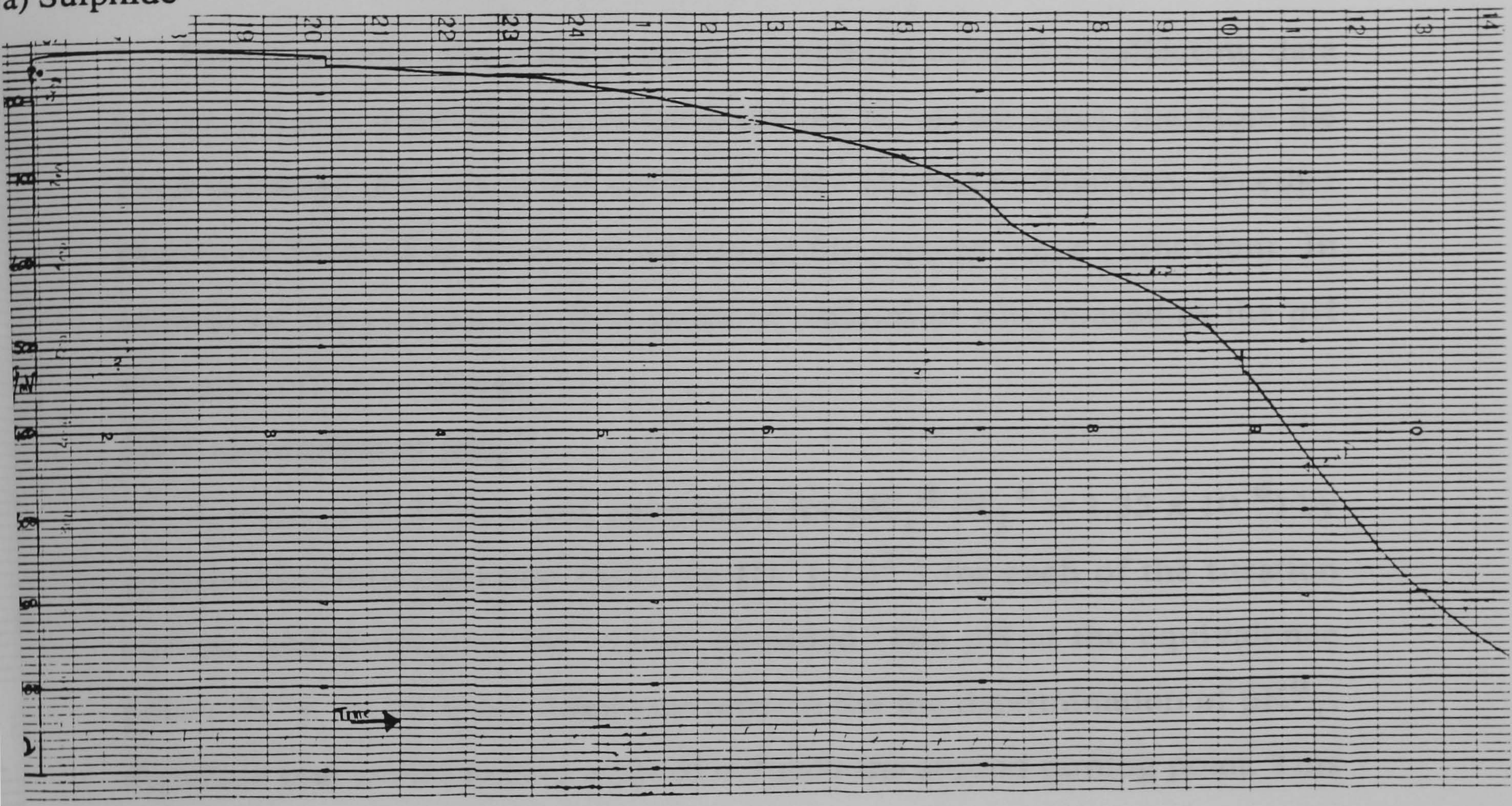

b) pH

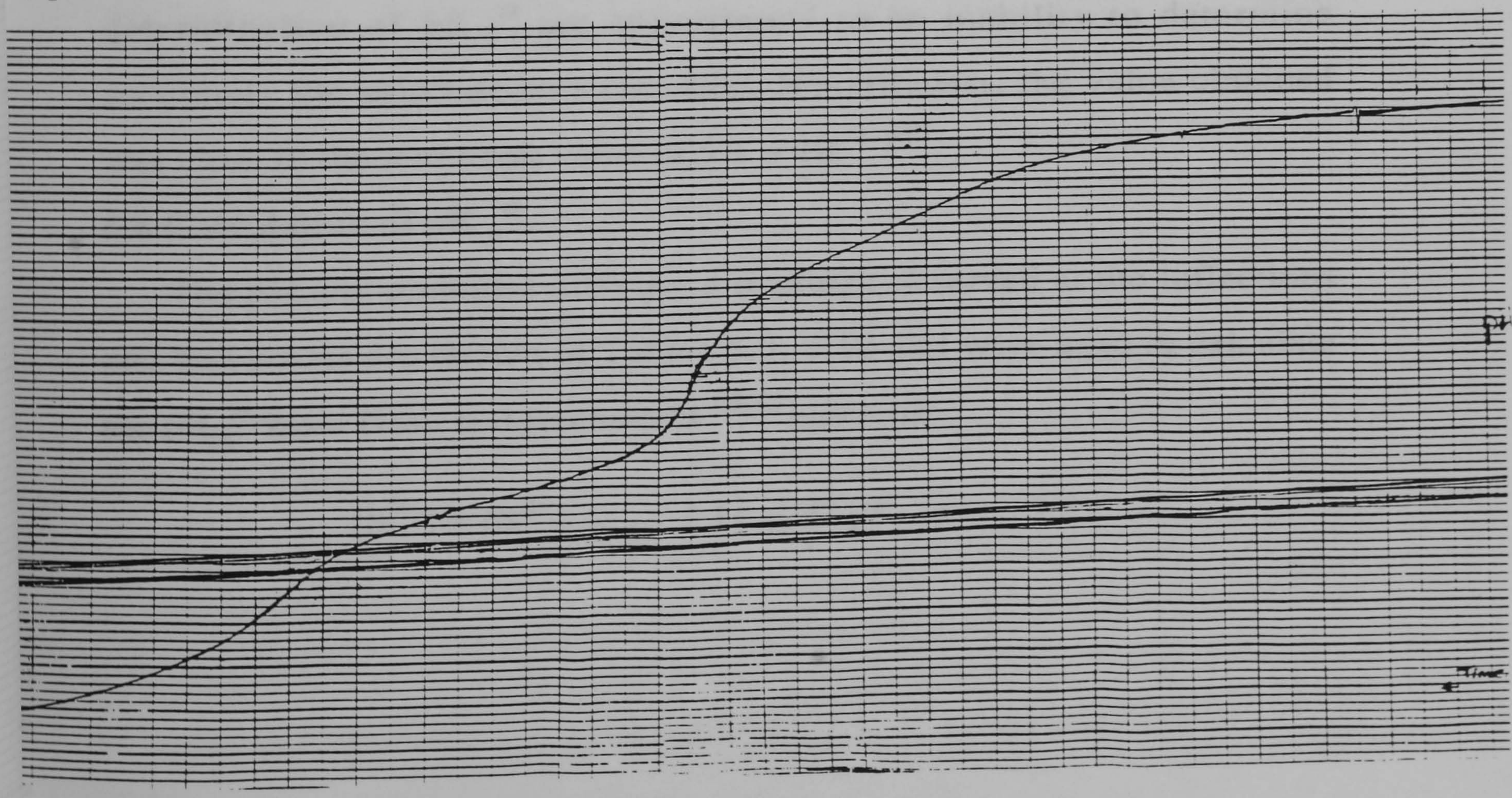

concentrations of hydroxide and bisulphide ion were not equal but given by the following equation;

$$[OH^-]_{present} = [OH^-]_{total} - [HS^-] - 2[S^{2-}] \qquad (5.15)$$

Unfortunately, the chart recorder speeds selected for collecting data for the pH and sulphide electrodes could not be set the same, therefore the chart recorder tracings could not be directly aligned to determine whether points of inflection from pH and sulphide curves were coincident. In several of the curves, the first point of inflection was missed as the pH was not sufficiently high.

5.7 Calculation of pK_1^d.

A value of 5.87 ± 1 was calculated for pK_1^d ($K_1^d = 1.35 \times 10^{-6}$) by substitution into equation (5:8) the $[H^+]$, $[S^{2-}]$ for each of the titration curves, and averaging the values obtained. The pH at the equivalence point, $[H^+]$, is the most dominant term in the the determination of pK^d_1, therefore one would expect a pH of ~ 7 near the second turning point. This was, indeed, the case, as is shown in Table 5:9, 5:10. Inaccuracies in the determination of pK_1^d are apportioned to an inability to determine accurately the sulphide concentration. Nevertheless, the value obtained was close to the text book value of 9.1×10^{-8} [67].

5.8 Calculation of pK_2^d.

The pH and potential difference readings observed at the inflections and end points are shown in Tables 5:9, 5:10 and were used to calculate the pK_2^d from Hseu and Rechnitz's [23] equation;

$$[S^{2-}] = [S^{2-}]_{TOT} / \{ 1 + ([H^+]/K_2)\} \qquad (5.8)$$

Table 5:9 pH Readings at the End Points and Turning Points during Coulometric Titrations of Sodium Sulphide, by Visual Inspection.

Sample Name	pH_i	pH_{calc}	pK_2	pK_1	ep(1)	ep(2)
1	11.3	10.7	10.9	6.5	8.9	5.2
2	11.8	12.0	10.3	6.2	8.1	5.3
3	10.9	10.7	10.9	6.3	9.1	4.9
4	12.4	12.0	11.8	7.3	10.0	6.3
5	10.1	10.4	10.1	6.6	8.5	5.4
6	12.5	12.0	11.8	7.9	9.7	6.6
H&R	12.8	13.0	11.5	7.9	10.0	4.2

pH_i is the initial pH of the sample

pH_{calc} is the maximum possible pH, calculated

Table 5:10 Potential Difference Values at the End Points and Turning Points during Coulometric Titrations of Sodium Sulphide, by Visual Inspection.

Sample Name	mV_i mV	pK_1 mV	pK_2 mV	ep(1) mV	ep(2) mV
1	-740	-730	-600	-680	-490
2	-845	-810	-530	-580	-350
3	-740	-720	-600	-680	-465
4	-795	-750	-580	-655	-500
5	-830	-795	-420	-595	-200
6	-685	-665	-320	-485	-200
H&R	-890	-850	-630	-730	-380

where mV_i is the initial potential difference value

For the calculation of pK^d_2, the value was found to be 12.08 ± 1.0 ($K_2^d = 8.32 \times 10^{-13}$) close to the text-book value of 11.96 ($K_2^d = 1.1$

x 10^{-12}) [67] and far removed from the new value proposed by Meyers [16], but in agreement with Kubli [1] and Hagisawa [68] who found pK^d_2 values of 10.44 and 11.0 respectively. Both workers used direct potentiometry, measuring the pH during titration of sodium sulphide with hydrochloric acid. The values obtained in Newcastle were reproducible for a range of solutions titrated. The activity coefficient of sulphide ions, taken as unity, was incorporated into the value of pK^d_2. This approach was also taken by Ellis and Golding [29].

From equation (5.8), the pH at the equivalence point is the most influential term in calculation of the dissociation constant. Substitution in equation (7.5) - (7.7) show that in order to obtain $pK^d_2 = 14$, a value of pH 13, greater than the initial pH (12.4) would be necessary at the equivalence point.

To determine the accuracy of the titrations carried out, the number of coulombs required to reach the second end point equivalent to the number of hydrogen ions generated, was compared with the number of moles 'available for titration' (sulphide ions + hydroxide ions). Table 5:11 shows that the experimental and expected (calculated) values agree well.

Table 5:11 Comparison of Available (calculated) and Experimental Titrated Moles.

Sample	Number of Moles	
Name	Calculated	Experimental (pH Curve)
1	1.5×10^{-5}	1.4×10^{-4}
2	1.1×10^{-4}	1.6×10^{-4}
3	1.5×10^{-5}	1.5×10^{-5}
4	1.1×10^{-4}	1.77×10^{-4}
5	1.25×10^{-5}	1.6×10^{-5}
6	1.01×10^{-4}	1.9×10^{-4}

5.9 Using SUPERQUAD to Determine pK_1^d, pK_2^d for Hydrogen Sulphide.

5.9.1 Manipulation of the Titration Curves.

Since data had been collected only by chart recorder tracings, with no numerical values attached to particular points on the graphs (other than those estimated from the calibration curve), a digitiser later was used to generate data points from the curves.

A Calcomp 91480 Digitising Tablet interfaced to an IBM PS/2 model 80 microprocessor using the ADS digitising module, from the ARC / INFO Geographical Information Systems (GIS) software, revision 3.3, was used to digitise and transform the data. This is a highly sophisticated package developed by the Environmental Systems Research Institute (ESRI), California; pc ARC / INFO, was revised in 1989. The graphs were plotted using the "GRAPHER" programme on a NIMBUS 286 microprocessor interfaced to a Hewlett-Packard 7475A A4 plotter. Figure 5:10 shows a characteristic digitised plot (for sample 4).

The digitised data was used in conjunction with SUPERQUAD (see Chapter 4) as a better method of determining the dissociation constants. ISEs have not often been used with SUPERQUAD. Gans [69] suggested that SUPERQUAD has not previously been used to analyse coulometric data, despite the 'JCOUL' option, which implies that coulometric data can be read directly into the refining programme.

5.9.2 Setting up SUPERQUAD.

Several modifications to the set up file (described in Chapter 4) had to be made to enable SUPERQUAD to analyse coulometrically obtained data. At present, the programme does not permit entry of charge passed, therefore it was necessary to convert these values into a 'volume equivalents'. The number of coulombs passed at each point was converted to give an equivalent volume of 10^{-1} or 10^{-2} mol dm^{-3} hydrochloric acid which would provide the same number of moles of H^+ as were

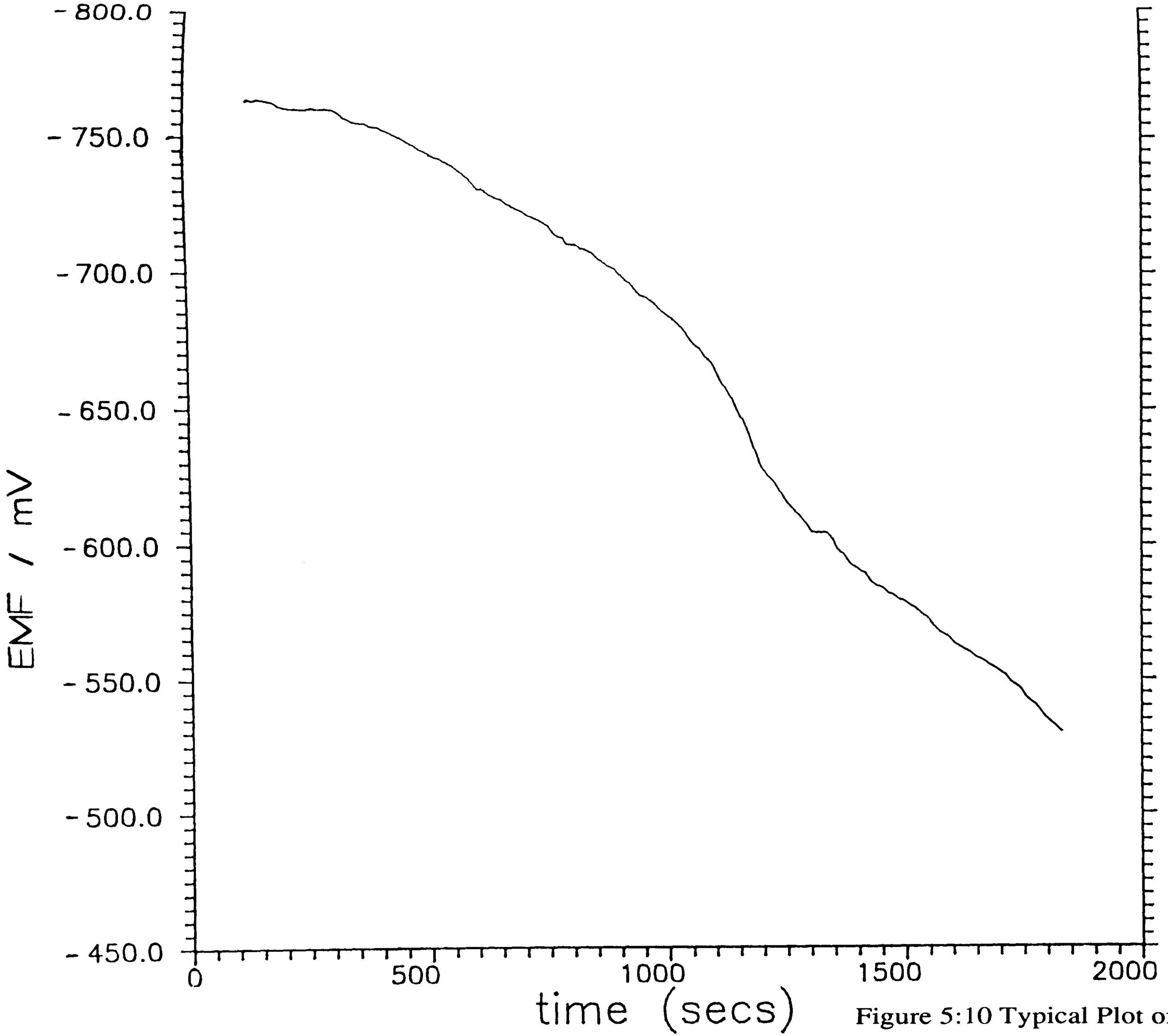

Figure 5:10 Typical Plot of Digitised Titration Data

Sulphide ISE Titration Data for Sample 4

coulometrically generated.

This is shown in the header file as concentration of 'hydrogen' added. There was no increase in volume of the sample during titration, normally corrected for in SUPERQUAD; this correction factor was bypassed by setting JCOUL to 1. In the header file for the pH electrode, the 'SLOPE' term (actually a fraction of the Nernst slope) was set to 1, which sets the slope to 59.16 mV dec^{-1} and 'EZERO' is set to zero; however, for the sulphide ISE, the slope must be set to 0.5 or the number of electrons transferred to 2. The EZERO value was set at a mV value corresponding to the potential difference for a 1.0 mol dm^{-3} sulphide ion concentration (see Appendix E for further information regarding setting up SUPERQUAD).

SUPERQUAD had been used previously in Newcastle for titration of nitrogen base buffers and for their metal-ion complexation constants, so no difficulties were anticipated in extending the treatment to determine β formation constants for hydrogen sulphide and thus the dissociation constants. In this work, the ligand was designated as the sulphide species, S^{2-}, which is successively protonated to give H_2S, thus the following series of equations may be used to correlate K^d and β formation constants. The association constant, K^a, is by definition, the reciprocal of the dissociation constant, K^d. Association and dissociation constants are consecutive, K_1^a, K_2^a etc., whereas the β formation constants are successive, that is the β constant is a product of protonation steps. Considering hydrogen sulphide, for the series of protonation reactions, the corresponding K^a and β constants are shown below,

$$S^{2-} + H^+ \underset{K_2^d}{\rightleftharpoons} HS^- \qquad (5.17)$$

$$K_2^a = [HS^-] / ([S^{2-}] A_{H+} \qquad (5.18)$$

designated β_1 in the header file

$$SH^- + H^+ \underset{K_1^d}{\overset{K_1^a}{\rightleftharpoons}} H_2S \qquad (5.19)$$

$$K_1^a = [H_2S] / [HS^-] A_{H+} \qquad (5.20)$$

Overall; $$2\,H^+ + S^{2-} \longrightarrow H_2S \qquad (5.21)$$

$$K_1^a K_2^a = [H_2S] / [S^{2-}] (A_{H+})^2 \qquad (5.22)$$

where A_{H+} is the measured hydrogen ion activity.

i.e. this was the overall reaction required and designated as β_2 in the header file.

Thus, it can be seen how the β formation constants refined in SUPERQUAD are related to the dissociation constants, K_1^d, K_2^d.

The hydrolysis of water is given by

$$H^+ + OH^- \longrightarrow H_2O \qquad (5.7)$$

$$K_w = [H^+] [OH^-] / [H_2O] \qquad (5.6)$$

However, here we were considering the back reaction of (5.7), therefore, $p\beta_1 = -pK_w$ and explains why a minus sign is attached to the β constant for water in the set up file. A value of -13.7 rather than -14.0 was assigned to pK_w, which takes into account the ionic strength effect on pK_w.

From equations (5.17) - (5.22), Item 5 in SUPERQUAD was produced, as shown in Table 5:12. The 'KEY' term indicates action about a β formation constant. If KEY = 0, then the β value will remain constant; if set at -1, then the β constant will be refined and if set at +1 the β constant will be ignored during refinement.

Table 5:12 The β Formation Constants used in the H_2S Header File.

Log β	M	L	H	KEY
12	0	1	1	-1
19	0	1	2	-1
-13.7	0	0	-1	0

Initial values of 12 and 19 were assigned to log β_1 and log β_2 as these agreed, approximately, with values obtained by visual inspection. Refinements of samples 1 and 2 were carried out. At present, SUPERQUAD can only accept up to 99 data points, therefore it was necessary to reduce the data (up to 300 data points were generated using the digitizer) ensuring no important detail was lost from the titration curves. SUPERQUAD requires the number of mmoles of reagents to be read into the header file, thus, for sample 1; 0.005 was set as the number of sulphide mmoles present in the sample initially, a negative sign was attached to the hydrogen ion concentration, -0.005, indicating that hydroxide ions, rather than hydrogen ions, were present in the sample. For sample 2, EDTA was either categorised as a discrete reagent, or the presence of EDTA was accounted for in the total hydrogen ion concentration.

As there was uncertainty in the concentration of sulphide present in the sample, before refining the β formation constants, the concentration of species required for titration and present in the sample were refined. The concentration of the titrant was determined first, the new value inserted into the header file then the sulphide and hydrogen ion concentrations in the sample refined. Since SUPERQUAD can only accept up to 99 data points, it was only possible to refine one parameter at a time, however, in the new revised version of SUPERQUAD, allowing 1000 data points to be analysed per titration curve, it will be possible to refine more than one parameter at a time.

As far as possible, both β constants were refined together. When refining two constants, SUPERQUAD initially evaluated both constants, then if the error of one was excessive, this constant was removed and the remaining β constant re-refined. SUPERQUAD uses $X^2 > 12.6$ value to determine whether a term is excessive. A more useful option in SUPERQUAD is a graphical display of the calculated *versus* experimental fit of data, which indicates how closely the model represents the titration data.

Table 5:13 shows the sulphide and pH header files for sample 1; the concentrations of each reagent were each refined before refinement of the formation constants.

5.10 Results of SUPERQUAD Analysis.

5.10.1 Determining the β Formation Constants.

β_1 and β_2 were refined as described above. It was found, however, that the presence of EDTA in SAOB influenced the two sets of data of sample 2. When sample 2 was refined using a similar set up file as sample 1 (Table 5:13), that is not including the β formation constants of EDTA, lower than expected log β values were obtained 10.07 and 10.00 for β_1 and 16.89, 16.63 for β_2. When the two EDTA β formation constants lying in the region of interest were included in the header file (Table 5:14), values of 11.64, 12.00 for log β_1 and 18.01, 18.49 for log β_2 were obtained, close to those values obtained for sample 1. The EDTA formation constants were refined, holding the sulphide β values constant, these and the sulphide β constants are shown in Table 5:15.

The log β values were used to calculate the pK_2^d, pK_1^d values for hydrogen sulphide; pK_2^d was determined as 11.82 ± 0.4 and pK_1^d as 6.71 ± 0.4 which agree with values obtained using visual inspection and inserting values in equation (5.8). The pK^d values are compared in Table 5:16.

Table 5:13 Header Files for Refinement of Data of Sample 2, excluding the EDTA β Formation Constants.

Sulphide ISE Data Refinement

MAXIT	IPRIN	MODE	TOL	ACCM	RELAC
20	6	1	0.10E-03	0.10E-74	0.298023E-07

Reactant 1- sulphide
Reactant 2- HYDROGEN

e Temperature of Solution(s) is 23.00 Degrees Centigrade

	Formation Constants	Log Betas	Refinement Keys	Stoichiometric Coefficients	
A	1.0000E 12	12.0000	1	1	1
B	6.3096E 18	18.8000	0	1	2
C	0.1698E-13	-13.7700	0	0	-1

Formation Constants to be refined

•

ırve 1 Initial Volume 10.10
Titre volume error 0.00003 Millilitres

Reactant	Initial No of Millimoles	Titrant Moles/Litre	Standard Potential MilliVolts	Electroa Error
sulphide	0.01080	0.00000	-839.99997	0.00200
HYDROGEN	0.00520	0.06000	No Electrode	

Glass Electrode Data Refinement

MAXIT	IPRIN	MODE	TOL	ACCM	RELAC
20	6	1	0.10E-03	0.10E-74	0.298023E-07

Reactant 1- sulphide
Reactant 2- HYDROGEN

Temperature of Solution(s) is 23.00 Degrees Centigrade

Formation Constants	Log Betas	Refinement Keys	Stoichiometric Coefficients	
1.0000E 12	12.0000	1	1	1
6.3096E 18	18.8000	0	1	2
0.1698E-13	-13.7700	0	0	-1

ormation Constants to be refined

ve 1 Initial Volume 10.10
Titre volume error 0.00003 Millilitres

Reactant	Initial No of Millimoles	Titrant Moles/Litre	Standard Potential MilliVolts	Electrode Error
sulphide	0.01080	0.00000	No Electrode	
HYDROGEN	0.00520	0.06000	10.0000 Assumed	0.11752

Table 5:14 Header Files for Refinement of Data of Sample 2, including the EDTA β Formation Constants.

Sulphide ISE Data Refinement

MAXIT	IPRIN	MODE	TOL	ACCM	RELAC
20	2	1	0.10E-03	0.10E-74	0.298023E-07

Reactant 1- sulphide
Reactant 2- HYDROGEN
Reactant 3- edta

The Temperature of Solution(s) is 23.00 Degrees Centigrade

	Formation Constants	Log Betas	Refinement Keys	Stoichiometric Coefficients		
A	4.3652E 11	11.6400	0	1	1	0
B	10.0000E 18	19.0000	1	1	2	0
C	0.1698E-13	-13.7700	0	0	-1	0
D	7.2444E 16	16.8600	0	0	2	1
E	1.0814E 10	10.0340	0	0	1	1

1 Formation Constants to be refined

Glass Electrode Data Refinement

MAXIT	IPRIN	MODE	TOL	ACCM	RELAC
20	2	1	0.10E-03	0.10E-74	0.298023E-07

Reactant 1- sulphide
Reactant 2- HYDROGEN
Reactant 3- edta

The Temperature of Solution(s) is 23.00 Degrees Centigrade

	Formation Constants	Log Betas	Refinement Keys	Stoichiometric Coefficients		
A	1.0000E 12	12.0000	0	1	1	0
B	10.0000E 18	19.0000	1	1	2	0
C	0.1698E-13	-13.7700	0	0	-1	0
D	2.1878E 10	10.3400	0	0	1	1
E	3.8019E 16	16.5800	0	0	2	1

1 Formation Constants to be refined

Table 5:15 Log β Formation Constants Refined by SUPERQUAD and corresponding K_2^d and K_1^d Values Calculated.

Data of Sample	Log β_1	Log β_2	pK_2^d	pK_1^d
1 pH Curve	11.91	18.80	11.91	6.89
1 S^{2-} Curve	11.73	18.80	11.73	7.07
2 pH Curve	10.07	16.89	10.07	6.82
2 S^{2-} Curve	10.00	16.33	10.00	6.33
2^* pH Curve	11.64	18.01	11.64	6.37
2^* S^{2-} Curve	12.00	18.49	12.00	6.49
$2^\#$ EDTA	9.38	14.63	9.38	5.25

where sample 2* takes into account the EDTA β formation constants for refinement of sample 2 β formation constants

sample $2^\#$ was the refinement of the β formation constants of EDTA

Table 5:16 Comparison of pK^d Values for Hydrogen Sulphide obtained by Visual Inspection and using SUPERQUAD.

	By Visual Inspection		Using SUPERQUAD	
Sample	pK_2^d	pK_1^d	pK_2^d	pK_1^d
1 pH	10.58	5.52	11.91	6.89
S^{2-}			11.73	7.07
2 pH	12.78	5.72	11.64	6.82
S^{2-}			12.00	6.33

5.10.2 Experimental *versus* Calculated Data.

For sample 1, without SAOB, it was possible to fit experimental data well to the calculated titration curve, that is, the model provided by the header files accurately described the systems. These curves are shown in figures 5:11, 5:12.

Better data fitting was possible for sample 2 without EDTA constants (figures 5:13, 5:14) than when EDTA constants were included (figures 5:15, 5:16), this was true for both the glass electrode and sulphide ISE titration curves. However, all 4 curves are similar. When the EDTA constants only were refined, although a reasonable fit was obtained at the start of the titration, this deteriorated after the first end point, it is possible, therefore, that only β_1 of sulphide is affected by the presence of EDTA. Comparing the acid dissociation constants of the SAOB reagents (se Appendix F (ii)), pK_3^d, pK_4^d of EDTA are close to the pK_1^d, pK_2^d of hydrogen sulphide. However, as the refinements of sample 2 showed, it is only pK_4^d which affects the titration results. The pK_d values of ascorbic acid also lie within the pH range of the titration curves. pK_1^d is too low to interfere with pK_1^d of hydrogen sulphide and, fortunately, the pK_2^d value is almost coincident with that of hydrogen sulphide and enhances the inflection . The effect of the SAOB is discussed further in 5.13.

Similar residuals plots were obtained for sample 2 with and without EDTA β formation constants. Figures 5:17, 5:18 show the typical output plots for the sulphide titration of sample 2. One can see that these analyses were similar. Sigma values (the residual standard deviation) of 33.9 and 30.5 were obtained for analyses without and with the EDTA constants. The X^2 value was considerably lower without the EDTA constants. It would, therefore, appear that for sample 2, where similar concentrations of EDTA and sulphide species were present in the analyte, that one observes foremost the titration of the sulphide species, however,

Figure 5:11 Experimental *versus* Calculated Titration Data using SUPERQUAD.

Sample 1, pH Curve

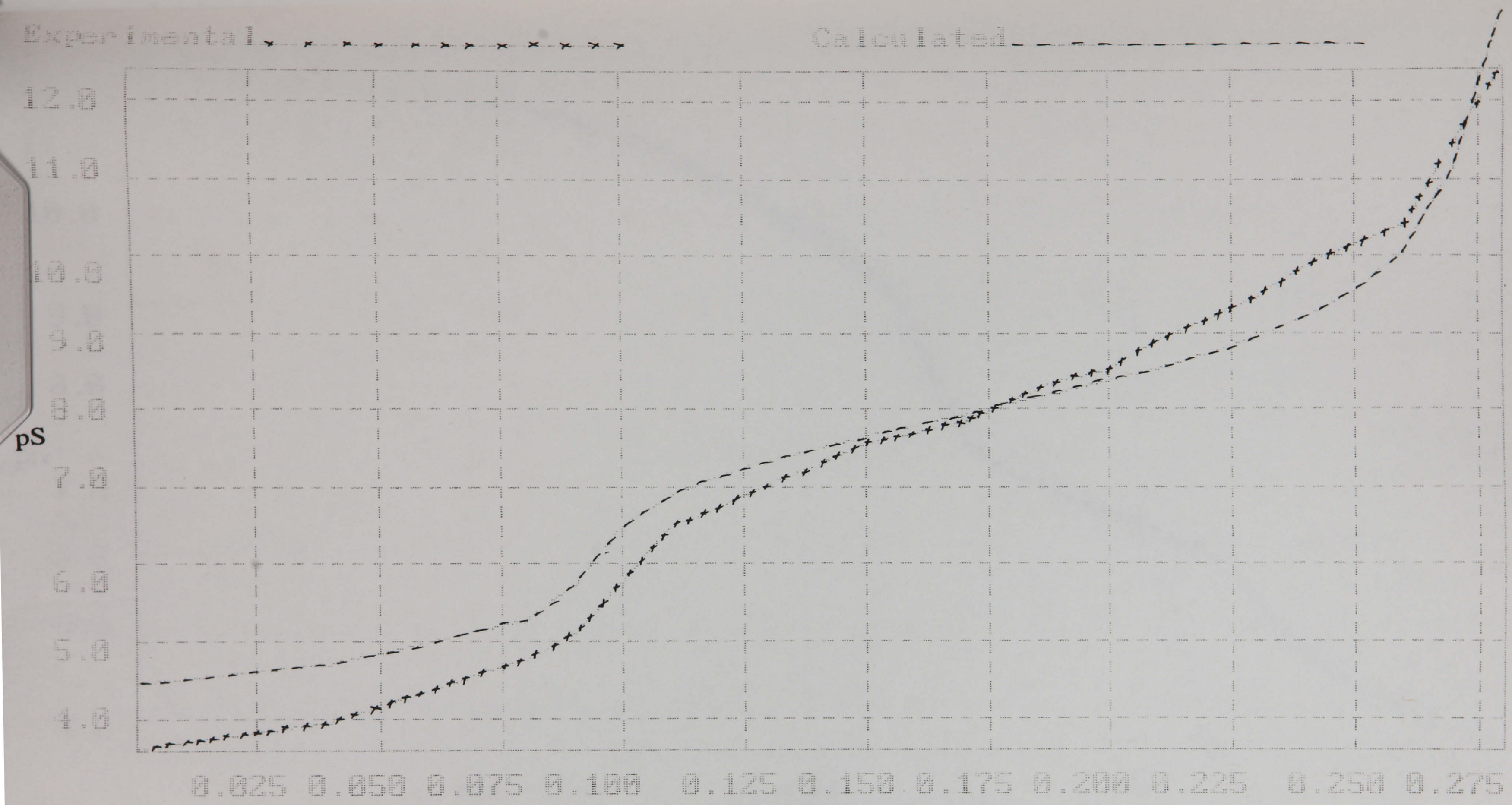

Figure 5:12 Experimental *versus* Calculated Titration Data using SUPERQUAD.

Sample 1, Sulphide Curve

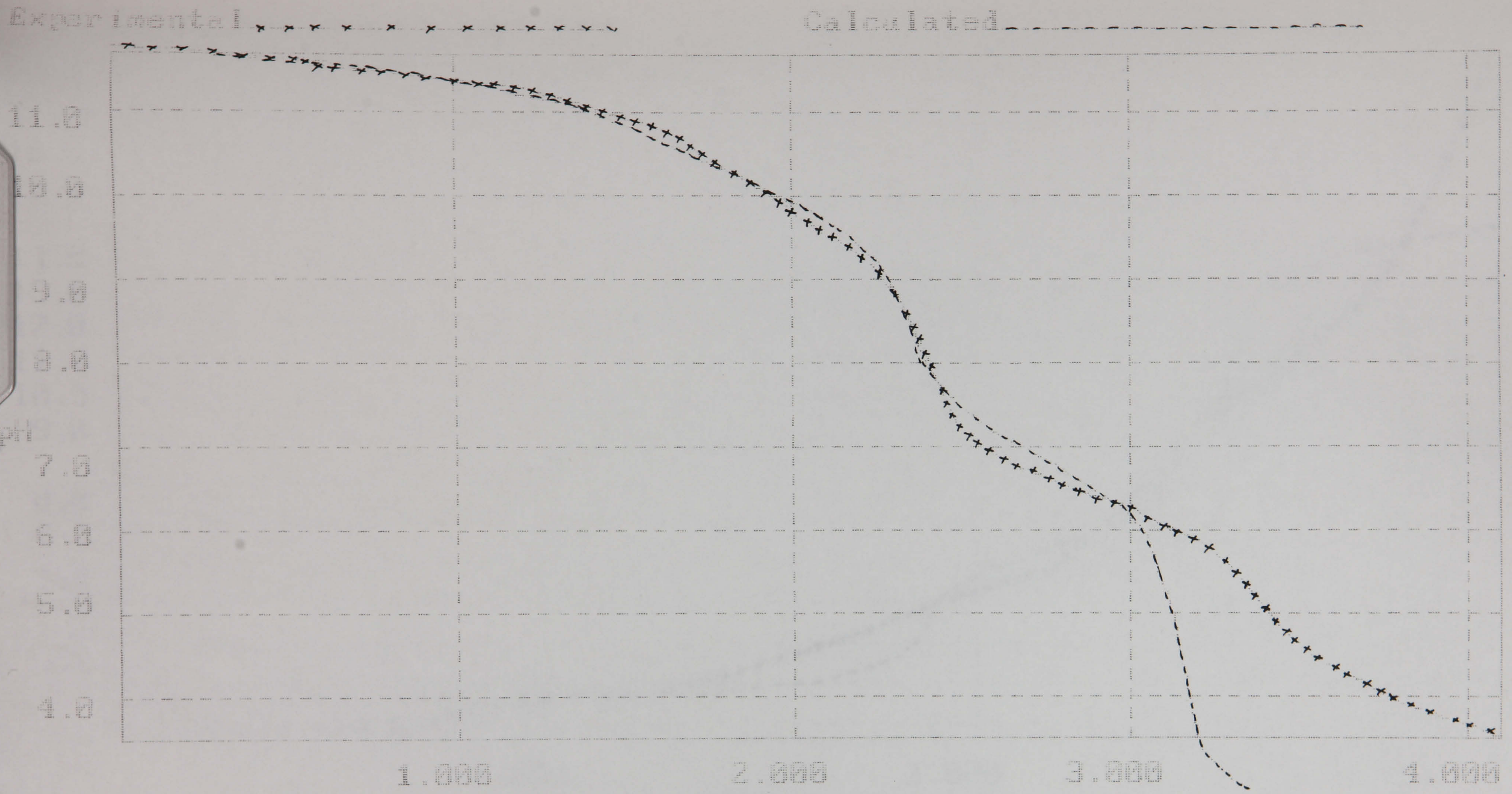

Figure 5:13 Experimental *versus* Calculated Titration Curve using SUPERQUAD.

Sample 2, pH Curve.

EDTA β Formation Constants not included during refinement.

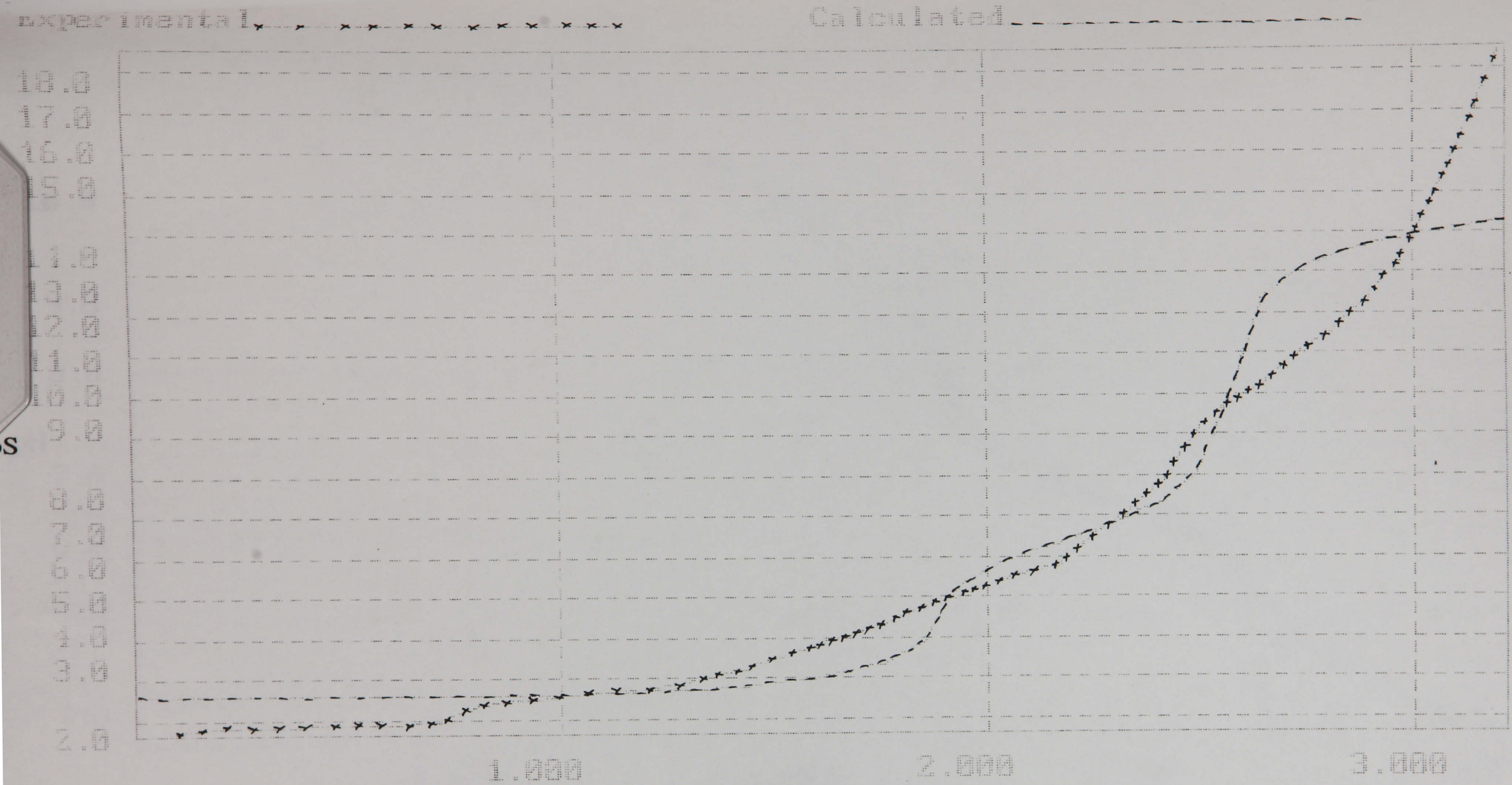

Figure 5:14 Experimental *versus* Calculated Titration Curve using SUPERQUAD.

Sample 2, Sulphide Curve.

EDTA β Formation Constants not included during refinement.

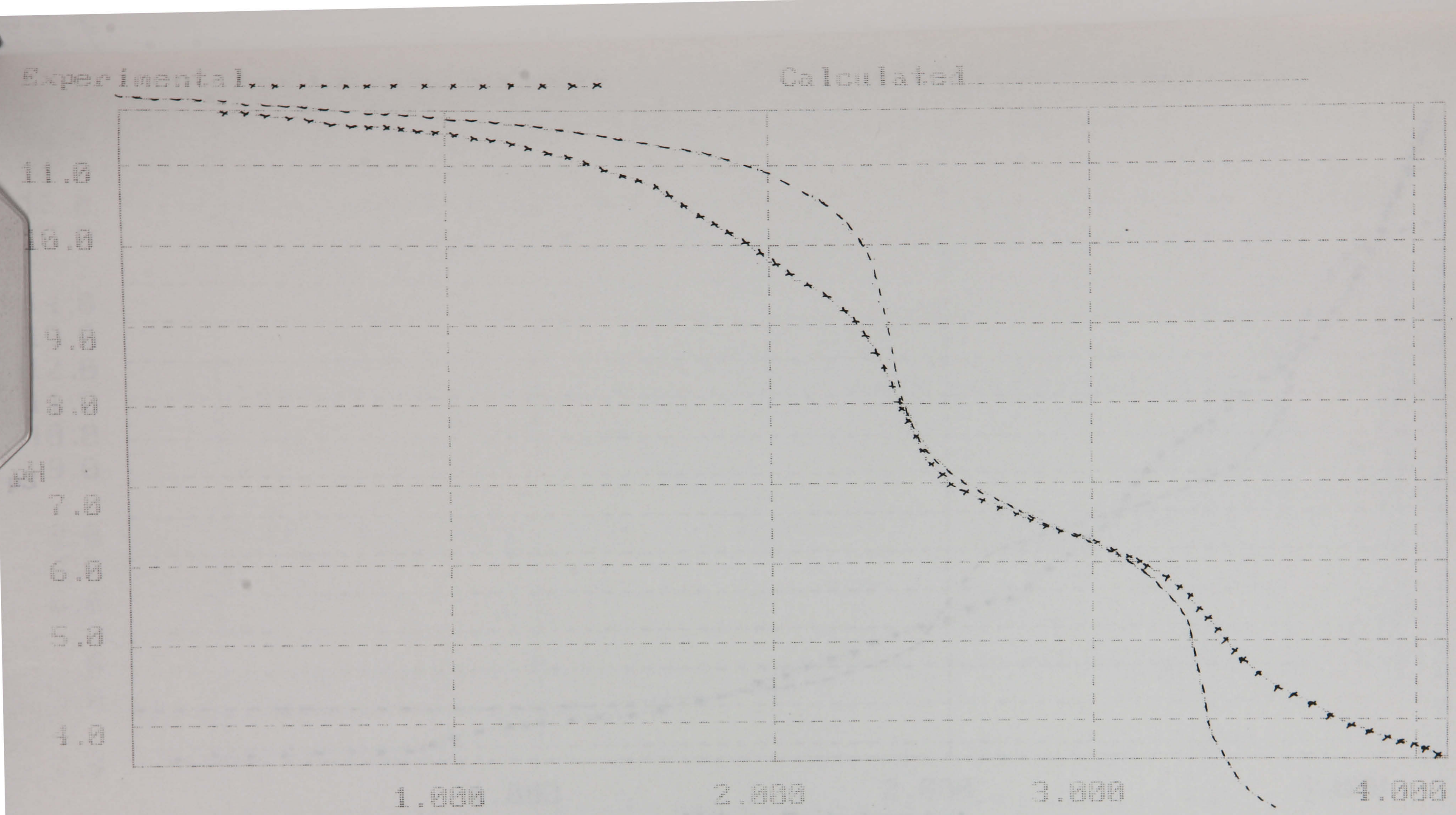

Figure 5:15 Experimental *versus* Calculated Titration Curve using SUPERQUAD.

Sample 2, pH Curve.

EDTA β Formation Constants included during refinement.

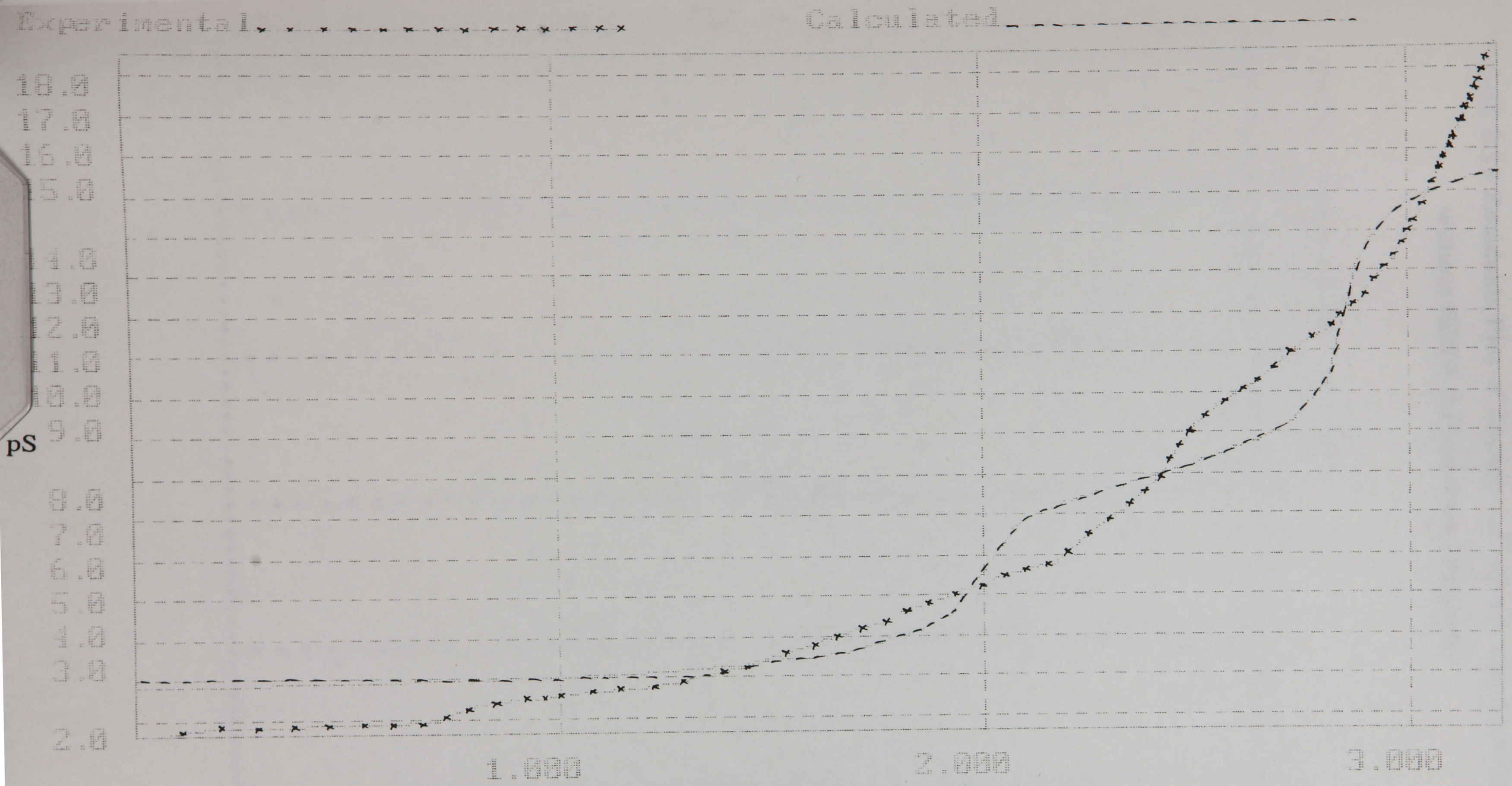

Figure 5:16 Experimental *versus* Calculated Titration Curve using SUPERQUAD.

Sample 2, Sulphide Curve.

EDTA β Formation Constants included during refinement.

Figure 5:17 Residuals Plot of Sample 2 Sulphide Titration Data Refined without EDTA β Formation Constants.

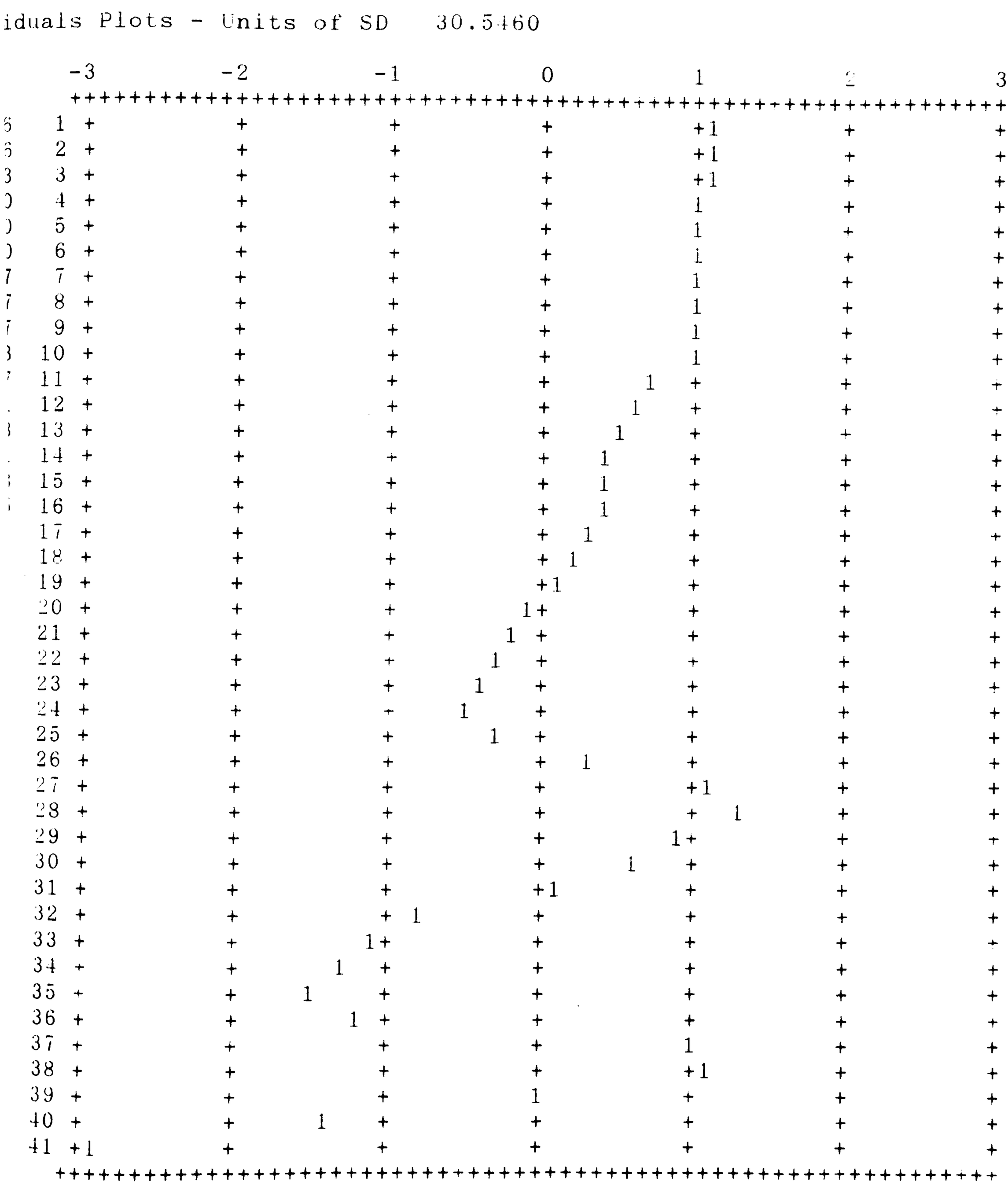

Figure 5:18 Residuals Plot of Sample 2 Sulphide Titration Data Refined with EDTA β Formation Constants.

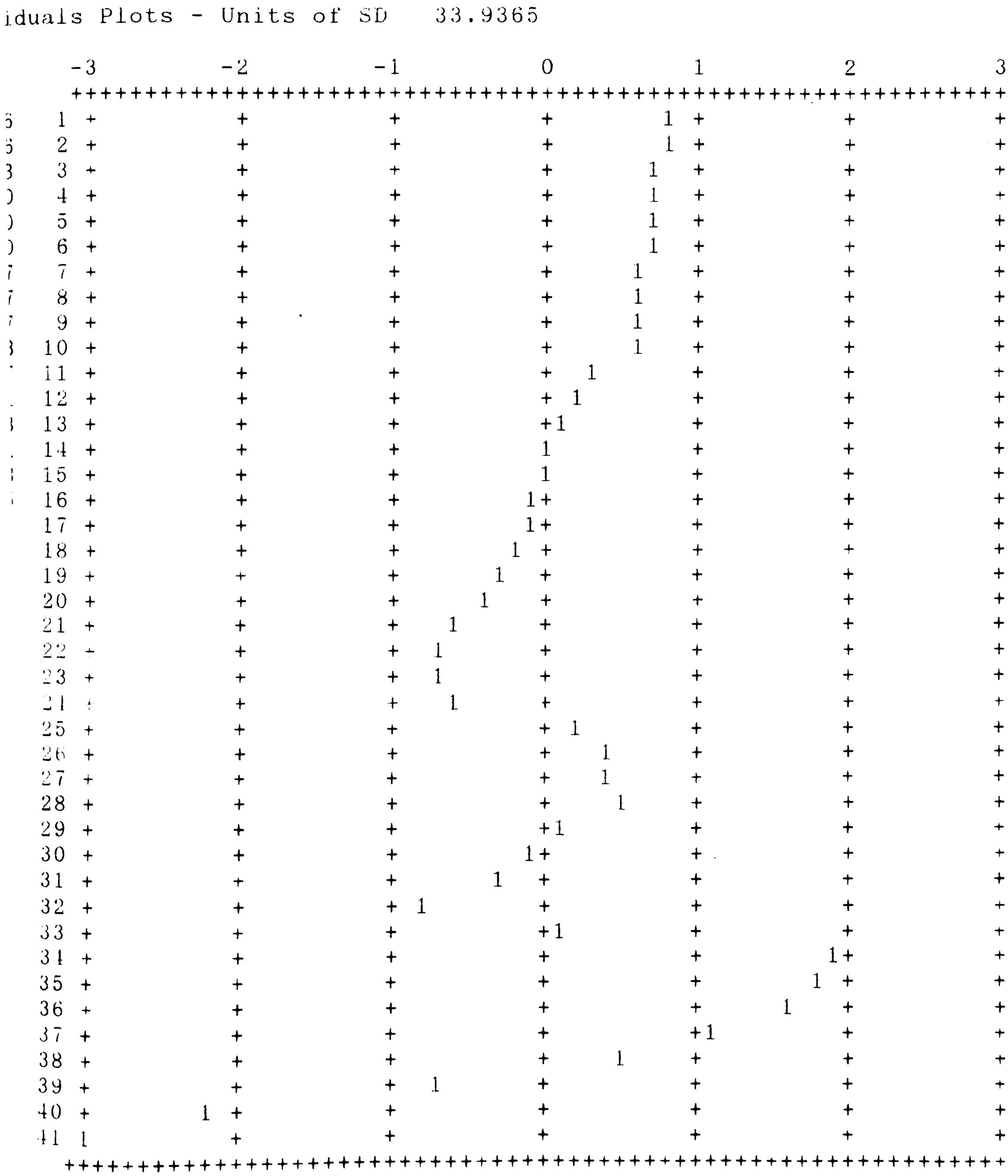

the titrated EDTA must also play a role as insertion of the β formation constants of EDTA, held constant during refinement of β_1, β_2 of sulphide, gave β_1, β_2 values similar to those obtained for sample 1 without EDTA.

5.11 Discussion.

SUPERQUAD is not generally used in conjunction with potentiometric titrations, which show minor variations in the potential difference, therefore, may incorrectly assigned minor "bumps" in the curves to points of inflection. The quality of the titration curves analysed here were not of high quality, but demonstrated well the application of SUPERQUAD. Using the standard deviation plots, it was possible to identify outlying points and remove them from the analyses. By ignoring one incorrectly recorded point, refinement of the titration proceeded which had not been possible before. Where poor quality data is to be refined, it may be necessary to remove outlying points from curves before running SUPERQUAD, however, one must ensure that no loss of details occurs.

Small volumes, 50 µl, of samples were taken, therefore, one might expect some difficulties in obtaining reproducable titration curves, however, this was not found to be the case. Hseu and Rechnitz [23] had used 5.5×10^{-2} mol dm^{-3} in volumetric analyses, and it was felt that by repeating their work, now with an anti-oxidant buffer, that coulometric titrimetry could be operated at considerably lower concentrations.

SAOB was shown to be necessary, in calibrations (Tables 5:5 - 5:7), to prevent aerial oxidation. However, from successful analyses carried out using sample 1, with 1.0 mol dm^{-3} sodium hydroxide rather than SAOB, it was shown that so long as the ionic strength was kept high and constant through out the titration, then aerial oxidation was inhibited. This agrees with work carried out by Hseu and Rechnitz [23] at constant ionic strength of 10^{-1} mol dm^{-3}.

The chart recorder traces do not allow easy visual inspection of the

titration curves, therefore the data analysed by SUPERQUAD of samples 1 and 2 were plotted, superimposing the pH and sulphide curves (figures 5:19, 5:20).

On comparing figures 5:19, 5:20, a longer lead in is shown for the SAOB titration. This is due to the higher pH initially, which must be reduced before the sulphide curve will show; it is the pK_2^d which determines the start of the equilibrium.

5.12 Experimental Considerations.

It is difficult to be sure of the true sulphide concentration of sodium sulphide nonahydrate due to the deliquescent nature of the sample, therefore standardisation of the stock solution should always be carried out using potassium iodate as oxidant. Sulphide ions in the stock solution are oxidised to sulphate ions and excess iodate is back titrated with sodium thiosulphate. In this work, however, not knowing the true sulphide concentration was not considered problematic. Calibration of the sulphide ISE used standards of 10 fold dilution, prepared by serial dilution from the stock solution, thus it was still possible to obtain the Nernst slope of the sulphide electrode. Also, SUPERQUAD is able to refine the concentration of sulphide present initially and use the 'new' refined value to determine β formation constants. Refinements of the sulphide concentration for samples 1 and 2 showed only a 5% error and values for pK_1^d, pK_2^d for hydrogen sulphide obtained by visual inspection and using SUPERQUAD agreed well. The standardisation procedure, however, is recommended for all further work using sodium sulphide nonahydrate.

Small sample volumes, 50 µl, were used in this work, however this should not introduce errors as most micro-pipettes are accurate to within 1% total volume. Preventative steps were taken to avoid aerial oxidation, therefore no loss of sample sulphide (to bisulphide) should occur, this is obviously a greater problem when handling micro samples.

Figure 5:19 pH and Sulphide Titration Curves, superimposed, of Sample 1

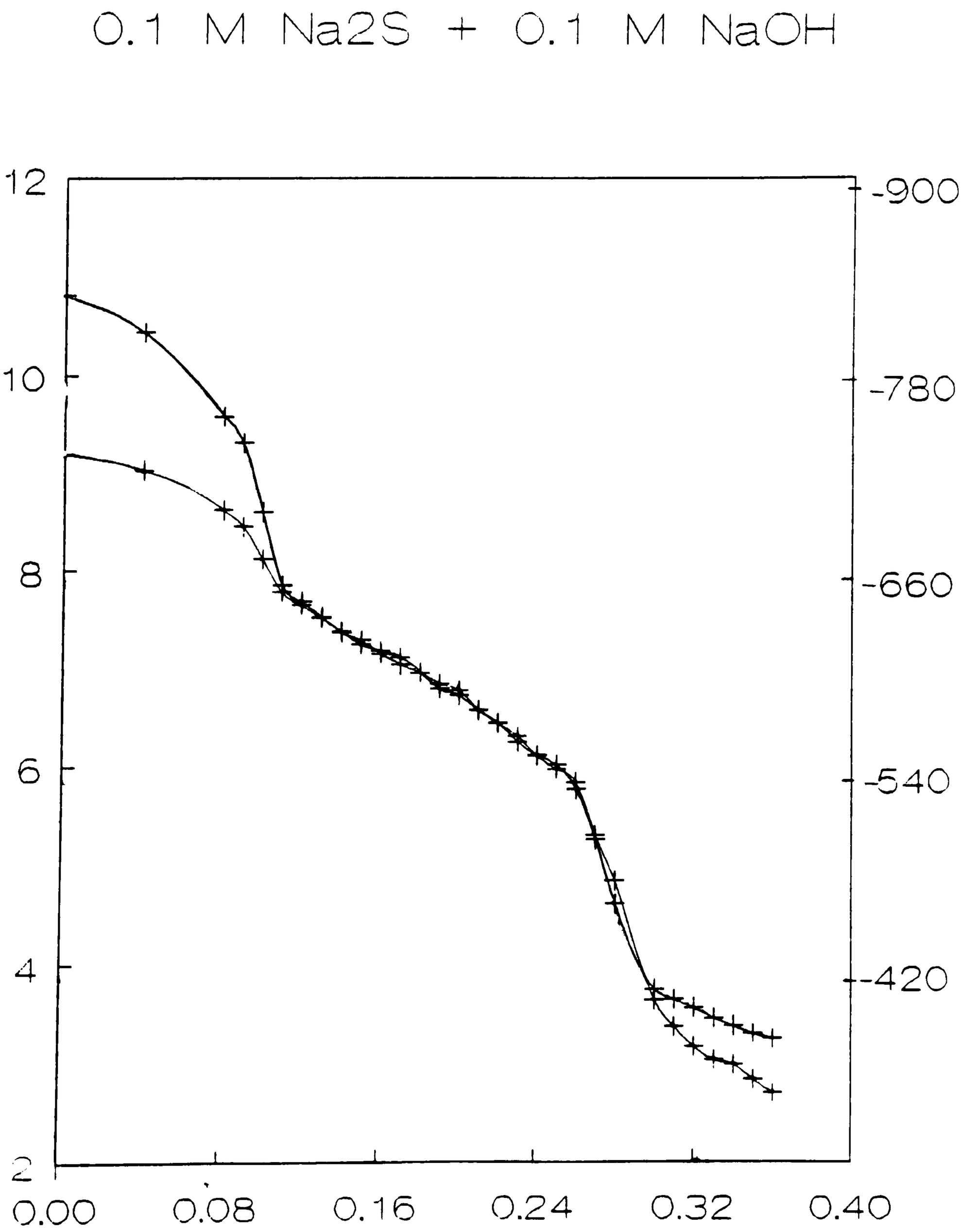

Figure 5:20 pH and Sulphide Titration Curves, superimposed, of Sample 2

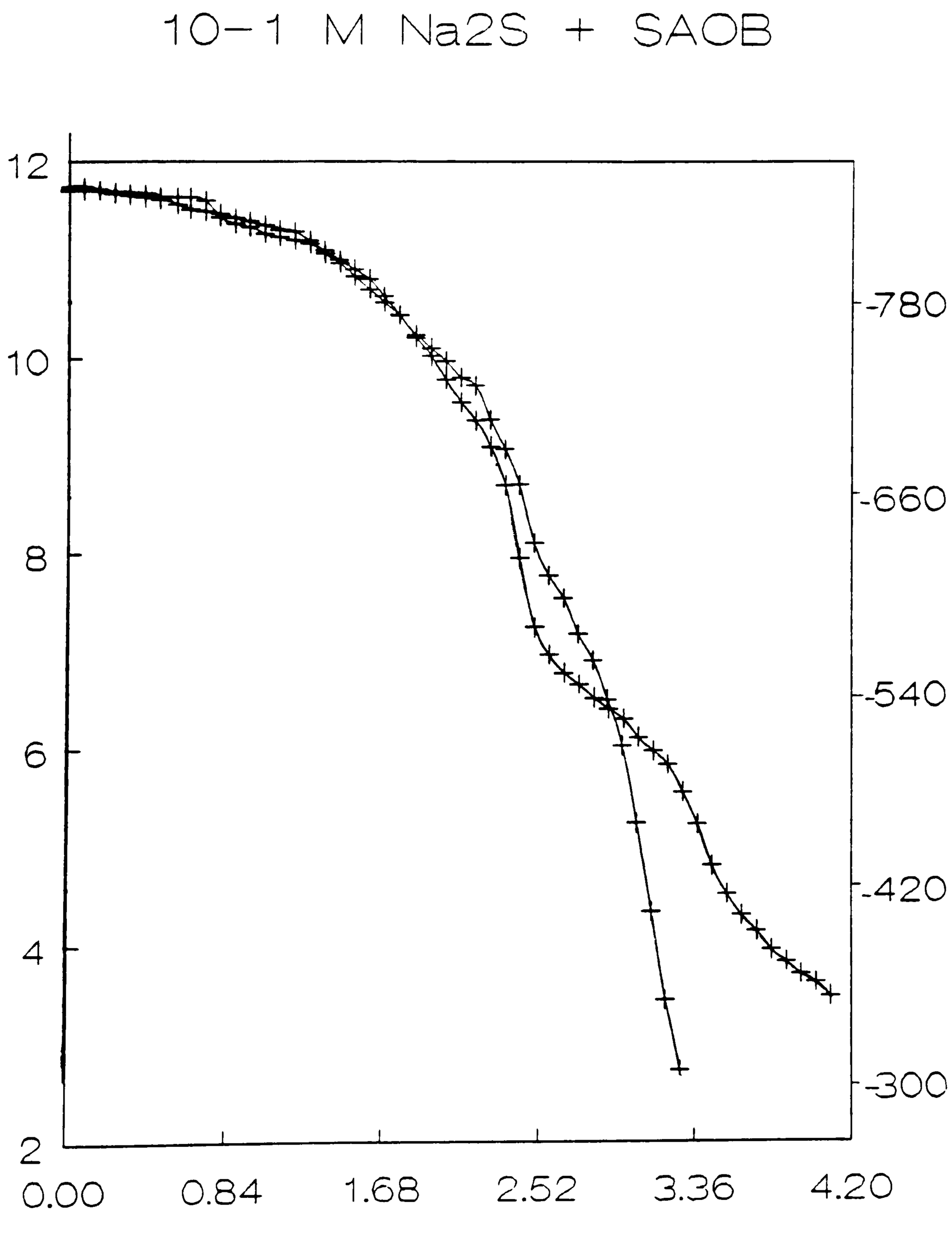

On digitising the titration curves, as this is done manually using a mouse on a control table, errors may be introduced. However, digitising also has the advantage of smoothing titration curves if necessary, e.g. removing mains spikes, and allowing an increased number of data points to be collected near the end points. As the titrator system is currently being transferred to a microprocessor controlled system, the sensor-actuator system, on-line with SUPERQUAD, digitising titration curves will become redundant, however this work has shown how useful a technique digitising can be.

Several non-linear least squares refining programmes are available. SUPERQUAD was used as the Newcastle group is most familiar with this programme. However, SUPERQUAD is extremely particular about the quality of data it will analyse and one must ensure that good quality titration curves are fed into SUPERQUAD. SCOGS2, which is less demanding in the quality of data refined, may be another possible programme to determine dissociation constants of weak acids, such as hydrogen sulphide.

5:13 Further Work.

Use of coulometry to titrate sulphide ions, with simultaneous potentiometric monitoring of the pH and sulphide during titration, has been shown to be an extremely effective method of determining the sulphide speciation as is shown in figures 5:21, 5:22 for sample 1, and thus to determine the dissociation constants. However, this study was only a preliminary test of the technique and if the work is to be continued, which the findings here suggest would be worthwhile, then several points must be made.

The composition of SAOB used in this work was that recommended by Orion Inc. [60] and used by other workers in this group [25]. However, a range of SAOB compositions exist and in future work, the EDTA concentration should either be reduced considerably, to *ca.* 1% of the

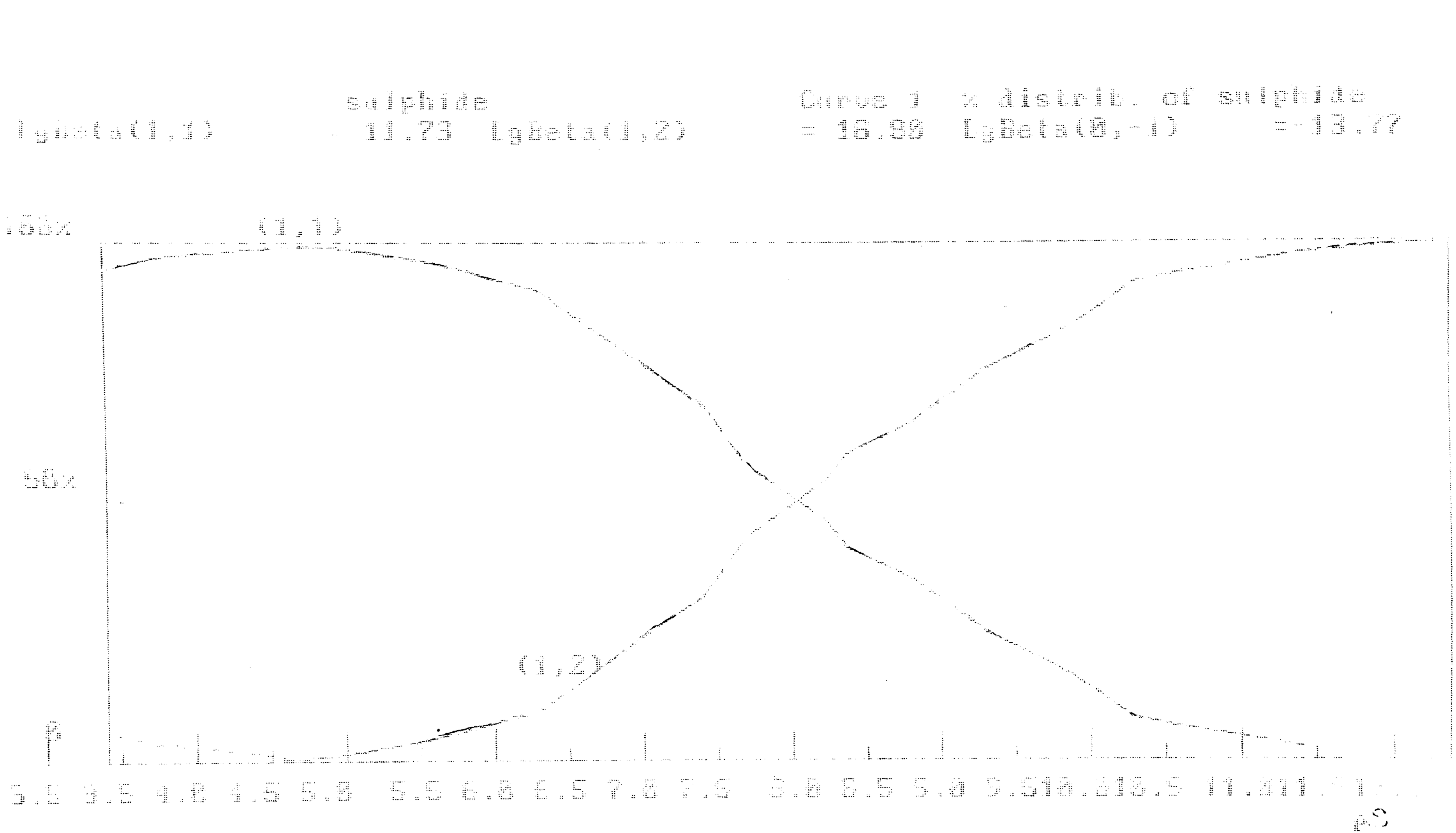

Figure 5:21 Sulphide Speciation Distribution Curve for Sample 1, using Sulphide ISE Titration Data.

sulphide

lgBeta(1,1) = 11.91 lgBeta(1,2) = 18.68 lgBeta(0,-1) = -13.77

Curve 1 : distrib. of sulphide

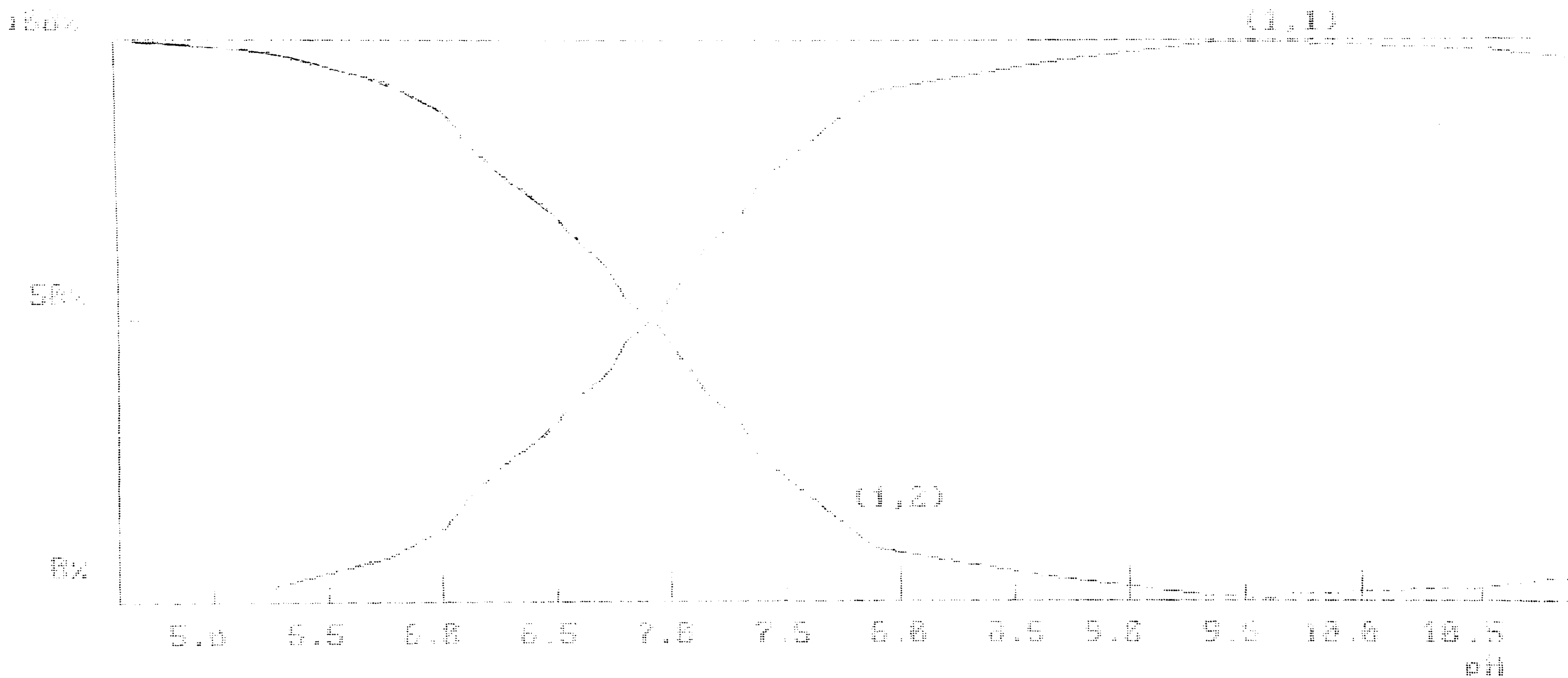

Figure 5:22 Sulphide Speciation Distribution Curve for Sample 1, using Glass Electrode Titration Data.

sulphide concentration, or not used at all. Keeping the ionic strength high and constant prevents conversion of sulphide to bisulphide ions and the presence of ascorbic acid, a sacrificial oxidant, is advised to prevent aerial oxidation. 2 mol dm^{-3} sodium hydroxide and trace ascorbic acid added to the samples in a 1:1 ratio with the sample is recommended as the SAOB composition in further work.

EDTA was used in SAOB compositions to prevent complexation of metal ions with sulphide species, however, this should not be necessary for studies of the dissociation constants and as was discussed in 5.10, the presence of EDTA affects the determination of pK_2^d of hydrogen sulphide due to the similarities in pK^d values. The pK_2^d value of ascorbic acid lies close to that of sulphide, therefore the inflections are superimposed and so ascorbic acid enhances the inflection observed for the sulphide species.

Before summarising the findings of this study, experimental work carried out by spectroscopic techniques will be discussed and compared with potentiometric techniques.

5.14 Comparison of Results of Spectroscopic and Potentiometric Studies.

Results obtained by Ellis and Giggenbach [35] contrast sharply with the present work. Using a silver / silver sulphide ISE [66], a good Nernstian response to a divalent ion (26.7 mV dec^{-1}) was observed for solutions of sodium sulphide in the range 10^{-1} to 10^{-5} mol dm^{-3} when rigorous oxygen exclusion measures were taken and no oxidation was considered to have occurred. This response was attributed to sulphide ions. The hypothesis was tested by repeating calibrations without precautions against oxidation, and a monovalent ion response was observed (65.5 mV dec^{-1}), due to the bisulphide ion. From previous studies carried out [70] no common interferent could cause such behaviour, nor would polysulphides, which Giggenbach suggests are present in sulphide solutions at pH 12. Potentiometric methods clearly distinguish between

monovalent bisulphide ions and divalent sulphide ions by nature of the Nernst slope.

Hseu and Rechnitz [23] showed that in the range pH 11.4 - 11.8, sulphide ions are present and observed Nernst slopes of 29.5 mV dec^{-1} down to 3×10^{-5} mol dm^{-3} sodium sulphide. They mention that at pH 11 there is more hydroxide ion than bisulphide ion; this was the cause of the slightly larger than expected volumes of acid required to reach the first equivalence point in the titration of sodium sulphide (figure 5:1).

Spectroscopic methods rely on correct band identification. Raman studies carried out by Meyer *et al.* [18] must be open to question. The concentration of bisulphide ion quoted as present in samples is determined from a calibration curve obtained from an unknown, or rather, unmentioned, calibrant. It is, therefore, possible that Meyer *et al.*[18] were actually observing sulphide ions and wrongly assigning these as the bisulphide.

Other workers using potentiometric methods [1, 68] also determined much lower values of pK^d_2 than Giggenbach and other spectroscopists, and it seems apparent that it is the method of determination that has given rise to such a large variation of K^d_2 (Table 5:17).

5.15 Conclusions.

Minimisation of aerial oxidation was of prime importance in this work, and all solutions were prepared with deoxygenated water and SAOB or sodium hydroxide to maintain a constant, high ionic strength throughout the titration. This necessity was verified by the series of calibration curves; under optimised conditions a Nernst slope of 27.0 mV dec^{-1} was obtained. At this stage, inhibition of polysulphide formation cannot be guaranteed. However, polysulphides would not give rise to the monovalent Nernst response observed in non SAOB containing solutions, or at low concentrations; this was attributed to bisulphide ions.

Thus, potentiometric methods using a sulphide ISE allow the the

Table 5:17 Quoted Literature Values for the Second Dissociation Constant of Hydrogen Sulphide (in Chronological Order).

Year	Author	pK_2^d	Method	Reference
1905	Kuster & Huberlein	14.92	Hydrolysis	72
1906	Knox	13.22	Hydrolysis	73
1922	Jellinek & Czerwinski	13.70	Conductance	74
1922	Wasastjerna	16.22	Hydrolysis	75
1931	Kolthoff	13 - 14	Solubility	76
1935	Kury *et al.*	12.58	Hydrolysis	77
1941	Hagisawa	11.0	Potentiometry	68
1946	Kubli	12.44	Potentiometry	1
1949	Konopik & Leberl	13.10	Colorimetric pH	20
1959	Ellis & Golding	14.0	UV Spectroscopy	29
1959	Maronny	13.62	Potentiometry	78
1960	Zavadhov & Kryukov	12.44	cited by Sillen	79
1961	Muhammad & Sundarama	13.85	UV Spectroscopy	19
1964	Widmer & Schwarzenbach	14.12	Potentiometry	81
1966	Dickson	15.0	Solubility	82
1967	Ellis & Milestone	13.80	UV Spectroscopy	9
1968	Wagman, Evans *et al.*	12.92	Calorimetry	83
1969	Stephens & Cobble	12.86	Calorimetry	55
1971	Schmidt & Pungor	12.70	Potentiometry	70
1971	Giggenbach	17.0	UV Spectroscopy	30
1974	Ellis & Giggenbach	17.0	UV Spectroscopy	35

1976	Tsonopoulus *et al.*	15.70	Titimetry	84
1977	Rao *et al.*	13.0	Calorimetry	85
1981	Meyer *et al.*	17.0	Raman	17
1982	Brewer	17.0	Thermodynamic Review	86
1984	Camoes *et al.*	12.64	Potentiometry	22
1985	Bard *et al.*	11.92	Solubility Study	87
1986	Meyers	19.0	Review	16
1987	Millero	14.92	Colorimetry	61
1987	Licht & Manassen	17.30	Flocculation/ Spectroscopy	47
1988	Schoonen & Barnes	18.51	Calorimetric	56
1990	CRC Handbook 72^{nd} edn.	11.96		67
1990	Licht *et al.*	15.10	Densometric	49

species S^{2-} and HS^{-} to be clearly distinguished, whereas there is still doubt as to the identity of bands at 27700 cm^{-1} observed by Blandamer[71] and the 'shoulder' observed at 40000 cm^{-1} by Ellis and Giggenbach [35].

These experiments using 50 µl samples of a chemically unstable reagent indicate the advantages of coulometric titrimetry, with in-situ generation of the titrate, over the conventional volumetric methods.

From Hseu and Rechnitz'[23] equation (5.8), the dissociation constants of hydrogen sulphide, pK^{d}_{1}, pK^{d}_{2}, were determined as 5.87 ± 1 ($K_1^{d} = 1.35 \times 10^{-6}$) and 12.08 ± 1.0 ($K_2^{d} = 8.32 \times 10^{-13}$) which are very close to the literature values, Table 5:17, shows that the values obtained are similar to those obtained using similar electrochemical techniques. Comparisons with Hseu and Rechnitz's work, (using volumetric

titrimetry), show that similar profile titration curves were obtained with closely coincident end points for the pH and sulphide electrodes.

The refinements carried out using SUPERQUAD showed how use of this programme may be expanded. Certainly, potentiometric titrations can be used in conjunction with SUPERQUAD not only to evaluate β formation constants of metal - buffer compexes, Average values of 11.83 ± 0.4 for pK_2^d and 6.71 ± 0.4 for pK_1^d were determined using SUPERQUAD. These values agree well with text book values and demonstrate the potential of SUPERQUAD, or similar programmes, to determine dissociation constants of weak acids. This work was to show the feasibility of using SUPERQUAD with ISEs and coulometry, one can expect greater precision from further data, of better quality, when experimental conditions have been optimised.

The presence of EDTA in the anti-oxidant buffer was found to be detrimental to studies; in pH plots, the titration curve of EDTA was superimposed on that of the sulphide species. This was not found to be problematic at high (10^{-1} mol dm^{-3}) concentrations of sodium sulphide, but problems are anticipated at lower sulphide concentrations when the EDTA concentration will greatly exceed that of the sulphide species. The composition of SAOB used in further work, therefore, should be composed of 2.0 mol dm^{-3} sodium hydroxide and trace ascorbic acid.

Further work, to compare directly the results obtained using both electrochemical and spectrophotometric techniques, should be carried out on highly alkaline solutions using a mercury/ mercury oxide reference electrode (stable in highly alkaline solutions) in order to examine the reasons for the disparity. It is suggested that the experiments are repeated and the solutions prepared also undergo spectroscopic studies.

References.

1. Kubli H.
   Helv. Chim. Acta 1946, **29**, 1962

2. Pomeroy R.
   Sewage Works J. 1941, **13**, 498

3. Eckert W. & Frevert T.
   Ion Selective Electrodes, 4
   Anal. Chem. Symposia Series, 1984, **20**, 359

4. Eriksson E.
   J. Geophys. Res. 1963, **68**, 4001

5. Al-Hitta I.K., Moody G.J. & Thomas J.D.R.
   Analyst 1983, **108**, 43

6. Al-Hitta I.K., Moody G.J. & Thomas J.D.R..
   Analyst 1983, **108**, 1209

7. Millero F.
   Mar. Chem. 1986, **18**, 121

8. D'yachova I.B. & Khodakovsky L.L.
   Geokhim. 1968, **11**, 615

9. Ellis A.J. & Milestone N.B.
   Geochim. Cosmochim. Acta 1967, **31**, 615

10. Champs P.R., Gulens J. & Jackson R.E.
    Can. J. Earth Sci. 1979, **16**, 12

11. Hersley J.P., Plese T. & Millero F.
    Geochim. Cosmochim. Acta 1988, **52**, 2047

12. Gulens J.
    Water Res. 1985, **19**, 201

13. "Mud Duck" Field Operation Manual
    Delphian Corporation, California

14. Ostlund H.G. & Alexander J.
    J. Geophys. Res. 1963, **68**, 3995

15. Almgren T. & Hagstrom I.
    Water Res. 1973, **8**, 395

16. Meyers R.J.
    J. Chem. Ed. 1986, **63**, 687

17. Latimer W.M.
    "The Oxidation States of the Elements and their Potentials in Aqueous Solution"
    2nd ed. , Prentice Hall, Englewood Cliffs, New Jersey 1952, pp 34

18. Meyer B., Ward K., Koshlap K. & Peter L.
    Inorg. Chem. 1981, **22**, 2345

19. Muhammad S.S. & Sundaram E.V.

J. Sci. Ind. Res. Sect. B 1961, **20**, 16

20. Konopik K. & Leberl G.
Monatsch. 1949, **80**, 787

21. Auerbach F.
Z. Physikal Chem. 1904, **49**, 220

22. Camoes M.F.G.F.C., Silva M.F.G. & Pereiva M.I.S.
ref. 3, p.321

23. Hseu T.M. & Rechnitz G.A.
Anal.Chem. 1968, **40**, 1054

24. Damjanovic A., Yeh R.L.S.& Hudson P.G.
J. Appl. Electrochem. 1982, **12**, 343

25. Dunn D.
unpublished work, University of Newcastle-upon-Tyne, 1986

26. Umezawa Y., Ito K., Hata H., Sugawara M., Harsanyi E.G., Toth K., Pungor E., Soma M. & Tanaka A.
Mikrochim. Acta 1990, I, 231

27. Crombie D.J., Moody G.J. & Thomas J.D.R.
Anal. Chim. Acta 1975, **80**, 1

28. Giggenbach W.
Inorg. Chem. 1971, **10**, 1333

29. Ellis A.J. & Golding R.M.
J. Chem. Soc. 959, **127**, 1

30. Giggenbach W.
Inorg. Chem. 1971, **10**, 1306

31. Giggenbach W.
Inorg. Chem. 1974, **13**, 1724

32. Giggenbach W.
Inorg. Chem. 1974, **13**, 1730

33. Clark R.J.M. & Cobbold D.G.
Inorg. Chem. 1978, **17**, 3169

34. Cotton F.A., Harmon J.B. & Hedges R.M.
J. Am. Chem. Soc. 1976, **98**, 1417

35. Ellis A.J. & Giggenbach W.
Geochim. Cosmochim. Acta 1971, **31**, 615

36. Blandamer M.J., Gross J.M. & Symons M.C.R.
Trans. Faraday Soc. 1964, **60**, 615

37. Smith M. & Symons M.C.R.
Trans. Faraday Soc. 1958, **54**, 338

38. Stein G. & Treinen A.
Trans. Faraday Soc. 1959, **55**, 1068

39. Blandamer M.J., Gough T.E., Symons M.C.R.

Trans. Faraday Soc. 1963, **59**, 1748

40. Stein G. & Treinen A.
Trans. Faraday Soc. 1960, **56**, 1393

41. Smith M. & Symons M.C.R.
Disc. Faraday Soc. 1958, **54**, 346

42. Smith M. & Symons M.C.R.
Trans. Faraday Soc. 1960, **56**, 1125

43. Branch G.E.K. & Calvin K.
"The Theory of Organic Chemistry"
Prentice-Hall, Englewood Cliffs, New Jersey, 1944 p.204

44. Levy D.E. & Myers R.J.
J. Phys. CHem. 1990, **94**, 7842

45. Wood R.H.
J. Am. Chem. Soc. 1958, **80**, 1559

46. Licht S.
Anal. Chem. 1985, **57**, 514

47. Licht S. & Manassen J.
J. Electrochem. Soc. 1987, **134**, 918

48. Licht S.
J. Electrochem. Soc. 1988, **135**, 2971

49. Licht S., Forouzan R.F. & Longo K.
Anal. Chem. 1990, **52**, 1356

50. Kielland J.
J. Am. Chem. Soc. 1937, **59**, 1675

51. Picknett R.G.
Trans. Faraday Soc. 1968, **64**, 1059

52. Brull L.
Gazz. Chim. Ital. 1934, **64**, 624

53. Bonino G.B. & Centola G.
Mem. Accad. Italia 1933, **4**, 445

54. Lito M.J.G.H.M., Camoes M.F.G.F.C., Ferra M.I.A. & Covington A.K.
Anal. Chim. Acta 1990, **239**, 129

55. Stephens H.P. & Cobble J.W.
Inorg. Chem. 1971, **10**, 619

56. Schoonen M.A.A. & Barnes H.L.
Geochim. Cosmochim. Acta 1988, **52**, 649

57. Coucouvas D.
J. Amer. Chem. Soc 1979, **101**, 3392

58. Moody G.J. & Thomas J.D.R.
ref. 3, p.218

59. Guterman H., Ben-Yakov S. & Abeliovich A.
Anal. Chem. 1983, **55**, 1731

60. Handbook of Electrode Technology
Orion Research Publication
Orion Research Inc., 1968, S-5

61. Millero F., Hubinger S., Fernandez M. & Garnett S.
Env. Sci. Tech. 1987, **21**, 439

62. Private Communication
Dr. K. Smith, Albright & Wilson, to J.Dick, Nov. 1989

63. Cunningham M.J.
3H Project Report, University of Newcastle-upon-Tyne, 1988

64. Private Communication.
Dr. F. Millero, Univ. of Miami, to Prof. A.K. Covington, Jan. 1990

65. Vesely J., Jensen G.J. & Nicolaisen B.
Anal. Chim. Acta 1972, **62**, 1

66. Ruzicka J., Lamm C.G. & Tjell J.Chr.
Anal. Chim. Acta 1972

67. Handbook of Chemistry & Physics
72nd edn. C.R.C. Press, Inc. Boca Raton, Florida, 1990-91

68. Hagisawa H.
Instit. Physic. Chem. Res. 1941, **20**, 384

69. Private Communication
P. Gans, Univ. of Leeds, to A.K. Covington, Oct. 1991

70. Schmidt E. & Pungor E.
Anal. Lett. 1971, **4**, 641

71. Blandamer M.J., Gross J.M. & Symons M.C.R.
Proc. Chem. Soc. 1963, 147

72. Kuster F. & Huberlain F.
Z. Anorg. Chem. 1905, **43**, 53

73. Knox J.
Z. Electrochem. 1906, **12**, 477

74. Jellinek K. & Czerwinski J.
Z. Phys. Chem. 1922, **102**, 438

75. Wasastjerna J.A.
Soc. Sci. Fenn. Com. Phys. Math 1923, **1**, 40

76. Kolthoff I.M.
J. Phys. Chem. 1931, **35**, 2711

77. Kury J.W., Zieles A.J. & Latimer W.M.
J. Electrochem. Soc. 1953, **100**, 468

78. Maronny G.

Electrochimica Acta 1959, **1**, 58

79. Zavadhov S.S. & Kryukova P.A.
cited by Sillen L.G. & Martell A.E., 1964 (ref. 80)

80. "Stability Constants of Metal Ion Complexes"
Sillen L.G. & Martell A.E.
The Chemical Society, London 1964

81. Widmer M. & Schwarzenbach G.
Helv. Chim. Acta 1964, **47**, 266

82. Dickson F.W.
Bull. Volcan. 1966, **24**, 605

83. Wagman D.D., Evans W.H., Parker V.B., Halow I., Bailey S.M., & Schumm R.H.
NBS Technical note 270-3,
U.S. Govt. Printing Office, Washington D.C., p. 43, 47

84. Tsonopoulus C., Coulson D.M. & Inman L.B.
J. Chem. Eng. Data 1976, **21**, 190

85. Rao S. Ramachandra & Hepler L.G.
Hydrometallurgy 1977, **2**, 293

86. Brewer L.
in "Flue Gas Desulfurization" Chap. 1
ed. Hudson J.L., Rochelle G.T.
Am. Chem. Soc., Washington D.C., Symposia Series No. 188

87. Bard A.J., Parsons R. & Jordan J.
" Standard Potentials in Aqueous Solutions", Chap. 6
IUPAC Comission on Electrochemistry and Electroanalytical Chemistry.
Marcel Dekker Inc., New York, 1985

CHAPTER SIX

CLINICAL ANALYSES

6.1 Introduction.

In Chapter 4 the advantages of coulometry and the relevance of coulometric techniques with potentiometric sensors were discussed. The objective of the project discussed in this chapter was to study the suitability of ion sensitive field effect transistors (ISFETs) for clinical work with special reference to the flow cell assembly provided by Bellhouse Medical Products (figure 6:1, 6.2). This was intended for use in the analysis of blood and serum, where the concentrations of specific ions, e.g. sodium, potassium, are of critical importance. Evaluations of the optical sensitivity of ISFETs and of a new membrane composition, for use in clinical chemistry, were made.

Several points have arisen in this investigation with regard to the cell requirements and these are discussed as appropriate.

6.2 Ex-vivo *versus* In-vivo Methods.

Ex-vivo monitoring has distinct advantages over in-vivo sensing. In in-vivo experiments the electrode must be removed from the patient if recalibration should be necessary during tests, thus increasing the chance of thrombi formation. In ex-vivo methods, it is possible to connect the flow cell / device directly to the patient via a cannula. Sterilization requirements for the devices are now unnecessary and it is possible to treat the sample, e.g. dilute or heparinize to prevent blood clotting, if necessary [1].

One problem which must be appreciated during ex-vivo analysis is the possible difference in temperature of blood and calibration solutions. A heat exchanger has been used in some systems to maintain thermal equilibrium within the system [2].

6.3 Clinical Methods.

6.3.1 Flame Photometry.

A detailed description of this technique can be found elsewhere [3]. The important points to note are that the blood samples are diluted one

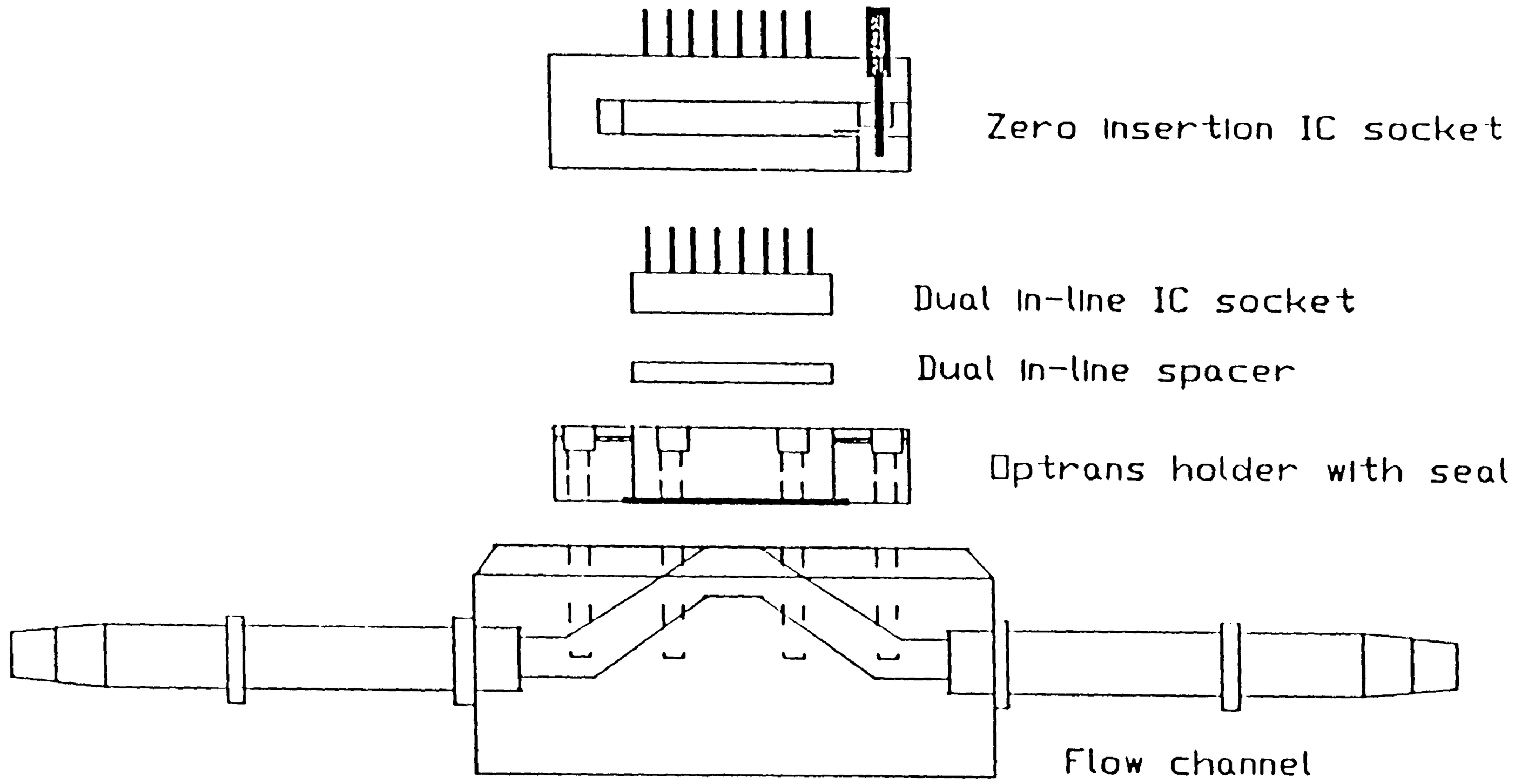

Figure 6:1 Schematic of the Bellhouse Dialysis Flow-cell Assembly.

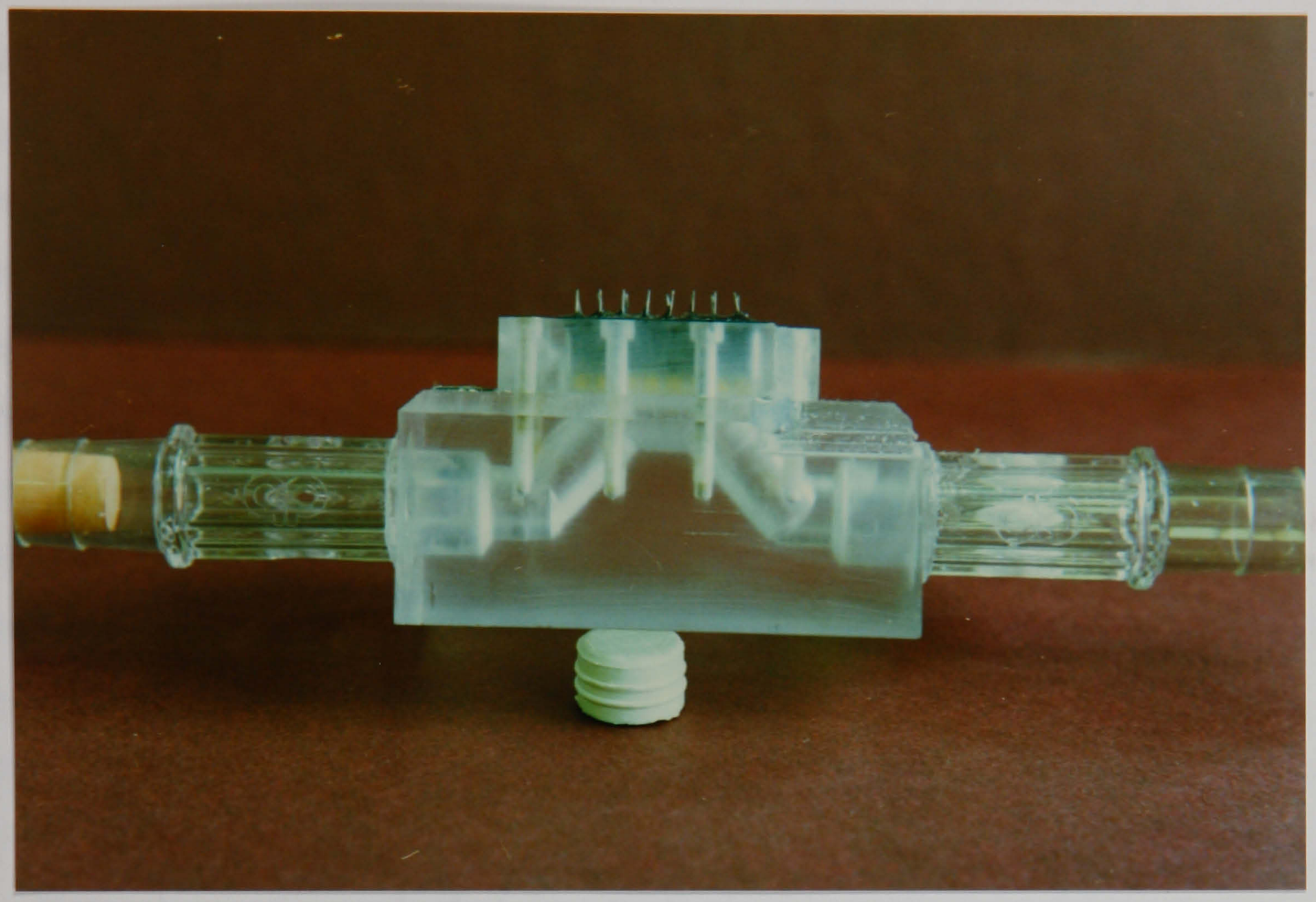

Figures 6:2 The Bellhouse Dialysis Flow-Cell Assembly.

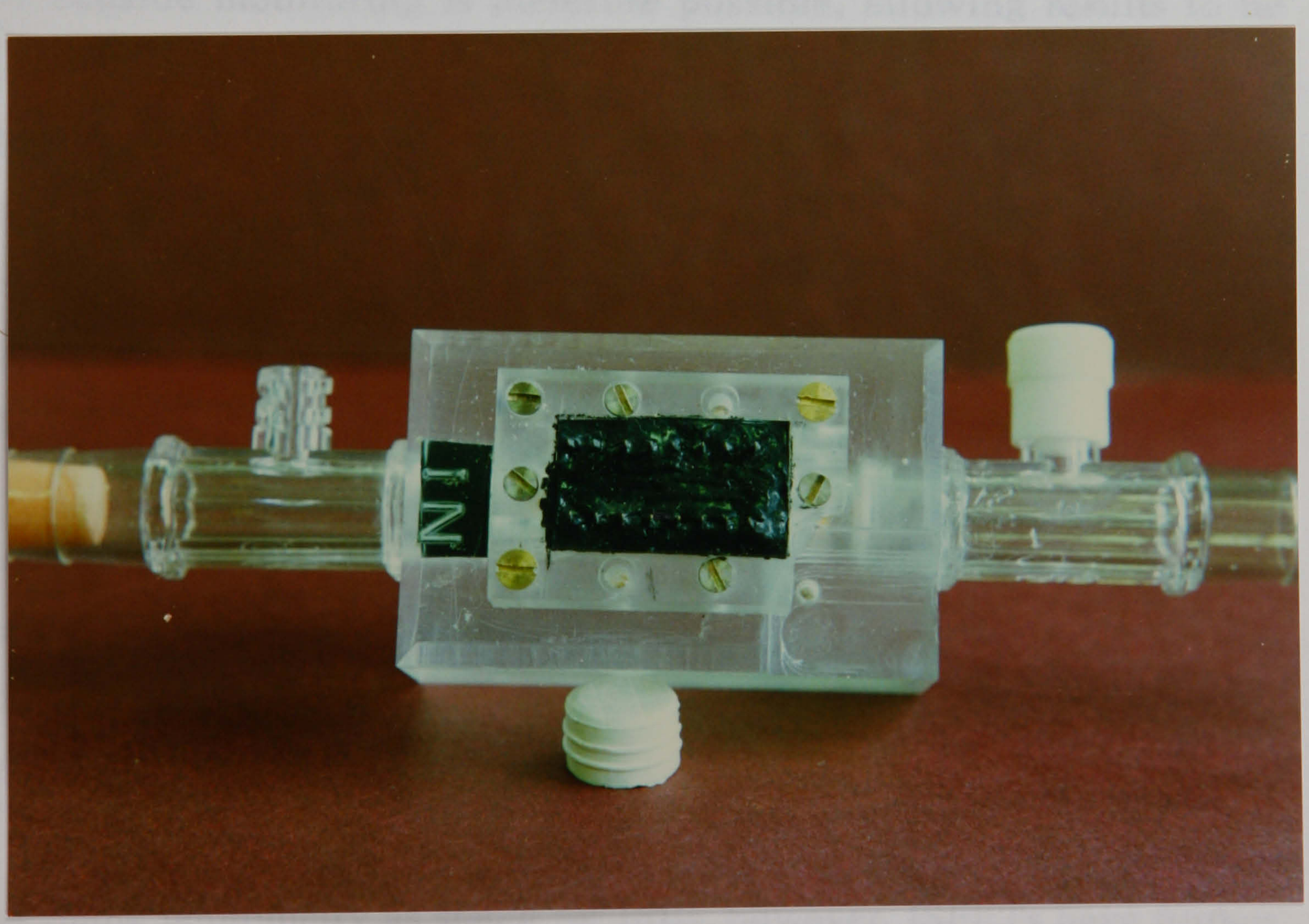

part sample to 199 parts diluent (depending on the ion and ion concentration) and that it is the **concentration** of ions (mmol l^{-1} water). and not **activity** that is determined. In reality, activity is a more important parameter as this is the available species [4], e.g. 50 % of calcium is protein bound [5], therefore unavailable, in serum. It is well known that proteins will bind to low molecular weight species [6], and that the degree of interaction is pH and temperature dependent (e.g. calcium and hydrogen ions will compete for binding sites). For sparingly soluble compounds this is a means of transportation e.g. calmodulin. Clinicians, however, are familiar with values indicative of total ion present and are reticent to changing convention.

6.3.2 Potentiometric Methods.

Potentiometric methods have distinct advantages over photometric techniques [7, 8]. No sample pretreatment, e.g. centrifuging, is necessary and bedside monitoring is therefore possible, allowing results to be obtained instantly without referral to the hospital central laboratory. Also, activity, the parameter of importance, is measured and the devices are simple, requiring very little training to operate.

ISEs have been used in-vivo [9, 10] but not yet as a commercial proposition. There are, however, many auto-analysers available for examination of ion concentrations in body fluids [11-14].

Mini-electrodes are used in these analysers, but due to the small membrane size, these electrodes can have a very high membrane resistance; this is a limiting factor in the construction of miniaturised ISEs [15].

6.4 Ion Sensitive Field Effect Transistors (ISFETs).

ISFETs possess all the advantages of direct potentiometric techniques over flame photometry as stated for ISEs, however, ISFETs have further advantages. ISFETs have a high input impedance, and corresponding low output impedance, so there is a less noisy signal and less dependence on

the buffer amplifier for signal processing compared with ISEs, and as there is no internal reference electrode, there is one less interfacial potential to consider.

ISFETs with a PVC / valinomycin membrane were shown by Moss *et al.* [16] to operate satisfactorily in the presence of proteins, encouraging the development of ISFETs as clinical sensors [17, 2]. The research did show a small negative drift over a three hour period which they believed arose due to desorption of protein from the membrane surface.

It was, therefore, extremely important that the drift characteristics of devices were studied before analyses, as a change from e.g. 4.0 mM to 4.1 mM potassium corresponds to a change of only 0.63 mV. Resolution of 0.1 mV is required of devices, i.e. a drift of less than 0.13 mV h^{-1} [1].

6.5 Blood Constituents.

As the cell was intended for use in monitoring serum, blood and other biological fluids, it is essential that the complex composition of blood is appreciated. Buffering in blood plasma is maintained by haemoglobin, bicarbonate and phosphates. Although haemoglobin has better buffering action, bicarbonate is easier to determine. The concentration of bicarbonate is related to pH and pCO_2 by the Henderson-Hesselbalch equation,

$$pH = pK_a - \log \{[CO_2] / [HCO_3^-]\} \qquad (6.1)$$

pH measurements alone are sufficient only for short term monitoring of respiratory conditions. This is because blood pH is affected by two mechanisms; the fast O_2 / CO_2 exchange of respiration and the slow oxidation of proteins and lipids into non-volatile acids. Hence simultaneous monitoring is necessary to distinguish between these processes.

Blood is composed of;

- plasmatic water, that is water, ions and small hydrophilic

constituents e.g. glucose

- proteins, lipids and lipoproteins
- corpuscles, erythrocytes, leucocytes and platelets.

In "normal", healthy patients this composition can be described by

		(6.2)
Plasma water = 93 % plasma water + 5.4 % protein + 0.6 % lipids		
composition	+ 0.9 % soluble salts and sugars	

Using this information, the total volume of water can be determined for healthy patients using Waugh's calculation [18];

Plasma water = 99.1	-	0.73	-	1.03 (6.3)
ml/100 ml		g/100 ml		mg/100 ml

Note that this equation refers to **concentration** of species as indicated by flame photometric techniques. In normal plasma, i.e. from healthy patients, 2.5% difference for Na^+ and K^+ concentrations are determined using plasma water rather than plasma volume values [19-22].

Using direct potentiometry with undiluted samples, rather than indirect dilution methods, 7% greater sodium and potassium ion concentrations were observed due to the volume displacement effects of proteins, lipids etc. [23], and a positive bias of 4 - 5 % arose for the concentration of calcium ions, cCa^{2+}, measurements in whole blood compared with the true value in plasma phase. However, this bias could be reduced by creating a larger area of contact between blood and the potassium chloride bridge solution and by correct choice of standards. Also, by taking into account variation in dissolved carbon dioxide content, avoiding calcium complexation and calcium / heparin binding [24].

Maas *et al.* [25] stated that ionic strength changes do not give appreciable differences between flame photometric and direct potentiometric results unless the water concentration changes greatly, as in hyperlipemia or hyper- or hypo-proteinemia. In these cases, the

normalisation factor used to account for the volume displacement of proteins, lipids etc., proportional to the mass concentration of water divided by the molar activity coefficient of the ion of interest in normal plasma, can no longer be used.

Using serum based standards, sodium ion analyses by the two techniques over a 6 month period were found to be similar, with more precise results using the ISE method [26]. Pioda *et* al. [27] also found direct potentiometric monitoring to be better than flame photometry for potassium analyses in centrifuged, undiluted serum samples.

6.6 Protein Interference.

When there is an increase in the concentration of protein there is an effective decrease in concentration of plasma water. Direct potentiometric methods of determining activity of species will not be affected by the increased volume and this leads to an increased bias of values from each method. Maas *et al.* [25] hope to introduce a conversion factor to integrate the two methods, as yet this has not been accomplished. They also suggested that use of protein-containing calibration solutions may alleviate the discrepancy.

As the concentration of protein increases, there is decreased recovery of potassium and sodium [28]. Although weak interaction of sodium - albumin has been noted by some groups [22], Ladenson [26] stated the effect was due to a non-protein, protein associated, compound which bound to the sodium. Hickling [29] later identified this as a sodium-binding polypeptide (with molecular weight of 5000) in ox-blood which may also be present in humans.

There is, therefore, much controversy as to the effect of proteins on ISE and ISFET experimental performance. Payne [30, 31], an advocate of the belief that proteins do interfere with ISEs, suggests that protein and other macro-molecules, surrounded by bound counterions, behave as neutral protein-water-ion micelles in the water-ion phase, giving rise to a

difference in the total ion concentration across the protein impermeable dialysis membrane. Payne and Jones [30] state that in measurements of ionised calcium, protein interferes with measurement of the reference liquid junction potential. Oesch *et al.* [32] suggested that interfacial changes at the membrane surface are produced by protein deposition; a change in the physical nature of the interface leading to a shift in the standard electrode potential, E_o. This shift in the standard potential has been noted by other workers [33, 34] and shown not to be a liquid junction potential. Thode *et al.* [35] found that this irreversible shift was not eliminated using albumin containing calibration solutions, but was eliminated using a cellophane dialysis membrane over the ion selective membrane. Rebelo [33] noted that both Visking ® and Europhen ® dialysis membranes were affected by protein, giving readings 1 mV higher than expected. As drifting was not observed, it was suspected that the dialysis membrane had introduced another liquid junction. Tests carried out for calcium [24], in a system as shown in figure 6:3, showed that a dialysis membrane did affect the time response. An increase from 1 s to 15 s for 95% response was observed, however, this was considered acceptable as the membrane was now protecting the sensor.

Impedance studies carried out at Newcastle show that albumin, used as the interferent protein in most investigations, does not affect the diffusion of ions at the membrane surface [36]. It would therefore be advisable to repeat tests initially carried out by Fogh-Andersen *et al.* [37] with proteins other than albumin e.g. globulin.

Utilising all this information, following the example of commercial analysers [12-14], it was considered advisable to use a cellophane dialysis membrane, integrated in to the flow cell, to separate the ISFET sensing membrane from the sample solution. The dialysis membrane, thereby, avoids sterilisation problems associated with protein and anti-coagulant adhesion on the FET.

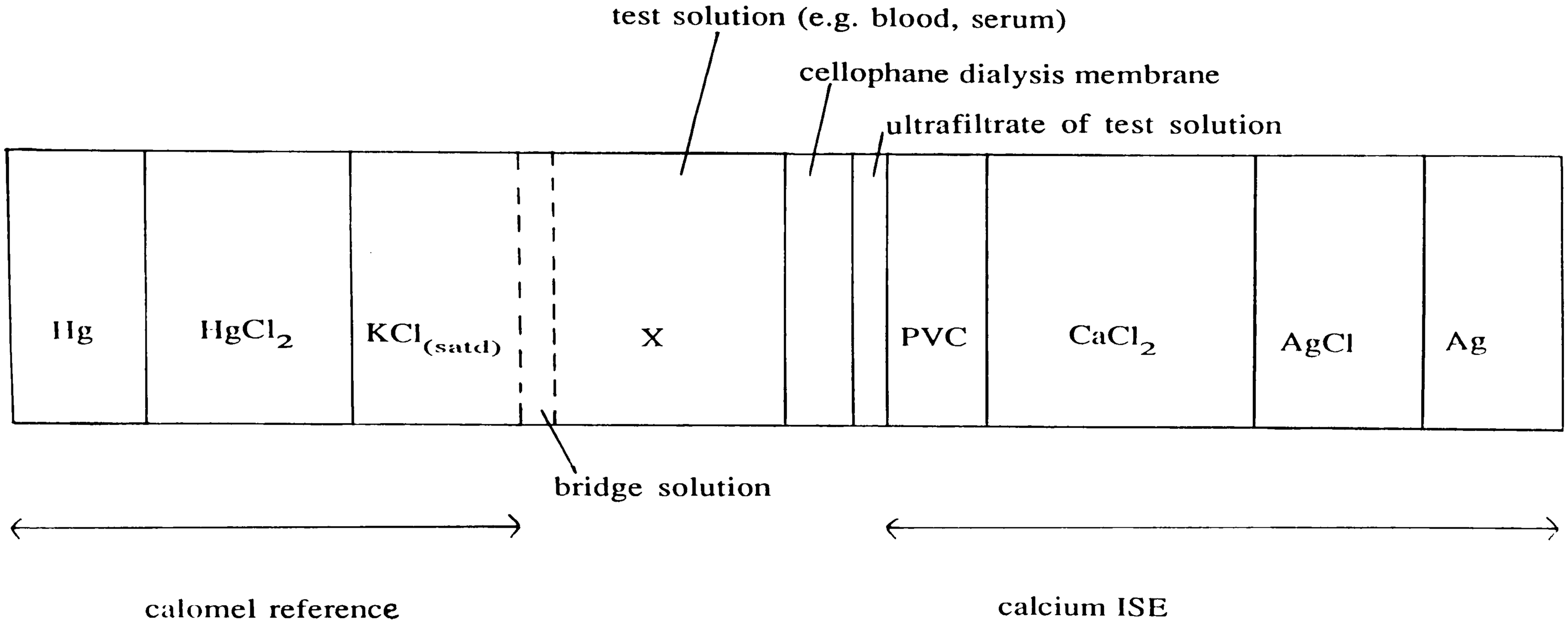

Figure 6:3 Schematic of the Electrochemical Cell with Cellophane Dialysis Membrane (Calcium ISE *versus* Calomal Reference Electrode).

Calibration solutions for the examination of biological samples should contain protein, thus resembling the sample as closely as possible.

6.7 Sterilization Techniques.

It is important that all devices and solutions are sterilised when making measurements in-vivo; migration of species can occur opposed to the flow of the system.

6.7.1 Autoclaving.

Autoclaving, the application of saturated steam under pressure has been used to sterilise ISEs, buffers and calibration solutions [38]. This method is inexpensive and easy to control.

6.7.2 Chemical Methods.

Chemical methods of sterilisation are also possible, e.g. gluteraldeyde due to its wide biocide activity. This has been used for sterilising PVC / potassium ISEs [39] but there is the danger of compromising the response of ISFETs. Gluteraldehyde is most often used to sterilise metallic and plastic objects, however, its use is now restricted for operator health reasons.

6.7.3 Cold Gas Method.

Ethylene dioxide gas, a cold method, can be used as a sterilising reagent, but again this can affect the behaviour of the ISFET. Ethylene dioxide can react with water in the membrane to produce toxic ethylene glycol, which reacts with hydrochloric acid to produce chlorohydrin, a suspected mutagen [40].

6.7.4 Irradiation.

Irradiation is also incompatible with ISFET sterilization, as this compromises the device performance by altering the crystal lattice defects [38].

The ISFET group in Newcastle has used chlorohexidene in alcohol and observed no detrimental effects [41]. For this work, however, autoclaving is recommended as a suitable means of sterilization.

6.8 Ion Selective Membrane.

When ISEs or ISFETs are placed in samples, e.g. whole blood, plasma, which have lipophilic character (e.g. proteins), favourable extraction of lipophilic membrane components, possessing only a moderate mobility, will occur, giving rise to a shift in E_o.

Oesch *et al.* [42] suggested that in experiments where the membrane is in contact with a flowing solution of blood serum, the lipophilicity, P (defined as the partition coefficient between water and octan-1-ol) [43], of the plasticizer should be at least 12.8. Simon's group used two new plasticizers, a benzophenone (ETH 2041) and a benzohydrol (ETH 2112) both of which have high lipophilicity due to their long alkyl chains (figure 6:4) which decrease mobility and restrict diffusion of valinomycin in the membrane [44]. An added advantage of these plasticizers is their favourable adhesion to PVC and silicon substrates making them particularly suitable for use with ISFETs. These components are also believed to be carbon dioxide impermeable. This has an important consequence for blood analyses. The buffering action in blood plasma is controlled by $NaHCO_3 \setminus H_2CO_3$ and $NaH_2PO_4 \setminus NaHPO_4$. Although, as stated earlier, haemoglobin is a better buffer, the action of these buffering systems is also important.

ETH 2041 (tetra-n-undecyl 3,3',4,4'-benzophenone tetracarboxylate) and DOS (bis (2-ethylhexyl) sebacate) plasticizers were used and their performances compared. Valinomycin was used as the ionophore.

All percentage compositions were by weight. The components were dissolved in freshly dissolved THF and well shaken.

Membrane Component		% Reagent
Valinomycin	Ionophore	1.02
High molecular weight Poly (vinyl chloride)	'Inert' matrix	32.22
ETH-2041 or DOS	Plasticizer	66.76

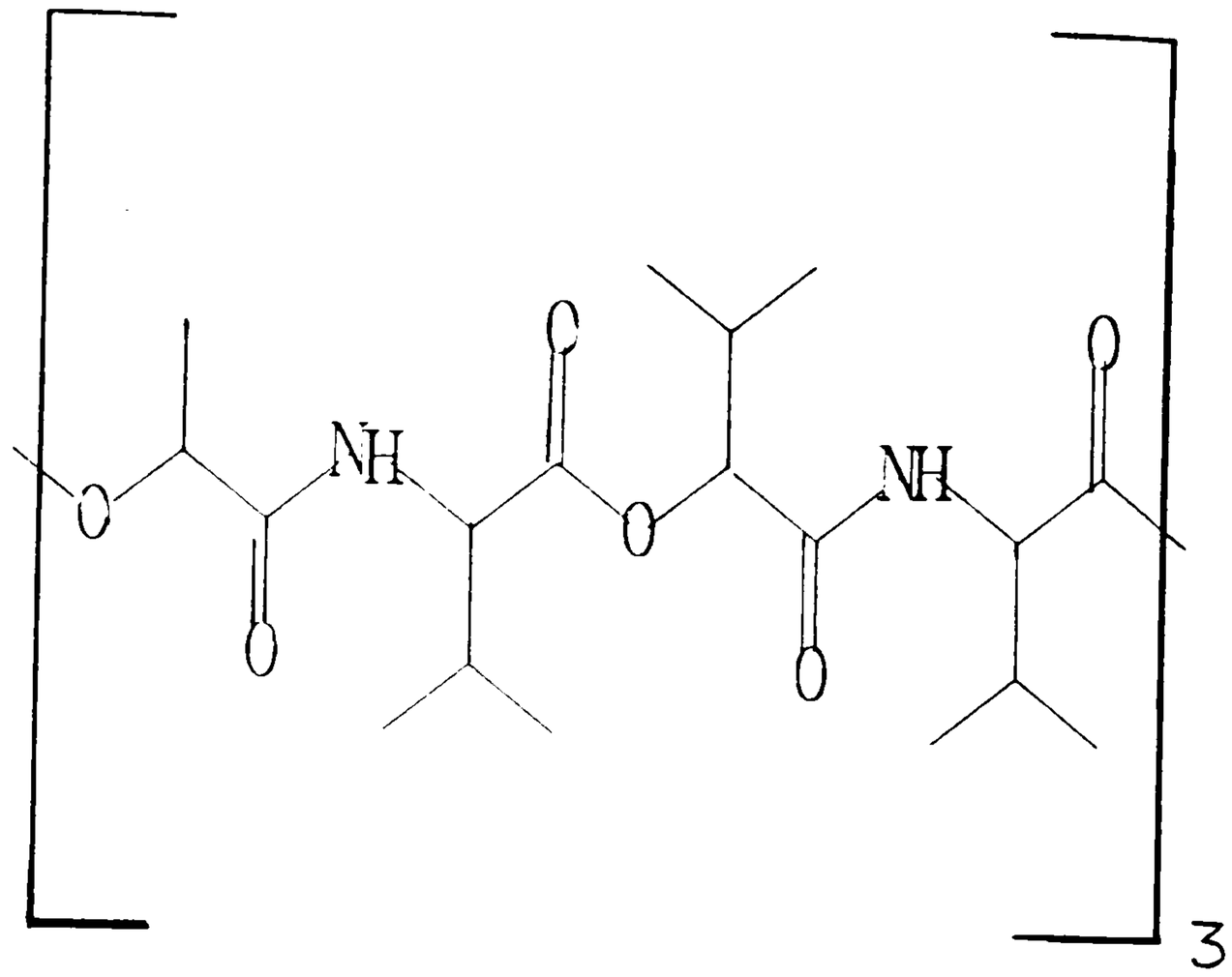

i) Valinomycin

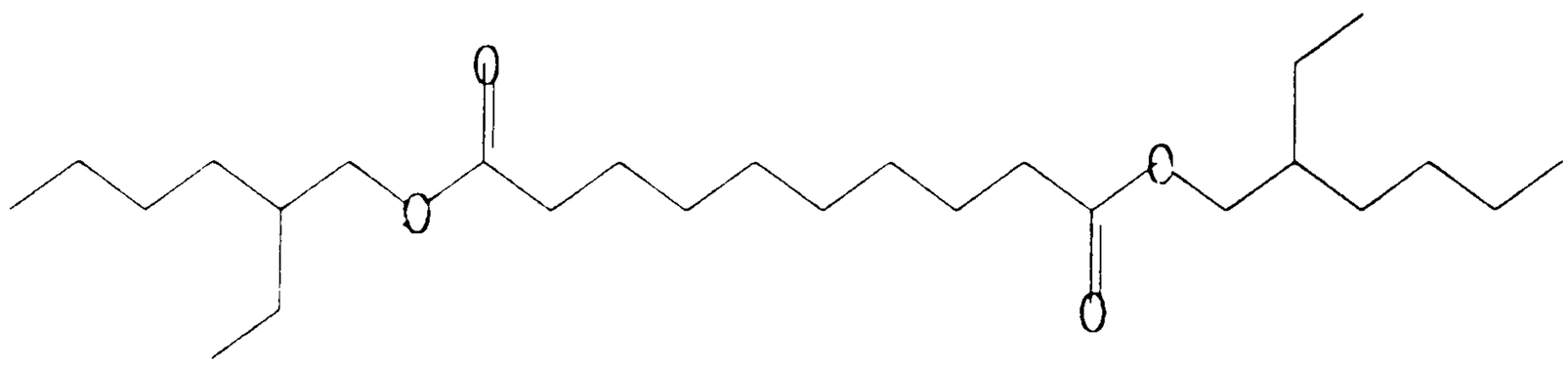

ii) bis (2-ethylhexyl) sebacate (DOS)

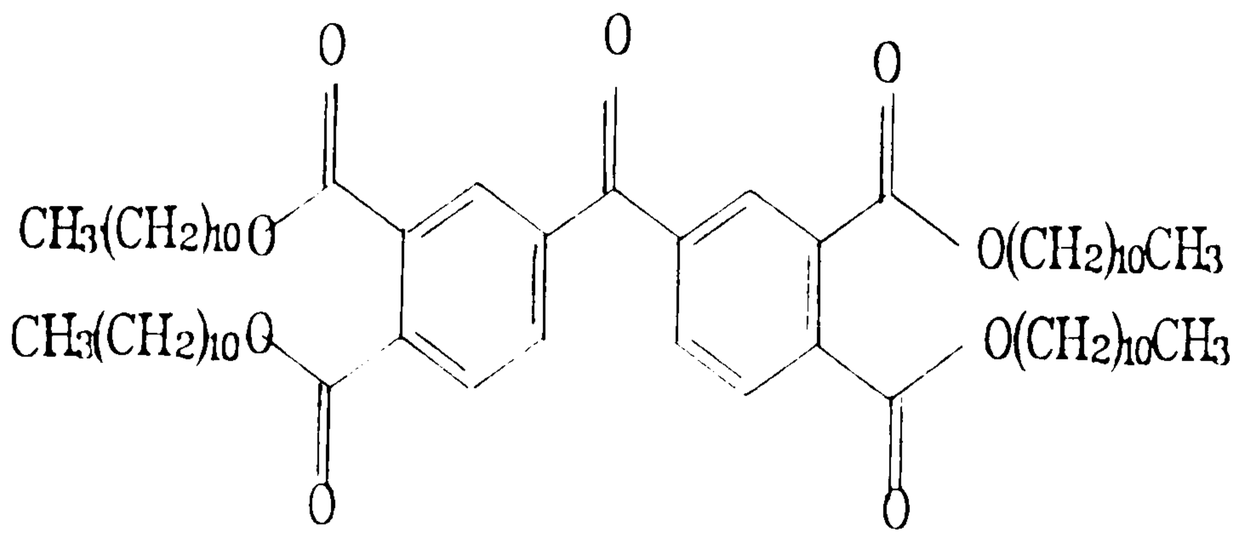

iii) tetra-n-undecyl 3,3',4,4'-benzophenone tetracarboxylate

(ETH 2041)

Figure 6:4 Potassium Selective PVC Membrane Components.

All reagents were specific for use in ISE work and supplied by Fluka Chemicals Ltd.

Before setting down the membranes, the ISFETs were thoroughly cleaned, as described in Chapter 2. It was found that the best method of depositing membranes was using the end of a plastic disposible pipette tip cut off at an oblique angle to form a shallow scoop. This tip was then dipped into the THF membrane solution and the solution could be deposited easily over the gate by tilting the scoop. This method is preferable to earlier membrane deposition techniques which used a disposable glass pipette. There were two main disadvantages of the latter method;

i) the dissolved membrane solution adhered to the sides of the pipette

ii) air bubbles were introduced to the membrane solution, which remained in the membrane on drying, obscuring the gate region.

It is now believed that several devices were discarded early on in the Nerwcastle ISFET project due to the second of these disadvantages, therefore in this work all devices were tested to ensure they functioned before and after membrane deposition. Also, after membrane deposition, devices were examined closely under a microscope to ensure no air bubbles obscured the gate region.

If air bubbles were found to be present, or if a new membrane was to be deposited on a device, the PVC membrane membrane was removed by easing the edges of the membrane from the chip using a scalpel then peeling the membrane from the device with fine tweezers. The device was then washed as before before deposition of a fresh membrane.

6.9 Calibration of Sensors.

The membranes were calibrated using the dip method with solutions in the range 10^{-1} to 10^{-5} mol dm^{-3} potassium chloride and also using the constant volume dilution method using a flow rate of 3.58 ml min^{-1} and a dilution vessel of 38.37 ml with a dilution vessel of 38.37 ml and a flow

rate of 3.58 ml min^{-1}. The results are shown in figures 6:5 - 6:8.

The selectivity coefficients, k_{ij}, of both membranes (ETH 2041 and DOS) were determined for calcium and pH using the constant volume dilution method.

6.10 The ChemFET Device.

6.10.1 Preliminary Tests.

All devices were packaged in 16 pin d.i.l. headers and prior to setting down the membranes the following tests were carried out.

The characteristics (i.e. I_D / V_{REF}) of the devices were determined, this was in order to observe the working range of the ISFETs. A typical characteristics plot is shown in figure 6:9. For comparison, since Bellhouse ultimately wished to extend the work to OPTRAN usage, the characteristics of OPTRANs, Eμ-358A, were identified. A plot is shown in figure 6:10. In this case, the bias voltage *versus* output voltage was recorded and the "switch on" potential noted.

The devices were also tested to ensure that none was liable to electrical leakage by connecting together the drain, source and substrate of the ISFET and polarizing from -3 V to +3 V against a low resistance (< 100 KΩ) reference electrode. No leakage current should be observed as the bias potential is increased. Any device with a leakage current greater than 1 nA was rejected. The characteristics of a leaky device are shown in figure 6:11. These experiments were repeated when the potassium membrane was set down.

Having satisfied this criteria, the drift, noise and optical sensitivity of the devices were determined. Between tests, ISFETs were stored with calibration solution (usually 10^{-2} mol dm^{-3} potassium chloride) over the membrane to prevent it drying out, and placed in specially designed electrostatic-free boxes (RS Components).

6.10.2 Optical Sensitivity.

Light on a reverse-biased p-n junction (here an ISFET) leads to the

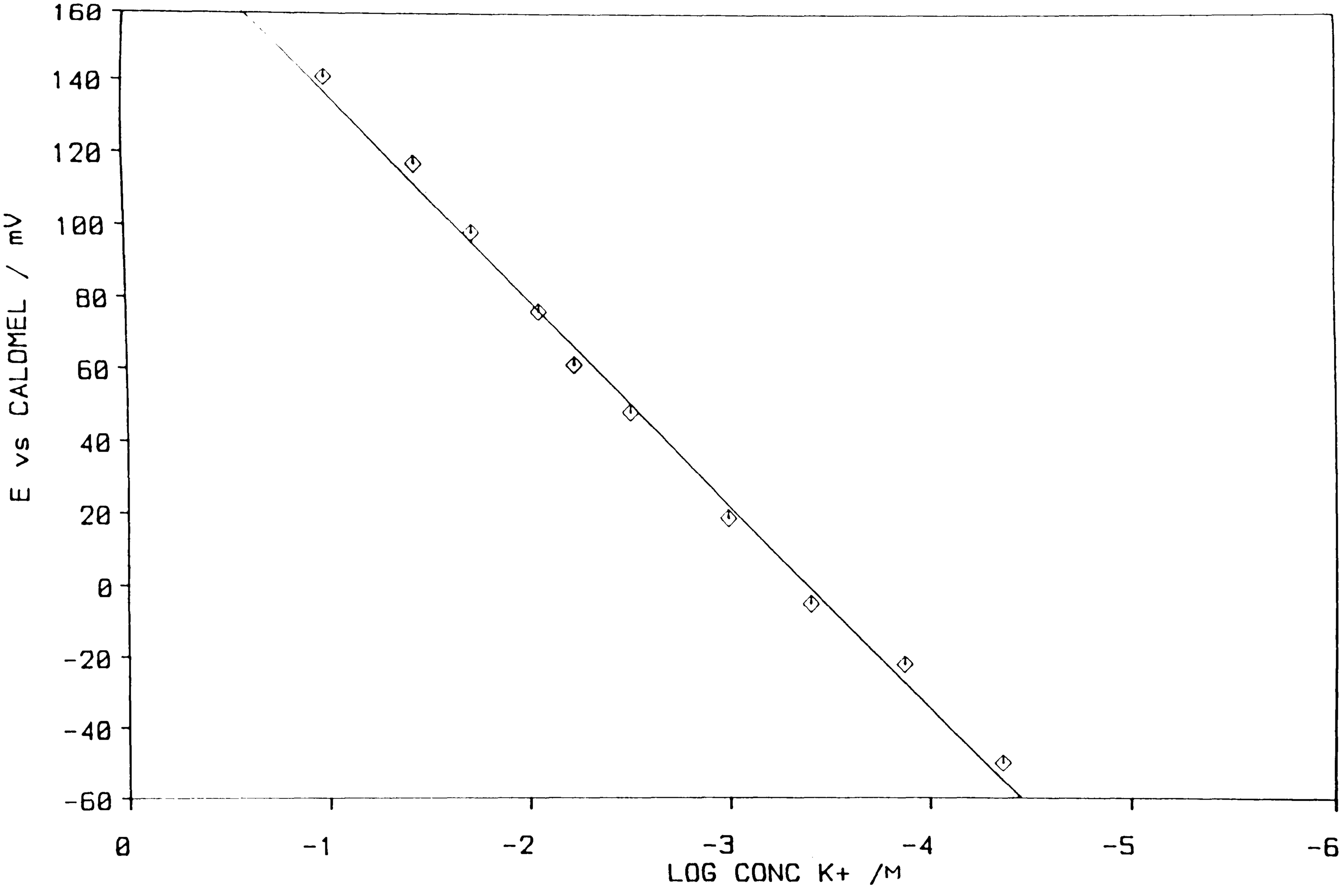

Figure 6:5 Calibration Curve of DOS-type Membrane using the CVD Method.

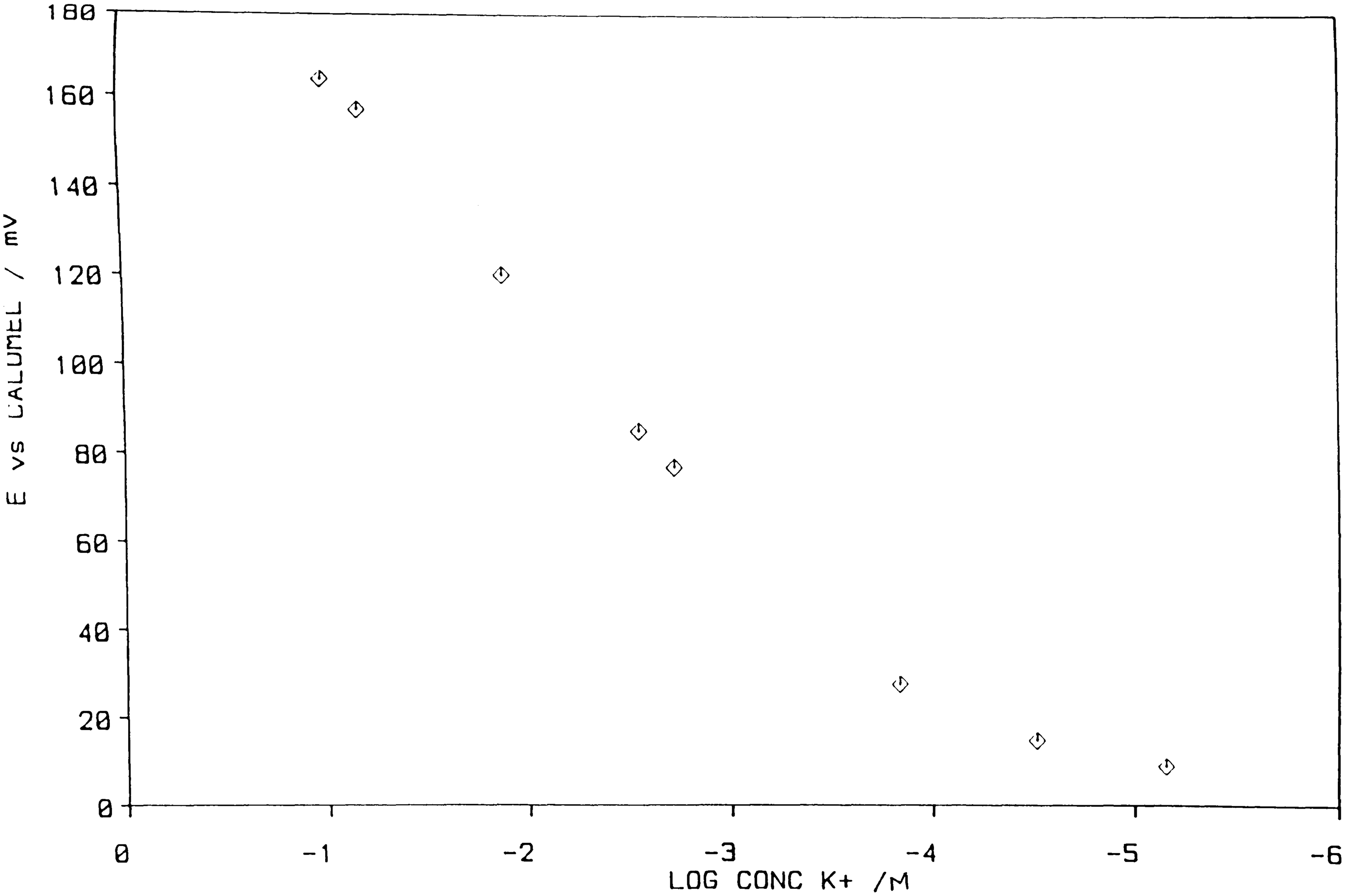

Figure 6:6 Calibration Curve of the ETH 2041-type Membrane using the CVD Method.

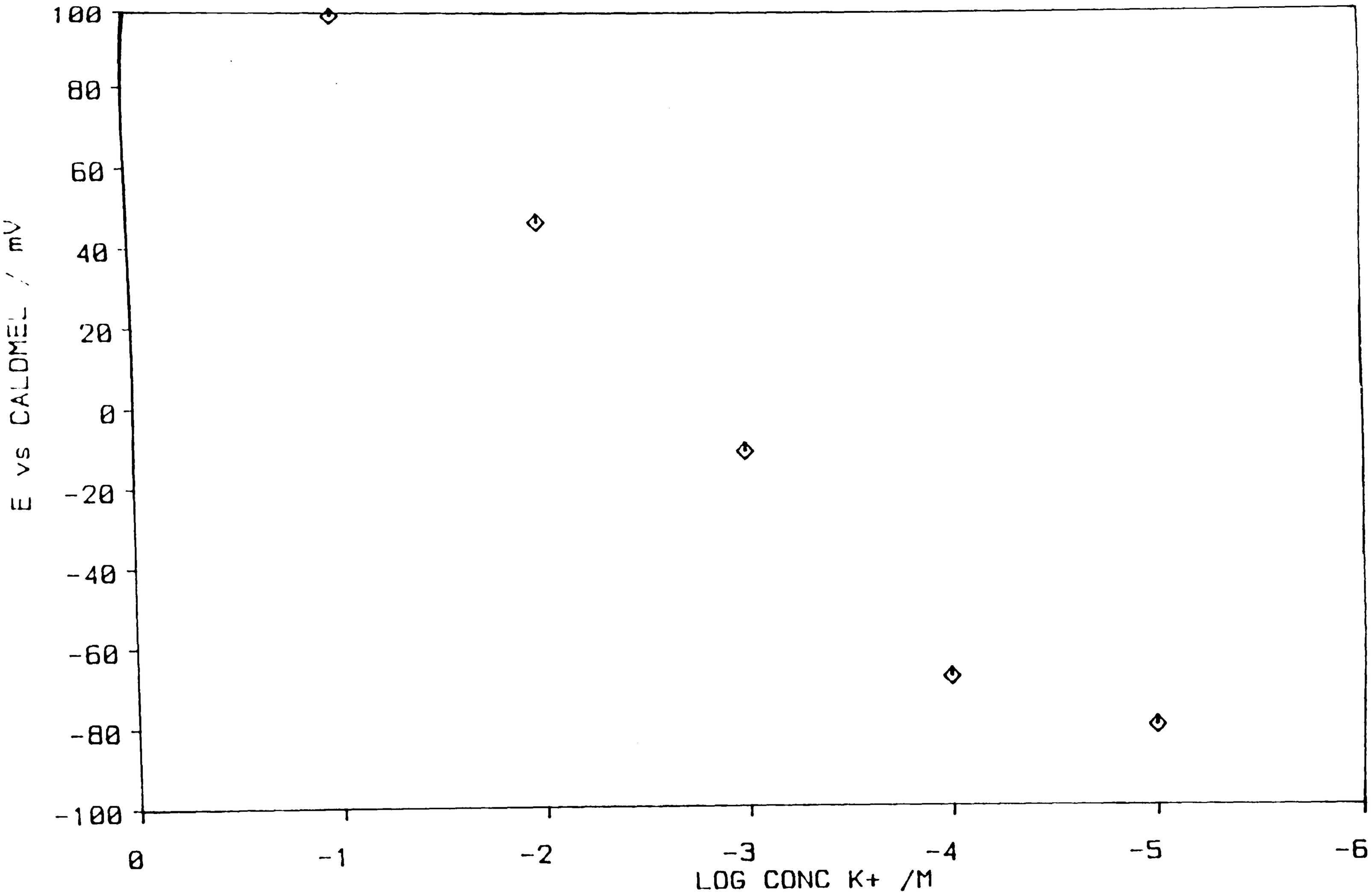

Figure 6:7 Calibration Curve of the DOS-type Membrane using the Dip Method.

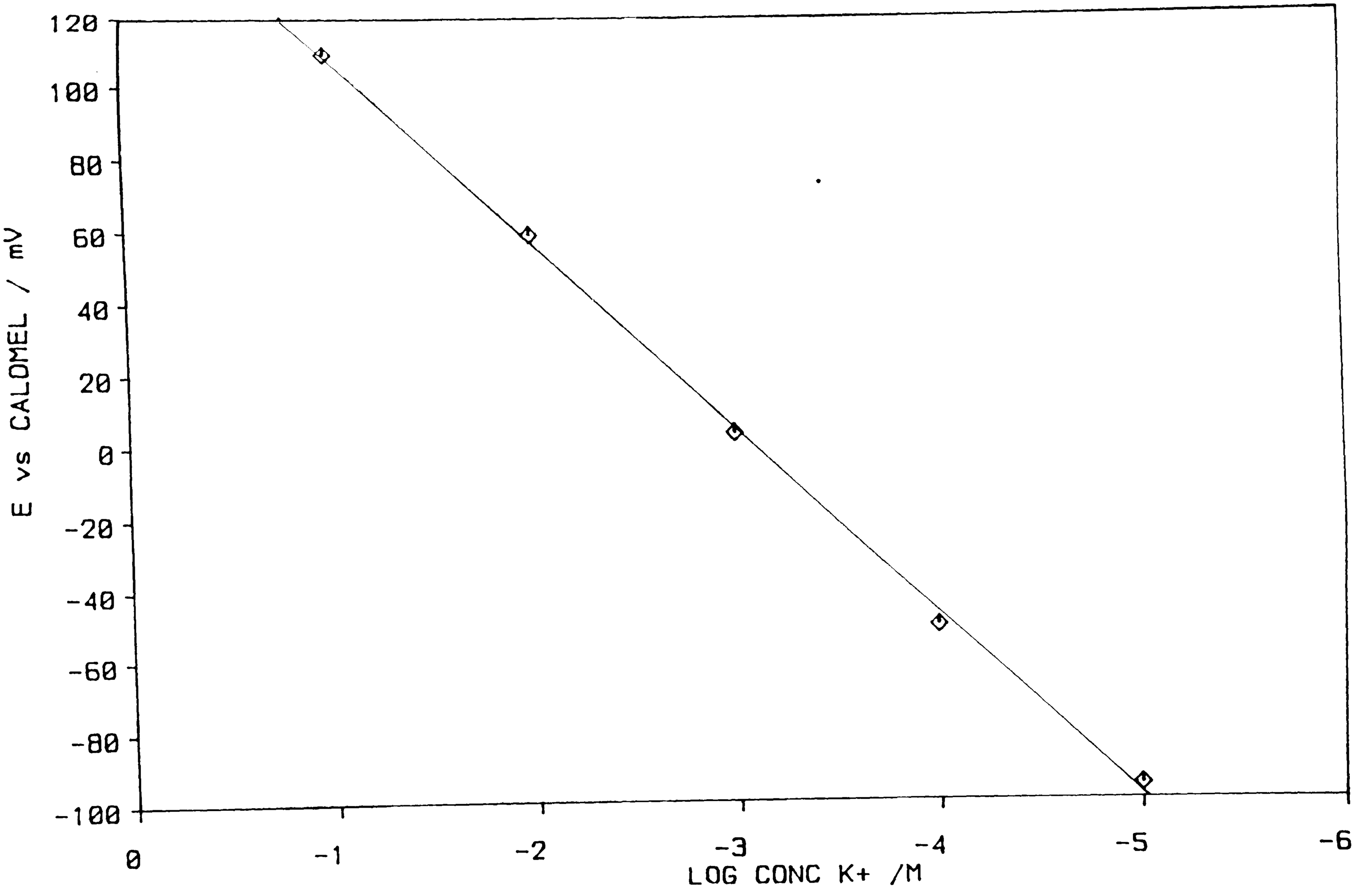

Figure 6:8 Calibration Curve of the ETH 2041-type Membrane using the Dip Method.

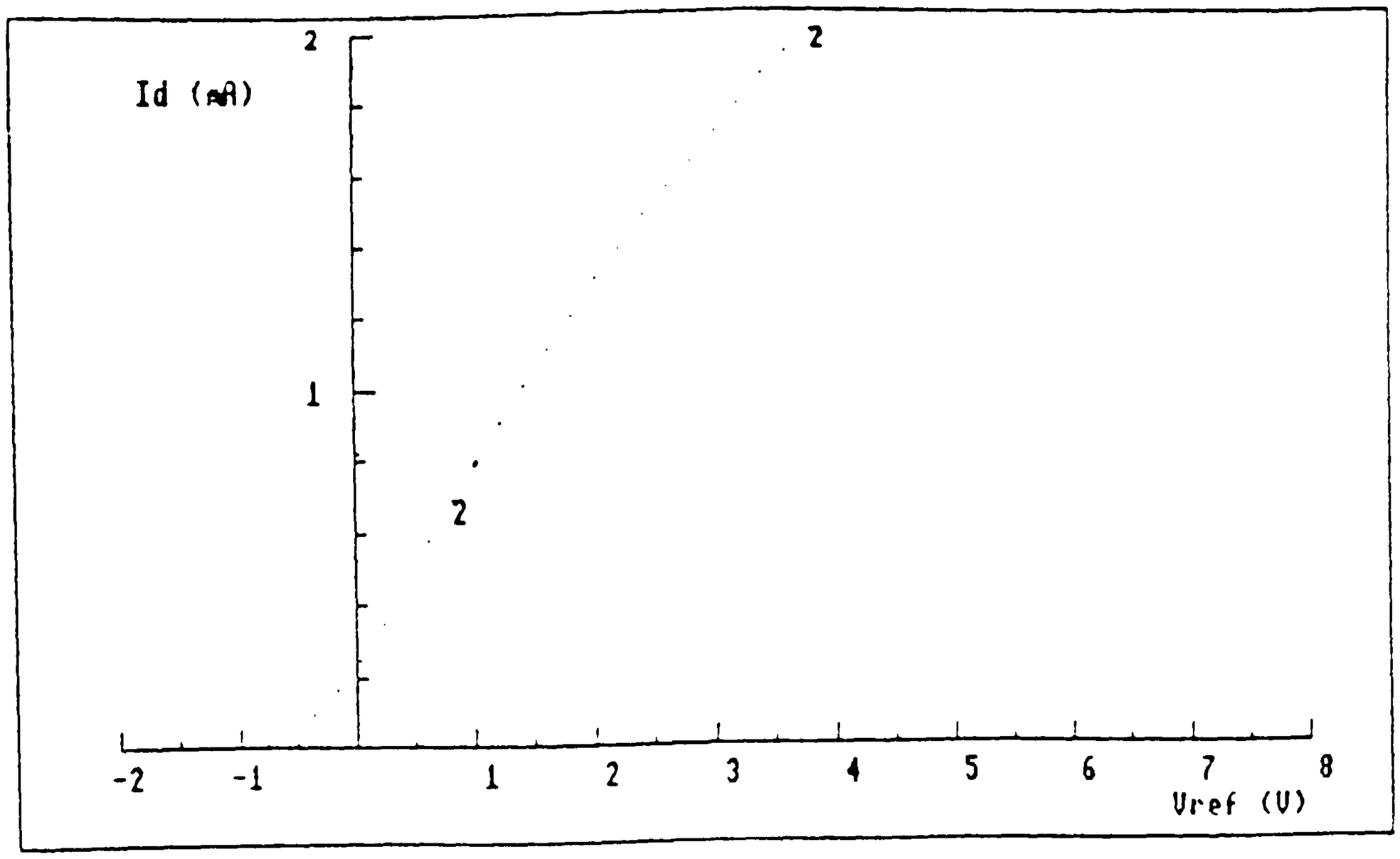

Figure 6:9 Characteristics Plot (I_D / V_{REF}) for a Potassium Selective Eμ-146 Device.

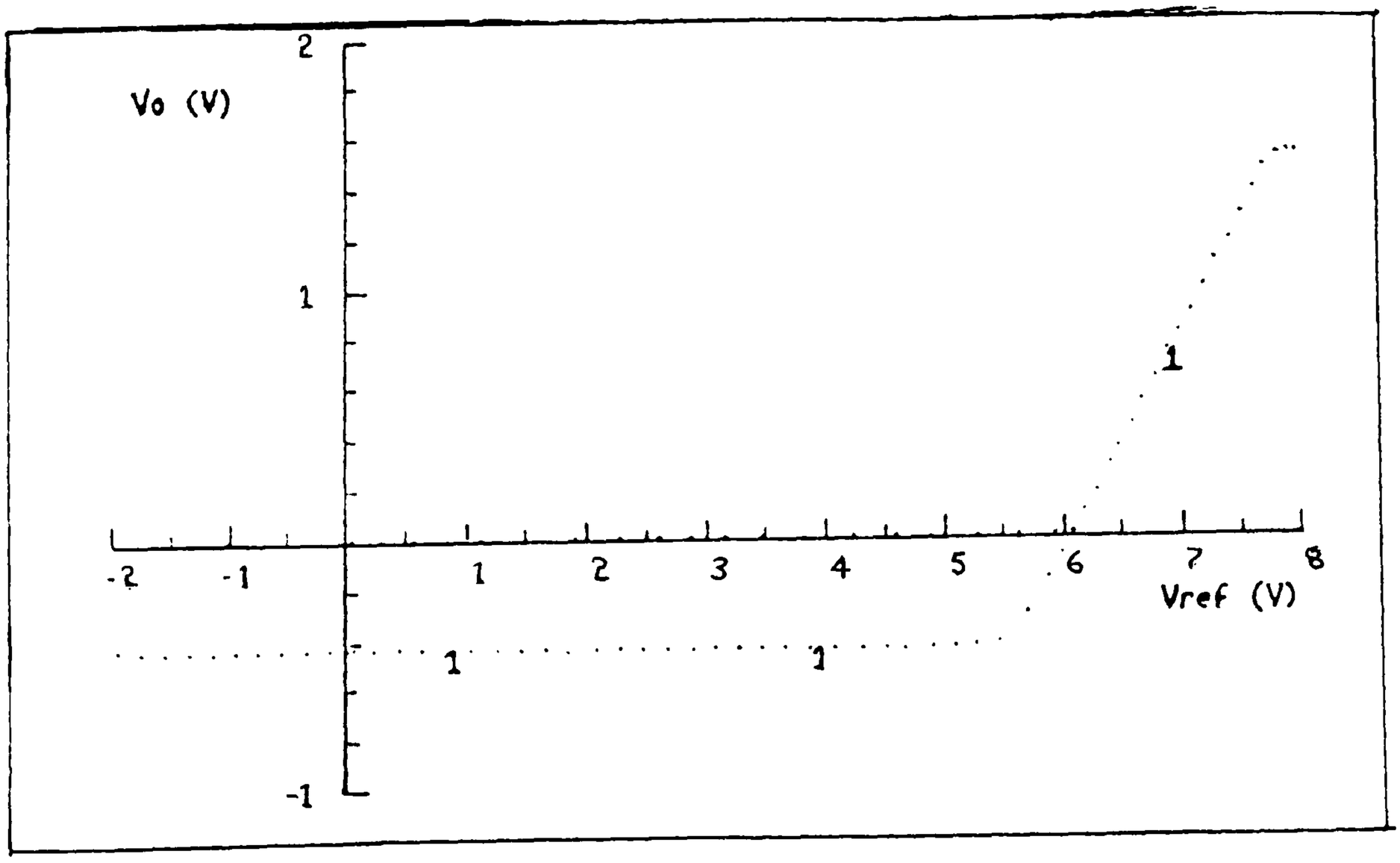

Figure 6:10 Characteristics Plot (Bias Voltage *versus* Output Voltage) for an OPTRAN, Eμ-358A.

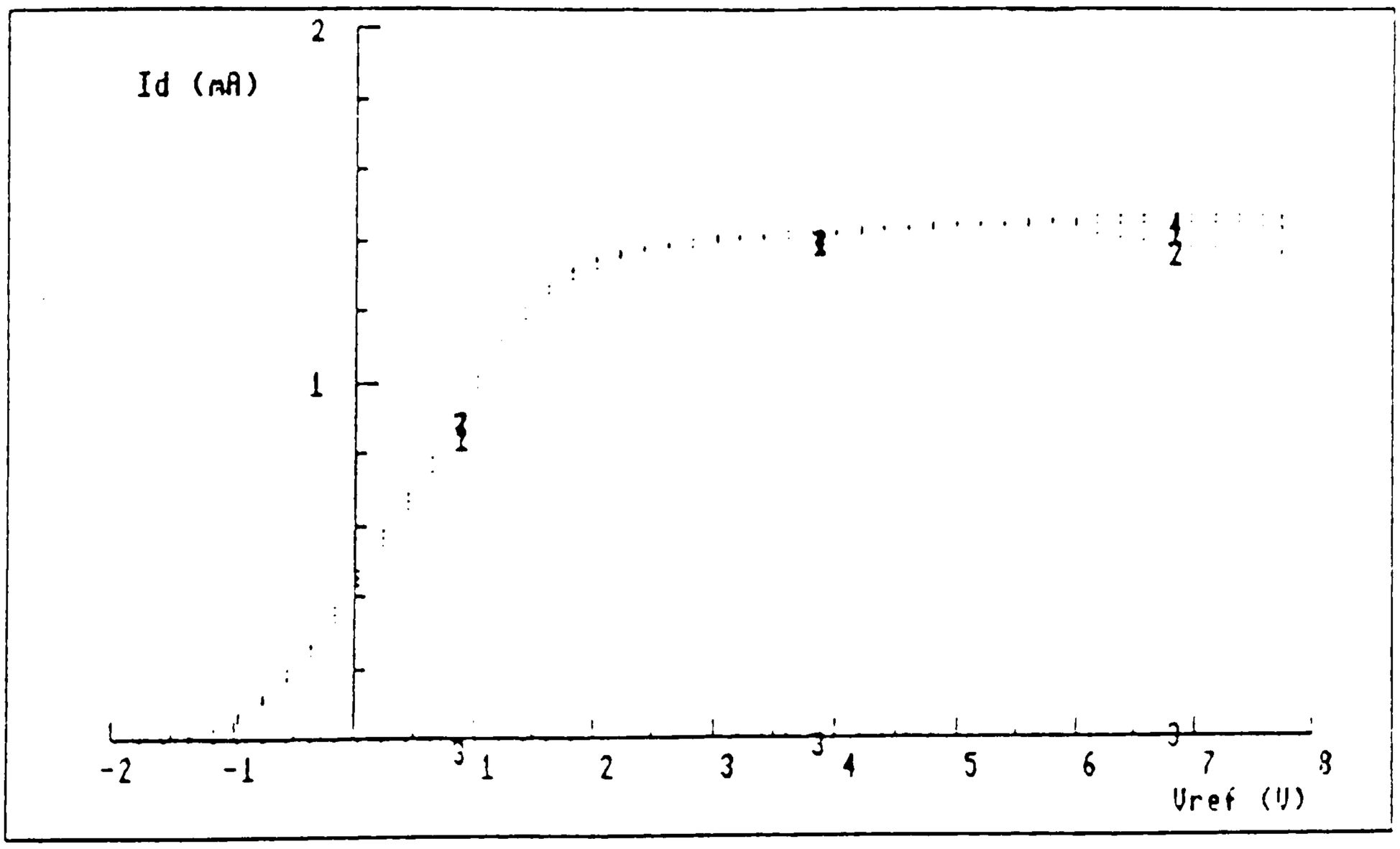

Figure 6:11 Characteristics of a Leaky Eμ-146 Device.

generation of electrons [45]. In the case of an ISFET, these are driven by the source to drain voltage and are therefore summed into the drain current, so that overall an increase in the drain current is observed. Sibbald [46] observed, typically 3 mV optical sensitivity at constant drain current.

It has been suggested that the use of opaque flow caps or opaque membranes could be used to reduce light sensitivity [46]; only preliminary tests were carried out by Sibbald, this should be further examined.

The characteristics and drift of the devices were determined under normal laboratory conditions (daylight and fluorescent strip lighting), complete darkness and with intense (100 w) light supplied by an overhead lamp shining directly on to the gate of the i.c. device.

6.10.3 Thermal Sensitivity.

This was discussed in Chapter Three, but it is reiterated that the two major affects of temperature are

i) to affect the threshold voltage, V_T, due to changes in the contact potential between the solution and the semi-conductor bulk material

ii) to influence the relationship between I_D / V_G due to a change in mobility of the charge carriers.

6.10.4 Electrostatic Damage.

An account of problems associated with electrostatic charging was given in the previous chapter. A wrist grounding strap was worn at all times when handling the devices. Although UV irradiation may return V_T to its original value, it is obviously better that this treatment is not necessary.

6.11 Assembly of the Bellhouse Flow Cell.

The ISFET was sealed into the perspex holder, incorporating the dialysis membrane and seal, using silicone rubber requiring 12 h curing. This assembly was then screwed into the main body of the cell. This was

then connected via thin, flexible PVC tubing to the sample and the peristaltic pump. This cell was designed for use with Bellhouse's vortex mixing system.

6.12 Results and Discussion.

6.12.1 Membrane Studies.

Membranes were prepared as described by Griffiths, Moody and Thomas [47] from the cast membrane solution, and the behaviour of these membranes was investigated. It was found that the DOS membrane showed good Nernst response in both dip tests and constant volume dilution calibrations (55.68 mV dec $^{-1}$, 57.31 mV dec $^{-1}$ respectively), whereas the ETH 2041 membrane showed sub-Nernstian responses using both calibration methods, this was most marked for the constant volume dilution calibration (see Table 6:1).

Table 6:1 Results of Potassium Ion Calibration Studies.

	Slope mV dec $^{-1}$	
Plasticizer;	DOS	ETH 2041
Calibration Method		
Dip Test	55.68	51.98
Constant Volume Dilution	57.31	48.84

The working range of the membranes extended to 10^{-4} mol dm^{-3} for ETH 2041 and 4.5 x 10^{-5} mol dm^{-3} for the DOS containing membrane. It would be prudent to repeat experiments with ETH 2041 in order to ascertain that these results were characteristic. Although the response and working range are acceptable, this plasticizer was reported [39] as having better behaviour than was observed here.

The selectivity coefficients, k_{ij}, of the membrane for calcium and hydrogen were determined graphically from results of the mixed solution method of the constant volume dilution technique and are shown in

figures 6:12 - 6:14. The CVD chart recorder traces used to obtain the selectivity coefficients of the DOS membrane are shown in figure 6:15. The values of k_{ij} obtained here are compared in Table 6:2 with the literature values, from a review by Pungor *et al* [48].

Table 6:2 Selectivity Coefficients for Potassium Ions.

	Literature Value				Experimental Value	
					DOS	ETH 2041
Reference	[42]	[47]	[48]	[49]		
$k_{k+,j}$	x 10^{-5}	x 10^{-4}	x 10^{-5}	x 10^{-2}	x 10^{-3}	x 10^{-3}
Na^{+}	7.9	2.0	6.0	6.9	-	-
H^{+}	6.3	-	-	-	32.2	2.83
Ca^{2+}	1.6	1.0	4.9	-	0.44	0.21

It was apparent that both DOS and ETH 2041 membranes were pH sensitive and a shift of 15 mV was noted for both electrodes when immersed in mixed solutions containing 0.1 mol dm^{-3} hydrochloric acid. This was not considered to be a problem for the physiological working range of pH 7. The membranes did not exhibit severe interference by calcium ions, and of the two membranes, the ETH 2041 membrane showed least interference. The experimental selectivity coefficients are, however, slightly higher than the literature values (Table 6:2).

If claims [52] suggesting ETH 2041 is carbon dioxide impermeable are justified, then this plasticizer should replace DOS in potassium membranes for use in plasma and serum studies where changes in pCO_2 can occur [53].

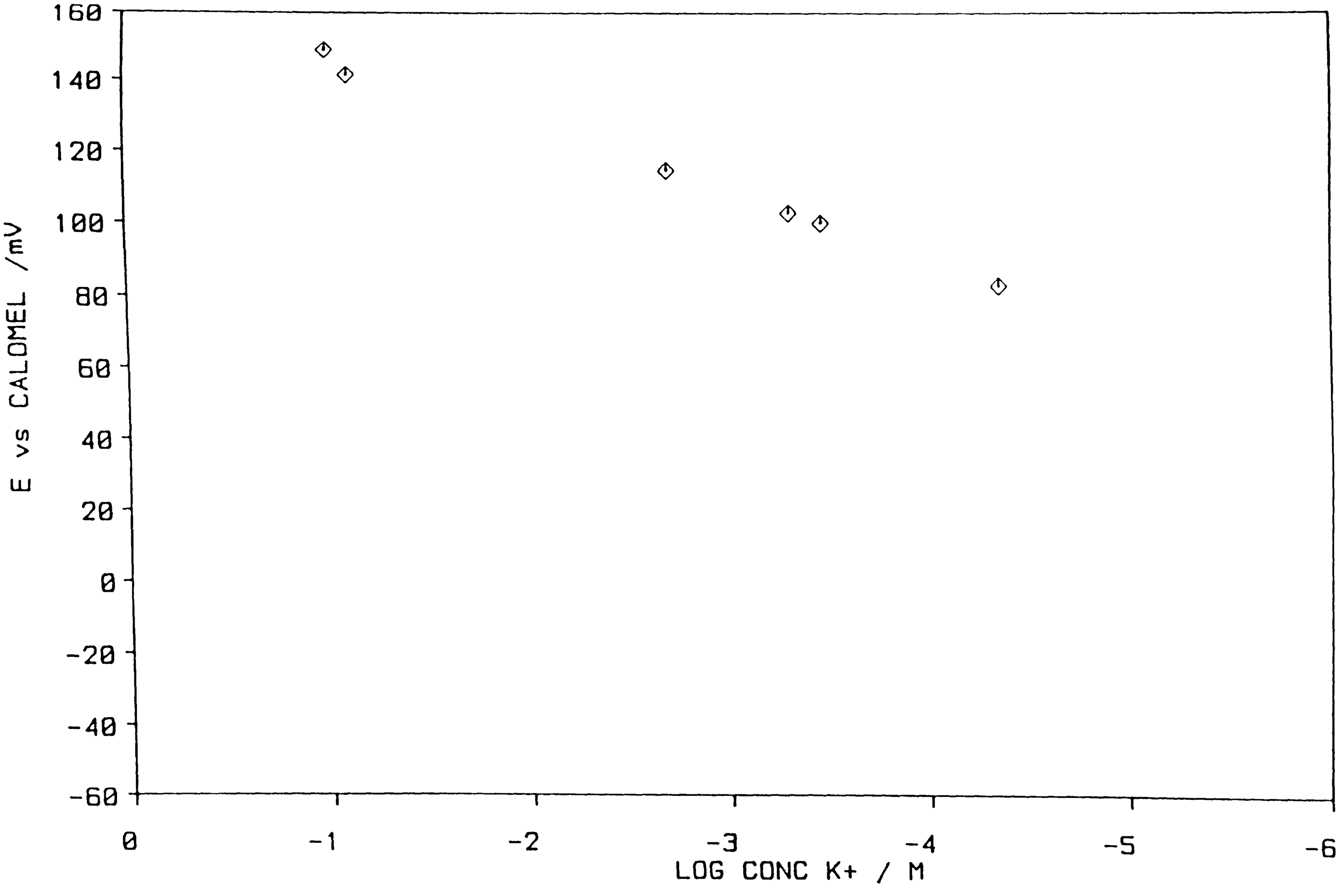

Figure 6:12 To Determine the Selectivity Coefficient, $k_{K+,Ca2+}$, of the DOS Membrane.

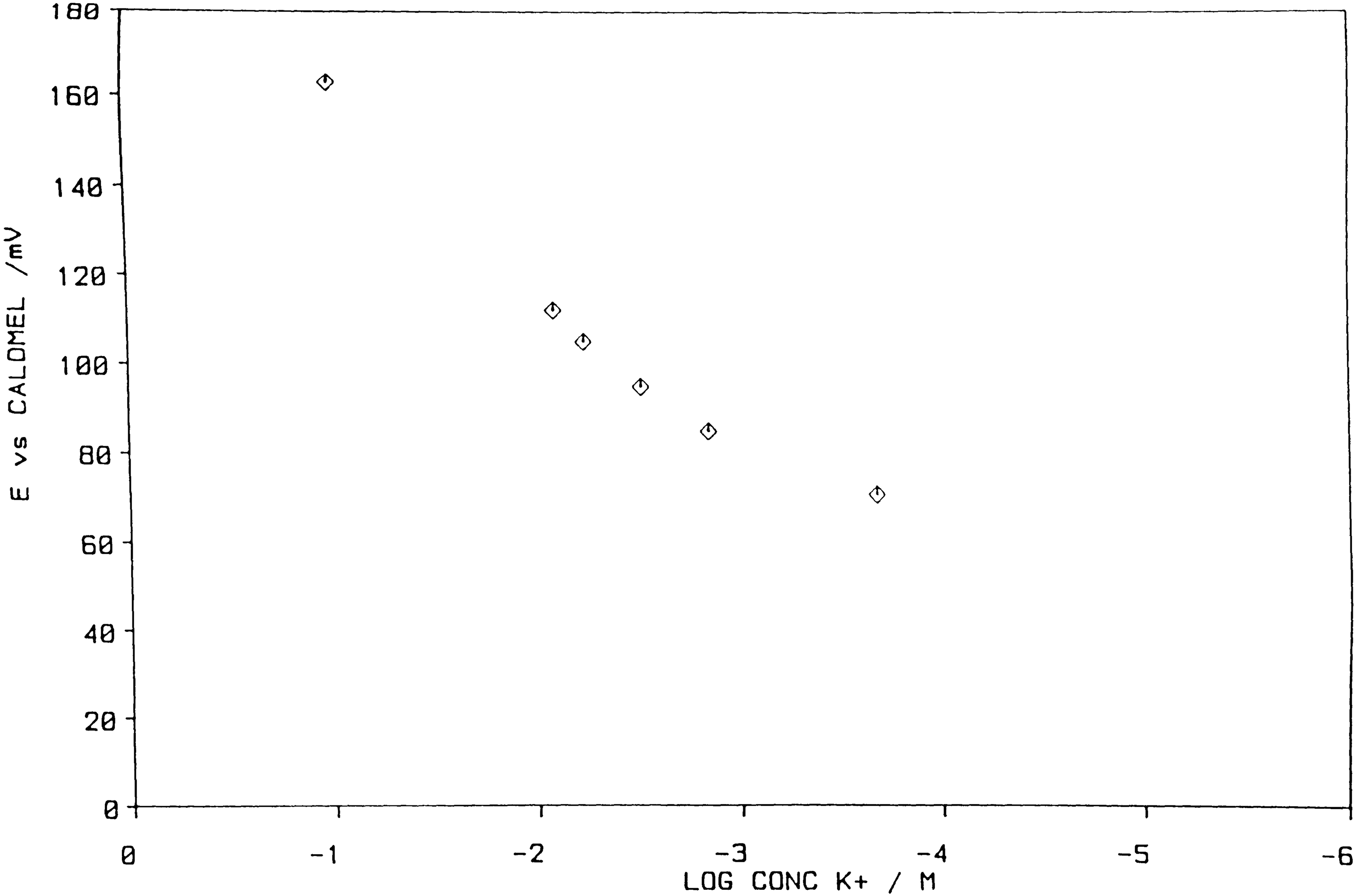

Figure 6:13 To Determine the Selectivity Coefficient, $k_{K+,Ca2+}$, of the ETH 2041 Membrane.

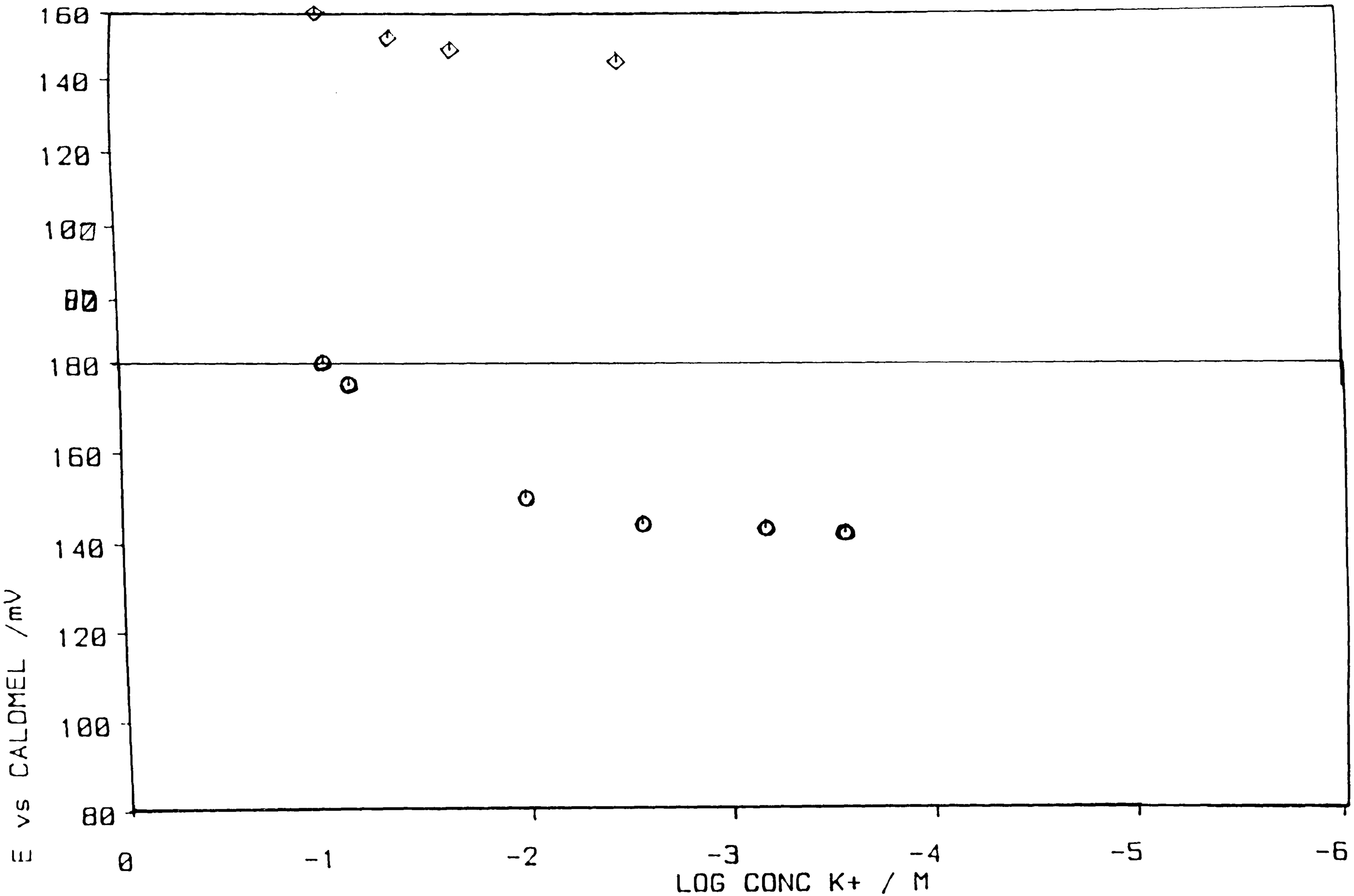

Figure 6:14 To Determine the Selectivity Coefficients, $k_{K+, Ca2+}$, of the DOS and ETH 2041 Membranes.

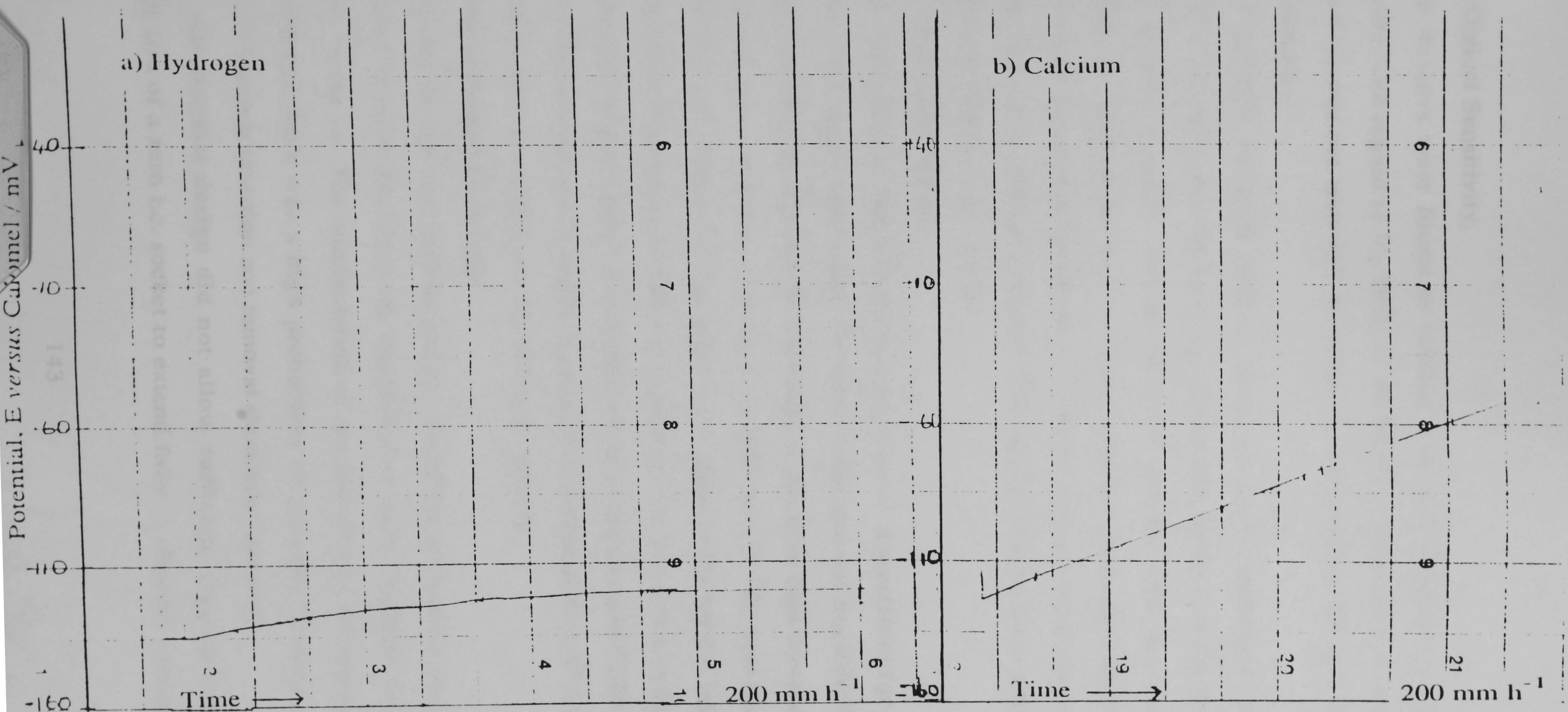

Figure 6:15 To Determine the Selectivity of the K^+ Selective DOS Membrane to Hydrogen and to Calcium Ions.

6.12.2 Optical Sensitivity.

The devices were found to behave well and showed no optical sensitivity with regard to V_T shift. A threshold voltage of -0.5 mV was recorded throughout tests and there was no variation in the I_D / V_{REF} characteristics.

The ISFETs did drift slightly under all light conditions. Initial drifts of + 1.0 mV were recorded for all devices tested, but the ISFETs settled to give a stable voltage, 0.5 mV greater than the starting potential. As this behaviour complies with the drift characteristics suggested by Covington & Sibbald [1], these devices were considered suitable for use in clinical analysis. The characteristics plots obtained are shown in figures 6:16 - 6:18.

6.12.3 Thermal Sensitivity.

The behaviour of the devices as a function of temperature for these devices is not easily monitored. To achieve the thermal insensitivity of non dip-type sensors, it would be necessary to put flow caps down on the devices and pass a solution warmed to, in this case 37 °C, over the gate via the flow cap. However, one must make allowances for the solution cooling whilst flowing, requiring the experiment to take place in an oven thermostatted slightly above the desired temperature (accurately known). This is obviously not easily practical and one could not predict 37 ± 0.1°C and this is only a suitable test for dip type sensors.

6.13 The Bellhouse Flow Cell.

The cell design has obvious pitfalls. Handling of devices should be minimised in order to reduce the likelihood of static charging from the operator to the i.c. The manipulation of the ISFET into the holder was awkward and there was a high probability of physical damage to the devices if frequent insertion and removal should be necessary.

As the original design did not allow sufficient clearance for the locking arm of a zero i.c. socket to extend fully a channel was cut into

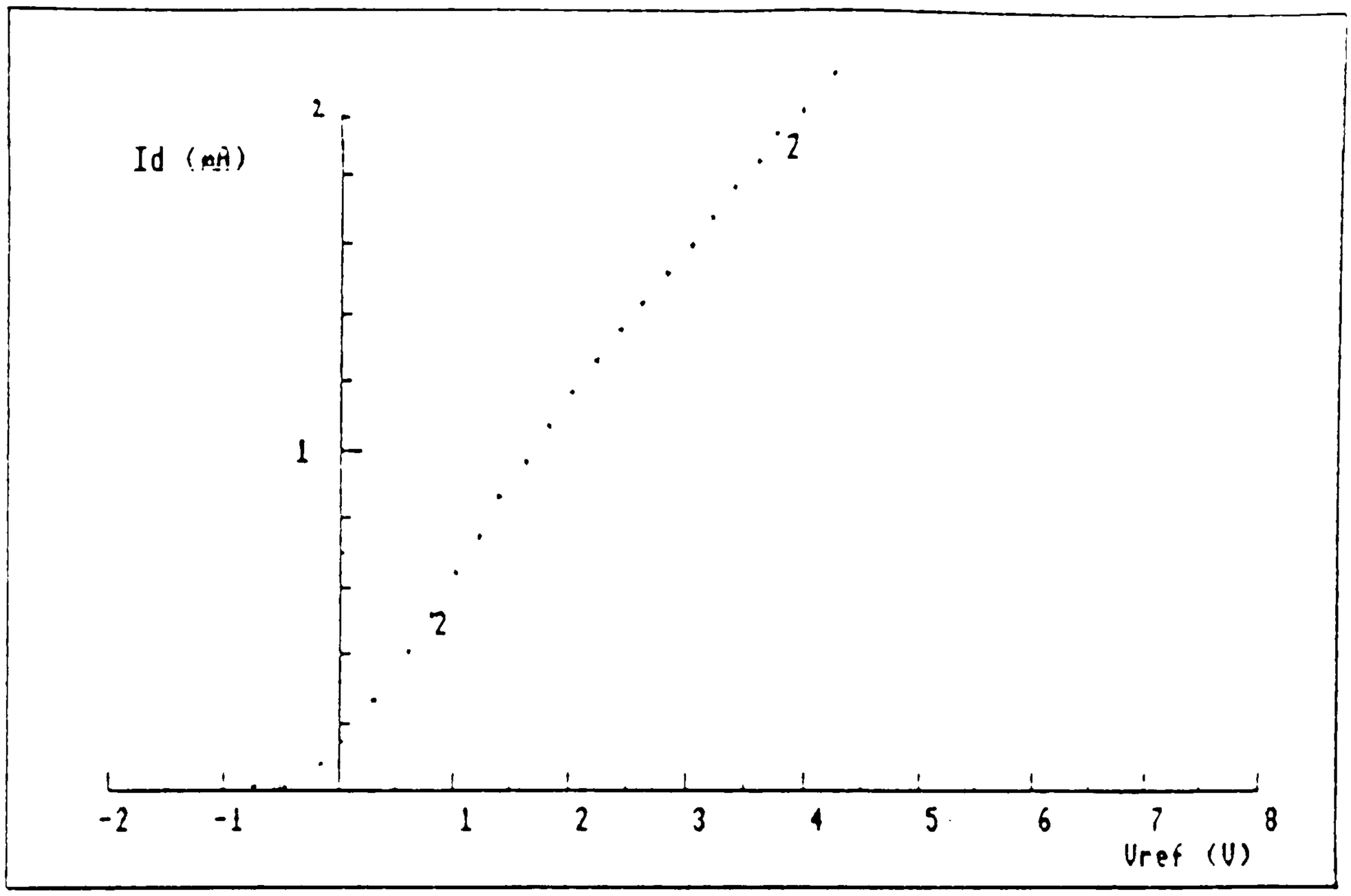

Figure 6:16 Characteristics of an Eμ-146 Device, No Light.

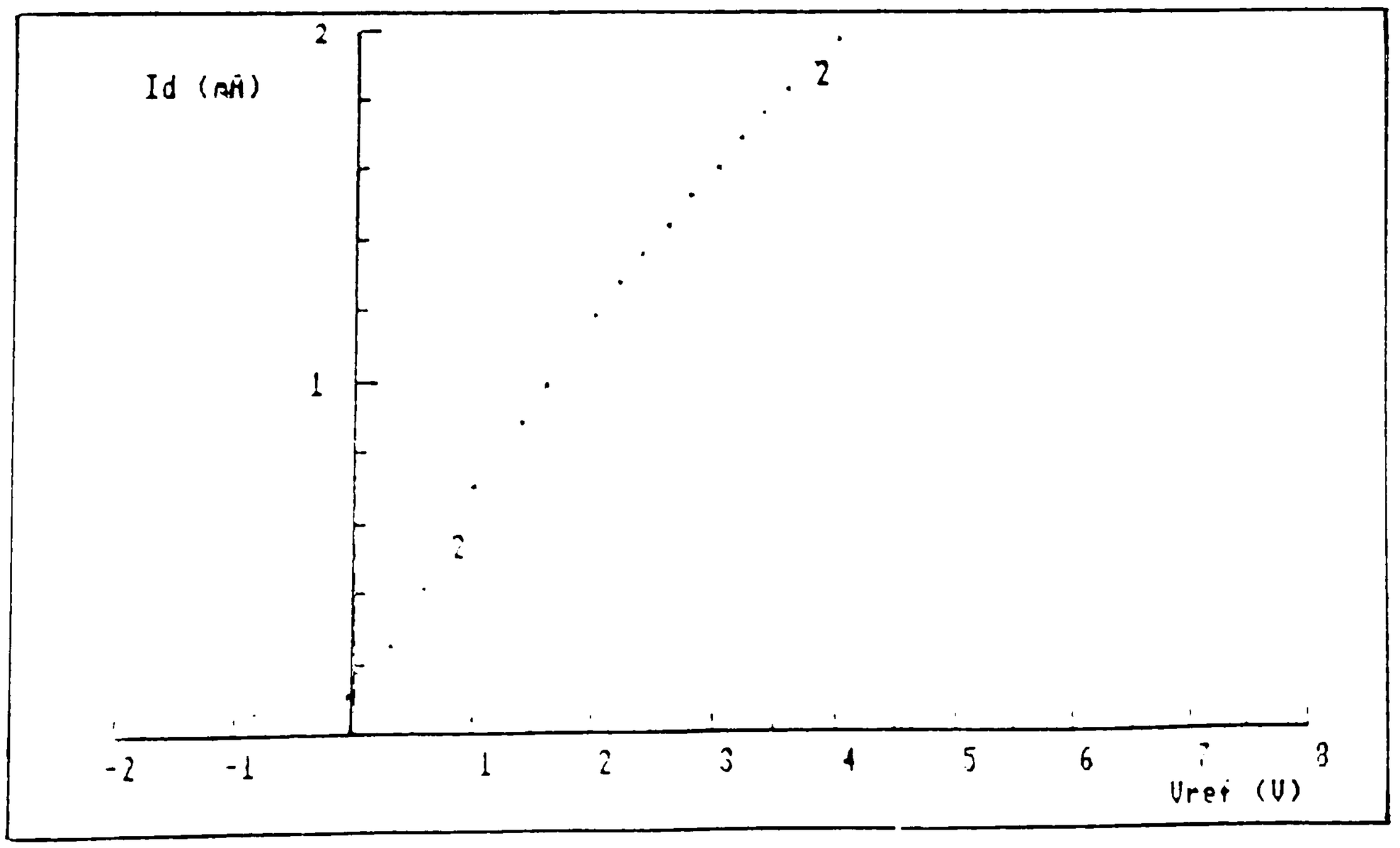

Figure 6:17 Characteristics of an Eμ-146 Device, Intense Light (100 w).

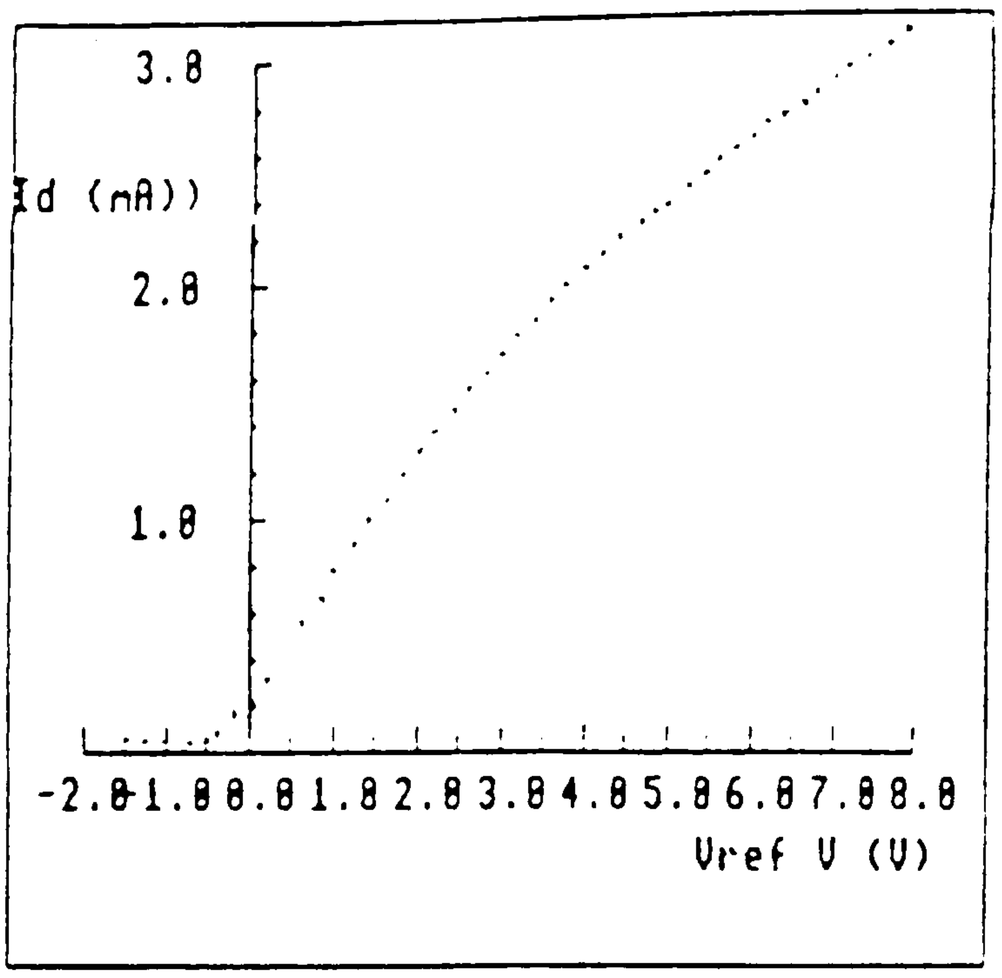

Characteristics

Figure 6:18 Characteristics and Drift of an Eμ-146 Device, Normal Laboratory Conditions.

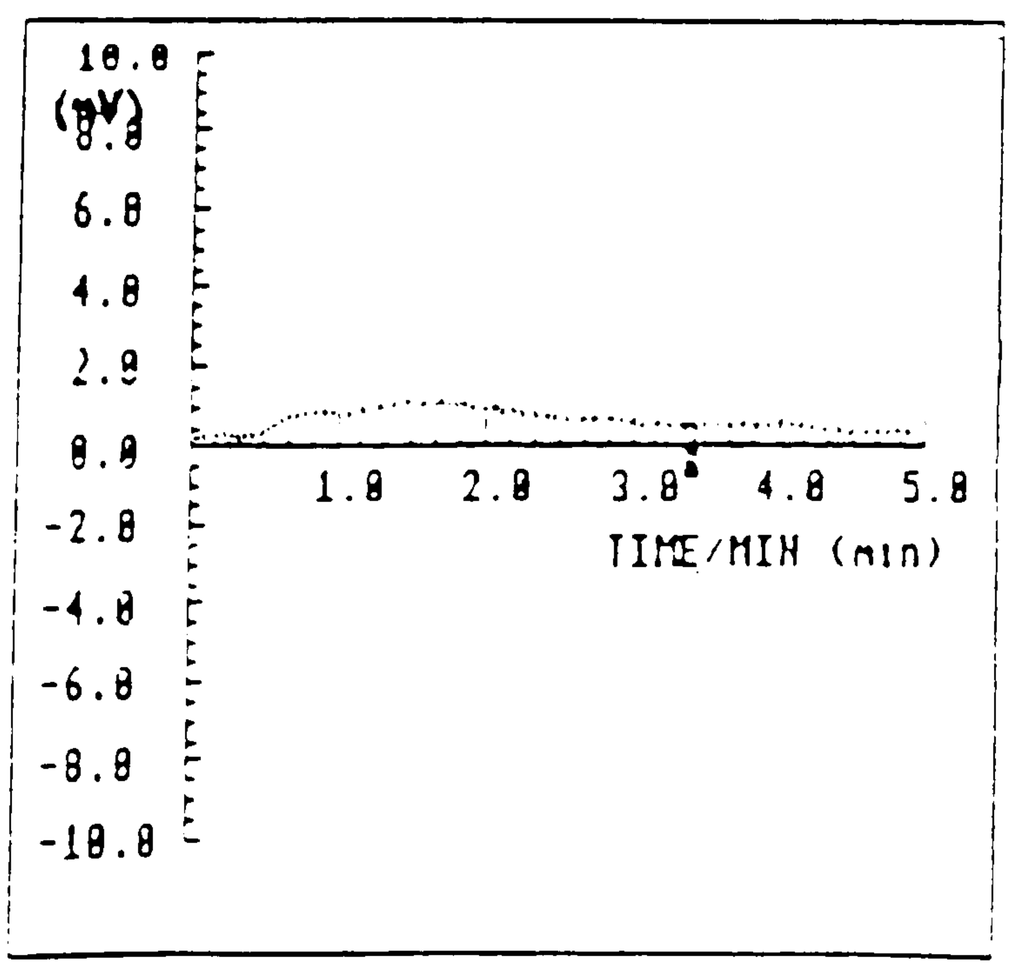

Drift Study

the main body of the flow cell and a small section removed from the FET holder to overcome this problem. Alternative solutions would be to place an extension between the locking arm and the i.c. socket or to replace the zero i.c. socket with a d.i.l. socket.

The most serious flaw in the system is the location of the sealing gasket; in the original design, because of the large recess in the cell for the FET holder, the flowing solution can come into direct contact with the "legs" of the device thereby short-circuiting it. This problem has been overcome by filling the pit around the header with silicon rubber but this must be removed and the cell cleaned thoroughly after each analysis, defeating the object of a simple, reusable cell. A more practical design would be one based on any of the flow caps designed at the University of Newcastle (figure 6:19); only the gate region is exposed to solution. The on-line remote sensor unit [54, 55], built in the Chemistry Department Workshops, University of Newcastle-upon-Tyne, incorporates such a flow cap, and it has been shown, in extensive laboratory tests, to operate well.

It was thought that it might be possible to use the cell (modified) in static experiments and monitor the response of the potassium ChemFET against a calomel reference electrode, when solutions of differing potassium concentrations were placed either side of the dialysis membrane. This was found to be impossible in practice due to the means adopted for fixing the FET-holder into the cell assembly. Once the FET is sealed into position it is not possible to replace the solution of the gate region. Should the ISFET drift, it must be possible to recalibrate in-situ. It is essential to incorporate some sort of serum cap for injection of new solution.

The internal diameter (i.d.) of the flow channel is too large, 16 mm, for a standard peristaltic pump to operate; i.d. values are normally in the region of 1 mm. The large i.d. initially used was to allow interfacing with the vortex mixing system; a design feature which must be considered

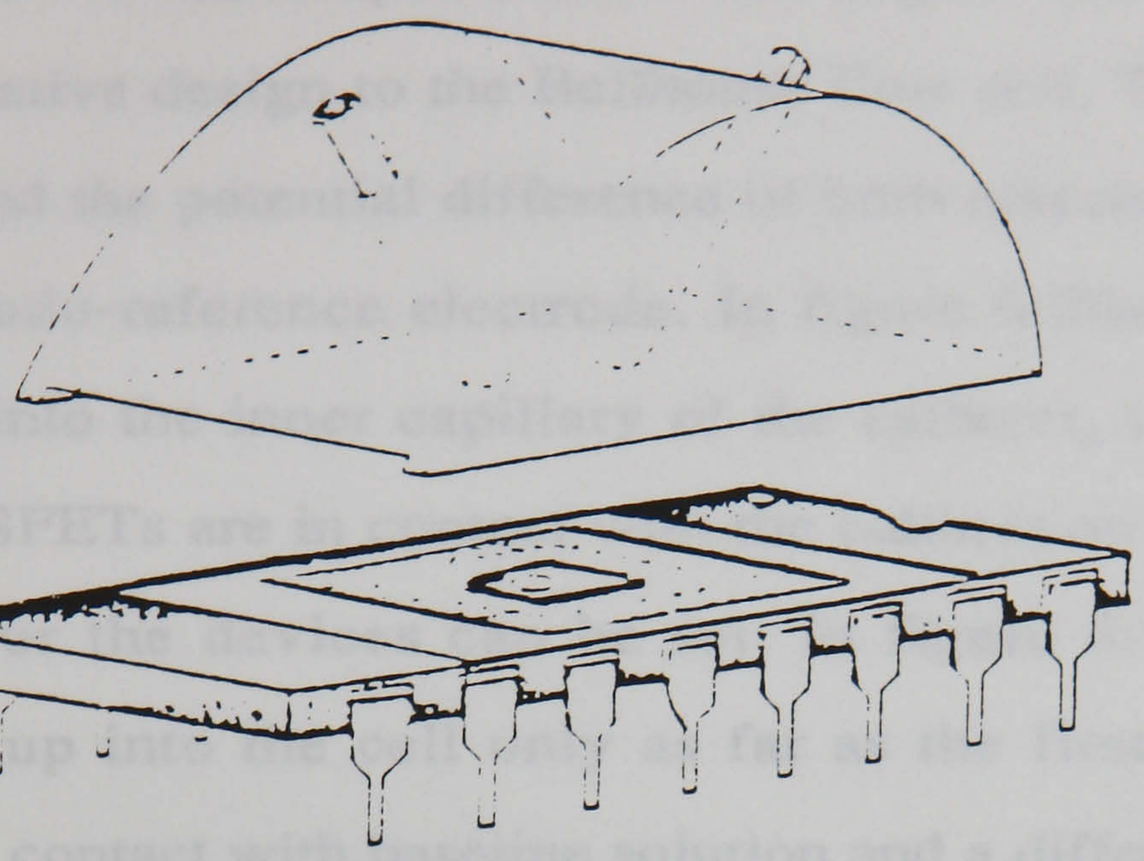

Figure 6:19 The Perspex Flow Cap Assembly, as used at the University of Newcastle-upon-Tyne.

separately.

Gumbrecht *et al.* [56] developed a micro-cell (figure 6:20) which may be a suitable alternative design to the Bellhouse flow cell. Two identical ISFETs are used and the potential difference of both measured against a platinum wire pseudo-reference electrode. In figure 6:20a, calibration solution is drawn into the inner capillary of the catheter, to the micro-cell, so that both ISFETs are in contact with the calibration solution and a baseline value for the devices can be set. In figure 6:20b, sample solution is drawn up into the cell only as far as the first ISFET; the second ISFET is in contact with baseline solution and a differential signal results. Sample solution then flows to the second device and the signal should revert to zero. As this whole process takes ~15 s, there should be no drift of signal. If protein and anticoagulant deposition is a serious problem, then this could cause error in the differential signal.

6.14 Conclusions.

From this work several conclusions can be drawn. The behaviour of the Eμ-146 devices substantiated claims by earlier workers [13, 55] that i.c.s are suitable as ex-vivo clinical sensors.

The optical sensitivity and drift of the devices in this work was very good. It is necessary, however, to design and implement a suitable method for determining thermal sensitivity. Bearing in mind that, as in all in direct potentiometry, ISFETs sense activity rather than concentration and that the devices are very small and easy to operate, then it would seem practical to use these devices in preference to flame photometry, currently being used.

Both membrane compositions gave good Nernst response with valinomycin as ionophore, though repeat calibration of the ETH 2041 should be carried out, with fresh plasticizer, to determine whether the sub-Nernst response was typical. The ETH 2041 plasticizer was found to yield devices which were more selective to potassium than the more commonly

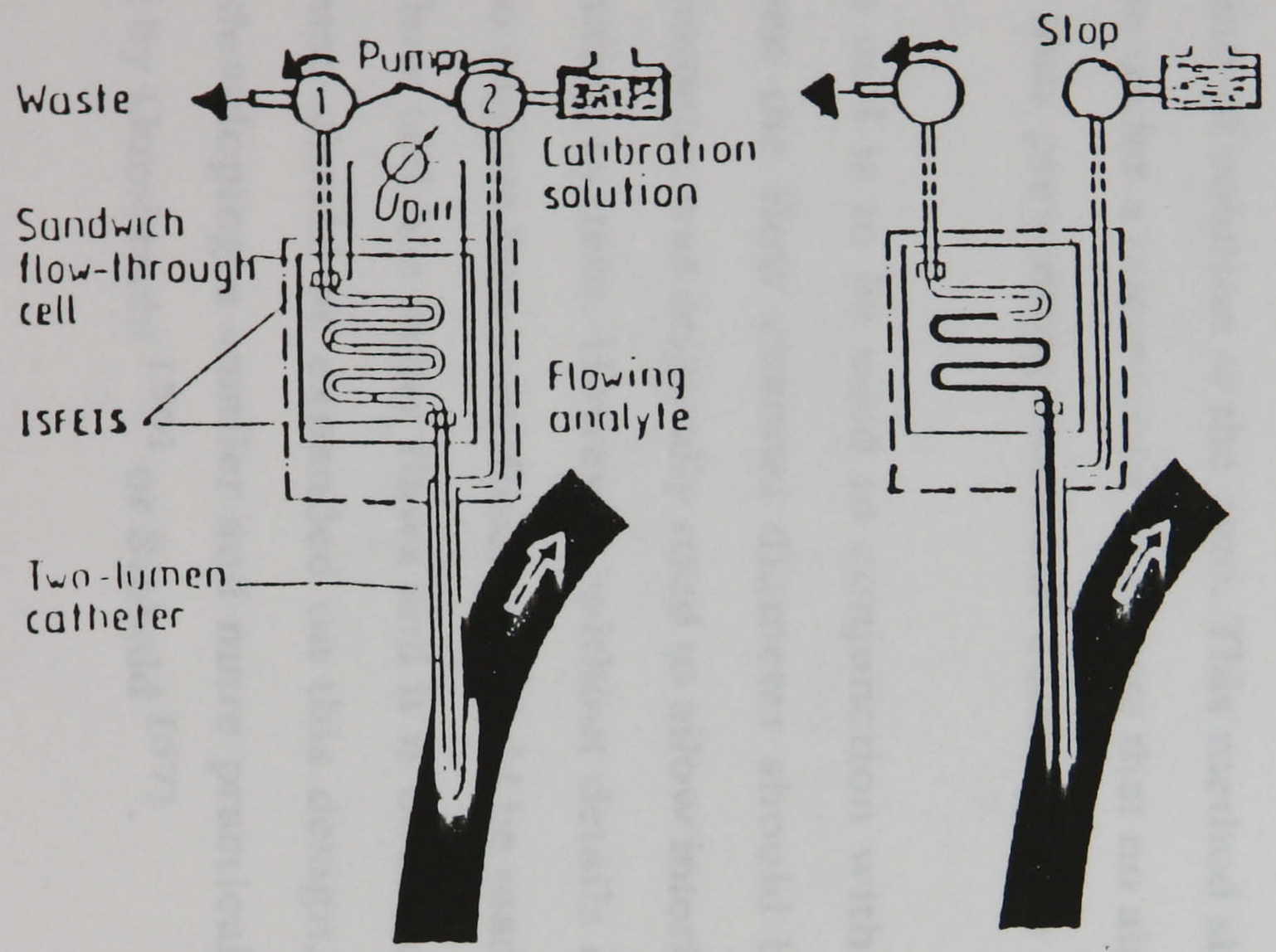

Figure 6:20 a)

Figure 6:20 b)

Figure 6:20 Gumbrecht's [49] On-line ISFET monitoring System.

used DOS and it would therefore seem wise to convert to the use of ETH 2041 in future potassium selective membranes for clinical analyses.

The cell design needs modifying with special regard to the large gap in the ISFET holder which allowed solution to come into contact with the device and therefore short circuit the electronics. Although silicone rubber has been used as a temporary filler, this is obviously not suitable if the cell is to be a successful commercial proposition. Future designs should also have channels pre-cut in the main body of the flow cell and in the FET holder to house the locking arm of the zero i.c. socket.

As it was necessary to seal the device into place (requiring 12 h drying), thus isolating the device, some method must be found to allow replacement of solution at the gate. This method should permit inspection of the gate under a microscope to ensure that no air bubbles are obscuring the gate, thus preventing electrical contact (gate / solution) from being made.

If the cell is to be used in conjunction with a standard peristaltic pump, then the flow channel diameter should be reduced. The large internal diameter was originally used to allow interfacing with Bellhouse's vortex mixing system. However, without details of this system it is not possible to suggest how modifications could be made.

The flow cell has many flaws and it is doubtful whether further time and expense should be expended on this design, it would be better to consider developing a smaller and more practical system such as those suggested by Gumbrecht [56] or Sibbald [57].

References.

1. Covington A.K. & Sibbald A.
Phil. Trans. Roy. Soc. London 1987, **B316**, 31

2. Sibbald A., Covington A.K., Cooper E.A. & Carter R.F.
Clin. Chem. 1982, **29**, 405

3. Dvorak J., Rubeska I. & Rezac Z.
"Flame Photometry, Laboratory Practice"
(English Translation by Hester R.E.)
Iliffe Books, London 1971

4. Ladenson J.H.
Anal. Proc. 1983, **20**, 554

5. Gosling P.
Ann. Clin. Biochem. 1986, **23**, 46

6. Worth H.G.J.
Analyst 1988, **26**, 992

7. Harry D.J., Davidson B. & Kenny M.A.
Clin. Chem. 1980, **26**, 992

8. Levy G.B.
Clin. Chem. 1981, **27**, 1435

9. Band D.M. & Treasure T.
J. Physiol. 1977, **266**, 12P

10. Band D.M., Heining M.P.D. & Linton R.A.F.
J. Physiol. 1983, **339**, 1P

11. Bernando A.J., Dreier G.H., Kelley T.F., Pistone D., Rolfe N.F.
Silverman N.D. & Webster M.E.
Clin. Chem. 1980, **26**, 992

12. KNA1 Sodium-Potassium Analyser Handbook
Radiometer, Copenhagen 1981

13. Electrolyte Analyser 902 (Corning)
Operating Manual Parts A & B, Issue 1, 1985

14. Beckman Astra Manual™ 015-555588

15. Simon W., Morf W.E. & Ammann D.
Mikrochem. J. 1987, **36**, 3

16. Moss S.D., Janata J. & Johnson C.C.
Anal. Chem. 1975, **47**, 2238

17. McKinley B.A., Houtchens B.A. & Janata J.
Crit. Care Med. 1981, **9**, 845

18. Waugh W.H.
Metabolism 1969, **18**, 706

19. Cowell D.C., Browning D.M., Clarke S., Kilshaw D., Randell J.,
& Singer R.

Med. Lab. Sci 1985, **42**, 252

20. Treasure T. & Band D.M.
Proc. Analyt. Div. Chem. Soc. 1977, **14**, 334

21. Annan W., Kirwan N.A. & Robertson W.S.
Clin. Chem. 1979, **25**, 643

22. Langhoff E. & Steines I.
Clin. Chem. 1982, **28**, 170

23. Czaban J.D., Cormier A.D. & Legg K.D.
Clin. Chem. 1982, **28**, 1936

24. Siggaard-Andersen O., Thode J. & Wandrup J.
"Proc. 5 th Meeting IFCC Expert Panel on pH and Blood Gases."
Copenhagen, Denmark 1980, pp.163

25. Maas A.H.J., Siggaard-Andersen O., Weisburg H.F. & Zijlstra W.G.Z.
Clin. Chem. 1985, **31**, 482

26. Ladenson J.H.
J. Lab. Clin. Med. 1977, **90**, 654

27. Pioda L.A.R., Simon W., Bosshard H.R. & Curtius H.Ch.
Clin. Chem. 1970, **29**, 289

28. Flear C.T.G., Roberts S.W., Omondi T.M., Serwedda D. & Holmes M.
Methodology and Applications of Ion Selective Electrodes,
IFCC Workshop, Graz, Austria 1986
ISE Determination of Na^+, K^+, pH.

29. Hickling M.J., Barclay J.A., White S.J. & White K.
Experimenta 1976, **32**, 554

30. Payne R.B.
Ann. Clin. Biochem. 1982, **19**,233

31. Payne R.B. & Jones D.P.
Ann. Clin. Biochem. 1987, **24**, 400

32. Oesch U., Ammann D. & Simon W.
Clin. Chem. 1986, **32**, 1448

33. Rebelo M.J.F. & Covington A.K.
in preparation

34. Buckley R.M., Rawson K.M. & Russell L.J.
Methodology and Clinical Applications of Ion Selective Electrodes
1987, **8**, 299

35. Thode J., Fogh-Andersen N. & Siggaard-Andersen O.
Ann. Clin. Biochem. 1983, **8**, 299

36. Hall C.A.
3H Project, University of Newcastle-upon-Tyne, Dec. 1989

37. Fogh-Andersen N., Christiansen T.F., Komarmy L.F. & Siggaard-Andersen O.
Clin. Chem. 1978, **24**, 1545

38. Treasure T. & Band D.M.
J. Med. Eng. & Tech. 1977, **1**, 271

39. Janata J. & McBride P.T.
J. Bioeng. 1979, **2**, 459

40. Sibbald A.
Ph.D. Thesis, University of Newcastle-upon-Tyne, 1982

41. Sibbald A., Covington A.K. & Carter R.F.
Clin. Chem. 1984, **30**, 135

42. Oesch U., Anker P., Ammann D. & Simon W.
"Ion Selective Electrodes"
Akademia Kiado, Budapest 1985, pp.81
ed. Pungor E. & Buzas I.

43. Oesch U., Xu A., Brzozka Z., Suter G. & Simon W.
Chimia 1986, **40**, 351

44. Oesch U. & Simon W.
"Opportunities of Planar Ion Selective Electrode Membrane Technology."
Transducers 1987, 4th International Conference on Solid State Sensors and Actuators.

45. Grove A.S.
"Physics and Technology of Semiconductor Devices"
J. Wiley & Son, New York 1967, Chapter 12

46. Valdes-Perezgasga F.
Ph.D. Thesis, University of Newcastle-upon-Tyne, 1990

47. Griffiths J., Moody G.J. & Thomas J.D.R.
Analyst 1972, **97**, 420

48. Pungor E., Toth K. & Hrabececzy-Pall A.
Pure & Appl. Chem. 1979, **51**, 1915

49. Mascini M. & Pallozi F.
Anal. Chim. Acta 1974, **73**, 375

50. Fiedler U. & Ruzicka J.
Anal. Chim. Acta 1973, **67**, 179

51. Papacostas S.
Ph. D. Thesis, University of Newcastle-upon-Tyne 1986

52. Oesch U., Malinowski E. & Simon W.
Anal. Chem. 1987, **59**, 2131

53. Wimberley P.D., Siggaard-Andersen O., Fogh-Andersen N., & Boink A.B.T.J.
Scand. J. Clin. Lab. Invest. 1985, **45**, 7

54. Sibbald A., Whalley P.D. & Covington A.K.
Anal. Chim. Acta 1984, **159**, 47

55. Sibbald A., Covington A.K. & Carter R.F.
Med. Biol. Eng. Comp. 1985, **23**, 329

56. Gumbrecht W., Schelter W. & Montag B.
Digest Eurosensors 1, (Cambridge), 1987, 155

57. Sibbald A., Covington A.K. & Harbinson T.R.
Presented at Utah Conference on "Electrochemical Sensors in Medicine and Medical Research"
Park City, Utah, Jan. 10-14th, 1982

CHAPTER SEVEN

ANALYSIS OF FERTILIZERS

7.1 Introduction.

In this project, ISEs, both home made and commercial, were used to analyse potassium in fertilizers. Previous work at Newcastle [1] had used ISFETs in a similar study. Conventionally, in industry, the composition of fertilizers is determined spectrophotometrically; this project aimed to investigate the advantages of electrochemical methods.

7.2 The Fertilizer Samples.

It is a tradition in the fertilizer industry that fertilizer compositions are expressed as a mass percentage (of the total); potassium is expressed as a percentage of potassium superoxide, K_2O. Although this species does not actually exist in fertilizer or in solution (the species present is actually a potassium phosphate based compound) this is the conventional means of showing the potassium content.

The samples were supplied by ICI plc, (Agricultural Division, Billingham) and were "NPK" fertilizers, containing the major plant nutrients. Several of the supplied samples are commercially available. "NPK" is the notation used for total nitrogen, i.e. ammonium and nitrate concentration together, P_2O_5 and K_2O. In simple terms, nitrogen compounds are used for leaf production, phosphates for root production and potassium compounds for flowering. Details of sample NPK content are given in Table 7:1.

7.3 Ion Selective Electrodes.

Home made and commercial electrodes, both with valinomycin as ionophore, were used. See Chapter 2 for a detailed preparative description.

7.3.1 Home made Electrodes.

The valinomycin membrane used had the following composition

All percentages by weight and membrane reagents supplied by Fluka, specifically for ion selective membranes.

The reagents were dissolved in freshly distilled tetrahydrofuran.

Valinomycin	Ionophore	0.6 %
Poly(vinyl) Chloride	Inert support	33 %

Bis (2-ethylhexyl) sebacate	Plasticizer	66 %
Potassium tetrakis 4-chlorophenyl borate	Salt	0.9 %

Table 7:1 The Composition of Fertilizer Samples (ICI plc.).

Sample Number	NPK Ratio	Sample Concentration	$[K_2O]$	$[K^+]$
		g dm^{-3}	mol dm^{-3}	mol dm^{-3}
1	15:15:21	0.5	1.062	2.124
2	15:15:21	1.0	2.123	4.240
3	25: 5: 5	0.5	0.271	0.542
4	25: 5: 5	2.0	1.083	2.166
5	10:25:15	0.5	0.791	1.581
6	10:25:15	1.0	1.582	3.164
7	5:15:30	10	6.0 *	3.0 *
8	20:10:10	10	4.4 *	2.2 *
9	15:15:15	10	1.0 *	0.5 *
10	26:14: 0	10	0.4 *	0.2 *
11	9:24:24	10	4.0 *	2.0 *

* values supplied by Manufacturer.

The membrane was prepared and the ISEs fabricated as described by Griffiths et al. [2] and conditioned over 12-24 h with 10^{-2} mol dm^{-3} potassium chloride internal solution and the membrane immersed in 10^{-2} mol dm^{-3} potassium chloride. An internal silver / silver chloride reference electrode was sealed into the electrode body, with the internal filling solution of 10^{-2} mol dm^{-3} potassium chloride, using silicone rubber (Dow-Corning, 3140 RTV).

Figure 7:1 The Corning Miniature Ion Selective Electrode.

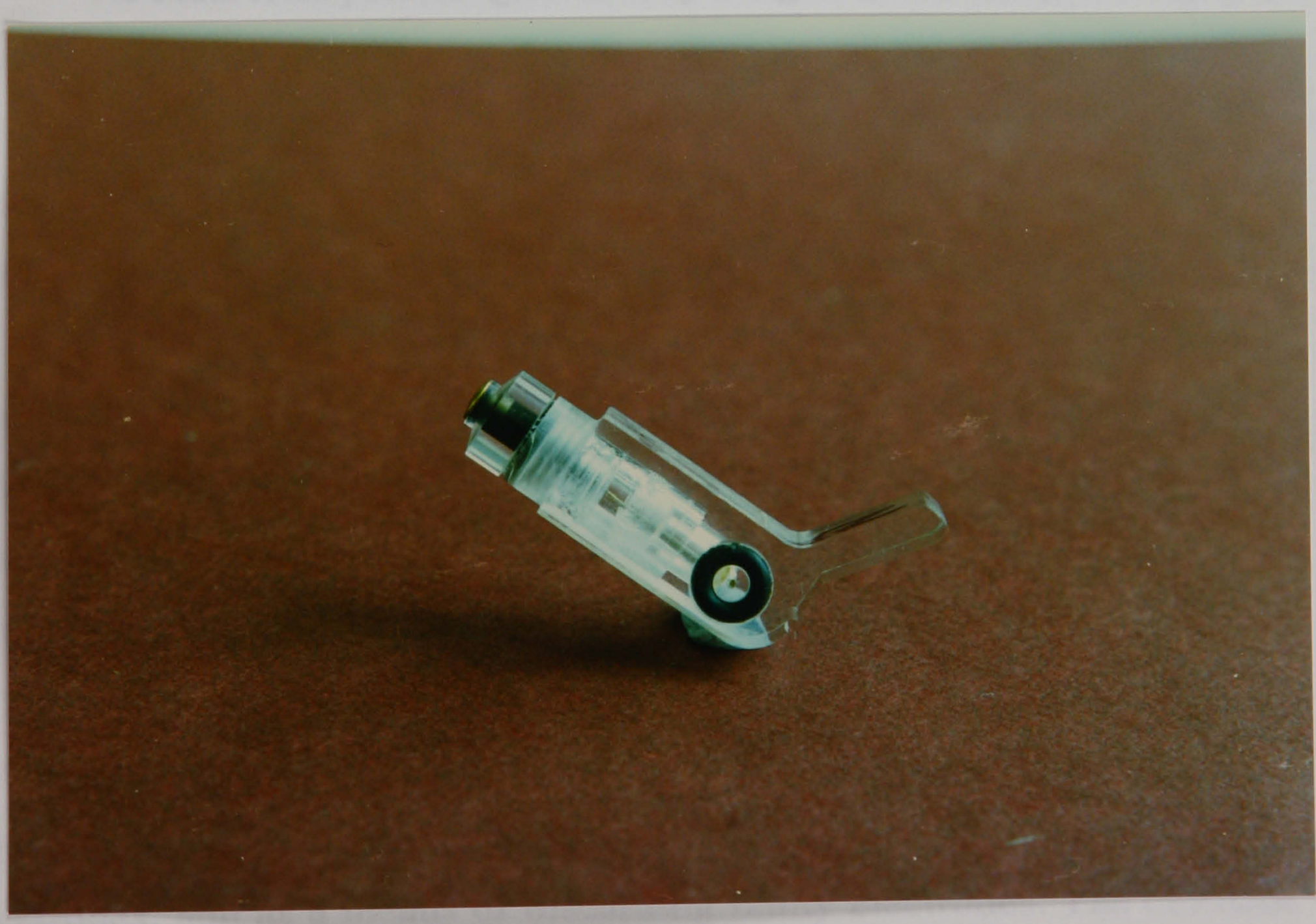

7.3.2 Commercial Electrodes.

A miniature Corning electrode (Type 476270, Corning Medical and Scientific, Massachusetts) was used. This electrode has a perspex body in two sections which screw together, sealed with a silicone "O" ring. The upper section contains the internal silver / silver chloride reference electrode, dipping in to the internal reference electrolyte, 10^{-2} mol dm^{-3} potassium chloride. This section has a small hole bored through which, when the mini-electrode is assembled, allows sample to come into contact with the ion selective electrode [3] (figure 7:1).

7.3.3 ISFETs.

The ChemFET devices used were Eμ-146 devices on which were set down membranes of the following composition;

Valinomycin	Ionophore	1 %
Poly(vinyl) chloride	Inert support	33 %
Bis (1-butylpentyl) adipate	Plasticizer	66 %

As before, all percentages were by weight, and all reagents supplied by Fluka.

The devices were integrated into an automated flow system [1] (figure 7:2).

7.4 Calibration Methods and Standards.

A double junction (3.5 mol dm^{-3} potassium chloride, 3.5 mol dm^{-3} potassium chloride) calomel reference electrode was used in studies for both ISEs and ISFETs. In experiments using ISEs, the system was set up as described in the previous chapter and all results were recorded on a Linseis Y / t chart recorder.

Potassium chloride solutions were used for calibration. Preliminary dip tests, as suggested in Chapter Three, were carried out to ensure that sufficient conditioning time had been given to newly prepared home made electrodes, and as a means of discarding faulty electrodes. The constant

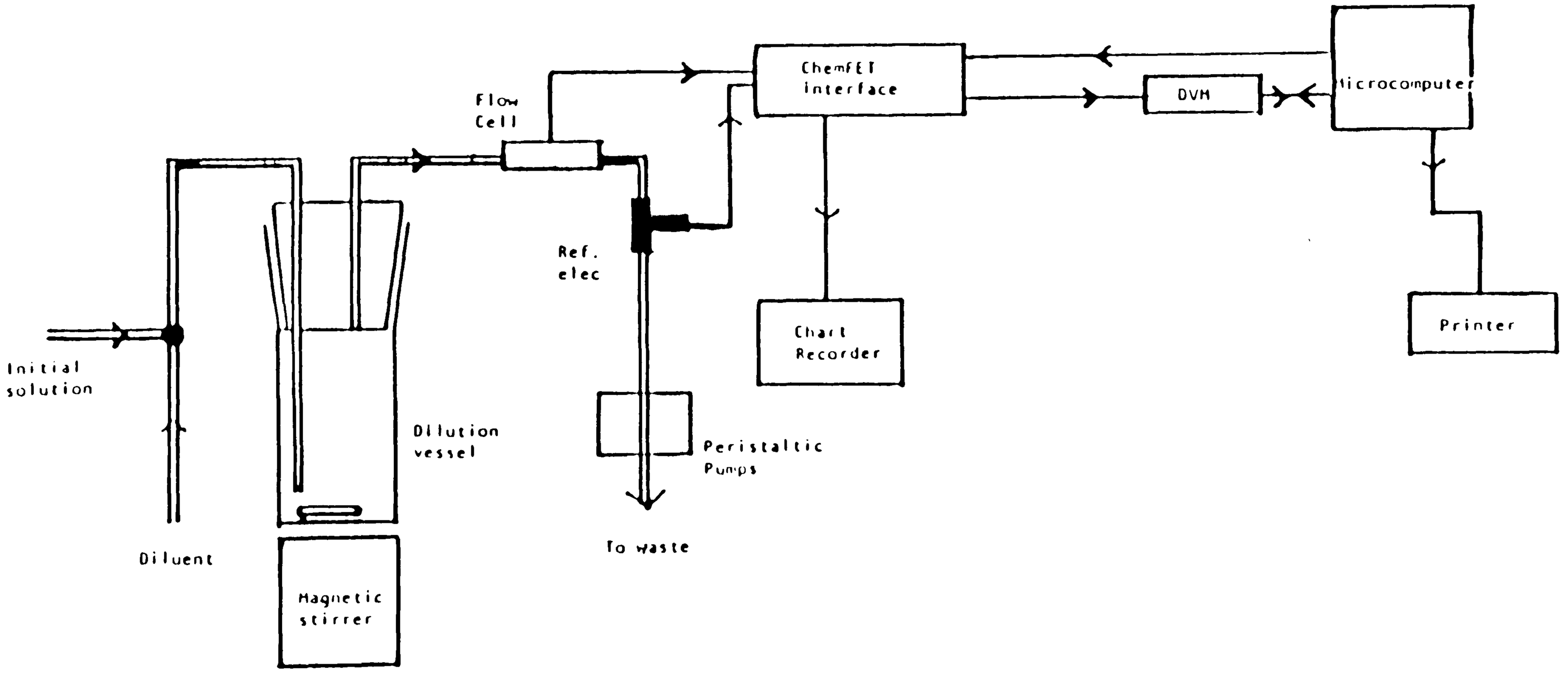

Figure 7:2 Automated Flow System for use with ChemFETs.

volume dilution technique was used to determine the Nernst response of both types of electrodes. On developing the Orion-type flow cap, described in Chapter Three, this replaced constant volume dilution as the means of calibration, thus matching method of analysis and calibration as closely as possible. Electrodes were calibrated immediately prior to each analysis; this was important as a base-line shift (variation in the standard potential) is often observed due to ageing of the system and variation in the flow rate, although the Nernst slope is not affected [4].

7.5 Experimental.

7.5.1 Analyses.

Samples 1 to 6 were analysed, as supplied, at dilute concentrations, 0.5 g dm^{-3} to 2.0 g dm^{-3}, and were untreated. 10 g dm^{-3} samples of fertilizers 7 to 11 were analysed. To these was added an ionic strength adjustment reagent (ISA), 2 mol dm^{-3} sodium sulphate in a 1:50 v/v ratio. None of the samples was filtered prior to analysis. This is in accordance with work carried out by Papacostas [1].

Analyses were carried out in a flow system, operated by a peristaltic pump fitted with pulse suppressor (as described in Chapter Three). In preliminary tests, the home-made ISE sat in a constant volume vessel (32.46 ml) containing a stirred solution of a particular fertilizer which also flowed through the system, in an attempt to minimize the static layer at the membrane surface. It was soon realised that this method was inadequate, as the vessel was too large, and the Orion-type flow cell was developed and used in all further analyses with the home made ISE.

The ISE was calibrated using potassium chloride solutions. A solution of 10^{-1} mol dm^{-3} potassium chloride was diluted using the constant volume dilution method, and calibrations with the 'Orion' type flow cell used 10^{-1} to 10^{-5} mol dm^{-3} potassium chloride solutions (prepared by serial dilution) passed in the flow assembly in random order. A Nernst response of 59.51 mV dec^{-1} was calibrated for the ISE.

7.5.2 pH Effects. Pretreatment of Samples.

The samples tested were in suspension; this can give rise to serious pH errors [5], which in turn can affect speciation. The fertilizers were filtered using a medium glass sinter (no.2). The pH of all the fertilizer samples, filtered and unfiltered was determined using a pre-calibrated glass electrode (Russell type CE7L), and the flow system used as before.

7.5.3 Ionic Strength Adjustor.

The effect of ISA on pH was also measured, as above, in both filtered and unfiltered samples of fertilizers 7 to 11.

7.5.4 Selectivity Studies.

Selectivity studies, using the mixed solution method, were carried out to determine $k_{K+,\ NH4+}$ using 10^{-1} mol dm^{-3} potassium chloride and 10^{-2} mol dm^{-3} ammonium chloride.

7.5.5 Effect of Phosphate.

Potassium is present in the fertilizers as a phosphate-based compound. The responses of the Corning and home made potassium selective electrodes were observed as the concentration of phosphate was increased. This was in keeping with studies carried out using ISFETs.

7.6 Electrode Poisoning.

As the project progressed, the performance of both types of ISEs deteriorated. Eventually, neither the Corning nor the home made electrode responded to potassium ions. Several attempts were made to reinstate the ISEs' response by soaking the membranes in progressively more concentrated (to 1.0 mol dm^{-3}) solutions of potassium chloride, for extended periods of time (12 h to several days).

It was suspected that ammonium ion, present in similar quantities to potassium ion in the sample (see Table 7:2) and of similar ionic radius was responsible for this behaviour. Several new membranes and ISEs were prepared to try to reproduce the observed effect in a controlled experiment using standards of known concentrations of ammonium ion. Both dip tests

and flow experiments were carried out.

Table 7:2 Concentration of Ammonium Ion Present in the 10 g dm^{-3} Fertilizer Samples.

Sample Number	$[NH_4^+]$ mol dm^{-3} Expected #	Experimental ‡
7	1.3×10^{-3}	58.9×10^{-3}
8	0.9×10^{-3}	1.0×10^{-3}
9	1.4×10^{-3}	86.6×10^{-3}
10	2.5×10^{-3}	80.7×10^{-3}
11	2.1×10^{-3}	57.6×10^{-3}

Values supplied by Manufacturer.

‡ Values determined by Papacostas [1].

7.7 Drift Studies.

A shift in the baseline was noted when the pump was initially switched on and off, and a drift of the electrode response had been noted when the electrode was in an unstirred sample solution, though not in a flow situation. This potential drift was recorded during steady state flow conditions and then for periods of up to 30 min after the pump action had stopped. The sample flow was then resumed for ca. 5 min before the process was repeated. It was important to determine whether this shift in the standard electrode potential was reversible. If an irreversible baseline shift was observed, re-calibration of the electrode may be necessary between analyses.

7.8 Results and Discussion.

Concentrations of samples were all determined graphically from calibrations carried out immediately prior to analysis. The calibration curves obtained for the home made ISE and the Corning miniature ISE are shown in figures 7:3, 7:4.

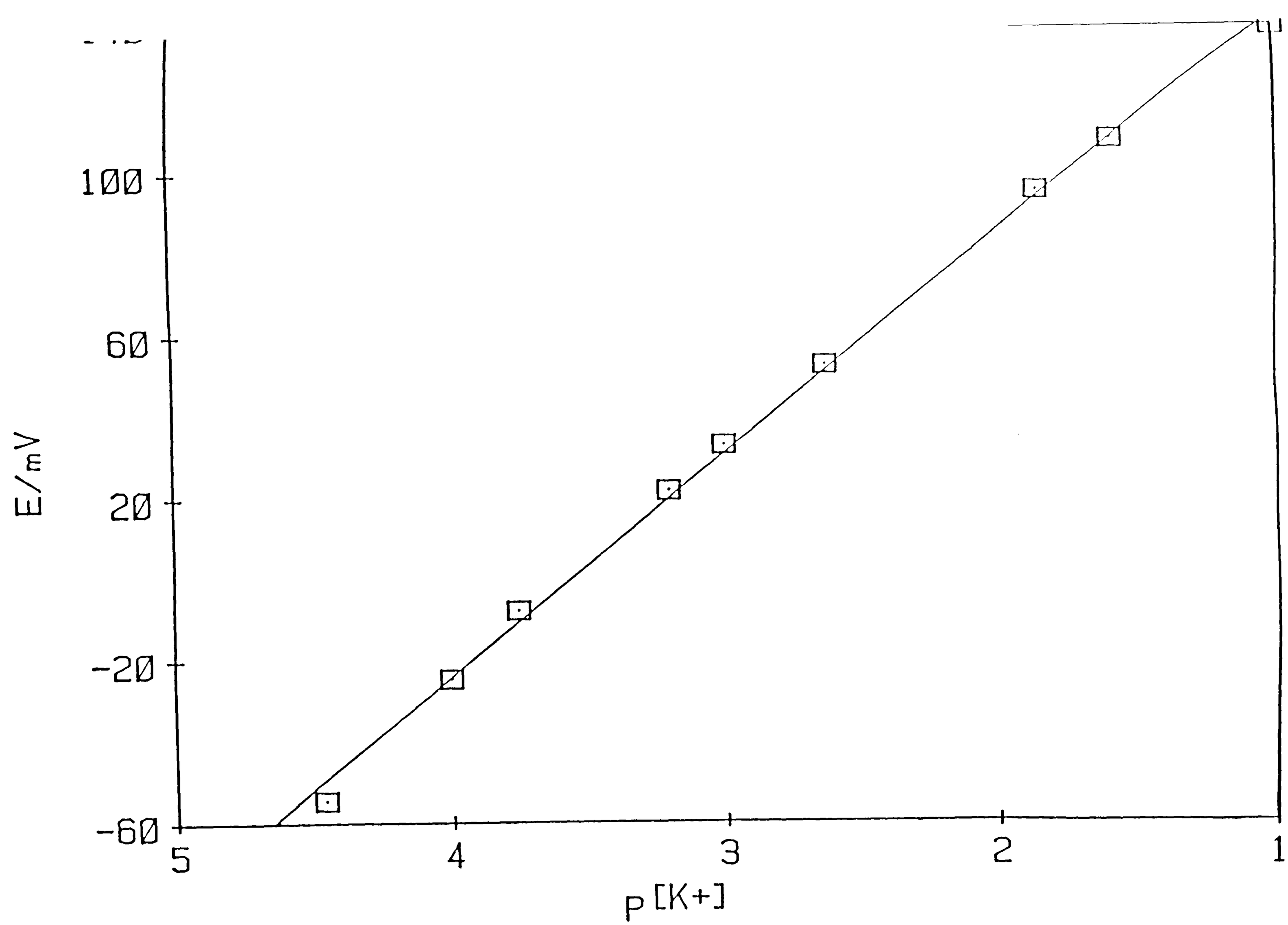

Figure 7:3 Calibration Curve for the Home-made Potassium Selective Electrode.

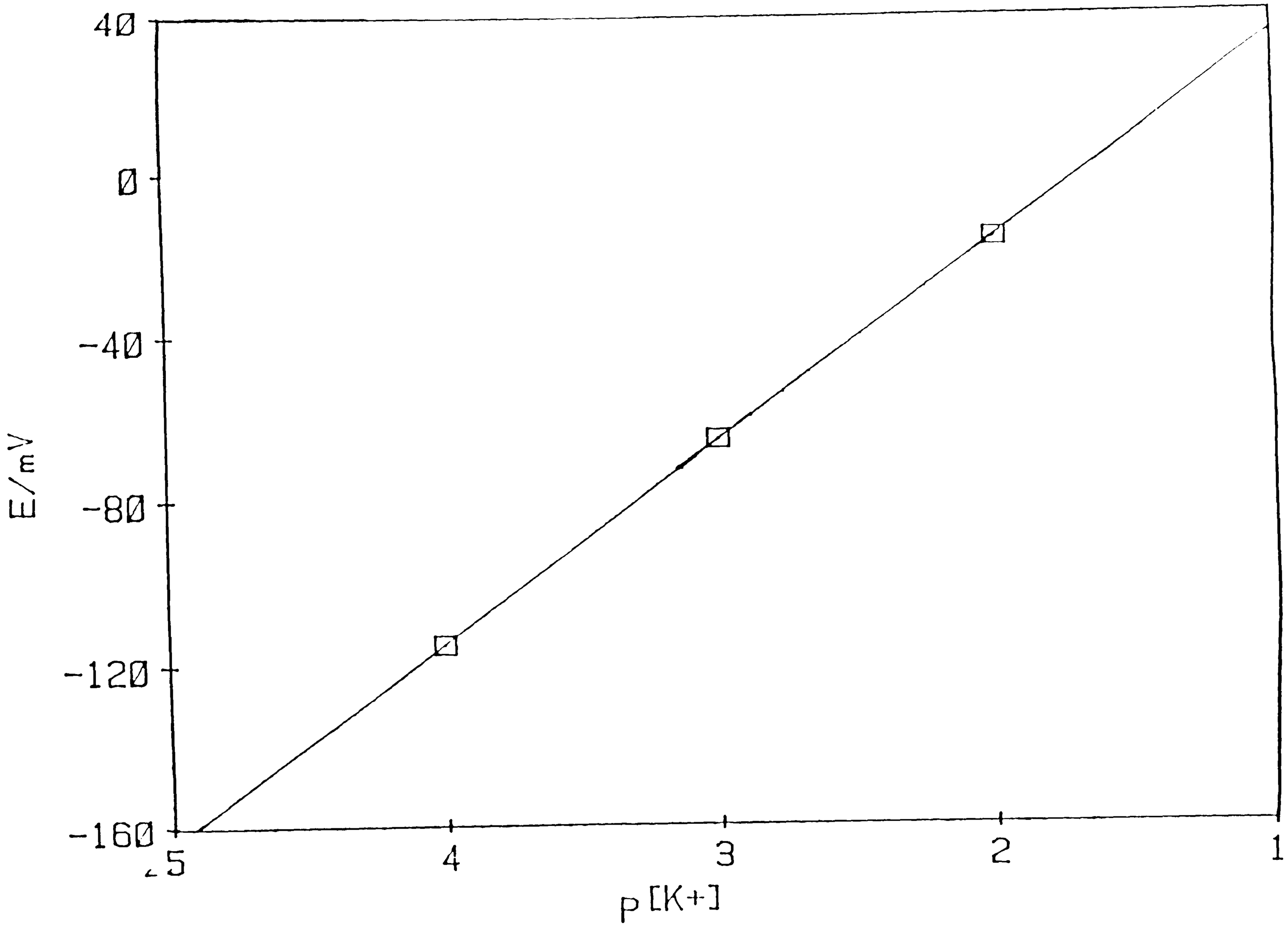

Figure 7:4 Calibration Curve for the Corning Miniature Ion Selective Electrode.

The potassium concentrations of the samples 1 to 6 as determined, with the home made electrode using the large constant volume dilution vessel, are shown in Table 7:3. Due to problems associated with the carry-over and dead space using this method, all further analyses were carried out using the Orion-type flow cap. The response time was much reduced using the latter method. Measurements determined using this flow cell, the Corning ISE and ISFET are compared with the expected (calculated) values and are shown in Table 7:4.

It can be seen that the values obtained using all methods was very close to the calculated value for fertilizers 1 to 4. However, there was a discrepancy between the expected and observed values for samples 5, 6. As this deviation was also found by Papacostas [1], it seemed possible that this was possibly an error in the analysis by I.C.I. plc, or more likely, incorrect data.

Table 7:3 Potassium Analysis of Fertilizers (1 - 6) with Home made ISE.

Sample Number	$[K^+]$ / mol dm^{-3} x 10^3 CVD Method	"Orion" flow cap	Expected (calculated)
1	17.3	2.51	2.124
2	28.8	2.69	4.246
3	1.33	0.75	0.542
4	22.9	2.51	2.166
5	15.5	2.11	1.581
6	22.4	4.47	3.164

This table clearly shows the potassium concentration values obtained using the constant volume dilution method were *ca.* 10 times greater than those values determined using the Orion type flow cap and the manufacturer's value. These results substantiated findings in Chapter 3; the dead space in the dilution cell gives rise to erroneous concentration

values of samples, due to inefficient mixing of sample and diluent, so that solutions appear to have higher concentrations than is actually the case.

Table 7:4 Comparison of Analyses Carried out on Fertilizers 1 - 6.

	$[K^+]$/ mol dm^{-3} x 10^3			
Sample Number	Home made ISE	Corning ISE	ISFET	Calculated
1	2.51	2.45	3.80	2.124
2	2.69	4.22	4.57	4.246
3	0.75	0.71	0.80	0.542
4	2.51	2.66	3.21	2.166
5	2.11	1.77	1.64	1.581
6	4.47	3.09	3.98	3.164

The potassium concentrations determined for samples 7 to 11 did not agree well with those values supplied by the manufacturers, but were in general ten times greater than the expected values, see Table 7:5. The trend in concentrations was similar, except for fertilizers 8 and 11, which had similar potassium concentrations and reversed positions in the expected trend. The ISFET analyses of these fertilizers also showed a discrepancy from the expected values, and were of the same order of magnitude for those obtained using ISEs. The results obtained for these fertilizers (using ISFETs) although close to the expected value was, therefore, considered suspect.

Why there should be such a large discrepancy for these analyses, when similar results were obtained for fertilizers 1 to 6, was disturbing. It was for this reason that the effect of filtering and ISA was investigated.

As the second batch of samples was more concentrated, 10 g dm^{-3} as opposed to 1.0 g dm^{-3}, there was a higher degree of suspended matter. It was also noted that no ammonium ions were detected by Papacostas[1] in

fertilizers 1 to 6, but significant amounts were present in samples 7 to 11.

Table 7:5 Comparison of Analyses Carried out on Fertilizers 7 -11.

	$[K^+]$/ mol dm $^{-3}$ x 10 ^{3}			
Sample Number	Home made ISE	Corning ISE	ISFET	Calculated
7	31.85	-	61.8	3.0 *
8	10.61	-	3.5	2.2 *
9	15.92	-	33.6	0.5 *
10	5.01	-	21.1	0.2 *
11	25.48	-	47.7	2.0 *

* Values supplied by Manufacturer.

Brezinski [6] emphasised the restrictions imposed on ISEs in colloidal samples with respect to colloidal charges and inhomogeneity of the sample. The pH difference between colloidal sediments and the supernatant liquid was assigned the term "suspension effect" by Pallman and Weigner [7]; they attributed this pH variation to the absorption of hydrogen ions by the dispersed phase [8, 9]. However, other workers found that this early explanation was insufficient as the position of the reference electrode affected the magnitude of the suspension effect. There is some dispute amongst workers as to whether this effect is real or artefact. The first explanation expands Pallman and Weigner's proposal, assigning the unequal partition of hydrogen ions between the supernatant liquid and the charged colloid particles as a result of a phase boundary potential, that is a Donnan potential at the solid supernatant interface. This theory was termed the Donnan explanation and is the one more often favoured by colloid chemists.

The artefact theory, expounded by Jenny *et al.* [10] advocates a liquid junction effect caused by a large number of charged particles at the bridge

interface, which affect the originally equitransferent diffusion rates of potassium and chloride ions. That is, in a true solution, potassium and chloride ions are equitransferent between the salt bridge and the intermicellular liquid, but in a suspension this balance is upset by the presence of charged particles. This theory considers the suspension effect as an extreme example of a liquid junction error and is the concept more usually accepted by analytical chemists.

These theories are further discussed elsewhere [11-13]. In general, the pH of a suspension appears lower than anticipated if a suspension effect is present. Jenny [10] reports an extreme example of this effect; a pH change of 4 was observed between a 10 % suspension and the supernatant liquid.

7.9 pH Effects.

No significant pH differences were observed here between filtered and unfiltered samples. In the most concentrated samples, 10, 11, a Δ pH of only -0.03 and +0.13 in pH, respectively, was observed between the filtered and unfiltered samples. These results are shown in Table 7:6.

It was also shown that the presence of ISA did not influence the pH readings in filtered or unfiltered samples (Table 7:7).

In neither of the pH tests was a trend observed. If any significance could be attached to the small Δ pH changes observed, one would expect all pH changes to be negative (between filtered and unfiltered samples), this is evidently not the case. Nor was the direction of pH change consistent in experiments concerning ISA.

It can, therefore, be concluded that no suspension effect was observed in this work and the changes in pH observed between experiments was not due to suspended matter.

Table 7:6 pH Effect of Filtering Fertilizer Samples.

Sample Number	Unfiltered	Filtered	
	pH	pH	ΔpH
1	6.59	6.59	-
2	6.56	6.57	+ 0.01
3	5.19	5.19	-
4	6.56	6.55	- 0.01
5	6.33	6.33	-
6	6.33	6.32	- 0.01
7	5.76	5.89	+ 0.13
8	6.51	6.60	+ 0.09
9	6.61	6.63	+ 0.02
10	6.45	6.41	- 0.04
11	5.84	5.81	- 0.03

Table 7:7 pH Effect of Addition of Ionic Strength Adjuster (ISA).

	pH Values					
Sample Number	Unfiltered Samples		ΔpH	Filtered Samples		ΔpH
	with ISA	no ISA		with ISA	no ISA	
7	5.99	5.94	- 0.05	5.84	5.90	+ 0.060
8	6.61	6.55	- 0.06	6.52	6.61	+ 0.090
9	6.66	6.68	+ 0.02	6.61	6.62	+ 0.01
10	6.51	6.50	- 0.01	6.47	6.52	+ 0.05
11	5.92	5.99	+ 0.07	5.89	5.94	+ 0.05

The discrepancy between the manufacturers' results and those using electrochemical methods may have arisen due to inherent properties of each technique. The ISEs and ISFETs detect only ionised potassium and report activity of the primary ion, whereas spectrophotometric methods

report total concentration of the species of interest. This further complicates the issue, as one would expect the manufacturers' results to be greater than those obtained by either electrochemical method.

The potassium calibration solutions used were potassium chloride 10^{-1} to 10^{-5} mol dm^{-3}), however, the fertilizer samples are extremely complex, containing phosphates, nitrates and other unknown species. The ionic strength of the fertiliser samples is, therefore, much greater than that predicted by the potassium concentration alone. The same standards were used for potassium determinations of fertilisers 1 to 6, and fertilisers 7 -11, of 0.5 - 2.0 g dm^{-3} and 10 g dm^{-3} sample concentration, respectively. There was, therefore, a considerable difference in the ionic strengths between the two batches of fertilisers, and therefore large differences in the liquid junction potentials experienced by each system. A twenty fold difference in concentration between samples 1, 3, 5 and 7 - 11 could give rise to a difference in the liquid junction potential, E_{LJ}, of *ca.*10 mV, which relates to a difference in the concentration of 1.67×10^{-2} mol dm^{-3} for a 10^{-1} mol dm^{-3} solution, this could explain, in part, why experimental values obtained for the potassium ion concentration of samples 1 to 6 were considerably nearer those values obtained for samples 7 to 11.

It is, therefore, important that the chemical composition of the standards should match as closely as possible that of the samples. A variation in the matrix between the calibrants and the samples can lead to a considerable liquid junction error. As a result of these inconsistencies, tests were also carried out to ascertain the effect of ammonium and phosphate ions.

7.10 Selectivity Studies.

7.10.1 Ammonium Solutions.

The results of mixed solution selectivity tests, shown in figure 7:5 (chart recorder traces) using the home made ISE were reproducible and

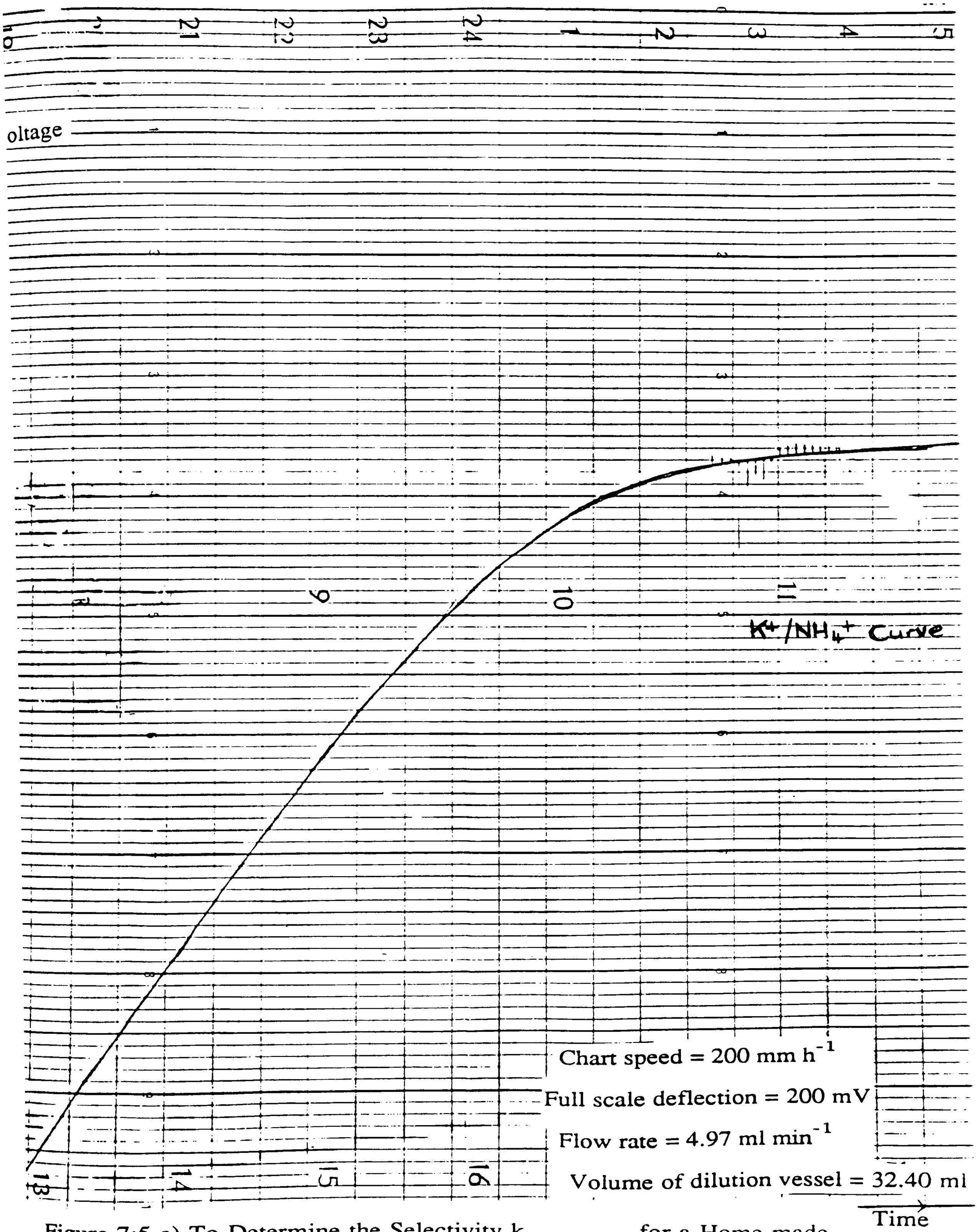

Figure 7:5 a) To Determine the Selectivity $k_{K+,NH4+}$ for a Home-made PVC / Valinomycin ISE; mixed solution.

K^+ calibration curve for the ISE.

Chart speed = 200 mm h^{-1}

Full scale deflection = 200 mV

Flow rate = 4.97 ml min^{-1}

Volume of dilution vessel = 32.40 ml

Nernst slope = 54.6 mV dec^{-1} K^+

Figure 7:5 b) Calibration of a Home-made PVC / Valinomycin ISE.

gave an average $k_{K+,NH4+}$ of 7.40 x 10^{-2} (Figure 7:6). This is in agreement with literature values (Table 7:8). As shown in Table 7:3, the concentration of ammonium ions is very similar to the potassium concentration, one would therefore expect some interference. This argument is further substantiated when one realises that samples 1 to 6, which contained an undetectable ammonium ion concentration gave values close to the manufacturer's specifications.

The effect of ammonium ion interference on the values of potassium ion is shown in Table 7:9. The combined concentration of potassium and interfering ammonium ions does predict a slightly larger signal will be observed by the potassium selective ISE, but this still does not fully explain the greater than ten fold difference between observed and expected potassium ion concentrations for all of 10 g dm^{-3} samples except sample 8. Sample 8 had the lowest phosphate ion concentration. The effect of phosphate on potassium ion ISEs is discussed in the following section. It was not, unfortunately, possible to repeat this work with a Corning electrode, as a functioning potassium selective electrode was not available.

Table 7:8 Literature Values of Selectivity Coefficients of Valinomycin Electrodes.

Electrode Type	Measuring Method	Interferent Concentration	$k_{K+,NH4+}$
		mol dm^{-3}	x 10^{-2}
Orion [15]	S.S. #	10^{-3}	5.0
Corning [16] Exchanger	M.S. *	10^{-2}	40.8
		5 x 10^{-2}	36.2
Silicone [17] Rubber	M.S.		2.3
PVC [18] Selectrode	M.S.	10^{-2}	1.3

S.S. = separate solution method

M.S. = mixed solution method

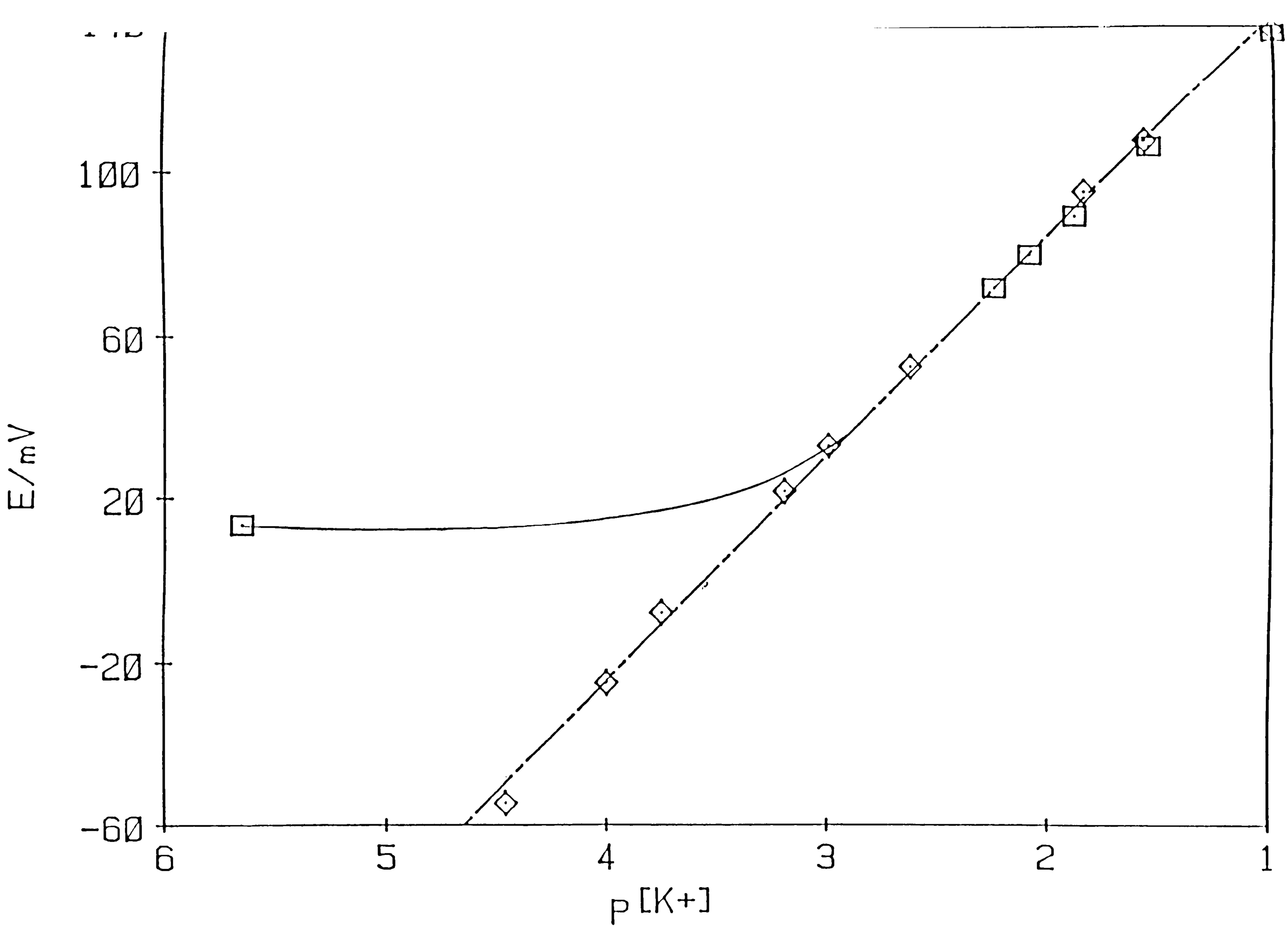

Figure 7:6 Selectivity Study of K^+ / NH_4^+ using a Home-made ISE by the Constant Volume Dilution Method.

Table 7:9 Effect of Ammonium Ions on Potassium Ion Signal.

Sample	Manufacturer's Values			Experimental Values	
Number	$[K^+]$	$[NH_4^+]$	$[K^+] + [NH_4^+]^*$	$[K^+]$ ISE	$[K^+]$ ISFET
7	3.0	1.3	3.0962	31.85	61.8
8	2.2	0.9	2.2666	10.61	3.5
9	0.5	1.4	0.6036	15.92	33.6
10	0.2	2.5	0.385	5.01	21.1
11	2.0	2.1	2.1554	25.48	42.7

All concentrations in mol dm^{-3}

* Using $K_{K+,NH4} = 7.40 \times 10^{-2}$, this value represents the combined concentration of the primary potassium ion and interfering ammonium ion.

7.10.2 Phosphate Solutions.

In flow tests using the Orion-type flow cell, the effect of phosphate (Table 7:10) was found to be twice that observed by Papacostas [1] (Table 7:11). As the phosphate concentration increased from 50 ppm to 250 ppm, more negative potentials were observed. A similar trend was observed with the Corning electrode (Table 7:12). The voltage difference observed for each 40 ppm change in phosphate concentration was not constant, but gave an average Δ mV of 14 mV (per 40 ppm phosphate concentration change). This effect was reproducible, but it was necessary to use a flow, not dip, method for the home made ISE. Papacostas reported only ca. 8 mV difference between solutions with ISFETs. This discrepancy may have arisen due to the different plasticizer; bis (2-ethylhexyl) sebacate *versus* bis (1-butylpentyl) adipate. Although, in theory, the plasticizer is inert, in practice it may affect membrane performance [18], e.g. by leaching of membrane components from the membrane.

Table 7:10 Composition of Phosphate Standards.

Solution	Phosphate Concentration	
	ppm	x 10^{4} mol dm^{-3}
A	50	3.674
B	90	6.613
C	130	9.552
D	170	12.49
E	210	15.43
F	250	18.37

Table 7:11 Effect of Phosphate on Electrode Readings (Home made ISE).

	(1)		(2)	
Solution	Response, V	Δ V	Response, V	Δ V
	mV	mV	mV	mV
A	+ 18.3		- 106.2	
		- 57.4		+ 12.1
B	- 39.1		- 94.1	
		+ 12.4		+ 15.9
C	- 26.7		- 110.2	
		+ 78.6		+ 18.8
D	+ 51.9		- 91.2	
		+ 4.7		+ 26.2
E	+ 56.6		- 65.0	
		+ 0.6		- 2.0
F	+ 57.2		- 67.0	

(1) Dip Test

(2) Flow Test

The effect of phosphates should therefore be taken into account and considered as a suspect interferent to potassium.

Table 7:12 Effect of Phosphate on Electrode Readings (Corning Electrode).

	(1)		(2)	
Solution	Response, V	Δ V	Response, V	Δ V
	mV	mV	mV	mV
A	- 103.8		- 113.3	
		+ 9.1		+ 6.0
B	- 94.7		- 107.3	
		+ 14.8		+ 14.9
C	- 109.5		- 94.4	
		+ 19.8		+ 34.1
D	- 89.7		- 60.3	
		+ 15.3		+ 3.9
E	- 74.4		- 56.4	
		+ 3.6		+ 0.4
F	- 70.8		- 56.0	

(1) Dip Test

(2) Flow Test

7.11 Electrode Poisoning.

The Nernstian response of the home made and the Corning electrodes deteriorated as the study continued from 58.73 mV dec^{-1} and 55.13 mV dec^{-1}, respectively, to no potassium response. Despite soaking in solutions of potassium chloride of strengths up to 1.0 mol dm^{-3} for several days, the potassium response could not be restored. This effect has been observed elsewhere [19] for miniaturised electrodes in the clinical analysis of urine where the cause was attributed to ammonium ions poisoning the membrane. Conversely, Ladenson [20] saw only a minimal influence of ammonium ions on potassium sensors and only for a maximum load of 200 to 300 mmol of dissolved ammonia per litre per 24 h. It, therefore, seemed reasonable to assume, taking into account the high "total nitrogen" content, that a similar phenomena may have occurred here. The previously determined selectivity coefficient of the home made electrode showed that

it was susceptible to ammonium ion interference.

It was impossible to reproduce this "poisoning" effect with any of several newly prepared home made electrode. An electrode dipping overnight in a 1.0 mol dm^{-3} ammonium chloride solution showed a Nernst response to potassium after being in 10^{-2} mol dm^{-3} potassium chloride for 2 h. Similarly, an electrode soaked for 60 h in a solution of 10^{-1} mol dm^{-3} ammonium chloride and 10^{-4} mol dm^{-3} potassium chloride showed a slight decline in performance, from 52.5 mV dec^{-1} to 48.4 mV dec^{-1}, but the Nernstian response was improved after being in 10^{-1} mol dm^{-3} potassium chloride overnight.

In order to determine how effectively ammonium ions remained in the membrane, sequential aliquots of a 10^{-1} mol dm^{-3} ammonium chloride / 10^{-4} mol dm^{-3} potassium chloride were added to a standard solution of 10^{-4} mol dm^{-3} potassium chloride, thus maintaining the background concentration of potassium ion throughout. When ammonium ions were clearly seen to be interfering, aliquots of 10^{-4} mol dm^{-3} ammonium chloride / 10^{-4} mol dm^{-3} potassium chloride were added, thus reducing the overall concentration of ammonium ion present in solution.

A decreased response to ammonium ions was observed as the concentration of ammonium ions in the solution was diminished (Table 7:13, Figure 7:7). This showed that these ions did not remain in the membrane but potassium, preferentially, set up an equilibrium between the membrane and the electrolyte solution. With time, the response of the ISE returned to the original value observed before the addition of ammonium interferent and the equilibrium position was reinstated.

It would appear, therefore, that although ammonium ions may act as interferent towards the ISEs, they do not remain in the membrane and were not responsible for the total electrode failure observed. As there may be many unknown compounds present in the sample, it is possible that one of these was poisoning the electrode.

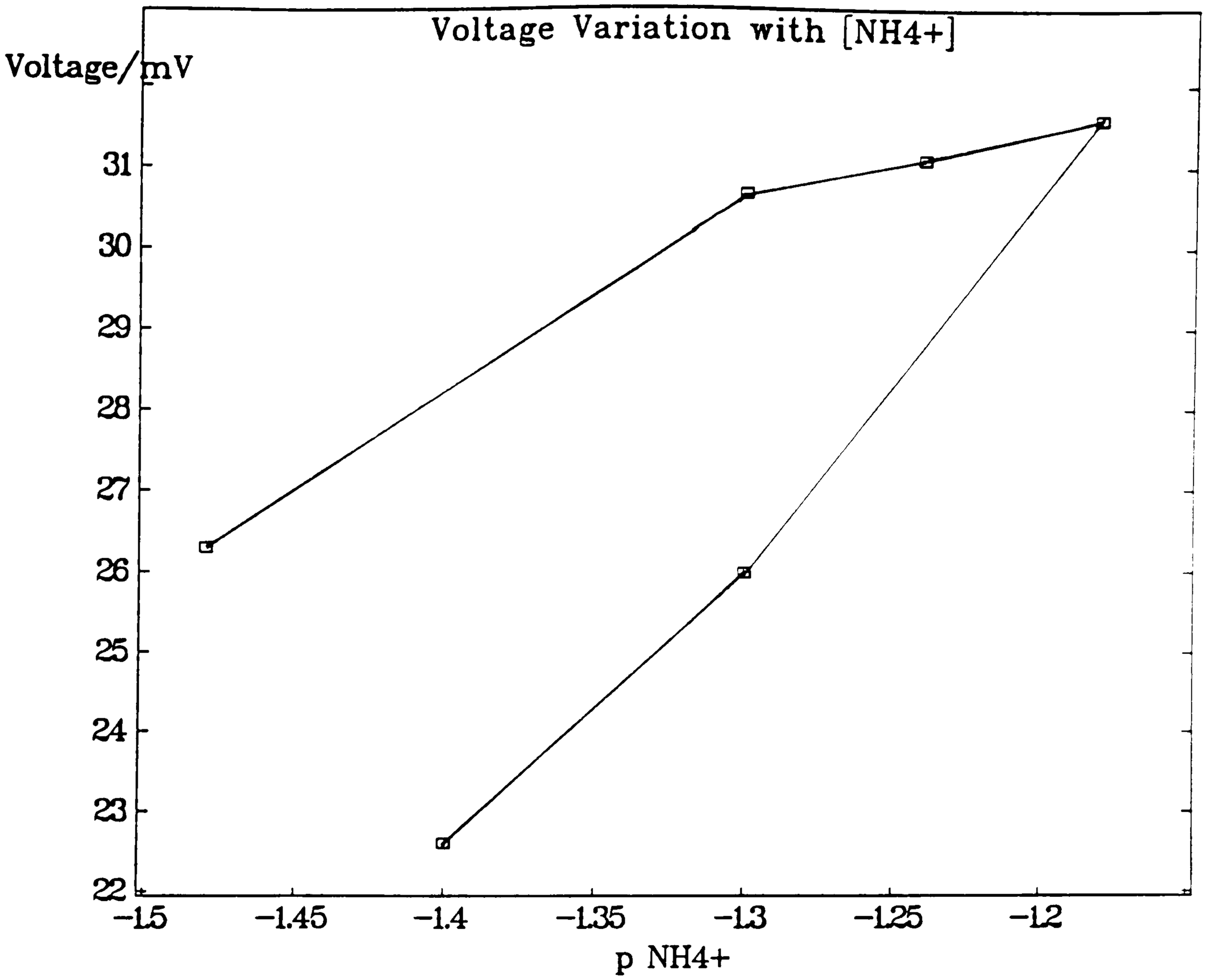

Figure 7:7 The Variation in Voltage with Subsequent Additions of Ammonium Ions.

Table 7:13 Effect of Ammonium Ions on Response of the Home made Electrode. Addition of Ammonium Chloride to a Background Solution of Potassium Chloride.

Volume of Aliquot Added ml	$[NH_4^+]$ Added mol dm $^{-3}$	$[NH_4^+]$ mol dm $^{-3}$	Voltage mV
-	-	-	+ 15.8
25	10^{-1}	3.33	+ 26.3
25	10^{-1}	5.00	+ 30.7
25	10^{-1}	6.00	+ 31.2
25	10^{-1}	6.67	+ 31.6
50	10^{-4}	5.00	+ 26.0
50	10^{-4}	4.00	+ 22.6

Jenny *et al.* [21], who observed similar effects in undiluted urine analyses, attributed this to anion interference as their results agreed with those observed in the presence of thiocyanate ions [22]. They were unable to determine which anion. Using silicone rubber, rather than PVC, as the support for the membrane, they were able to reduce this effect drastically. Other workers [23, 24] have also found neutral carrier based electrodes to exhibit anion interference due to anion extraction (from the electrolyte) by the membrane phase. The problem was overcome, as it was by Jenny *et al.*, by substitution of the PVC membrane for a silicone rubber membrane, thus reducing the extraction properties of the electrode.

A prime suspect of this poisoning effect, however, must be phosphate. As shown in 7.11.2, a potential shift was observed when the potassium selective ISE was placed in phosphate solutions; it is now believed that the total lack of potassium selectivity of the electrode was due to phosphate ions entering the membrane due to a breakdown of the Donnan Exclusion Principle. This is explained in the following section.

7.12 The Donnan Exclusion Principle.

Consider a plasticized PVC membrane with no ionophore present but

with anionic sites and hydrogen counter ions (~ 10^{-7} mol dm^{-3}). On exposing the membrane, from lower to higher concentration solutions of potassium chloride (an equitransferent salt), since the concentration of anion sites in the membrane is much greater than that of the potassium ions, hydrogen ions, in very low concentrations, are transferred to the bathing solution. This leads to a boundary potential potential at each interface which draws the potassium ions in to the membrane in higher concentrations (than the hydrogen ions). The anions in the membrane prevent chloride ions entering, thus cation permselectivity is created [25]. This effect, known as the Donnan Exclusion Principle, is the exclusion of ions of one charge, here anions, from the membrane.

On addition of an ionophore to the membrane, here valinomycin, a potassium selective ionophore, potassium ions are more easily extracted in to the membrane which results in a lower boundary potential, E_B, at the interface thus there is less exclusion of the free anions from the bathing solution. Hence, the Donnan Exclusion Principle fails more easily in membranes with a good ionophore. This phenomenon is also known as Donnan Breakdown or Co-ion Exclusion Failure.

Buck [22] showed that 10^{-2} mol dm^{-3} potassium thiocyanate led to the onset of Donnan Exlusion Failure for a valinomycin potassium selective ISE. Thiocyanate is intermediate between halide ions and tetraphenylborate with respect to extraction ability and Buck [26] found in mixed solutions of potassium thiocyanate / potassium chloride that a large uptake of hydrophobic thiocyanate ions occured in preference to the hydrophilic chloride ions.

It is now thought that the poisoning observed for the potassium selective ISE may have been due to phosphate ions, HPO_4^{2-}, from the fertiliser solutions, entering the membrane due to violation of the Donnan Exclusion Principle. This would explain why tests with ammonium solutions could not reproduce the poisoning effect. Preliminary flow tests

carried out with phosphate solutions showed a more negative potential reading as the concentration of phosphate solution was increased from 50 - 250 ppm. This effect was observed for both the home made electrode and the Corning electrode. Papacostas [1] recorded only a slight variation in potential, *ca*. 8 mV (per 40 ppm phosphate concentration change) between phosphate solutions and did not note poisoning of his devices.

7.13 Drift Studies.

During sampling, the electrode gave good, stable responses of + 0.05 mV and no drift was observed. When the pump was switched off, an immediate base-line shift, to a more negative potential (i.e. indicating less potassium ion), was recorded. After ca. 15 min, the signal settled to a minimum and then crept back to the new "stationary" base-line potential. When flow action was continued, the base-line returned to its original value. Several workers have reported this effect [27] and have associated it with ageing of the electrode, stirring or flow rate. By carrying out calibrations and analyses in succession, without bringing the pump to a halt, this problem can be avoided. In dip tests, this would be a problem, but by maintaining a flow rate of *ca*. 4 ml min^{-1}, the extent of deposition is minimised [28]. The cause of this effect was attributed to the deposition of particulate matter at or near the membrane surface, affecting the laminar diffusion layer.

It was found that a dead-space existed even in the Orion type flow cell and it was necessary to flush the system copiously with the next sample and wait for a steady signal before making any measurements. By analysing in a random order and repeating recordings, it was possible to ensure that potential measurements were consistent and were not subject to systematic errors.

7.14 Conclusion.

Rapid and reproducible analysis of fertilizers, using on-line electrochemical detectors, ISEs and ISFETs, is possible. Pre-calibration

was found to be necessary before analysis as an irreproducible base-line shift was observed between analyses. Analyses using the CVD method gave potassium ion concentrations *ca.* 10 times greater than those determined experimentally using the Orion type flow cell and the manufacturer's supplied values. This reinforced the claims in Chapter 3 that the CVD method must be used with care.

The composition of the calibration solution should match as close as possible that of the sample solution, otherwise large liquid junction potentials errors may occur. These variations in liquid junction arise due to large differences in the ionic strengths between calibrant and sample solutions, and was believed to be true of the Batch 2 fertilizers and calibration standards.

Ammonium ions were shown to interfere reversibly, with $k_{K+,NH4+}$ of 7.4×10^{-2}, this is due to the similar ionic radius of the potassium and ammonium ions. This would explain, in part, the unexpectedly high potassium concentrations determined in samples 7 to 11.

The "poisoning" effect of the ISEs was attributed to some unknown species, possibly an anion, in the fertilizer. Without a more detailed knowledge of the sample composition and subsequent testing, it is impossible to state definitely the interferent. Ammonium ions were originally suspected as interfering, but the effect could not be repeated with ammonium solutions. It is now believed, however, to be phosphate ions present in the fertiliser solution, which entered the membrane due to Donnan Exclusion Failure. Further work should be carried out to ascertain the effect of phosphate ions on the potassium selective membrane. As this effect was not observed for the ISFET, it would appear that ISFETs have distinct advantages over ISEs in these analyses.

Further work should, therefore, be carried out to determine the selectivity of the membrane towards phosphate.

References.

1. Papacostas S.
Ph.D. Thesis, University of Newcastle-upon-Tyne 1986

2. Griffiths J., Moody G.J. & Thomas J.D.R.
Analyst 1972, **97**, 420

3. Corning (private communication from L.J. Russell to A.K. Covington)
1986

4. Ruzicka J. &. Tjell J.C.
Anal. Chim. Acta 1969, **47**, 475

5. Mattock G. & Band D.M.
In "Glass Electrodes for Hydrogen and Other Cations"
ed. Eisenman G.
Marcel Dekker 1967, Chapter 2

6. Brezinski D.P.
Talanta 1983, **30**, 347

7. Weigner G., Pallman H., Musierowicz A. & Alberado J.M.
Polish Agr. Forestal. Ann. 1932, **28**, 323
cited in ref. 6

8. Weigner G.
Kolloid Z. 1930, **51**, 49
cited in ref. 6

9. Pallman H.
Kolloidchem. Beihefte 1930, **34**, 334
cited in ref. 6

10. Jenny H., Nielson T.R., Coleman N.T. & Williams D.E.
Science 1950, **112**, 164

11. Overbeek J.T.G.
J. Colloid Sci. 1953, **8**, 593

12. Marshall C.E.
Science 1951, **113**, 43

13. Eriksson B.
Science 1951, **113**, 419

14. Lal S. & Christian G.D.
Anal. Lett. 1970, **3**, 11

15. Davies J.E.W., Moody G.J., Price W.M. & Thomas J.D.R.
Lab. Pract. 1973, **22**, 20

16. Pick J., Toth K., Pungor E., Vasak M. & Simon W.
Anal. Chim. Acta 1973, **64**, 477

17. Fiedler U. & Ruzicka J.
Anal. Chim. Acta 1973, **64**, 179

18. Ammann D., Morf W.E., Anker P., Meier P.C., Pretsch E. & Simon W.
Ion Sel. Elec. Rev. 1983, 5

19. Private Communication (J.M. Thompson, Queen Elizabeth Hospital, Birmingham to A.K. Covington)

20. Ladenson J.H.
Clin. Chem. 1979, **25**, 757

21. Jenny H.B., Reiss C., Ammann D., Magyar B., Asper R. & Simon W.
Mikrochim Acta 1974, **46**, 1765

22. Buck R.P., Toth K., Graf E., Horvai G. & Pungor E.
J. Electroanal. Chem. 1987, **223**, 51

23. Oesch U. et al.
Analytical Chemistry Symposia Series
Vol. 22 Ion Selective Electrodes, 4 pp.81
ed. Pungor E.

24. Lindner E., Wuhrman D., Simon W. & Pungor E.
In "Proc. 2nd Symposium on Ion Selective Electrodes"
Matrafared, Hungary "Ion Selective Electrodes"
ed. Pungor E. & Buzas I.
Akademia Budapest, 1977 pp.159

25. Van den Berg A.
Ph.D. Thesis University of Twente., The Netherlands 1988

26. Buck R.P., Stover F.S. & Mathis D.E.
J. Electroanal. Chem. 1979, **100**, 63

27. Van den Winkel P., Mertens J. & Massart D.L.
Anal. Chem. 1974, **46**, 1765

28. Shatkay A.
Anal. Chem. 1976, **48**, 1039

CHAPTER EIGHT

CONCLUSIONS

8.1 Introduction.

As a result of the studies carried out, ISEs and ISFETs have been shown to be extremely good electroanalytical tools for a diverse range of applications. Before considering these, a few points must be made with regard to the operating conditions and measuring systems used.

8.2 Calibration and Measuring Systems.

Flow systems were found to be far superior to dip test, 'beaker-to-beaker', methods of calibration; this was due to the make-and-break [1] of the electronic circuit, leading to polarisation of the ISE.

In Chapter 3, the constant volume dilution (CVD) method, used for determining the Nernst slope and selectivity of ISEs and ISFETs was examined. It was found that the technique, presented by Horvai [2], must be used with careful consideration of the operating conditions; at fast flow rates, the solution within the cell was unable to mix efficiently and there was a large discrepancy between the expected and observed concentrations of solution within the dilution vessel as shown using a separate means of determining concentration, UV-vis spectrophotometry.

Equation (3.1) is based on first order kinetics for dilutions using the CVD method.

$$c = c_o \exp(-Wt / V_r) \qquad (3.1)$$

where c = the concentration of the solution in the dilution vessel at time t, in mol dm^{-3}

c_o = initial concentration in the dilution vessel, in mol dm^{-3}

W = flow rate of diluent, in ml min^{-1}

t = time, in min

At slow flow rates, first order kinetics was almost obeyed, but there was still a disparity between the experimental and theoretical (predicted) concentrations. It was concluded that this difference was due to inefficient mixing within the dilution vessel, that is, there was a dead

space in the flow cell, reducing the working volume of the cell and thus reducing the efficiency of the dilution. However, it was not possible to correct for the dead space in the cell as there was a problem modelling diffusion of materials out of the dead volume.

On reducing the flow rate, to *ca.* 2.5 ml min^{-1}, and size of the dilution vessel, from *ca.* 35 ml to *ca.* 15 ml , concentrations closer to that predicted by Horvai in equation (3.1) were observed. These conditions are advised, therefore, for further work using the CVD method and the conditions under which a CVD experiment are run should be quoted. As was discussed in Chapter 3, if the lag time can be compensated for, and thus the x axis (time, correlated concentration of substrate in the dilution vessel) corrected, then it should be possible to make reliable measurements of selectivity coefficients in mixed solutions.

The limitations of the CVD method were shown clearly in Chapter 7 when the results of fertilizer analyses carried out using calibration by the CVD technique were compared with those using a small 'Orion' type flow cell and on-line analyses. The potassium concentration of samples obtained using the CVD calibration curve were 10 times greater than the manufacturer's predicted concentrations and the values obtained using the smaller flow cell. This clearly demonstrated the inefficiency of sample mixing during dilution experiments.

In Horvai's original paper [2], it was noted that the response time of the ISE (or ISFET) should not be too slow. Obviously, it is important that the electrode can respond rapidly to the change in concentration of solution in the dilution vessel. At very fast flow rates it was shown, using an iodide selective ISE and potassium iodide solutions, that the ISE was unable to follow the dilution.

Thus, it was concluded that whilst the constant volume dilution is a simple and adaptable method of calibrating electrochemical sensors, it must be used with caution giving careful consideration to the flow rate.

volume of dilution vessel, design of the cell, and, most importantly, the response time of the device.

8.3 Potentiometric Titrations.

ISEs and ISFETs allow very accurate end point determinations in potentiometric titrations, where much sharper end points are reached than when using conventional colorimetric techniques. An auto-titration unit, for both volumetric and coulometric titrations, with a sensor-actuator system, was designed to exploit further the advantages of potentiometric detectors.

Coulometric generation of the titrant is particularly suitable for micro-analysis or for use with chemically unstable reagents. The auto-titrator was designed with an option for volumetric titrations, interfaced to a Mettler DV11 auto-burette, or for coulometric titrations, interfaced to a pulse generator and constant current source. The generating electrode pair needed varies with the titrate, but in general it was found that using silver anode / platinum cathode for titration of acids and platinum anode / platinum cathode for titration of bases gave good, reproducible titration curves and thus showed that a similar sensor-actuator system to that developed by Bergveld *et al.*[3] could be developed in Newcastle.

Two-compartment cells were used to reduce contamination by side reagents produced at the auxiliary electrode and consequently more stable titration curves were obtained. The arrangement of electrodes in the reaction vessel was shown to be important and should be considered before experimental work is carried out. In order to prevent interference of the generating electrode with the indicator electrode(s), the indicator electrode(s) should be placed near the working electrode but not between the generating electrode pair.

The set-up developed here was used only for preliminary work, however, it was shown to be a highly adaptable system, worth developing, and, therefore, the system is to be transferred to an on-line IBM computer.

8.4 Determination of the pK_d^2 Value of Hydrogen Sulphide.

8.4.1 Potentiometric *versus* Spectroscopic Methods.

Coulometric titrations were used to confirm the pK^d_2 value for hydrogen sulphide. In a recent review [4], Meyers postulated a new value of 19 ± 1 for pK_2^d of hydrogen sulphide. Results of this work, carried out by simultaneously monitoring the pH and sulphide ion concentration during coulometric titration of sulphide sample solutions, dispute the value proposed by Meyers and agree with the text book value of pK_2^d [5].

The average pK^d values for hydrogen sulphide were found to be 5.87 ±1 and 12.08 ± 1, using visual inspection and Hseu and Rechnitz's [6] equation (equation (5.8)).

$$[S^{2-}] = f_{S2-}[S^{2-}]_{TOT}/\{1 + ([H^+]/K_2^d)\} \quad (5.8)$$

The titration data was fed into SUPERQUAD to obtain the β formation constants of hydrogen sulphide, and thus a second determination of the dissociation constants. The β formation constants for hydrogen sulphide were calculated and used to obtain pK^d values of 11.83 ± 0.4 and 6.7 ± 0.4, which agree well with values obtained by visual inspection Both sets of pK_d values agree well with the text book values of 7.04 and 11.96 [5] and are far from the new valueput forward by Meyers [4].

Sulphide solutions are vulnerable to aerial oxidation and therefore experiments were carried out under nitrogen with either a sulphide anti-oxidant buffer (SAOB) or with sodium hydroxide (10^{-1} or 5×10^{-2} mol dm^{-3}) in a 1:1 volume ratio with the sulphide solution, prepared using degassed water.

Calibration of the electrodes in solutions with and without SAOB clearly demonstrated the necessity of using SAOB to prevent oxidation of sulphide to bisulphide. In the presence of SAOB a 30 mV dec^{-1} Nernst slope was observed for the sulphide ISE in sulphide solutions and the pH remained high (*ca.* 12.4). Without SAOB, a Nernst slope of *ca.* 60 mV

dec^{-1}, typical of a monovalent ion (here HS^-) was observed. The pH dropped considerably, to 7.4, as the sulphide concentration of the calibration solution decreased.

Thus, the calibration curves show that ISEs can easily distinguish between sulphide and bisulphide ions, whereas in spectroscopic studies correct identification of sulphide species is a major source of debate. To compare spectroscopic and potentiometric systems, it is suggested that coulometric titrations are carried out in highly alkaline solutions, as used in spectroscopy studies, with a mercury / mercury reference electrode, and the pK_d values calculated as before. Spectroscopy studies should be undertaken in tandem with this work so that the two techniques can be compared directly and the controversy surrounding pK_2^d of hydrogen sulphide resolved.

8.4.2 Sulphide Anti-Oxidant Buffers.

The composition of SAOB used in this work contained EDTA (see Appendix F (i)). This composition is well recommended [7] and has been used by other workers in Newcastle [8], however, it was found to be unsuitable for this work and in further work the SAOB composition should be 2.0 mol dm^{-3} sodium hydroxide and trace asorbic acid..

EDTA in SAOB, present in similar concentration to sulphide in the sample, was found to cause slight interference on refining the β constants for hydrogen sulphide. Two of the acid dissociation constants of EDTA lie in the pH range of pK_1^d, pK_2^d for hydrogen sulphide (see Appendix F (ii)). When the β_1, β_2 formation constants of EDTA were included, but kept constant, in the header file for refinement of β_1, β_2 of sulphide, values closer to the literature values [4] were obtained for pK_1^d, pK_2^d of hydrogen sulphide. Refinement of the EDTA β_1, β_2 formation constants showed that it was only β_1 which affected the sulphide refinement. Although not problematic at 10^{-1} mol dm^{-3} sulphide concentrations, problems are anticipated at lower sulphide concentrations. EDTA is,

therefore, not recommended for further work to confirm pK^d values of hydrogen sulphide.

The second dissociation constant of ascorbic acid (11.52) (see Appendix F (ii)) lies very close to the pK_2^d of sulphide, however, rather than obscure the pK_2^d of sulphide, ascorbic acid enhances the sulphide inflection, that is, it is not possible to discriminate between titration of the sulphide and absorbic acid.

8.5 Modifying SUPERQUAD.

SUPERQUAD is normally used to refine the β formation constants for metal-ligand complexes and it would appear that this programme had not been used much with ISEs or with coulometrically generated titration data. The results of this work show the potential of expanding the applications of SUPERQUAD.

If SUPERQUAD is to be used routinely for analysis of coulometric data, for which it has been shown there are distinct advantages, then the programme requires slight modification. An improvement currently being introduced is an increase in the number of data points which SUPERQUAD will read; at present only 99 data points are accepted, this is being increased to 999. SUPERQUAD allows the concentration of each reagent present to be refined; with a limited amount of data it is necessary to refine each parameter individually, however with the revised programme, it will be possible to refine several parameters at once. Since it was possible to refine the sulphide concentration, it was not necessary to know the absolute concentration of sulphide present in the sample. Most importantly, at present in order to read into SUPERQUAD the number of coulombs generated during titration, it is necessary to calculate the volume equivalents (for a fixed concentration of titrant) of the charge passed and insert this value into the programme.

SUPERQUAD is very particular about the quality of data it will accept. Potentiometric titration curves for micro-litre samples are not

always smooth and if refined unmodified, SUPERQUAD may assign these minor "bumps" as inflections. This problem can be overcome by ignoring outlying points, identified using the residuals plot; this was shown to be a useful function in SUPERQUAD. It would be interesting to compare the performance of SUPERQUAD with other non-linear least squares programmes, such as SCOGS2, which do not require titration data of such a high quality as SUPERQUAD.

8.6 Novel Designs of Flow Cells.

8.6.1 Ion Selective Field Effect Transistors.

A range of flow cells and flow caps are available for analyses with ISFETs and are of particular importance in clinical analyses where the advantages of small size and relative robustness of ISFETs are fully exploited. The Bellhouse cell examined (Chapter 6), however, was found to have serious design errors and is not recommended as a commercial proposition. The flow cell did not allow easy insertion of a FET, increasing the likelihood of electrostatic damage to the device, moreover, the major fault of this cell was the siting of the device holder / socket, which allowed direct contact of the holder and sample solution, thus short circuiting the ISFET. Other systems are available for use in clinical analyses [9, 10], several of which have been designed, and successfully used, in Newcastle.

8.6.2 Ion Selective Electrodes.

New style flow caps for ISEs were designed to reduce the dead space and carry-over of the larger, more conventional flow cells available and were used, as far as possible, to replace the constant volume dilution method.

Particularly efficient was the two-piece, glass electrode flow cell which prevented residual solution remaining trapped behind the bulb of the electrode; a major source of carry-over. By blocking off this part of the cell, without reducing the ion selective region of the glass bulb,

improved response times were obtained. Two types of flow cap were designed for the standard, flat membrane ISE; an 'Orion' type flow cell and the 'straight walled' flow cap. All three flow cells were shown to behave extremely well in calibrations of ISEs, and the latter two flow caps were used in the analysis of fertilizers, described in Chapter 7. No carry-over of sample or calibrants was observed.

8.7 Experimental Considerations.

The optical sensitivities of the Eμ-146 ISFETs were studied in Chapter 6. When bright illumination (100 w) was shone on to the FETs, a slight drift in potential, + 1.0 mV, was observed initially. After several minutes, the devices stabilised to give a potential 0.5 mV greater than the starting potential. No improvement in stability of response was observed when devices were operated in darkness. One can conclude, therefore, that the devices were optically sensitive, but this was not a problem for normal working conditions, and could be compensated for if experiments were to be carried out under bright lights.

ISFETs are more prone to electrostatic noise and electrostatic damage, therefore, care had to be taken when handling ISFETs. An earthing bracelet must be worn at all times when using these devices to minimise damage. ISEs, which have high impedance, required earthed systems. Systems for both ISEs and ISFETs can be electrically isolated, if required, by carrying out experiments in a Faraday cage.

8.8 Fertilizer Analyses.

8.8.1 Matrix Effects.

As discussed in 8.6.2, the newly designed Orion and 'straight walled' flow cells were used in analysis of fertiliser solutions. No carry-over effects were observed during on-line calibration and sample testing, and it can be concluded that this method is superior to the constant volume dilution method, the results of analyses carried out were compared and discussed in 8.2.

During the work, the importance of matching sample and standard was examined. A twenty fold variation in concentration, and therefore ionic strength, existed between the samples which can give rise to a variation in the liquid junction potential of *ca.* 10 mV. In accordance with work carried out by Papacostas. however, [11], the same calibration standards were used throughout.

Analyses of batch 1 fertilizer samples, of similar ionic strength to the calibration standards, gave potassium concentrations similar to the manufacturers specified concentrations. By comparison, the batch 2 fertilizers, of higher ionic strength than the calibration standards, gave potassium ion concentrations of up to 30 times (sample 9) greater than the value supplied by the manufacturer.

Poor matching of standard and sample was only partially responsible for the discrepancy in potassium ion concentration for the experimental results observed here and the manufacturer's values. It was noted, however, that the less concentrated samples gave potassium ion concentrations nearer to the manufacturer's values than the batch 2 fertilizers. It was concluded, therefore, that the matrix composition of the standard should resemble that of the sample as closely as possible.

8.8.2 Electrode Poisoning.

The poisoning effect observed for the potassium selective ISE was shown not to be due to ammonium ions present in the fertilizer samples. Selectivity tests showed that ammonium ions do interfere with valionomycin, potassium selective membranes, with an average $k_{K+,NH4+}$ of 7.40×10^{-2}, which agrees with literature values [12], due to similar ionic radii of the ammonium and potassium ions. However, this interference was a reversible process and ammonium ions could be displaced from the membrane by increasing the potassium ion concentration in the bathing solution, and a Nernst response to potassium ions was reinstated.

It is now believed that this poisoning effect was due to phosphate ions, HPO_4^{2-}, present in the samples, which led to Donnan Breakdown arising from failure of permselectivity at the membrane interface so that HPO_4^{2-} anions, normally excluded from the membrane now cross the bathing solution / membrane interface [13, 14]. This was fully discussed in section 7:12.

Further work should be carried out with potassium selective ISE and ISFETs using phosphate solutions in order to investigate fully this interference.

8.9 Summary.

Overall, one can see that ion selective devices may be used in a wide range of applications with advantages over conventional methods. Flame photometric techniques, can measure low concentrations, submicro-litre, of samples, however, no information is given about the speciation of the element and this is usually more important. In clinical studies, for example, it is the concentration of available ionized calcium which is required. Similarly, in analysis of fertilizers, it is the uncomplexed, free potassium ion concentration that is important.

In work to re-determine the pK_2^d of hydrogen sulphide, again electroanalytical techniques proved to be superior to spectrometric techniques. ISEs could distingiush between sulphide and bisulphide ions using a simple set-up; spectroscopists still debate the band assignation of sulphide species.

Coulometric generation of the titrate during potentiometric titrations allows very small, sub micro-litre, samples to be titrated. With the development of the sensor-actuator system to control the production of coulometrically generated species, electrochemical systems, giving information with regard to speciation of the analyte are a challenge to more conventionally employed spectroscopic methods.

References.

1. Johansson G., Karlberg G. & Wikby A.
   Talanta 1975, **22**, 953

2. Horvai G., Toth K. & Pungor E.
   Anal. Chim. Acta 1976, **82**, 45

3. Bergveld P., van der Schoot B.H., & Onckiewicz J.H.L.
   Anal. Chim. Acta 1983, **151**, 143

4. Meyers R. J.
   J. Chem. Ed. 1986, **63**, 687

5. Handbook of Chemistry & Physics
   73rd edn. C.R.C. Press, Inc. Boca Raton, Florida, 1991-92
   D-167

6. Hseu T.M. & Rechnitz G.A.
   Anal. Chem. 1968, **40**, 1054

7. Handbook of Electrode Technology
   Orion Research Publication
   Orion Research Inc., 1968, pp. S-5

8. Dunn D.
   Unpublshed work, Univ. of Newcastle-upon-Tyne 1986

9. Sibbald A., Covington A.K. & Harbinson T.R.
   Presented at Utah Conference on "Electrochemical Sensors
   in Medicine and Medical Research"
   Park City, Utah, Jan. 10-14th, 1982

10. Gumbrecht W., Schelter W. & Montag B.
    Digest Eurosensors 1, (Cambridge), 1987, 155

11. Papacostas S.
    Ph. D. Thesis, University of Newcastle-upon-Tyne, 1986

12. Ammann D., Morf W.E., Anker P., Meier P.C., Pretsch E. & Simon W.
    Ion Sel. Elec. Rev. 1983, 5

13. van den Berg A.
    Ph. D. Thesis, Twente University, Netherlands, 1988

14. Buck R.P., Stover F.S. & Mathis D.E.
    J. Electroanal. Chem. 1979, **100**, 63

APPENDICES

Appendix A.

(i) Distillation of Tetrahydrofuran (THF).

To the THF are added 3 μg of benzophenone and *ca.* 1 g potassium metal. Prior to distillation, the still glassware should be flushed through with nitrogen gas (dried over NaOH) to remove water from the apparatus. This is necessary as water forms an azeotrope with THF. A nitrogen flow is not used during distillation, as this would remove the THF vapour.

Potassium effectively removes peroxides in THF; the formation of peroxides leads to an extremely unstable mixture. Benzophenone acts as an indicator by forming complexes with potassium and thus showing the extent of the reaction. During the process quinoline, a peroxide stabiliser in THF, is also removed.

In order to reduce peroxide build up, the distillate should be stored under nitrogen and the container wrapped in aluminium foil to protect from light.

(ii) Preparation of Silver Oxide.

To 338 g of silver nitrate dissolved in 3 litres of deionised water, dropwise add a solution of 80 g sodium hydroxide dissolved in 400 ml water. The silver nitrate solution should be stirred vigorously throughout and the final precipitate should contain a slight excess of silver.

This precipitate should be washed thirty to forty times with distilled water until the conductance of the washings is constant.

Appendix B.

ChemFET Encapsulation using Polyimide / Photoresist.

The following procedure should be followed;

1. Mount the silicon spacers in headers using H54 epoxy. Cure for 15 min at 100 °C, then fill gaps around the spacers with H54 and cure for 30 min at 100 °C.

2. Mount the chips in headers using H54 and cure for 30 min at 100 °C.

3. Clean the chips using the following procedure;

i) 2 % Decon "Neutracon" for 20 s ultrasonically

ii) distilled water for 20 s ultrasonically x 2

iii) propan-2-ol for 20 s ultrasonically

iv) blowdry with N_2 and inspect

If the chip is clean then proceed, otherwise repeat stages iii) and iv).

4. Bond the chips and keep under a glass cover.

5. Blow the chip surface clean with a jet of N_2.

6. Apply a thin layer of polyimide; drop small drops then tease out with a syringe needle under the microscope to cover all the chip and bonding wires.

7. Oven dry at 125 °C for 30 min, then raise the temperature gradually to 170 °C for a further 30 min. Leave to cool very slowly to prevent cracking the encapsulant.

8. Apply thickened KPR-4 (a). This should form a meniscus slightly proud of the chip surface. Stand overnight in a fume hood.

9. Cure KPR-4 for 1 h at 125 °C then raise to 140°C for 3-4 h.

10. Dot KPR-4 with carbon ink from a Rotring pen.

11. Expose the chip to UV for 20 min at < 5-10 cm.

12. Remove the Rotring carbon ink as follows;

i) with Rotring ink remover for 15 s, ultrasonically

ii) spray (25 lb in^{-2}) with water

iii) blowdry with N_2 and inspect

iv) dry at 100 °C for 10 min.

13. Etch chips (KPR-4);

i) agitate the chips in KPR-4 developer for 10 min

ii) spray (25 lb in^{-2}) with KPR-4 developer in the area of the hole

iii) spray with xylene in the area of the hole

iv) blowdry with N_2 and inspect

v) dry at 100 °C for 10 min.

Repeat this procedure using progressively shorter developing times (5 min, 2 min, 1 min, 30 s, etc.) until all KPR-4 is removed from the pit. The remaining few traces require short development times (10-20 s) with oven drying in between to prevent under-cutting.

14. When all the KPR-4 has been removed from the pit, dry the chip at approx. 100 °C overnight.

15. Etch chips with polyimide;

i) agitate the chips manually for 1 min in hydrazine etch

ii) wash ultrasonically in water for 10 s

iii) blow dry with N_2 and inspect

Repeat with shorter etch times (10-30 s) until all the polyimide has been removed from the pit. Special care should be taken of the gate region during etching.

16. Wash the chips;

i) with Decon "Neutracon" ultrasonically for 10 s

ii) immerse in water

iii) with water, ultrasonically, for 10 s x 2

iv) with propan-2-ol, ultrasonically, for 10 s

v) blowdry with N_2 and inspect

If the chip is not clean then repeat stages iv), v).

17. Dry chips at 100 °C for 15 min then raise the temperature slowly to 140 °C and bake for approx. 3-4 h. Raise the temperature slowly to 170 °C and bake for a further 1 h before allowing to cool slowly.

a) Ordinary KPR-4 is thickened by heating to 40 °C under reduced pressure (400 mm Hg) in a vacuum oven for 2-3 days until the KPR-4 is reduced to 60 % of its original volume.

b) Hydrazine etch; this is a 50/50 mixture of 1,2-diaminoethane (ethylene diamine) and hydrazine hydrate, 99-100 %

Appendix C.

Composition of Buffers. *

The following compositions are all made up to 1 litre with deionised water.

Buffer	Composition	pH
B2	7.5 g glycine	2.49
	50 ml 1.0 mol dm^{-3} HCl	
B4	4.724 g succinic acid	4.21
	5.844 g NaCl	
	60 ml 1.0 mol dm^{-3} NaOH	
B6	20.924 g Bis Tris	6.58
	50 ml 1.0 mol dm^{-3} HCl	
B7	18.171 g Tris	7.90
	100 ml 1.0 mol dm^{-3} HCl	
B9	3.054 g ethanol amine	9.38
	30 ml 1.0 mmol dm^{-3} HCl	
B11	10.644 g piperidene	11.34
	50 ml 1.0 mol dm^{-3} HCl	
B12	30 ml 1.0 mol dm^{-3} NaOH	12.60
	54.7 g TMAH	

Tris; tris (hydroxymethyl) methylamine

Bis Tris; 2,2-bis (hydroxymethyl) -2,2'2''-nitrilo triethanol

TMAH; tetra methyl ammonium hydroxide

* Covington A.K. & Ferra M.I.A.
Anal. Chem. 1977, **49**, 1363

Appendix D. BASIC Sensor-Actuator Programme for Volumetric and Coulometric Titrations.

```
10 REM 15/6
20*KEYOMODE4|M
30*KEY2RUN|M
40 @%=&20306:MODE4
50GOTO 370
```

```
60 DEF PROCINIT:JJ%=&FCC8:KK%=JJ%+1:LL%=JJ%-8:?(LL%+2)=255
70 ?(JJ%+3)=32:I%=0:T%=100:L%=I%:?LL%=0:?(LL%+3)=255:NL%=LL%+1:?NL%=0
80J%=&FE68:K%=J%+1:L%=J%-8:?(L%+2)=128+3
90?(J%+3)=32:ENDPROC
```

PROCINIT sets up addresses for the burette, buffer amplifier etc.. initialising the system

```
100    DEF PROCCLERCNT
110?JJ%=255:?LL%=128
120?KK%=255:?LL%=0:ENDPROC
```

```
130 DEF PROCRADC
140 Y%=0
150 FOR X=1 TO 10
160?J%=255:?L%=128+I%:0%=0
170TIME=0:?K%=255:?L%=0:?L%=I%
180 IF TIME>=T% THEN 190 ELSE 180
190 N%=?J%+256*?K%:N%=65536-N%-10002
200IF N%>19999 THEN PRINT"OVER RANGE"
210IF (?L% AND 32)=0 THEN N%=-N%
220 Y%=Y%+N%
230 NEXT X
240 MV=(Y%/10)*1002/8088
250ENDPROC
```

PROCRADC instructs the computer to take a reading of the voltage difference

```
260 DEF PROCSETPULS
270 FOR TON=1 TO ON%
280 ?NL%=255
290 FOR A=0 TO 100:NEXT A
300 ?NL%=0:FOR A=1 TO 100:NEXT A:NEXT TON:ENDPROC
```

```
310    DEF PROCPULS:TIME=0
320?LL%=255
330IF TIME<PL% THEN 330
340?LL%=0:ENDPROC
```

PROCSETPULS instructs the counter to supply a number of pulses, corresponding to a given volume or charge pulse

```
350 PRINT"AUTO-TITRATION PROGRAM"
360 PRINT"THIS PROGRAM ALLOWS COULOMETRIC OR VOLUMETRIC TITRATIONS TO BE CARR
ED OUT"
370 PRINT"TO CALIBRATE ELECTRODES USING TWO POINT CALIBRATION"
380 PRINT"**********************************"
390A=2:DIM P(A):DIM MV(A):DIM N%(A)
400 FOR Z=1 TO A :@%=&20001
410 PROCINIT
420 PRINT"YOUR CHOICE OF BUFFERS SHOULD BE MADE WITH RESPECT TO THE PH OF YOU
SAMPLE"
430PRINT"**********************************"
440 PRINT"PUT ELECTRODES IN BUFFER ";Z
450 INPUT"PH OF SOLN IS";P(Z):PRINT"WAIT..."
460 PRINT"**********************************"
470@%=10:PROCRADC:MV(Z)=MV
480 PRINT"V";Z"=";MV(Z)"mV"
490 NEXT Z
500 SL=-(MV(1)-MV(2))/(P(1)-P(2))
510 PRINT"SLOPE=";SL"mV/DEC":PROCINIT
520 PRINT"**********************************"
530 PRINT"SET UP FOR TITRATION, PLACE ELECTRODES IN SAMPLE SOLUTION"
540 INPUT"INPUT 'SET' WHEN READY":SS$
550 IF SS$="SET" THEN GOTO 570
560 PRINT CHR$7:GOTO 530
570 PROCRADC:IMV=MV:I%=0
580 INPUT"TYPE OF TITRATION:VOLUMETRIC (V) OR COULOMETRIC (C)":TT$
590 IF TT$="V" THEN GOTO 650
600 IF TT$="C" THEN GOTO 810
610 PRINT CHR$7:GOTO 530
620 PRINT"SET UP PARAMETERS FOR THE EXPERIMENT"
```

Calibration of Electrodes; ensures the ISE has a Nernstian response

```
640 INPUT"INITIAL PULSE LENGTH IN 1/100 SEC";IPL%:GOTO 690
650 INPUT" CONCENTRATION OF TITRANT (mol/dm-3)";MO
660 VD=0.001
670 INPUT"INITIAL VOLUME OF EACH BURETTE DELIVERY .mL" IVN
680 IDN%=IVN/0.001
690INPUT ENDPOINT DIFFERENCE IN MILLIVOLTS=";ENDPOINT
700 IDMV=2
710INPUT"INITIAL DECREASE IN ALIQUOT VOLUME";DVL:DPL%=DVL/VD
720 INPUT"VOLUME OF ANALYTE USED/ml";VV
730 PRINT
740 SQ$="PH"
750IF SQ$="PH" THEN GOTO 780
760IFSQ$="MV" THEN GOTO 780
770PRINT CHR$7:GOTO740
780 INPUT"NUMBER OF ENDPOINTS EXPECTED";H%
790 INPUT"CHARGE OF THE SAMPLE IS ? (+ or -)";S$
800 PRINT"**********************************"
810 PRINT"NOW WE CAN START"
820 TP%=0:VT=0
830 PRINT"PLACE YOUR DATA-DISC IN DRIVE 0"
840 INPUT"INPUT A FILENAME FOR YOUR DATA";F$
850 FFF=OPENOUT(F$                    FFF = OPENOUT (F$) opens the file, on disc, to accept titration da
860 F=300:DIM B(3,F):T=0:@%=&20309
870IF TT$="V" THEN GOTO 1150
880 IF TT$="C" THEN GOTO 890
890 PRINT"CHARGE/mA","     PH","EMF/MV"
900 FOR J=1 TO H%:@%=&20309
910 PROCINIT
920PL%=IPL%:PROCPULSE
930 PROCRADC:P=(P(1)+((MV(1)-MV)/SL))
940 TP%=PL%+TP%:CH%=TP%*ICP%
950 B(1,F)=CH%:B(2,F)=P:B(3,F)=MV
960 PRINT CH%,P,MV
970 IF SQ$="PH" THEN PRINT£FFF,CH%,P ELSE PRINT£FFF,CH%,MV
980 OMV=MV:PROCRADC
990IF ABS(MV-OMV)> ABS(IDMV) THEN IPL%=IPL%-DPL%
1000IF IPL%=0 OR IPL%<0 THEN IPL%=1
1010 IF ABS(MV-OMV)>ABS(ENDPOINT) THEN GOTO 1020 ELSE GOTO 920
1020 PRINT
1030 PRINT"ENDPOINT=";MV;"MILLIVOLTS":IMV=MV
1040 PRINT"TOTAL CHARGE=";CH%"mA"
1050 CONC=(CH%*1000)/(VV*96485)
1060PRINT"CONC=";CONC"M""  PH IS ";P
1070 @%=10:@%=&20001
1080 IF S$="-" THEN GOTO 1100
1090 PRINT"PKa(";J")=";((2*P)-CONC-14):GOTO 1110
1100 PRINT"PKb(";J")=";(14-CONC-(2*P))
1110 @%=10
1120 PRINT
1130 NEXT J
1140 CLOSE£FFF:GOTO 1430
1150 PRINT"VOL/mL","    pH","EMF/mV"
1160 FOR K=1 TO H%:@%=&20309
1170 PROCINIT
1180 IDN%=IDN%:PROCSETPULS
1190 VP=VD*IDN%
1200 VT=VT+VP
1210 P=(P(1)+((MV(1)-MV)/SL))
1220 B(1,F)=VT:B(2,F)=P:B(3,F)=MV:PROCRADC
1230 PRINT VT/2,P,MV
1240 IF SQ$="PH" THEN PRINT£FFF,VT,P ELSE PRINT£FFF,VT,MV
1250 OMV=MV:PROCRADC
1260 IF ABS(MV-OMV)>ABS(IDMV) THEN IDN%=IDN%-DPL%
1270 IF IDN%=0 OR IDN%<0 THEN IDN%=1
1280 IF ABS(MV-OMV)>ENDPOINT THEN GOTO 1300 ELSE 1290
```

```
1290 GOTO 1130
1300 PRINT
1310 PRINT"ENDPOINT=";MV "mVOLTS":IMV=MV
1320 PRINT
1330 PRINT"TOTAL VOLUME =";VT"mL"
1340 CONC=((MO*VT)/VV)
1350 PRINT"CONCENTRATION OF ANALYTE IS ";CONC"mol/dm3"
1360 @%=&20001
1370 IF S$="-" THEN GOTO 1390
1380 PRINT"pKa(";K")=";((2*P)-CONC-14):GOTO 1400
1390 PRINT "pKb(";K")= ";(14-CONC -(2*P))
1400 @%=10:PRINT
1410 NEXT K
1420 CLOSE#EFF
1430 END
```

Appendix E.

(i) HELP File to assist in using SUPERQUAD.

```
* This is a HELP file for the entry of data for a METAL-HYDROGEN-LIGAND
* system.  All lines starting with '*' are comment lines to assist in the
* entry of data shown in the other lines.  All '*' lines MUST be omitted
* from true data files!

* Title, up to 52 Characters
 NICKEL-GLYCINE TITRATIONS
*MAXIT IPRIN NMBE MODE
   25   005     3     0
*(IPRIN: 1=Results only, 2=Residuals Plots, 3=Plots of Concs (recommended)
* 4=Refinement monitor, 5=Print of Titn. curves, 6=Table of residuals
* 7=Table of Concs, 8=Extra info on Chi-sq, 9=Total & free concs
* 10=echo of titn points.)
*(NMBE: Total number of reactants (mass balance equations))
*(MODE: normally 0=weights depend on data, 1=all weights are 1.)
* Names of each chemical reactant (KEMIC), total of NMBE in all
   NICKEL
   GLYCINE
   PROTON
* Temperature
  25.0
* Log Beta      M     L     H    KEY
   5.6          1     1     0     1
  10.3          1     2     0     1
  13.7          1     3     0     1
   9.64251      0     1     1     0
  12.05487      0     1     2     0
 -13.69         0     0    -1     0
* Log Beta values, followed by NMBE stoichiometric coefficients in order of
* reactants in KEMIC above, followed by refinement key, -1=beta ignored,
* 0= beta fixed in value, 1=beta to be refined. Terminate with a blank line

*JFP JNMB TOTMM     ADDC       LOCK1 LOCK2
  1 1    0.10340    0.00000      0     0
    2    0.33560    0.00000      0     0
    3    0.75840   -0.24540      1     1
*(JFP=Print controls, normally 1. JNMB=index of reactant from list in KEMIC
* TOTMM=Total no. millimoles of reactant initially present in vessel,
* ADDC=Conc of reactant in burette in moles/litre. LOCK1=refinement key for
* total millimoles, LOCK2=refinement key for burette conc. Terminate with a
* blank line)

*JCOUL   VINIT       SIGMAV
0       47.00000    0.00030
*(JCOUL normally 0 but 1 for coulombic titrations, VINIT=initial volume (ml
* SIGMAV=error in titre vol (ml).
JPH JEL IFC EZERO SIGMAE     LOCK     SLOPE
1 0 3    0.0         0.0017     0        0.0
* (JPH=1 for pH, 0 for mV.  This can be 'switched' in SUPERQUAD, if desired.
* by changing LINE 153 in the FORTRAN text file SUIN.FOR as instructed.
* JEL=No. electrons transferred,0 defaults to 1,
* IFC(Col 5)=Index of reactant in KEMIC to which electrode corresponds,
* EZERO may be 0 for pH, SIGMAV=error in electrode in mV or pH as appropriat
* LOCK=EZERO refinement key, SLOPE=Nernstian slope factor, 0 defaults to 1.
* Terminate electrode information with a blank line.)
```

```
*    TITRE(ml)    pH(or mV)    KEY   If KEY=1 point is ignored
       1.840       5.765
       1.860       5.851
       1.880       5.931
       1.900       6.008
       1.920       6.078
         ....                etc.


*terminate with a blank line. Next set of data as above
  1 1    0.10340    0.00000      0      0
    2    0.33560    0.00000      0      0
    3    0.75840   -0.36740      1      1

         47.00000    0.00030
0   3                0.0017       0

         1.200       5.509
         1.220       5.679
         1.240       5.821
         1.260       5.947  etc.

*Termniate all with 5 blank lines.
```

(ii) Starting to use SUPERQUAD. Documentation to assist in setting up SUPERQUAD.

The discs supplied contains files which include the program (versions for EGA and Hercules graphics), test data and test results, together with the original FORTRAN source code. Two discs are required with the files divided between them. The executable files are SUPERE.EXE (for EGA and CGA graphics) and SUPERH.EXE for Hercules and CGA graphics. Both versions can be used without graphical output or with output directed to a disc file or printer.

Hints on running the program

The IBM (or IBM compatible) computer should have a mathematics co-processor (8087 or 80287) installed. Ideally SUPERQUAD should be installed on a hard disk (with data files in a data directory). The program can be run via a .BAT file so that it can accessed directly from the Text Editor you choose. We find the editor from Turbo Pascal very useful. Alternatively you can prepare your data file using any text editor and SUPERQUAD can then be run by typing SUPERE (or SUPERH) followed by <ENTER>.

Data input for SUPERQUAD

For a description of SUPERQUAD see P. Gans, A. Sabatini and A. Vacca, J. Chem. Soc., Dalton Transactions, 1985, 1196.

SUPERQUAD uses fixed format data input. The formats have been chosen for ease of operation and almost all end in a column number that is a multiple of 5. Integer formats (I) must be right-justified, that is, the least significant digit must be in the right-most column of the data field. Floating point formats (F) contain a pre-defined decimal point; this can be overridden by putting a decimal point in the data. In both I and F formats a blank is equivalent to a zero.

Table 1
Standard layout for SUPERQUAD data

```
      Column number
          1 2 3 4 5        10        15        20        25        30
35
          .. . . . . . . . . . . . . . . . . . . . . . . . . . . . .
.
      Item          .         .         .         .         .
.
      1   < Title ------------------------------------------------> column
52
      2   < MAXIT  >< IPRIN  >< NMBEO  >< MODE  >          .         .
.
      3   <   Name of reactant   >      .         .         .         .
.
                    .         .         .         .         .         .
.
      4   <    Temperature   >          .         .         .         .
.
      5   <     Log beta     ><a or KEY><b or KEY><c or KEY><d or KEY>< (KEY)
```

```
      ...      .        .        .        .        .
.
      6 Blank line      .        .        .        .
.
      7      1*  2*< Total millimoles >< Burette conc. >< LOCK  >< LOCK
>
      ...      .        .        .        .        .
.
      8 Blank line      .        .        .        .
.
      9           3*<  Initial volume  >< Error in titre >        .
.
      10 4*  5*  6*<Standard potential>< Error on emf   >< LOCK  >------>
*7
      ...      .        .        .        .        .
.
      11 Blank line     .        .        .        .
.
      12 <      Titre      ><      emf 1      ><      emf 2      >< JUMP
>.
      ...      .        .        .        .        .
.
      13 Blank line
      14 Options: new titration curve or blank line
      15 Options: new models or blank line
      16 Options: new system or blank line
      Notes
       1* Item 7  column 3  Print control for species distribution plots
       2*      7         5  Index of reactant
       3*      9         5  Coulometric data flag - usually zero
       4*     10         1  Type of electrode
       5*     10         3  No. of electrons transferred
       6*     10         5  Index of reactant to which
                             electrode responds
       7*     10        40  Slope for electrode response
```

Table 1 gives the overall form of the data. There are five items which may contain a variable number of records (lines). In item 3 there may be up to 4 records, one for each reactant. In item 5 there may be up to 18 records, one for each formation constant in the basis set. In item 7 there may be up to NMBEO records, one for each reactant in that titration curve. In item 10 there may be up to 2 records, one for each electrode used in that titration curve. In item 12 there may be up to 250 records, one for each titration point in that curve. There now follows a detailed description of the individual entries in Table 1.

Item	columns	format	variable	Meaning
1	1-72	52A1	NAME	A descriptive title
2	1-5	I5	MAXIT	The maximum number of refinement cycles. (Must be a positive integer)
	6-10	I5	IPRIN	Print control integer. Printing of the following information occurs if the print

priority is less than or equal to IPRIN

1 Results page only
2 Plot of residuals
3 Plots of concentration (recommended)
4 Refinement monitor
5 Print titration curves
6 Table of residuals in emf
7 Table of concentrations in moles/litre
8 Extra information on chi-squared
9 Table of total and free concentrations

11-15 I5 NMBEO The total number of reactants in the system

16-20 I5 MODE Choice of weighting scheme.
0 Weights based on experimental data (normal mode)
1 Unit weight for all points
2 Weights are recalculated after a refinement, from a theoretical titration curve
3 As with 2 but starting with unit weights

3 1-12 12A1 KEMIC The names of each chemical reactant.

4 1-10 F10.6 TEMP The reaction temperature (degrees C)

5 1-10 F10.6 BETA The logarithm to base 10 of the formation constant.

11-15
16-20
21-25 I5
26-30
31-35

These fields contain the NMBEO stoichiometric coeffecients of the species formed followed by the refinement KEY for the beta.
The KEY may have the values:

-1 Beta is ignored in the first refinement
0 Beta has a fixed value
1 Beta is to be refined

6 A blank line to signify the end of the formation constants.

7 3 I1 JFP Print control for species distribution plot (only active if IPRIN > 2)
0 No plot
1 Plot of the concentration of this reactant divided by the total concentration

5 I1 JNMB Index of reactant from the list given in item 3, i.e. 1 for the first, 2 for the second etc.

6-15 F10.6 TOTMM Total number of millimoles of this reactant initially present in the titration vessel

16-25 F10.6 ADDC The concentration of this reactant in the burette (moles/litre)

	26-30	I5	LOCK	Refinement key for total millimoles
	31-35	I5	LOCK	Refinement key for burette concentration
8	A blank line to signify end of reactants information			
9	5	I5	JCOUL	Normally zero but 1 would signify a coulometric titration
	6-15	F10.6	VINIT	Inital volume in the titration vessel (ml)
	16-25	F10.6	SIGMAV	Error in titre volume (ml)
10	1	I1	JPH	Type of electrode.
			0	Reading in mV
			1	Reading in pH units
	3	I1	JEL	Number of electrons transferred at this electrode. A value of 0 defaults to 1.
	5	I1	IFC	Index of the reactant to which this electrode responds, from the list given in item 3
	6-15	F10.6	EZERO	Standard potential of this electrode (mV). If the electrode reads in pH it may be 0.
	16-25	F10.6	SIGMAE	The error in an electrode reading (in mV or pH units, as appropriate)
	26-30	I5	LOCK	Refinement key for standard electrode potential
	31-40	F10.6	SLOPE	Factor by which the Nernstian slope must be multiplied to obtain the experimental slope. A value of 0 defaults to 1, i.e. ideal slope
11	A blank line to terminate the electrode information			
12	1-10	F10.4	TITRE	Titre volume (ml)
	11-20	F10.4	EMFC	First electrode reading (mV or pH)
	21-30	F10.4	EMFC	Second electrode reading (if present, mV or pH)
	31-35	I5	JUMP	A flag to indicate whether to include this point in the calculation. If zero it is included, otherwise it is ignored.
13	A blank line to terminate data for one titration curve			
14	Either new titration curve (repeat items 7-13)			
	or blank line to signify end of titration curves			
15	Either new models			
	or blank line to signify end of models			
16	Either new system (1 in column 5, then repeat items 1-15)			
	or blank line to signify end of data			

Up to 75 new models may be specified in item 15. Each new model consists of a set of refinement keys equal in number to the number of records in item 5, having values of -1,0 or 1, in fields of I2 format.

Dangerous parameters

The quantities TOTMM, ADDC and EZERO can be held constant (LOCK=0) or refined. For simple refinement of a dangerous parameter set the corresponding LOCK equal to 1. However dangerous parameters can also be constrained to refine together. When so constrained they will change by the same proportion, so if the initial values are equal, the final values will also be equal. To impose a constraint set the corresponding LOCK to the same number greater than 1. More than two dangerous parameters can be included in the same constraint. Up to 20 different constraints can be applied.

Coulometric titrations

In some experiments hydroxide ions may be generated by electrolysis, rather than being added from a burette. This type of data will be flagged by JCOUL=1 in item 9, column 5. Subsequently the "titre" values will be assumed to have a different meaning. Since the product of "titre" and "burette concentration" (ADDC) is a number of millimoles, "titre" may be units of time, and "burette concentration" may be millimoles per unit of time. The total volume of the system will be assumed to be constant and equal to the initial volume in the titration vessel.

Overall limitations

In addition to the limitations indicated above, the following also apply, though not necessarily consistently!

No more than	32 titration curves	MAXTC
...	350 titration points overall	MAXTP
...	600 electrode readings overall	MAXEMF
...	700 weights overall	MAXWS
...	45 variable parameters	MAXV

(only accepts 99 poi per titratio

Sample data sets

The sets of data supplied with the program illustrate the different kinds of data that can be handled by SUPERQUAD. The selection is by no means exhaustive, but designed to illustrate the more common types of experimental situations.

1. This is the Nickel-Glycine data discussed in the original paper. Users may wish to explore the effect of refining various dangerous parameters.

2. Sartrigly. This contains the data for a simple titration of a dibasic ligand with alkali. The titration data is in the form of volume/pH. Two dangerous parameters are refined.

3. Nickel-tpt. This will be familiar to users of the MINIQUAD program. It illustrates a set of three titration curves for the system in which alkali is added to a mixture of metal and ligand. The data is in the form of volume/emf.

4. Nickel-histidine-proline. Investigation of ternary complexes, the formation constants for the various binary complexes having been determined in previous experiments. Electrode readings are in units of pH.

5. "Perfect" data. This was produced by an arbitrary simulation in which it was assumed that the correct model was the one used, and that the only experimental errors present were normally distributed errors in titre volume and emf. This data set illustrates how titration curves of different types may be included in the same refinement. Not only does the number of reactants vary from curve to curve but also the number of electrodes also varies.

6. "Synt3". Another set of synthetic data which should provide a good test of how well the program functions on various computers. All the calculated correlation coefficients are above 0.995!

Interpretation of output

It is essential that SIGMAE and SIGMAV (data items 9, cols 6-15 and 10, cols 16-25) are determined experimentally before starting to use the program, as all the statistics are based on these quantities. SIGMAV is an estimate of the error in burette reading. For illustration, a standard 50 ml grade A burette graduated in 0.1 ml divisions has an error of ca. 0.005 ml if read with a magnifying glass. If an autoburette is being used (e.g. a syringe) it is suggested that SIGMAV be determined by weighing the amount of liquid delivered for various increments. SIGMAE is a estimate of the random error in the potentiometer system, that is, the error in a reading ignoring long-term drift. DO NOT ATTEMPT TO DETERMINE SIGMAE AND SIGMAV USING SUPERQUAD (this would involve an essentially circular argument).

It is also recommended that the burette be calibrated to find out what is the actual volume delivered. An error of 0.1% in the absolute volume of an increment from the burette can be significant! When SIGMAE and SIGMAV have been correctly estimated, and when the standard weighting scheme (MODE 0) is being used, the s statistic (SIGMA in the SUPERQUAD output) should ideally be near to 1. To understand this let us suppose that we have a system with one electrode. If SIGMAV were equal to zero the weights would all be equal to 1/SIGMAE squared, and SIGMA will be nearly equal to the root mean square of the unweighted residuals, divided by SIGMAE, i.e. it will be the ratio of the rms residual in emf to the estimated error in an emf reading. When SIGMAV is not zero the weights will all be different, and ideally they should be equal to the inverse of the squared error in each observation; equating the errors and residuals each weighted squared residual should be 1, and so the rms weighted residual should also be 1. A similar argument applies when there are two electrodes.

If SIGMA values < 1 are obtained it is probable than SIGMAV and/or SIGMAE are too large. If large values of SIGMA are obtained possible causes are:

1) SIGMAE and/or SIGMAV are too small.
2) The model is incorrect, e.g. an important species is missing.
3) There are systematic errors in the data.

Deal with the first two possibilities directly. Systematic errors are treacherous to deal with. Ideally they should be minimised at the experimental stage, but inevitably some systematic errors will persist in real data. For example, systematic differences between two or more titration curves relating to the same system will usually become apparent when the data from all curves is included in one refinement. No-one knows exactly what causes these differences, though electrode calibration is an obvious candidate. If large systematic differences appear, more careful experimental work is indicated.

In the model selection process we can reject a model which gives a large SIGMA value, but we must decide what constitutes "large". It has been proposed that any value greater than 3 is "large" but in general this is somewhat optimistic. The value is based on the idea that if SIGMAV were zero this would correspond to the average residual being more than three times the estimate of error in potential. We suggest that the experimental set-up and quality of the data obtained from it be evaluated using systems in which the model is known with some certainty, e.g. the nickel/glycine system with three or more titration curves (not duplicates, but using different concentrations etc.).

A second statistic, chi-squared, is also useful for model selection. If SIGMA is acceptable but chi-squared is large this suggests that there are systematic trends in the residuals, indicative of systematic errors in the data and/or the model.

When an unacceptable fit is obtained, examine the plot of residuals. A single large residual probably indicates an erroneous data point. Otherwise the largest residuals usually appear near the end-points in the titration curve. This is probably caused by the fact that the emf changes rapidly near a end-point, making precise determination difficult. Also, there is a technical problem associated with the calculation of the weights in MODE 0 when there is a very sharp end-point, so that the weights may not be calculated accurately from the titration curve. If all the residuals near an end-point have the same sign there is probably a systematic error in the data. Sometimes this feature can be eliminated by refining a dangerous parameter but this is very risky if one is not sure of the source of the systematic error. Try a titration of glycine with alkali: this exhibits a very sharp end-point and the titration curve is difficult to fit.

Selection of suitable data for the calculation is very important. The experimental data may range from a region in which there is essentially no complex formation to a region in which complex formation is essentially complete. Data from these regions should be excluded from the calculations since they contribute no information regarding the formation constants. They represent only the effects of dilution and their inclusion can adversely affect the quality of the fit, as judged by SIGMA and chi-squared.

Conventions used to represent hydroxide ions

In the test data supplied the convention is used that hyroxide ion concentrations are given a negative sign, that is, addition of a solution containing hydroxide ions reduces the total hydrogen ion

concentration. With this convention the self disscociation constant for water, Kw, is included by specifying OH- as a complex, with stoichiometric coefficients such as (O -1) or (O O -1).

[OH]=Kw(1/[H])

Kw should be regarded as an empirical quantity appropriate to the ionic medium and temperature used in the experiments. Kw does not need to be specified unless the titration data extend to a region of high pH.

Deprotonated species are specified with negative stoichiometric coefficients. For example a metal complex might be specified by the coefficients (1 1 -1). This could either be a complex in which the ligand has lost a proton, MLH(-1), or a hydrolysed metal complex. In the latter case the formation constants are related by

Beta MLH(-1) = Kw * Beta(ML(OH))

It is generally preferable, when using this convention, to designate the most hydrolysed form of the substance as "reactant". E.g. for glycine we define the glycinate anion as the reactant L, and glycine itself is denoted as LH.

It is important to note that if a convention of this kind is adopted, and if a protonated form of the ligand is used to make up the reaction mixture, the total millimoles of proton (data item 7 cols 6-15) must include one millimole for each millimole of proton present in the ligand. For example, using the convention that glycine is denoted as LH, the total number of millimoles of proton should be given a number equal to the number of millimoles of glycine plus the number of millimoles of proton added as mineral acid. If the ligand were denoted as LH(subscript 2) the total number of millimoles of proton should be given a number equal to twice the number of millimoles of ligand plus the number of millimoles of proton added as mineral acid, etc.

Since the total hydrogen ion concentration can become negative the species distribution plots relative to the total hydrogen ion concentration are not usually very meaningful.

Appendix F.

(i) Composition of Sulphide Anti-oxidant Buffers.

a) Composition used in this work [60]

2.0 mol dm^{-3} sodium hydroxide

0.2 mol dm^{-3} ascorbic acid

0.2 mol dm^{-3} ethylene diamine tetra-acetic acid

prepared from the disodium salt, (Na_2H_2L)

where L is a negatively charged 4- ion

All reagents were supplied by BDH Chemicals Ltd. and the SAOB was used in a 1:1 v/v ratio with the sulphide sample solutions.

b) Composition recommended[58, 59] for further work

2.0 mol dm^{-3} sodium hydroxide

trace ascorbic acid

c) Composition used by Bock and Puff*

Glycine-sodium hydroxide buffers (no concentrations given) were used successfully for sodium sulphide solutions, 1.0 - 10^{-3} mol dm^{-3}, to inhibit bisulphide formation.

* Bock R. & Puff H.J.

Z. Anal. Chem. 1968, **240**, 351

(ii) Dissociation Constants of Reagents Present in SAOB.

pK^d Values of EDTA

H_4L	pK_1^d	1.99
H_3L	pK_2^d	2.67
H_2L	pK_3^d	6.16
H_1L	pK_4^d	10.26

from The Chemical Society, Special Publication no. 6, 1957

"Stability Constants. Part I. Organic Ligands."

ed. Bjerrum J., Schwarzenbach G., Sillen L.G.

pK^a Values of Ascorbic Acid.

pK_1^d	4.22
pK_2^d	11.52

from "Dissociation Constants of Organic Acids in Aqueous Solutions"

IUPAC Section on Analytical Chemistry Commision of Electrochemical Data, pp. 510

ed. Kortum G., Vogel W., Andrussov K.

London, Butterworths 1961